REFERENCE ONLY

UNIVERSITY OF LONDON THESIS

Degree PhD Year 2006 Name of Author BROADBENT, S.A

An investigation into neuronal nicotinic acetylcholine receptors with complex compositions

Steven David Broadbent
University College London
PhD Pharmacology

ProQuest LLC
789 East Eisenhower Parkway
P.O. Box 1346
Ann Arbor, MI 48106-1346

I confirm that the work presented within this thesis is my own work unless otherwise noted.

Steven Broadbent

ABSTRACT

Neuronal nicotinic acetylcholine receptors (nAChRs) are ligand-gated ion channels of the nicotinic superfamily. They are found widely in the autonomic nervous system and in selected regions of the central nervous system and are thought to be of importance in the progression and/or treatment of a number of disorders. Despite all this the exact role of cholinergic neurotransmission remains unclear and current cholinergic drug treatments leave a lot to be desired. As such nAChRs remain areas of immense interest and potential.

One of the problems with nAChR research has been that the simple receptors obtained in heterologous expression systems probably bear little resemblance to the more complex stoichiometries seen *in vivo*. Therefore my PhD dealt with the characterisation of some more complex nAChR compositions and the development of research tools to aid in the research of not just nAChRs but other ligand-gated and voltage-gated ion channels with complex compositions. In this I primarily used two-electrode voltage clamp methods in *Xenopus laevis* oocytes.

My initial research investigated the role of β3 subunit incorporation into a range of nAChRs; surprisingly this subunit, which produced only subtle effects when incorporated into α3β4 receptors, completely abolished the currents produced by all other pair and homomer receptors tested. Similar findings were obtained when hippocampal neurones in primary culture (which have α7-like responses) were transfected with the β3 subunit. This suggests a possible major role for β3 in nAChR regulation.

One widely used method of constraining receptor stoichiometry is the use of "tandem" subunits. My research however uncovered serious flaws in this method which may render it worse than useless. Subsequent work showed that expression of "pentamer" constructs has greater potential, as it allows much greater control over receptor composition yet avoids the problems seen with the tandem approach.

TABLE OF CONTENTS

LIST OF FIGURES

ACKNOWLEDGEMENTS

"Art is I, science is we" Claude Bernard (1813-1878)

This work was supported in part by a Medical Research Council grant. Part of my conference expenses were paid for by the Brains Trust. A special mention to all the employees of Scottish & Newcastle, I couldn't have done it without you, and to the playing staff of NUFC for teaching me the true meaning of frustration. I wish to thank Dr. Chris Shelley, Dr.Andrew Plested, Dr. Stephanie Schorge, Dr. Chris Hatton, Dr. Sergio Elenes, Dr. Philippe Behe, Dr. Bob Janes and Professor David Colquhoun for advice. I wish to thank Chris Courtice and Steve Coppard for technical assistance and warranted abuse. Thanks to Paola Imbrici, Helena Da Silva, Lola Wheat, Dr. Susan Griffin, Dr. George Peters, Dr. Carles Canti and the rest of the oocyte group. For the receptor binding studies can I thank Dr. Patricia Harkness and Dr. Neil Miller. I wish to thank the visiting members of my research group, Jenny Davie, Uta Schneiders, Martina Theuer, Kasia Bera, Skevi Krashia, Seb Kracun and Giovanna Hoffman for all their hard work and their tolerance of my bad jokes, with particular apologies to all those from abroad, after years studying English the last thing you needed was to be greeted by a Geordie. Cheers to Dr. James Boorman for showing me which end of an electrode to stick into an oocyte and for teaching me how to feed the horse. A big thank you to Dr. Marco Beato for all your help and for not resorting to any of the slow execution techniques you've threatened me with over the years. To Dr. Valeria Burzomato, hope you and the "pamelas" go on to have lots of foon together, thank you for not throwing anything worse than your shoes at me. Dr. Paul Groot-Kormelink, thanks for defrosting the RNA, I know it's a little more complicated than that, I'll keep my eyes peeled for

"een kleine muis op klompjes, daar op de trap". Special thanks to my second supervisor, Professor Trevor Smart, for all his assistance. To my friends, thanks for keeping me sane, sort of, don't worry I'll still talk to you all. Many, many thanks to my family for all their support over the years, particularly to my Grandma and Grandad, I'm sorry I had to move away but I never stopped thinking about you, to Floss, good luck for when we return you to live with the other monkeys and "me muva en fava" for not sending me back when I was born, its done you can stop getting cats now, words can't say how much you all mean to me.

Last and certainly not least, Lucia. I'm eternally grateful to you for providing me with this opportunity, thank you for all your guidance, for your example, for reining in my crazier flights of fancy and for all your patience, I understand that the urge to throttle me has been very strong at times. I hope you can look forward to many more years of productive research and that you never lose your joy in your work.

In loving memory of Elsie Angus, you'll always be in our hearts.

CHAPTER 1

Introduction

1.1 History of acetylcholine.

The history of our understanding of the acetylcholine (ACh) ligand-gated ion channel (LGIC) is in many ways the history of our understanding of pharmacology.

From long before Europeans arrived in the Americas the Native Americans have used tobacco as an entheogen and shortly after colonisation tobacco products were being widely smoked, chewed, "dipped" and sniffed recreationally across Europe. The tobacco industry was one of the main driving forces in the colonisation of what was to become the Southern US and tobacco excise taxation provided a third of the US government's internal revenue up until 1883. The main active ingredient in tobacco, nicotine, is named after Jean Nicot who was praising the recreational and medicinal benefits of tobacco as far back as 1550. It was not long before some of its less desirable effects became apparent with King James VI of Scotland and I of England denouncing it as a "custome lothsome to the eye, hatefull to the Nose, harmefull to the braine, dangerous to the Lungs, and in the blacke stinking fume thereof, neerest resembling the horrible Stigian smoke of the pit that is bottomelesse" in his famous polemic A Counterblaste to Tobacco (1604). Punitive tariff rates were to follow in a pattern which was to become common. The alkaloid itself was first isolated in 1828, its molecular formula elucidated in 1843 and its first synthesis achieved in 1904. Given all this, pharmacologists seem to come onto the stage late. In 1856, Claude Bernard, arguably the greatest physiologist of all time, published his most famous work demonstrating that a Central American arrow poison called curare, a cholinergic antagonist, selectively blocked the motor nerve endings (Frutton, 1979). In 1892 Langley definitely proved that nicotine, an ACh agonist, could

potently activate neurones (Langley & Anderson, 1892) and this provided the basis for Langley to make the first explicit formulation of receptor theory, the idea that "receptive substances" on cells combined with pharmacologically active compounds as their specific physiological targets, in 1905 building on the "side-chain" theory of Ehrlich (Langley, 1905; Ehrlich, 1897). Nicotine and curare were then extensively used by Langley and led to him postulating the presence of excitatory and inhibitory "receptive substances" in effector cells. As such the nicotine receptor became the first to be recognised and named (Langley, 1907), though the pharmacological action of choline and ACh on the adrenal medulla had already been described by Hunt in 1900 (Hunt, 1901). In 1914 Dale identified two types of ACh action and named them muscarinic and nicotinic, due to the different actions of the ACh agonists, muscarine and nicotine, a nomenclature which remains today (Dale, 1914; Dale *et al.* 1936). In 1920 *Vagusstoff*, later identified as ACh, became the first recognised neurotransmitter with Loewi's demonstration that activation of the vagus nerve could affect frog hearts even at a distance (Loewi, 1921). The ACh nicotinic receptor was the focus of the seminal work by del Castillo and Katz which remains the basis of models of drug-receptor interactions (del Castillo & Katz, 1957). In the 1950s the ACh receptor claimed another first when it became the first receptor to be studied electrophysiologically (Katz & Thesleff, 1957) and from this many of the different techniques of electrophysiology were developed. The muscle-type nicotinic ACh receptor (nAChR) remains the best characterised of all LGICs (reviewed in Changeux, 1990). So as can be seen many of the major milestones of pharmacology, and biological sciences in general, have revolved around ACh receptors. However despite the long and successful history of scientific research into ACh there still remain many

questions to be answered and so ACh transmission remains the centre of a lot of scientific research.

1.2 Acetylcholine and pathophysiology

Cholinergic neurotransmission is not only of importance to the history of pharmacology but also as a potential target for therapy. Acetylcholine is thought to be of importance in the progression and/or treatment of a host of diseases including (but not exclusively) Parkinson's disease, Alzheimer's disease, Huntingdon's chorea, schizophrenia, neuropathic pain, epilepsy (particularly the extremely rare autosomal dominant nocturnal frontal lobe epilepsy), Tourette's syndrome, myasthenia gravis, attention deficit disorder and ulcerative colitis. Given the morbidity and mortality attributed to smoking there is also a lot of interest in pharmacological approaches (particularly nicotinic) to smoking cessation, and these may also be of use in treating other addictions. Paradoxically, many of the "pleasurable" aspects of smoking such as anxiolysis, analgesia, improved learning and memory, cognitive enhancement and hunger suppression are of also of great interest. If these, along with the putative neuroprotective effects of smoking, could be mimicked safely and non-addictively it would be of great benefit. Hence, not only is cholinergic research of great historical interest and a good starting place to hone experimental techniques and approaches but there is also a considerable amount of potential for cholinergics in a wide range of fields.

1.3 Divisions of the cholinergic system

Cholinergic receptors are divided up in a variety of ways depending on their receptor superfamily subunit composition, their location in the body, their actions, their pharmacology etc. One of the oldest divisions was initially based purely on differences in pharmacology, some receptors were observed to be activated by muscarine while others were activated by nicotine, it was only later these differences were shown to correspond closely to the main physiological functions of ACh in the body.

1.3.1 Muscarinic acetylcholine receptors

Muscarinic acetylcholine receptors are so-called as they were found to be activated by muscarine, one of the active principles of the fly agaric mushroom, *Amanita muscaria*. They are G protein-coupled receptors found in the autonomic nervous system (ANS) and also extensively in the central nervous system (CNS). They are also found widely in non-neuronal tissues such as the parietal cells of the stomach, exocrine glands, smooth muscle, vascular endothelium, and in the heart (atria and cardiac conducting tissues). These receptors are thought to mediate the majority of the inhibitory and excitatory effects of ACh on central neurones and the peripheral tissues (Caulfield, 1993), the effect of their action being dependant on the downstream actions of the receptor such as the activation of phospholipase C, inhibition of adenylate cyclase or activation or inhibition of an ion channel.

1.3.2 Nicotinic acetylcholine receptors

Nicotinic acetylcholine receptors (nAChRs) are ligand-gated ion channels (LGICs) found in the ANS, somatic nervous system (SNS) and parts of the CNS. Ligand-gated ion channels mediate fast signal transmission at synapses and produce their effects by allowing the movement of ions across the cell membrane. This can affect the cell either directly, by changing the electrical potential of the cell by altering the internal concentrations of specific ions, or indirectly, by regulating the internal concentration of an ion, usually Ca^{2+}, which in turn affects the activity of a range of other proteins. The majority of my research was concentrated on the nAChRs, particularly the neuronal nAChRs although a little work was also carried out on 5-HT_3 and Glycine α1 ion channels. Much of the work, particularly that carried out on concatenated ion channel subunits, is of wider practical relevance within the nicotinic superfamily.

The nAChRs are made up of by a pentamer of subunits of which 17 have been so far discovered in vertebrates. These are named α1–α10, β1–β4, γ, δ and ε. These are further sub-divided into two groups, the muscle (α1, β1, γ, δ and ε) and neuronal nicotinic (α2–α10, β2–β4) subunits.

1.4 Structure of the nicotinic acetylcholine receptors

Despite the differences between the different subunits and the two main classes of receptors they form, a number of characteristics are consistent. Both muscle and neuronal nicotinic receptors are formed in the cell membrane by a pentamer of subunits arranged around a central ion-permeable pore (Figure 1.1B). Each subunit itself is made

up of a large extracellular N-terminal, four transmembrane domains (labelled TM1-TM4), a large cytoplasmic loop between TM3 and TM4 and a relatively short extra-cellular C-terminal (Figure 1.1A).

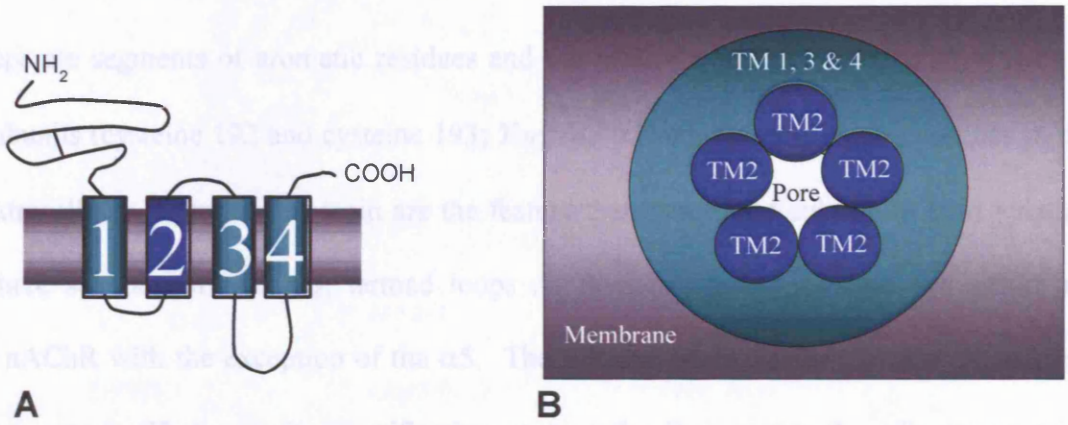

Figure 1.1: A) Representation of the four transmembrane domains of one subunit, showing the long extracellular ligand binding N-terminal (NH_2) domain with cysteine bond. The pore lining TM2 domain is highlighted in blue. B) A representation of the nAChR as seen from above. The five TM2 domains (highlighted in blue) create the pore-lining region. The non-TM2 domains (TM1, TM3-4) are represented by a structural ring in the membrane surrounding the TM2 domains. (Adapted from Boorman, 2002)

Of the two types, and in fact of all the LGICs, the muscle nicotinic remains the best characterised, although most of what is known for the muscle nAChRs probably holds for the neuronal nicotinics, and the other LGICs.

The large N-terminal is thought to contain the residues important in forming the binding site. The TM2 domain is thought to have a dominant α-helical structure conformation which lines the channel pore and contains the residues which govern the ion channel's selectivity and conductance (Karlin & Akabas, 1995). Between TM3 and TM4 there is a long cytoplasmic loop which is involved in targeting the receptor to

specific parts of the subsynaptic membrane (Williams *et al.* 1998) and contains a number of possible phosphorylation sites (their exact function is presently unclear, Moss *et al.* 1996). The principal binding domain of the muscle nicotinic was thought to be formed within the tertiary structure of the α1 subunit, created by interactions between three separate segments of aromatic residues and the pair of adjacent cysteines specific to α subunits (cysteine 192 and cysteine 193; *Torpedo* α1 numbering). These cysteines in the extracellular N-terminal domain are the feature that classifies a subunit as an α subunit. Three sections of residues, termed loops A, B and C, are conserved throughout all α nAChR with the exception of the α5. The α5 is most similar in terms of amino acid sequence to β3 despite its classification as an α (as it possesses the adjacent cysteine residues 192 and 193). An argument could be made that both subunits should be renamed. The three loops form a binding pocket that can interact with the ester moiety of the ACh molecule (Karlin & Akabas, 1995) (see Figure 1.2.).

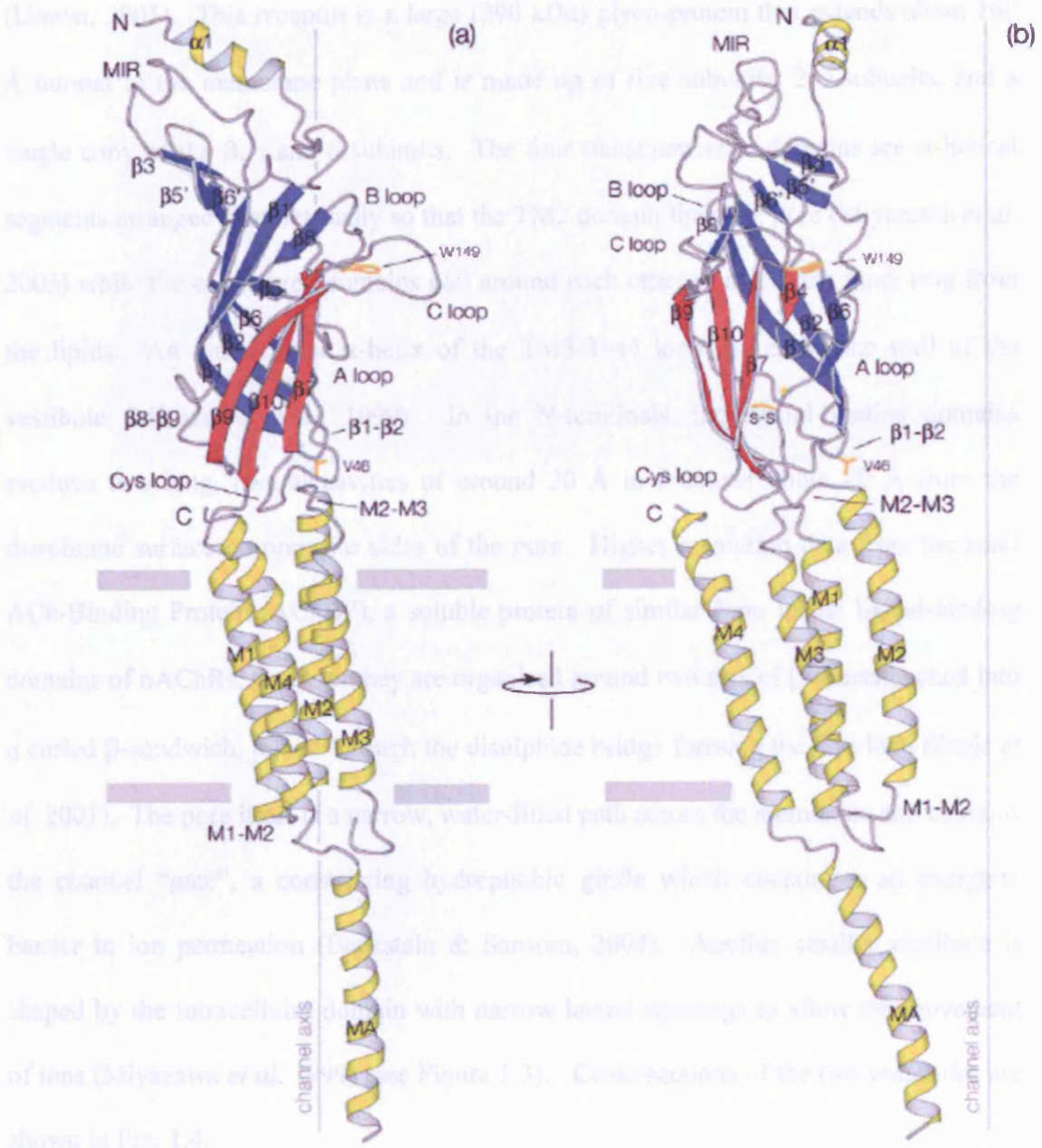

Figure 1.2: Ribbon diagrams of a single α subunit viewed parallel with the membrane plane, in orientations such that the central axis of the pentamer (vertical line) is (a) at the back and (b) to the side. The α helices are shown in yellow, the β-strands are in blue and red (inner and outer respectively). Locations of the N and C terminal, the Cys-loop disulphide bridge and the three binding loops are indicated. (from Unwin, 2005).

The structure of the membrane-associated *Torpedo* ACh receptor has been imaged by the group of Unwin using electron microscopy, most recently at a resolution of 4 Å

(Unwin, 2005). This receptor is a large (290 kDa) glyco-protein that extends about 160 Å normal to the membrane plane and is made up of five subunits; 2 α subunits, and a single copy of the β, γ and δ subunits. The four transmembrane domains are α-helical segments arranged symmetrically so that the TM2 domain lines the pore (Miyazawa *et al.* 2003) while the other three domains coil around each other to shield the inner ring from the lipids. An intracellular α-helix of the TM3-TM4 loop makes up the wall of the vestibule (Miyazawa *et al.* 1999). In the N-terminals, the ligand-binding domains produce two long, central cavities of around 20 Å in diameter about 40 Å from the membrane surface on opposite sides of the pore. Higher resolution data from the snail ACh-Binding Protein (AChBP), a soluble protein of similar form to the ligand-binding domains of nAChRs, suggests they are organised around two sets of β-sheets packed into a curled β-sandwich, joined through the disulphide bridge forming the Cys loop (Brejc *et al.* 2001). The pore itself is a narrow, water-filled path across the membrane and contains the channel "gate", a constricting hydrophobic girdle which constitutes an energetic barrier to ion permeation (Beckstein & Sansom, 2004). Another smaller vestibule is shaped by the intracellular domain with narrow lateral openings to allow the movement of ions (Miyazawa *et al.* 1999) (see Figure 1.3). Cross-sections of the two vestibules are shown in Fig. 1.4.

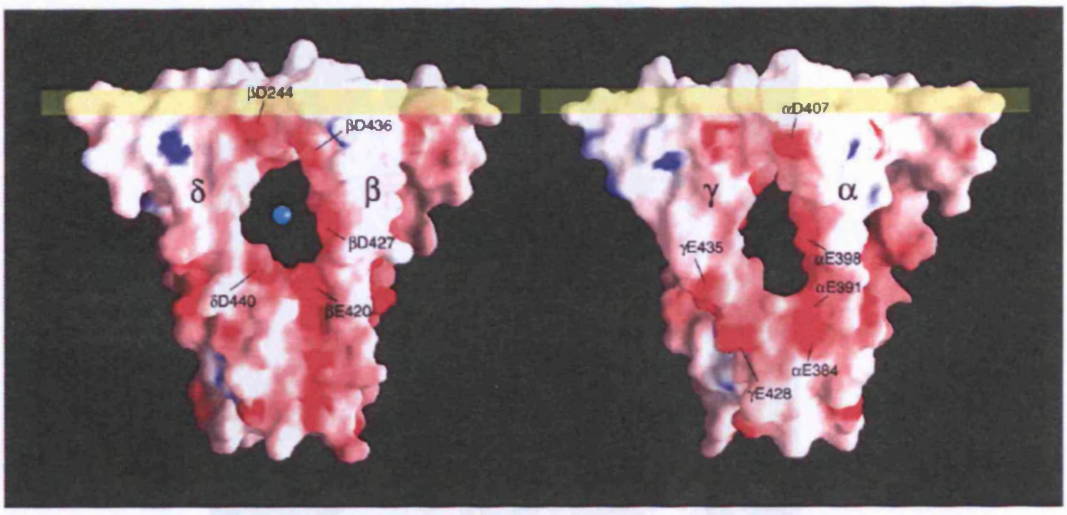

Figure 1.3: Electrostatic potential surface representations showing entry/exit windows for cations between the helices of different subunits of the muscle nicotinic receptor on the intracellular side of the membrane. The window between δ and β is shown on the left and the window between γ and α_δ are on the right. The location of the intracellular membrane surface is indicated by the horizontal bar and the sphere in the δ/β window is the size of a potassium ion (2.7 Å diameter). Exposed charged side-chains are labelled. (from Unwin, 2005)

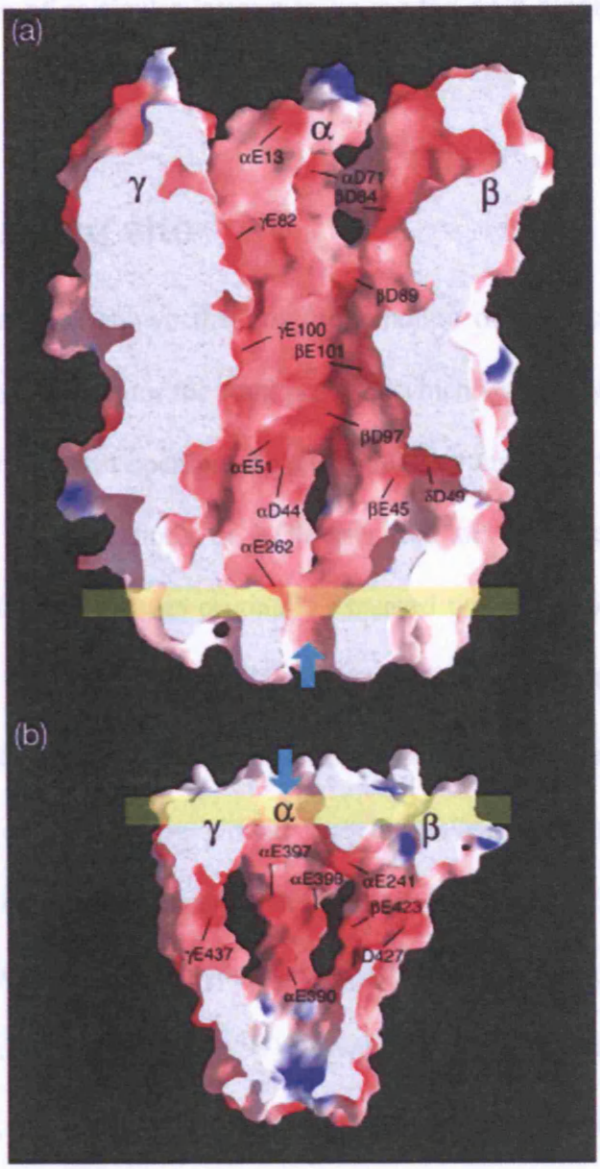

Figure 1.4: Central sections showing the inner surface of (a) the extracellular and (b) the intracellular vestibules. Both vestibules are lined by an excess of negatively charged groups, promoting a cation-stabilising electrostatic environment. Exposed side-chains are labelled and the locations of the membrane pores (arrows) and membrane surfaces (horizontal bars) are indicated. (from Unwin, 2005)
(**A**) View looking towards the α_δ–β subunit-subunit interface
(**B**) View looking towards the α_γ subunit with γ and β on either side.

The two structures of particular interest to us are the ACh-binding sites and the channel gate.

1.5 The ACh-binding site

Single channel data has shown that for full function of the receptor, two ACh molecules have to bind to the receptor the final proof of which was shown by Colquhoun & Sakmann, 1985. Monoliganded openings do occur but they are usually rare and minor events unless very low concentrations of ACh are used or the receptor contains a mutation. As mentioned earlier, it was originally assumed that the two ACh molecules bind solely to the two α subunits, however it was later suggested that the ACh-binding sites are found at the interface between an α and non-α subunit. The α-only binding model was championed originally by Unwin due to his early electron microscopy findings, however in his most recent papers (see for instance Unwin, 2005) he appears to have back-tracked somewhat from this hypothesis. Earlier imaging at lower resolutions, 9Å (Unwin, 1993) and 4.6Å (Miyazawa, 1999) showed that the α subunits differed most from the non-α subunits, not in the interface regions, but closer to the centre of what we now know is a β-sandwich. As the α subunits displayed weaker densities in their centre, this led this region to be identified as the putative ACh-binding site. Imaging in 2005 at the higher resolution of 4Å revealed that the more open appearance was a consequence of the distinct inner- and outer-sheet arrangements in the α subunits. As an example. the β9-β10 hairpin of the α subunits is around 1.5Å further from the oppositely facing inner β2 and β6 strands than it is in the other subunits at the level of the binding sites. Therefore the earlier identification was a mistake and the putative binding site is closer to

the γ and δ-subunit interfaces putting them in locations equivalent to those found in the ACh-Binding protein (Brejc *et al.* 2001). Unwin also notes a number of sites of potential contact between the α1 subunits and the γ or δ subunits, however he maintains that the γ and δ subunits, particularly the β5 and β6 strands merely help shape the binding pocket, while the α1 subunit binds directly. For instance, he identifies the conserved Y190, Y198 and C192 sidechains of the C-loop and the W149 of the B-loop in the α1 subunit as coordinating with the bound ACh analogue, carbamylcholine, in the complex with AChBP (Celie *et al.* 2004).

The two resulting distinct types of binding site, αγ and αδ, would account for binding site non-equivalence. The high affinity ACh binding site is thought to be formed at the α–δ interface (with the low affinity at the α–γ, see Fig. 1.5.), on the basis of the affect of site directed mutagenesis on the binding affinity of d-tubocurarine at *Torpedo* nAChRs (O'Leary *et al.* 1994).

Single channel data has confirmed that the two binding sites display different binding affinities for ACh (Zhang *et al.* 1995). This leaves an interesting question about the neuronal nicotinic receptors, are the two ACh-binding sites of a receptor such α3β4, presumably formed at the interface between the α3 and β4 subunits, equivalent?

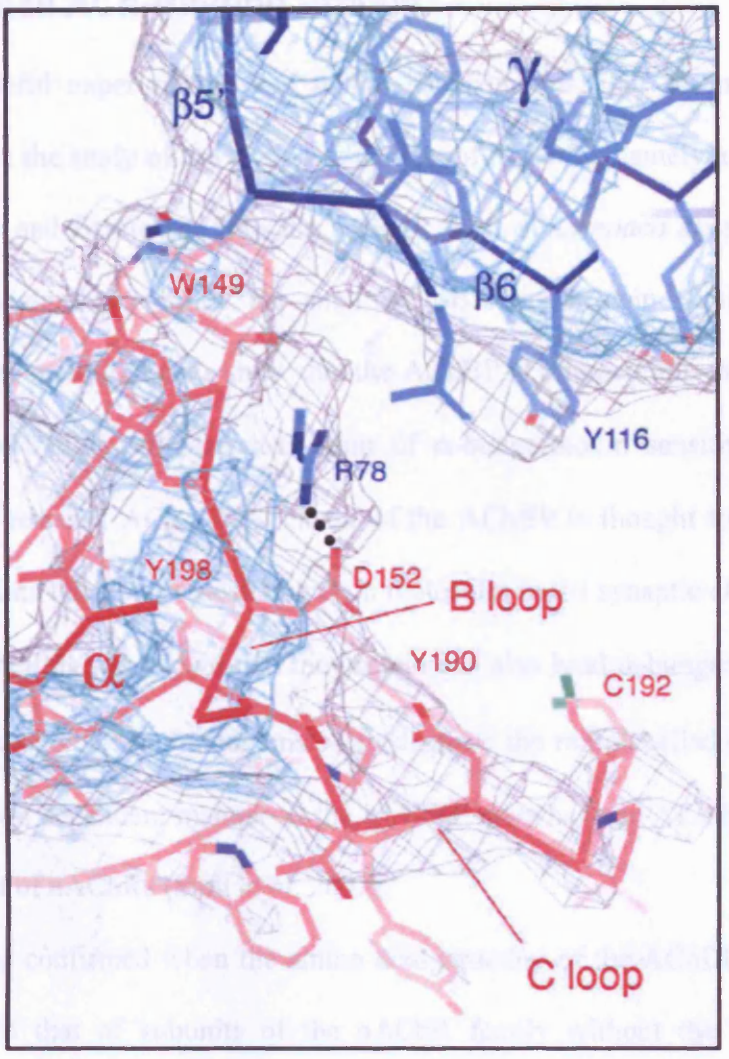

Figure 1.5: Interpretation of the ACh-binding region of the closed channel at the interface between the α and the γ subunits, showing the loops B and C (α subunit), the adjacent strands, β5 and β6 (γ subunit) and the attached amino acid side-chains. The slab is of the upper part of the Ach-binding region, viewed from the synaptic cleft. Some key residues implicated in ACh binding are labelled. the C^{α} backbone and side-chains are in red (α) and blue (γ). A salt-bridge is indicated between αD152 and γR78 is thought to be involved in stabilising the B loop. (from Unwin, 2005).

1.5.1 The snail ACh-Binding Protein

One useful experimental tool which has come to light recently has helped immeasurably in the study of the ACh-binding site of nAChRs, namely a soluble protein that binds ACh and is released into the synaptic cleft of *Lymnaea stagnalis,* the great pond snail, imaginatively called the snail ACh-Binding Protein (Smit *et al* 2001). Recordings from snail glial cells show that the AChBP is released into the synaptic cleft from perisynaptic glial cell after activation of α-bungarotoxin sensitive nAChRs by presynaptically released ACh. The release of the AChBP is thought to dampen down cholinergic transmission by sequestering ACh molecules in the synaptic cleft.

Radiolabelling has shown that the protein can also bind α-bungarotoxin and that known nicotinic agonists and antagonists can displace the radiolabelled α-bungarotoxin in a concentration dependent manner so the ACh-BP must have an ACh binding site that is similar to that of nAChRs (Smit *et al.* 2001).

This was confirmed when the amino acid structure of the AChBP was shown to be analogous to that of subunits of the nAChR family without the transmembrane domains i.e. mostly the extracelullar ligand-binding domain. The N-terminal domain of the AChBP contains a cysteine loop analogous to the loop formed by cysteine 128 and 142 in the nicotinic AChR subunits (with the slight difference that the two Cys are separated by 12 residues in AChBP and 15 residues in the nAChRs). The closest sequence similarity is with nAChR α subunits, containing the adjacent cysteine residues (Cys 192 and Cys 193). The majority of the residues involved in forming the loops in the subunit interface model of the binding site are also conserved, those being Tyr 93, Trp

149, Tyr 190, Tyr 198 and Trp 55 (numbering of *Torpedo* α1) and as mentioned above is quoted as proof of the α–γ/α–δ binding site model.

The crystal structure of the AChBP indicates that 5 identical AChBP 'protomers' form a pentameric cylinder 62 Å high, 80 Å diameter surrounding a central hole of approximately 18 Å (Brejc *et al.* 2001). Positive and negative sides have been identified for each protomer, allowing the protomers to form dimer interfaces with their neighbours, with the first protomer interfacing its plus side with its neighbour's negative side. At 4.6 Å resolution these dimensions of the AChBP pentamer are found to be in good agreement with those of the *Torpedo* nAChR although small differences became apparent at 4 Å (Miyazawa *et al.* 1999). The AChBP pentamer is also analogous to the nAChR in its orientation with the N-terminal domain at the extracellular face of the nAChR and the C-terminal at the cytoplasmic.

Two cavities have been identified in the AChBP (Brejc *et al.* 2001). The first is a large uncharged, hydrophobic pocket framed by β-strands which is thought to be analogous to the pocket that was originally thought to be the ACh binding pocket of *Torpedo* (Miyazawa *et al.* 1999). A distinct second cavity, which can be occupied by a HEPES molecule in the crystal, has been suggested as the location of the ligand-binding site (Brejc *et al.* 2001) (see Fig. 1.6.). Residues lining this second cavity are conserved from the presumed ACh binding site of the muscle nAChR. These are located close to the outer edge of the pentamer, at the interface between the protomers. Aligning the amino acid sequence of the AChBP with the nAChR subunits, reveals that many of the binding site loops of the AChBP are conserved in the nAChR subunits (see Table 1.1). This has made the AChBP a useful tool for investigating ACh-binding in the nAChRs,

has added evidence for the binding site controversy detailed above and has opened up interesting areas of research using AChBP chimeras (Bouzat *et al.* 2004).

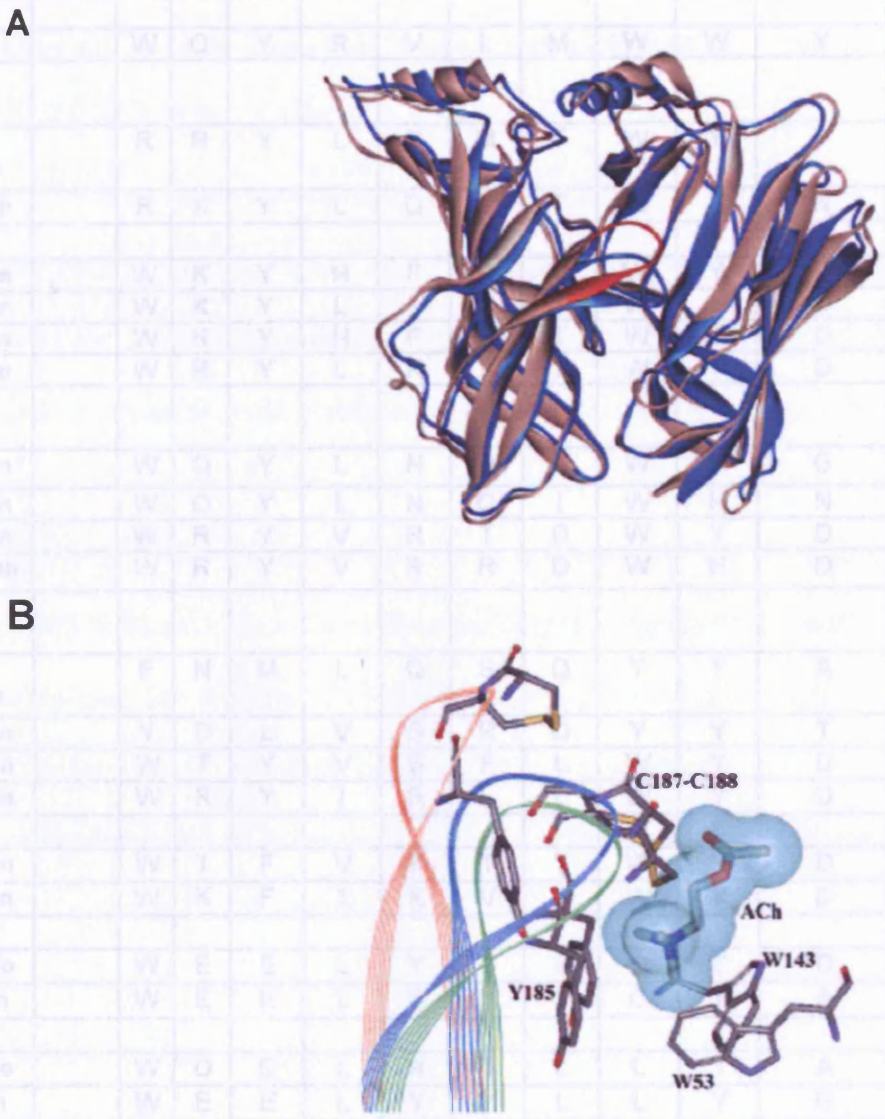

Figure 1.6: Representation of the structure of the AChBP binding site with and without agonist bound.
A) Superposition of the ribbon structure of the AChBP (subunits c and d shown) unbound (brown) and with 5 molecules of ACh bound (blue). Note the mobile C-loop highlighted in red.
B) Close-up superpositions of the C-loop for the ACh-free structure (brown), with ACh bound (blue) and with carbamylcholine bound (green). Side-chains of Cys187, Cys188 and Tyr185 are shown together with Trp143 and Trp53 in orientations obtained with 5 molecules of ACh-bound (from Gao *et al.* 2004)

	Loop	D		A	E				B		F	C			
	No.	53	55	89	104	106	112	114	143	145	164	185	187	188	192
AChBP		W	Q	Y	R	V	L	M	W	W	Y	Y	C	C	Y
α1 Torpedo		R	R	Y	L	D	M	T	W	Y	T	Y	C	C	Y
α1 Human		R	K	Y	L	Q	T	T	W	Y	N	Y	C	C	Y
α2 Human		W	K	Y	H	F	H	V	W	Y	D	Y	C	C	Y
α3 Human		W	K	Y	L	K	T	I	W	Y	D	Y	C	C	Y
α4 Human		W	K	Y	H	F	Q	T	W	Y	D	Y	C	C	Y
α6 Human		W	R	Y	L	K	T	T	W	Y	D	Y	C	C	Y
α7 Human		W	Q	Y	L	N	Q	L	W	Y	G	Y	C	C	Y
α8 Human		W	Q	Y	L	N	Q	I	W	H	N	Y	C	C	Y
α9 Human		W	R	Y	V	R	T	D	W	Y	D	Y	C	C	Y
α10 Human		W	R	Y	V	R	R	D	W	H	D	Y	C	C	Y
β1 Torpedo		F	N	M	L	Q	S	Q	Y	Y	A	S	D	P	Y
β1 Human		Y	D	L	V	S	R	Q	Y	Y	T	P	D	P	R
β2 Human		W	T	Y	V	S	F	L	W	Y	D	P	D	S	Y
β4 Human		W	K	Y	I	R	L	L	W	Y	D	P	D	P	Y
α5 Human		W	T	F	V	R	T	T	W	Y	D	D	C	C	Y
β3 Human		W	K	F	I	K	V	T	W	Y	D	D	V	Y	Y
γ Torpedo		W	E	E	L	Y	Y	L	Q	Y	D	W	L	T	F
γ Human		W	E	E	L	S	Y	L	Q	Y	A	P	A	P	H
δ Torpedo		W	D	Q	L	R	T	L	L	Y	A	P	K	F	Y
δ Human		W	E	E	L	Y	Y	L	L	Y	G	P	A	P	R
ε Human		W	G	E	L	Y	T	L	Q	Y	A	H	G	A	E

Table 1.1: Alignment of muscle and neuronal nAChR amino acid sequence with the residues of the AChBP model of the ACh binding site. Note the conservation of residues in the binding loops of nicotinic subunits and the AChBP.

1.6 The channel gate

Although it is widely accepted that the channel gate is in the pore-lining TM2 domain, there still remains debate over its exact nature and location. There are two hypotheses for the location of the channel gate.

Sequentially mutating the residues of the TM2 domain of α1 to cysteine provides the main evidence for the first hypothesis, first advanced by Arthur Karlin and co-workers. Methanethiosulfonate-ethylammonium (MTSEA) can covalently react with the inserted cysteine residue and block the channel. This is only possible when MTSEA can reach the cysteine residue. When the channel is open, it allows access to MTSEA to the whole of TM2. When the receptor is not activated, the channel is closed and allows MTSEA access only as far as the channel gate. Comparing the extent and rate of block in each case for a series of cysteine mutants gives an indication of the location of the channel gate. This work suggested that the location of the channel gate is near the intracellular end of the channel, at least as close as the 3rd residue downstream from the NH_2-terminal end of TM2 (Leu 3') (Akabas *et al.* 1994).

In contrast, the majority of the rest of the data indicates a more extracellular location of the channel gate. There is a hydrophobic amino acid residue at the 9′ position in many LGICs and in the majority of nAChRs subunits and for glycine, $GABA_A$, 5-HT_3 and the invertebrate glutamate-gated chloride channels (GluCl) this 9′ residue is a leucine (Labarca *et al.* 1995) (see Figure 1.7). Mutations of this residue to make it become more hydrophilic decrease the EC_{50} value of the receptors, a phenomenon we make liberal use of in this thesis. These mutations do not affect the receptor binding site, as is shown by the unchanged K_d value of d-tubocurarine in mutated muscle nAChRs (Filatov & White,

1995) suggesting an effect on gating. Single channel data from α7 homomeric receptors mutated this way show that although the mutation does not affect the main conductance state, it does introduce a higher-conducting second state, results which were interpreted as the mutation disrupting the desensitised state of the receptor to make it conducting (Revah *et al.* 1991). The most likely explanation of this is that the 9' residues constitute the channel gate. Data from homomeric ρ1 GABA also support the view that 9' mutations affect gating, mutating the 9'Leu here results in spontaneous, non-liganded openings, indicated by an increase in holding current in the absence of agonists (Chang & Weiss, 1998). These spontaneous openings are sensitive to picrotoxin at much higher concentrations than the wild-type.

Note that if only one out of the five 9' leucines is mutated to threonine (i.e. in the γ subunit of muscle nAChR) only a reduction in EC_{50} is observed with no additional conductance state (Filatov & White 1995).

Some of the discrepancies may be explained by electron microscopy of the muscle nAChRs which showed the closed channel being occluded near the midpoint of the channel around the 9′ residues (Figure 1.7A) by bends in the α helices thus forming the channel gate (Unwin, 1998). Higher resolution imaging however showed that the leucines were too far apart to fully occlude the pore but rather they left a hole of around 3.5Å in diameter in the centre, large enough to allow the passage of hydrated Na^+ and K^+ ions (Unwin, 2000). Therefore to prevent the movement of ions through the pore Unwin proposed that the channel is "closed" by a hydrophobic "girdle", spanning between the 9′ residue and the conserved 13′ residue, rather than a single "gate". This girdle located a turn of the α helix above the 9' would stop ion permeation by preventing the partial

stripping of the hydration shell from Na^+ and K^+ and so preventing them "squeezing" through the "hole" in the gate (Unwin, 2005) (see Figure 1.8).

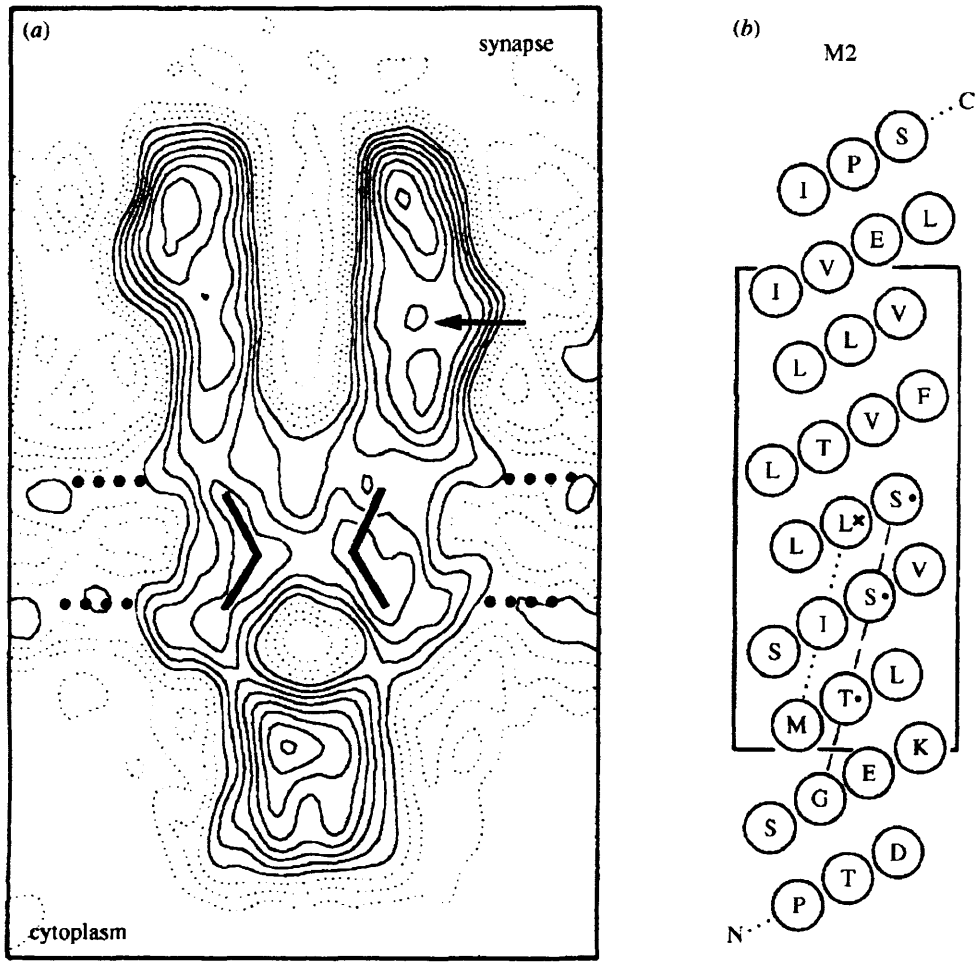

Figure 1.7: Interpretation of the closed-channel gate at 9 Å. (from Unwin, 2000)
(a) Channel in profile showing the positions of the pore-lining M2-rods (black lines), the ACh-binding pocket (arrow) and the estimated limits of the lipid bilayer (dotted lines).
(b) Helical net plot of the amino-acid sequences around the segment M2 of the Torpedo α-subunit. Highlighted are the conserved leucine residue thought to form the gate (cross) and other residues (dots) shown to affect the binding affinity of open channel blockers and ion flow through the open pore.

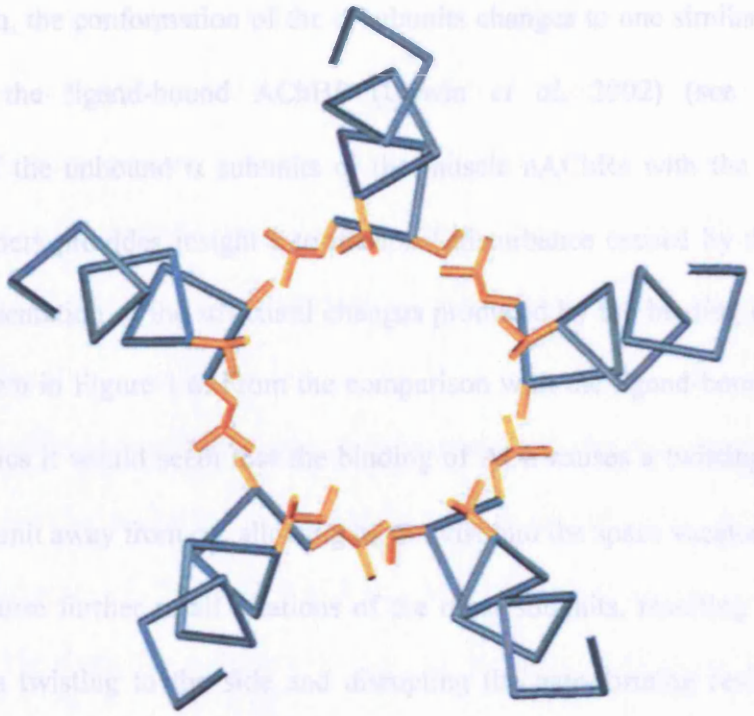

Figure 1.8: Higher resolution maps suggest that the gate is made up of a hydrophobic girdle (yellow) created by leucine and valine side-chains (from Unwin 2000).

1.7 The open pore

The binding of ACh induces changes in the structure of the receptor which results in the opening of the channel and thus allows the permeation of ions through the pore. Analysis of the structure of *Torpedo* nAChRs suggests that the extracellular domains of the subunits of the muscle nAChRs can exist in two conformations (Unwin, 2005). In the closed channel one conformation is characteristic of the two α subunits, the other characteristic of the three non-α subunits. On an axis normal to the membrane plane, the inner sheets of the β-sandwich of the α subunits binding domain are rotated 10° relative to the non-α subunits. Several interactions between different subunits have been identified that may stabilise this "special" conformation of the α subunits. On the

binding of ACh, the conformation of the α subunits changes to one similar to the non-α subunits and the ligand-bound AChBP (Unwin *et al.* 2002) (see Figure 1.9.). Comparison of the unbound α subunits of the muscle nAChRs with the ligand-bound AChBP protomers provides insight into the local disturbance caused by the binding of ACh. A representation of the structural changes produced by the binding of ACh to the AChBP is shown in Figure 1.6. From the comparison with the ligand-bound AChBP, in muscle nicotinics it would seem that the binding of ACh causes a twisting of α_γ which pulls the β subunit away from α_δ, allowing α_δ to twist into the space vacated by β. These disturbances cause further small rotations of the other subunits, resulting in the kinked TM2 α helices twisting to the side and disrupting the gate-forming residues (Unwin, 1998). This has a two-fold effect. First, the twisting of the α helices transiently increases the pore diameter allowing ion permeation. Secondly, it exposes the polar side chains of threonine and serine residues found at 2′ which are thought to constitute the channel selectivity filter (see Figure 1.10). It is these residues which are thought to render the channel permeable to only Na^+, K^+ and to a lesser extent Ca^{2+} under normal physiological conditions.

Site directed mutagenesis of the TM2 of *Torpedo* nAChRs has indicated that four hydrophilic residues in and close to the TM2 domain of each subunit face the pore. The residues at three of these positions (-4', -1' and 20') are charged and are the main determinants of the single channel conductance of these receptors expressed in oocytes (Imoto *et al.* 1988; 1991). These residues are present in each subunit and as such create hydrophilic rings at the –4', -1', 2' and 20' positions of the TM2 which, when the channel is closed, act to prevent movement of ions through the pore. They are named the

cytoplasmic ring (-4'); the intermediate ring (-1'), central ring (2') and the outer ring (20'). The cytoplasmic, intermediate and outer rings have a net negative charge due to the side chains of the residues present, whereas the central ring is hydrophilic and uncharged. The net charges and hydrophilic nature of these rings is conserved throughout most of the nicotinic subunits. The net effect of these negative charges is to make the nAChRs cation-conducting.

Reducing the net negative charge on the cytoplasmic, intermediate or outer 'rings' by inserting a positively charged or neutral residue results in a decrease in the single channel conductance of *Torpedo* nAChRs, with the conductance decrease being proportional to the change in net charge in the ring, independent of which subunit carries the mutation (Imoto *et al.* 1988). The greatest decrease in conductance was observed when the mutation was inserted into the outer ring. With the appropriate set of mutations the channel can even be made anion conducting! (Galzi *et al.* 1992).

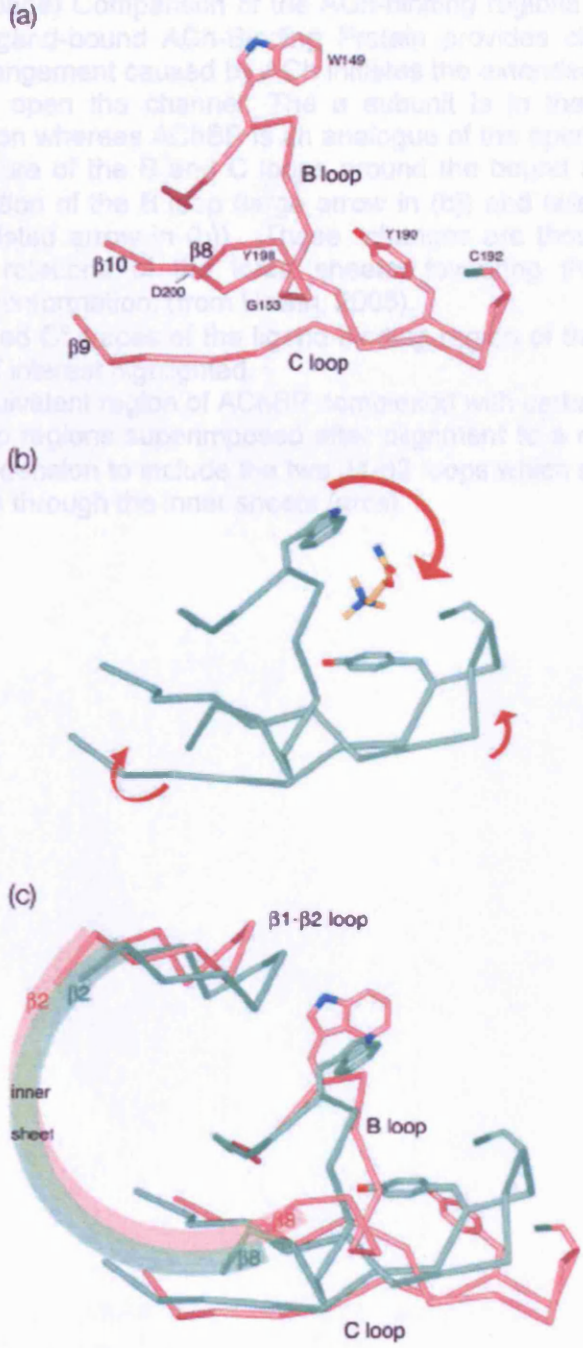
(a)
W149
B loop
β10
β8
Y198
Y190
C192
D200
G153
β9
C loop
(b)
(c)
β1-β2 loop
β2
β2
inner
sheet
B loop
β8
β8
C loop

Figure 1.9: (previous page) Comparison of the ACh-binding regions in the α-subunit with the ligand-bound ACh-Binding Protein provides clues to how the local rearrangement caused by ACh initiates the extended conformational change to open the channel. The a subunit is in the closed-channel conformation whereas AChBP is an analogue of the open or desensitised state. Closure of the B and C loops around the bound agonist changes the orientation of the B loop (large arrow in (b)) and twist of the β9-β10-hairpin (twisted arrow in (b)). These changes are thought to drive the clockwise rotations of the inner sheets, favouring the open-channel extended conformation. (from Unwin, 2005).
(a) Simplified C^{α} traces of the ligand-binding region of the α-subunit with residues of interest highlighted.
(b) The equivalent region of AChBP complexed with carbamylcholine.
(c) The two regions superimposed after alignment to a common rotation axis and extension to include the two β1-β2 loops which are connected to the B loops through the inner sheets (arcs).

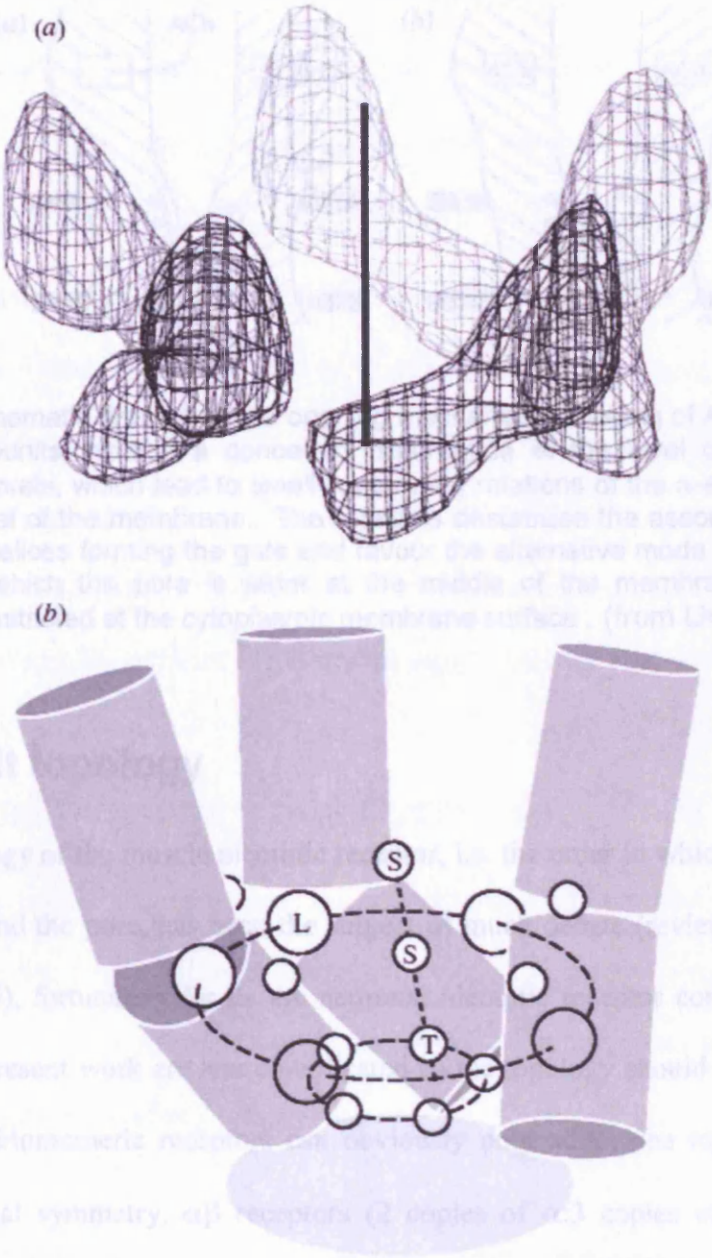

Figure 1.10: Transient configuration of M2 rods around the open pore and interpretation at 9 Å. (from Unwin, 1995)
(a) A barrel of a-helical segments, having a pronounced twist, forms in the cytoplasmic leaflet of the bilayer, constricting the pore maximally at the cytoplasmic membrane surface. The bend in the rods.(as shown in Fig.1.7A) are no longer pointing inwards but have rotated to the side.
(b) Schematic representation of the most distant three rods with a tentative alignment of the amino-acids with the densities suggesting that a line of polar residues (serines and threonines) should be facing the inner pore.

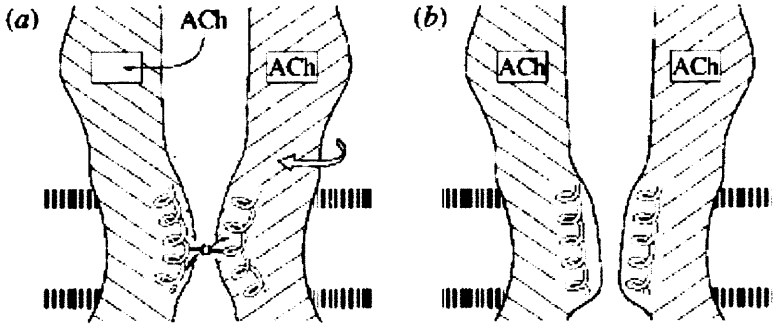

Figure 1.11: Schematic drawing of the opening mechanism. Binding of ACh to both α-subunits initiates a concerted disturbance at the level of the binding pockets, which lead to small (clockwise) rotations of the α-subunits at the level of the membrane. The rotations destabilise the association of bent a-helices forming the gate and favour the alternative mode of association in ehich the pore is wider at the middle of the membrane and most constricted at the cytoplasmic membrane surface . (from Unwin, 2000).

1.8 Subunit topology

The topology of the muscle nicotinic receptor, i.e. the order in which the subunits are arranged around the pore, has been the subject of much debate (reviewed by Karlin and Akabas, 1995), fortunately for us the neuronal nicotinic receptor combinations we deal with in the present work are less complicated so the topology should be reasonably straightforward. Homomeric receptors can obviously only adopt one topology while, assuming rotational symmetry, αβ receptors (2 copies of α:3 copies of β) can only produce two different topologies with the α subunits either together or separated by a single β (and *vice versa* for the putative 3:2 form), of which the second topology is most likely given what we know of the topology of the muscle nicotinic. It is only when a third subunit (such as β3) is introduced that multiple different topologies become possible. Our work on the incorporation of β3 into the α3β4 receptor showed the β3 had

minimal effect on the pharmacology of competitive antagonists. This suggests that either the sequence in the binding domain of β3 is too similar to that of β4 to cause a change or that β3 does not participate in the binding site. If the second hypothesis holds, β3 becomes analagous to the non-binding site subunit in the muscle nicotinic, the β1, in which case a clockwise topology of α3β4α3β3β4 becomes most likely. This is however not certain and it is not clear whether this would hold for the other types of triplet receptor such as α5-containing and the other putative β3 receptors. It had been hoped that the use of concatenated subunits would help us resolve these questions for both muscle and nicotinic nAChRs. Problems with the concatamer technique, at least in its tandem+monomer form, have meant that this hope hasn't materialised (see below).

1.9 Neuronal nicotinic acetylcholine receptors

Whilst the muscle nicotinic receptors are very well characterised, the nAChRs found throughout the peripheral and central nervous system, the neuronal nicotinic acetylcholine receptors, are much less well-understood. It is this class of receptor the majority of my research would be focussed on.

1.9.1 Comparison of the muscle and neuronal nicotinic receptors

The differences between the muscle and neuronal nicotinic receptors have been known for over 50 years since the work of Paton and Zaimis (Paton & Zaimis 1949, 1951) described the specific effects of decamethonium and hexamethonium in blocking nicotinic activity on neuromuscular and ganglion nAChRs respectively.

Both receptors are known to be cation-conducting, pentameric ligand-gated ion channels, found on post-synaptic membranes and are activated by two molecules of acetylcholine or nicotine. Also, like muscle nicotinics, functional neuronal nicotinics require at least two α subunits (not α5) to be present because the α subunits provide an essential part of the ACh-binding site. There is also a lot of common features in the structure and function of the two types of receptor such as the TM2 domain and it is likely the residues which are of importance in the muscle receptor will also be of importance in the neuronal, so the study of the structure of the muscle receptor and the ACh-Binding Protein will also be of interest to those studying neuronal receptors.

The human α1 (muscle) and α3 (neuronal) subunits share a 51% amino acid sequence identity showing a common evolutionary ancestor but when compared with the 76% identity between Torpedo and human α1 subunits it is clear the neuronal and muscle subunits diverged a long time ago (Le Novere & Changeux, 1995). One of the most obvious differences between the two types of nAChRs is the sheer number of neuronal nicotinic subunits. We do not know whether this diversity has an adaptive value, especially since pharmacological and biophysical characterisation of native receptor types only shows relatively few classes (α7, α6*, α4β2* and α3β4*). As noted above, work on the ε and γ subunits of muscle nicotinic has shown a developmental switch in which these subunits are involved and that this switch gives different properties to the resulting adult and embryonic receptors. Separate but related genes on different chromosomes code for the 12 neuronal nicotinic subunits (α2, α3, α4, α5, α6, α7, α8, α9, α10, β2, β3 & β4) and so provide for a potentially vast number of different receptor combinations although the likelihood is that most would not be functional. Even taking

only the most basic homomeric, pair and triplet combinations which are known to form receptors (even if not always particularly functional ones) in heterologous expression systems, around 20 different types of nAChRs combinations are known. Nevertheless work on native receptors suggests that nAChRs made up by at least four different subunits do form and this would increase the number of possible receptor combinations many times (Forsayeth & Kobrin, 1997; Conroy & Berg, 1998). Clearly, it is important to determine which nAChR combinations are functional, in what ratios subunits participate and how incorporation of each subunit affects the receptors characteristics.

1.9.2 Localisation of the neuronal nicotinic receptors

Neuronal nAChRs are found in both the sympathetic and parasympathetic divisions of the ANS and in a number of regions of the CNS. nAChRs are also found in other non-neuronal tissues such as striated muscle, epithelia, lymphocytes, granulocytes, skin and bone (for a review see Gotti *et al.* 1997). The physiological role, if any, of the nAChRs in these non-neuronal tissues is unclear. Nevertheless, these receptors may be activated pharmacologically in smokers. One disturbing possibility, for instance, is that the nAChRs present in the lung may play a role in the proliferation of cancers in smokers (both active and passive) and may even suppress the activity of anti-cancer drugs such as the retinoids (Schuller *et al.* 2000; Chen *et al.* 2002).

1.9.3 Function of the neuronal nicotinic receptors

In the ANS, ACh acts on nAChRs as a classical fast excitatory neurotransmitter in a manner very similar to that at the NMJ and as such governs fast synaptic

transmission between preganglionic and postganglionic neurones in both the sympathetic and parasympathetic systems.

In comparison to the ANS, such examples of cholinergic neurotransmission utilising nAChRs in the CNS are fairly rare and so neuronal nAChRs are thought to have a predominately modulatory, presynaptic role. While CNS neuronal nAChRs are found in both presynaptic and postsynaptic membranes (McGehee *et al.* 1995; Coggan *et al.* 1997), their physiological role is not yet known. It is not even known whether presynaptic nAChRs can actually be activated by synaptically released ACh. In contrast, exogenous application of nicotinic agonists (including nicotine self-administration by smokers) is known to produce widespread effects on the CNS.

The activation of presynaptic neuronal nAChRs may occur at the presynaptic terminal and also the preterminal level. The activation of these nAChRs by nicotinic agonists may enhance the release of a variety of neurotransmitters. Evidence of this has been shown using *in vivo* microdialysis where systemically administered nicotine was seen to increase the release of dopamine from ascending dopaminergic pathways, predominantly in the cell-body areas (Wonnacott, 1997) and, more recently, endogenous cholinergic activity has been shown to regulate dopamine release in the striatum (Zhou *et al.* 2001).

At the postsynaptic level, nicotinic agonists can depolarise neurones in several brain areas though whether all the nAChRs expressed in the CNS (both pre- and postsynaptic) are ever activated by synaptically released ACh remains an unanswered question. Currently hard evidence for the involvement of postsynaptic neuronal nAChRs in fast synaptic transmission in the CNS exists for only a few synapses, namely in the

spinal cord, between recurrent axons from spinal motoneurons and Renshaw cells (Eccles *et al.* 1954), in the retina (Feller *et al.* 1996) and in the ferret visual cortex (see Roerig *et al.* 1997; reviewed Sivilotti *et al.* 2000). More recently, synaptic transmission at nAChRs in rat hippocampal organotypic cultures and slices has also been reported (Hefft *et al.* 1999). Nevertheless, it appears that nicotinic synapses contribute little of the excitatory drive to the postsynaptic cell that receives them. However it may be that neuronal nAChRs, specifically those containing the α7 subunit, are involved in development in the CNS. However, the data is limited and any role is still controversial (reviewed by Role & Berg, 1996).

Irrespective of the physiological function of nAChRs, and of their role in smoking and its effects on such complex behaviours as addiction, learning and memory, it has also been noted that the localisation, number and function of neuronal nicotinics can be affected in a number of diseases of the CNS. The most noted of these is the marked decrease in numbers of nAChRs present in patients suffering from Alzheimer's disease but the neuronal nicotinics are also thought to play a role in the progression and/or pathophysiology of Parkinson's, schizophrenia, Tourette's syndrome, epilepsy and lung tumour development (for reviews see Gotti *et al.* 1997 and Lindstrom, 1997). Anecdotal evidence indicates a strong correlation between schizophrenia and smoking addiction with 70% of schizophrenic individuals being found to smoke currently, 54% of which were classified as heavy smokers compared to around 35% and 11%, respectively, for non-schizophrenics (McCreadie *et al.* 2003). It has been argued that this could be self-medication for schizophrenics who claim tobacco helps ameliorate their symptoms although these observations could be just as easily be interpreted as schizophrenics being

more susceptible to addiction or tobacco-smoking being a causal factor in schizophrenia, some reports have even indicated that nicotine addiction may actually be a side-effect of anti-psychotic medication (see de Haan *et al.* 2005 for an example). Additionally, the α7 subunit gene contained in the chromosome 15 loci has also been indirectly linked to a neurological deficit in schizophrenia (De Luca *et al.* 2004). The neurochemical changes underlying schizophrenia remain a poorly understood field with even the cherished dopamine hypothesis under fire so it isn't surprising that the exact role of the cholinergic system remains unclear. Smoking has also been claimed to be neuroprotective in Alzheimer's, although the use of pharmacological therapies aimed at the cholinergic system has only met with limited success so far (van Duijn *et al.* 1994, although see Almeida *et al.* 2002 for evidence of smoking being a risk factor in Alzheimer's).

There is however at least one disease state where the role of neuronal nicotinics can not be disputed. A rare form of inherited epilepsy, autosomal dominant nocturnal frontal lobe epilepsy (ADFNLE) is known to be due to mutations in either the nicotinic α4 or β2 subunit (Steinlein *et al.* 1995, 1997, for review see Combi *et al.* 2004). Six mutations have been identified so far, four in the α4 and two in the β2. The four α4 mutations are made up of three missense mutations (S252F, S256L and T265I) and an insertion of a leucine at position 263. The two β2 mutations both affect the same conserved valine residue at position 287 with it being replaced by either a leucine or a methionine (Combi *et al.* 2004). Not all affected families carry these mutations which only account for 12% of ADFNLE cases, suggesting that this disease is genetically heterogenous and is more likely to be a collection of closely related disorders rather than a singular disease. Other specific forms of idiopathic generalised epilepsy have been

linked to the region of the human genome containing the β3 subunit, indicating a functional role for β3 in the CNS which was surprising considering the supposedly "orphan" status of β3 at the time (Durner *et al.* 1999).

Knock-out studies have now been carried out to try and shed light on the role of the cholinergic system, for instance the use of gene targeting in mouse embryonic stem cells has highlighted interesting features. Mesencephalic dopamine-containing neurons in β2 knock-out mice have been shown to have lost the normal response to nicotine. Behaviourally the mice do not show intravenous nicotine self-administration unlike their wild-type counterparts (Picciotto *et al.* 1998). Both α4 and β2 knock-out mice also show a marked reduction in nicotine-elicited antinociception, incidentally providing further evidence that α4β2* receptors are likely to be a major neuronal nAChR subtype (Marubio *et al.* 1999). When α3 or both β2 and β4 are knocked-out the mice are seen to survive until birth but display impaired growth and increased perinatal mortality, effects thought to be due to the impairment in function of autonomic ganglia where α3β4* receptors are predominately expressed (Xu *et al.* 1999). Evidence of this was seen in the bladders of the survivors where impaired autonomic activity resulted in a hypertrophied mucosa and an increased tendency towards urinary infections and stones.

α7 and α9 knock out mice surprisingly displayed no obvious phenotype (Urtreger *et al.* 1997; Vetter *et al.* 1999). As α9 was only thought to be present in cochlear hair cells (Elgoyhen *et al.* 1994) the development and function of cochlear efferent neurones were studied in these α9 knock-out mice. The majority of outer hair cells in these knock-out mice were found to be innervated by only a single large terminal rather than the

multiple smaller terminals seen in wild-type animals, which may indicate a role for α9 in the maturation of synaptic connections.

Knock-in studies have also been carried out, with the insertion of gain-of-function mutations. Mice homozygous for the $\alpha7^{L250T}$ mutation display a marked decline in α7 protein levels in the brain with extensive apoptosis of neurones throughout the somatosensory cortex particularly in layers 5 and 6. Such mice die within 24 hours of birth. In comparison, mice heterozygous for this mutation display only a 25-30% reduction in α7 protein levels and are otherwise viable, anatomically normal with wild-type-like levels of apoptosis in the brain (Orr-Urtreger *et al.* 2000). Analysis of cultured hippocampal neurones from the heterozygous mice however did reveal an abnormal α7-like current with a slower desensitising component and a greater sensitivity to low concentrations of nicotine as would be expected from the incorporation of the $\alpha7^{L250T}$ mutation. Another gain-of-function mutation, a leucine to alanine 9′ point-mutation in mice α4 subunits has highlighted the importance of α4* receptors in nicotine-induced reward, tolerance and sensitisation (Tapper *et al.* 2004).

Of particular interest to our group has been the work on β3 knock-out mice. The initial work showed that these mice had increased locomotor activity which was thought to be due to alterations in the nicotine-induced dopamine release in the striatum and/or other areas of the CNS where β3-containing receptors are present in the pre-synapse (Cordero-Erausquin *et al.* 2000). Null-mutation mice also showed enhanced nicotine-stimulated dopamine release from striatal synaptosomes, increased activity in the open-field arena (Cui *et al.* 2003) and reduced anxiety in the elevated plus maze (Booker *et al.* 2000). Preliminary results have also shown that mice lacking the β3 subunit showed

much higher tyrosine hydroxylase activity (Butt *et al.* Society for Neuroscience Conference 2004). These effects of β3 knock-out may tie in with the observed induced decrease in nAChR activity produced by β3 insertion in the majority of nAChR subtypes as reported in Chapter 6.

1.9.4 Diversity of the neuronal nicotinic receptor

One of the main causes of the difficulty in characterising the neuronal nicotinic receptors compared to the muscle is the greater number of neuronal nAChR subunits which have been identified. Currently nine α subunits (α2 through to α10) and three β subunits (β2 to β4) are known and whereas the composition of muscle nAChRs is consistent, there are a variety of ways functional neuronal nAChRs can form. Theoretically thousands of different subunit combinations are possible. However, thankfully, work with heterologous expression systems has suggested that there are a number of restrictions on which subunit combinations can form a functional receptor. "Traditionally" two basic types of combinations of subunit were thought to form functional neuronal nAChRs. α7, α8 and α9 can form functional homomeric receptors i.e. they are capable of forming a LGIC using five copies of themselves. These channels are sensitive to α-bungarotoxin. whereas α2, α3, α4 and α6 can only form a functional receptor when expressed together with β2 or β4 subunits to give the so called "pair" receptor (Luetje & Patrick, 1991; Fucile *et al.* 1998). This simple separation of receptors into homomeric and heteromeric is now known to be flawed with evidence existing for both α9α10 and α7β3 pair receptors (Sgard *et al.* 2002; Palma *et al.* 1999).

However these compositions are only minimal requirements and don't necessarily mean that *in vivo* only these homomeric and pair combinations are present. Neuronal cells express multiple nicotinic subunits including the so-called "orphan" receptor subunits, α5 and β3, which remain well conserved in a wide variety of species. It would seem uncharacteristically wasteful for cells to retain and produce such proteins if they had no function. We now know that α5 and β3 can only be assembled into functional receptors when co-expressed with another *two* different subunits, for instance as α4β2α5 or α3β4β3 receptors (referred to as 'triplet' receptors).

It is worth noting that it is official IUPHAR nomenclature to qualify the composition of a nAChR as –say- *α3β4** where the asterix indicates that there may be other subunits involved. Such caution has proven to be well-founded with the discoveries that *α10* can form a "pair" receptor with *α9* (Elgoyen *et al.* 2001) and that the main nAChR in chick parasympathetic ciliary ganglia is made up of three or four different subunits (*α3β4α5* and *α3β2β4α5*) (Vernallis *et al.* 1993; Conroy & Berg, 1995); the receptor composition is even more complex in chick sympathetic ganglia (Listerud *et al.* 1991; Yu & Role, 1998). *α5* subunits have been shown to form "triplet" receptors with other combinations and the incorporation of an *α5* subunit has also been shown to lead to significant changes to the properties of the receptor such as single channel conductance and desensitisation properties (Ramirez-Latorre *et al.* 1996; Sivilotti *et al.* 1997; Gerzanich *et al.* 1998; Nelson & Lindstrom, 1999). Recently the last "orphan" subunit *β3* has also been shown to be incorporated into "triplet" receptors (Groot-Kormelink *et al.* 1998). Because of the similarity between *α5* and *β3* both in amino acid sequence, evolution, incorporation into receptors and putatively in role, there are calls to reclassify

$\alpha 5$ and $\beta 3$ into a third non-α, non-β group of nAChR subunits (Le Novere & Changeux, 1995). The incorporation of β3 into an α3β4β3 triplet receptor was only shown by the use of a reporter mutation approach (Groot-Kormelink *et al.* 1998) while more extensive work only highlighted subtle effects caused by the β3 insertion into the α3β4 nAChRs (Boorman *et al.* 2003). The examination of the effect of β3 insertion into other nAChR combinations, varying the stoichiometry of pair receptors and the development and evaluation of tools to restrict and report LGIC receptor stoichiometry would form the bulk of the work covered in this thesis.

1.9.5 Stoichiometry of neuronal nicotinic receptors

The different stoichiometries of neuronal nAChRs are summarised in Figure 1.12.

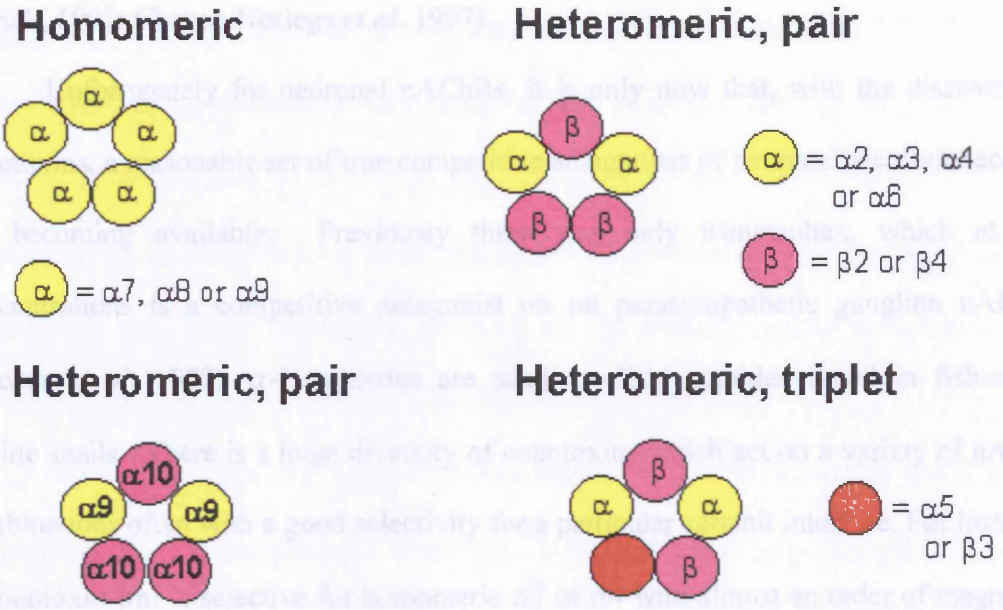

Figure 1.12: Different stoichiometries of neuronal nAChRs

In the previous section we have discussed the homomeric or heteromeric composition of nAChRs. Among heteromers, 'pair' receptors are pentamers with an α:β stoichiometry originally thought to be 2:3, as shown by radiolabelling and single channel studies on chick α4β2 receptors expressed in oocytes and from our own reporter mutation work (Anand *et al.* 1991; Cooper *et al.* 1991; Boorman *et al.* 2000) but as covered in Chapter 9 this sort of receptor may also exist in a 3:2 ratio.

1.9.6 Characterising neuronal nicotinic acetylcholine receptors

The pharmacology of neuronal nAChRs was also recognised to depend on their subunit composition, which allowed neuronal nAChRs to be characterised to some extent

by their sensitivity to different agonists and antagonists (see for example Luetje & Patrick, 1991; Chavez-Noriega *et al.* 1997).

Unfortunately for neuronal nAChRs, it is only now that, with the discovery of conotoxins, a reasonable set of true competitive antagonists of neuronal nicotinic receptor are becoming available. Previously there was only trimetaphan, which at low concentrations is a competitive antagonist on rat parasympathetic ganglion nAChRs (Ascher *et al.* 1979). α-Conotoxins are small cyclical peptides found in fish-eating marine snails. There is a huge diversity of conotoxins which act on a variety of nAChR combinations often with a good selectivity for a particular subunit interface. For instance, α-conotoxin-ImI is selective for homomeric α7 or α9 with almost an order of magnitude difference in affinity compared to 'pair' neuronal nAChRs expressed in *Xenopus* oocytes (Johnson *et al.* 1995) and acts competitively at α-bungarotoxin sensitive (i.e. α7-containing) neuronal nAChRs in rat hippocampal neurons (Pereira *et al.* 1996). In contrast the α-conotoxin AuIB is selective for α3β4 over other 'pair' neuronal nAChRs expressed in *Xenopus* oocytes, although it has not been shown to act competitively (Luo *et al.* 1998). Of most interest to us are the α-conotoxin MII, which may be selective for β3-dependant receptors and the α-conotoxin PIA, which is selective for α6/α3β2β3 nAChRs (McIntosh *et al.* 2000; Dowell *et al.* 2003). This continuing research on conotoxins offers the tantalising prospect of soon having a large library of truly subtype selective antagonists. Other compounds which are known to show a degree of selectivity between nAChRs combinations include methyllycaconitine (MLA) which has been shown to act competitively on α7 homomeric receptors expressed in *Xenopus* oocytes, demonstrating around a million-fold affinity for α7 over 'pair' receptors (Palma *et al.*

1996). It has also been shown that strychnine acts competitively on α-bungarotoxin sensitive neuronal nAChRs and (at very high concentrations) as an open channel blocker on α-bungarotoxin insensitive neuronal nAChRs (mostly α4β2) in rat hippocampal neurones (Matsubayashi *et al.* 1998). Finally Dihydro-beta-Erythroidine (DHβE) has been shown to act competitively on α7 and α4β2 expressed in *Xenopus* oocytes (Bertrand *et al.* 1992) and to be reasonably selective for the latter. These compounds have provided useful tools for the study of nAChR combinations.

The nature of the β subunit is also known to have an affect on the sensitivity of neuronal nAChRs to antagonists (Cachelin & Rust, 1995). This paper reported that α3β4 receptors are markedly more sensitive to block by mecamylamine, pentolinium, hexamethonium and trimetaphan than α3β2. However, the rank order of antagonist potency was found to be unchanged by the different β subunits.

The expression of the human nAChRs in *Xenopus* oocytes has allowed their characterisation with the nicotinic antagonists, DHβE, d-tubocurarine (d-Tubo) and mecamylamine (Meca) and the nicotinic agonists, acetylcholine, nicotine, cytosine and 1,1-dimethyl-4-phenylpiperazinium (Chavez-Noriega *et al.* 1997). This demonstrated that the each subunit composition (with both the α and β subunits being of importance) produced an unique selectivity profile. For some agonists a lower n_H was observed for β2-containing receptors compared to β4-containing nAChRs. Of the antagonists, DHβE and d-Tubo act reversibly on αβ pair and α7 homomers, whereas Meca produces an incomplete reversible block. The α4β4 was found to be more sensitive to Meca than α4β2, while Meca was equally potent at α2β2, α4β2 and α7. These three receptor subtypes could be differentiated by their different sensitivities to DHβE and d-tubo with

α2β2 being equally sensitive, α4β2 being more sensitive to DHβE than d-tubo and α7 being more sensitive to d-tubo than DHβE (Chavez-Noriega *et al.* 1997). Neuronal bungarotoxin (NBT) has been reported to potently block α3β2 receptors, but has no affect on α2β2 responses to ACh when expressed in *Xenopus* oocytes (Luetje *et al.* 1993). To further examine this, chimeras of α2 and α3 were created and showed that it was the first 181 amino acid residues in the ligand-binding N-terminal domain that were important for the NBT sensitivity of α3β2 receptors. Replacing the first 195 amino acid residues of α3 with the corresponding residues of α2 was found to abolish the block by 100 nM NBT on the resulting $\alpha3^{195\alpha2}\beta2$ receptor (Luetje *et al.* 1993). However, it was also found that to achieve block by 100 nM NBT on α2β2 receptors, the first 215 amino acid residues in the ligand-binding N-terminal domain had to be replaced with the corresponding residues of α3, producing an $\alpha2^{215\alpha3}\beta2$ receptor.

Similarly, Harvey and Luetje reported that NBT and DHβE are more potent at blocking α3β2 than α3β4 when expressed in *Xenopus* oocytes (Harvey & Luetje, 1996). Chimeras of β2 and β4 were use to show that, in the ligand-binding N-terminal domain, it is the first 133 amino acid residues that play an important role in DHβE and neuronal bungarotoxin (NBT) sensitivity of α3β2 and α3β4 receptors (Papke *et al.* 1993; Wheeler *et al.* 1993; Harvey & Luetje, 1996). Replacing these residues of the β2 with the corresponding residues of β4 produced DHβE and NBT potencies equal to α3β4 receptors in the resulting $\alpha3\beta2^{133\beta4}$ receptor (Harvey & Luetje, 1996). These findings show that the potencies of both DHβE and NBT on 'pair' receptors are determined by the nature of both the α and the β subunits.

1.10 The β3 subunit

The β3 subunit was first cloned and identified as a neuronal nAChR subunit from rat brain (diencephalon) cDNA libraries in 1989 (Deneris *et al.* 1989). It was named β3 as it lacked the adjacent cysteine residues 192 and 193, in common with all neuronal β subunits. Initial *in situ* hybridisation probes revealed that β3 was expressed along with α2-α4 and β2 in the rat medial habenula (ventromedial part), substantia nigra *pars compacta*, ventral tegmental area (Le Novere *et al.* 1996; Charpantier *et al.* 1998) and in the reticular nucleus of the thalamus and the mesencephalic nucleus of the trigeminal (Liu *et al.* 1998). Expression of β3 was also reported in the rat locus coeruleus (Le Novere *et al.* 1996). RT-PCR analysis by Anderson showed that β3 is co-expressed with in α2-α7, β2 and β4 in the Scarpa's ganglia and with α3, α5–α7, α9, β2 and β4 in vestibular end-organs of the rat, the organs responsible for transducing linear and angular linear acceleration of the head (Anderson *et al.* 1997). Immunoprecipitation studies have shown that β3 is expressed together with β4 in rat striatum, cerebellum and also faintly in the hippocampus (Forsayeth & Kobrin, 1997). RT-PCR data has also demonstrated the expression of β3 in the spiral ganglia of the rat cochlea (Morley *et al.* 1998). Northern blot analysis of RNA isolated from various regions of the chick CNS showed β3 expression in: retina, telencephalon, cerebellum and spinal cord (Hernandez *et al.* 1995). In the periphery, β3 mRNA was found to be expressed in developing trigeminal and dorsal root ganglia, with low levels detectable in superior cervical and sympathetic ganglia. Polymerase chain reaction (PCR) analysis of the cochlea of the mouse has

shown the co-expression of β3 with β2 and α2–α6 (Drescher *et al.* 1995). The co-localisation of α6 and β3 has become of particular interest as covered in Chapter 6. Analysis of the amino acids sequence of chick β3, found it to align most closely with the chick α5 subunit. α5 and β3 have similarities in amino acid sequence, including having both identical amino acids and conservative substitutions (68.2% amino acid sequence similarity in chick; Hernandez *et al.* 1995; 80% in human, Groot-Kormelink *et al.* 1998). These subunits were therefore classified in a separate group within the nAChR phylogenetic tree (Tsunoyama & Gojobori, 1998). The α5 and β3 shared another similarity in that both were initially considered "orphan" subunits for failing to appear to participate in functional "pair" receptors. For instance, Deneris *et al.* (1989) were unable to express functional β3 containing receptors with any of the known neuronal nAChR α subunits (α2–α4 at the time) leaving the β3 with no known function. Since then the α5 has been shown to participate in a functional "triplet" receptor (Ramirez-Latorre *et al.* 1996; Wang *et al.* 1996; Sivilotti *et al.* 1997).

All these findings presented a bit of a quandary. It was clear from the work covered above that the β3 was present and expressed in discrete parts of the brain yet (like the α5 before it) it didn't appear to participate in functional receptors, as expressed by heterologous expression systems such as the *Xenopus* oocyte. Tackling this problem to show, first, that the β3 could participate in forming a functional receptor and then elucidate what effect the incorporation of the β3 subunit has on these receptors has been one of the major areas of study for our group over the last seven years. In 1998 a reporter mutation approach showed that β3 can form a functional α3β4β3 'triplet' receptor when expressed with an α3β4 pair (Groot-Kormelink *et al.* 1998). More recently the

incorporation of β3 into a 'pair' α7β3 receptor has also been demonstrated by Palma *et al.* (1999). The work of Groot-Kormelink *et al.* 1998 was followed up by my group and formed the basis of this current study. Having shown that the β3 subunit could co-assemble with the α3 and β4 to form a functional receptor our group proceeded to show that the stoichiometry of the α3β4β3 receptor was 2:2:1 (Boorman *et al.* 2000) however, despite exhaustive work, we failed to show dramatic effects on the function of α3β4 receptors caused by the incorporation of the β3 subunit.

We knew the receptor was expressed *in vivo* in high concentrations in discrete nuclei, we knew that β3 knock-out studies showed effects on the behaviour of mice and we knew that functional receptors could be formed incorporating this subunit yet it appeared that this subunit had no significant effect on the function of nAChRs. Addressing this conundrum would be the main thrust of my PhD.

Chapter 2

Aims of the Project

The primary aim of my PhD was to research the β3 subunit of the neuronal nicotinic acetylcholine receptor. In particular I set out to determine if β3 co-assembles with neuronal nicotinic subunits other than α3β4 and if it did, with what stoichiometry and with what effect on the properties of these receptors

A secondary and complementary goal was to adapt, develop and evaluate techniques to aid in, primarily, the study of the β3 subunit but which would also be of further use in studying other ligand-gated (and even voltage-gated) ion channels beyond the nicotinic family. As such, dosing protocols, reporter mutations and concatemeric constructs.

A final objective was, time permitting, to use these above techniques to study other aspects of the neuronal nicotinic story and as such, variations in the stoichiometry of the α3β4 receptor were also examined.

The chapters which follow will cover the progress I made in accomplishing these aims.

CHAPTER 3

Materials & Methods

3.1 Materials

Acetylcholine chloride (ACh.), collagenase (Type 1A), glycine (Gly.) mineral oil (M-5904), sodium chloride (NaCl), potassium chloride (KCl), magnesium chloride ($MgCl_2$), calcium chloride ($CaCl_2$), sodium hydrogen carbonate ($NaHCO_3$), Tris buffer, tricaine, atropine sulphate, sodium hydroxide (NaOH), hydrochloric acid (HCl), trimetaphan camyslate, N-(2-Hydroxyethyl)piperazine-N`-(2-ethanesulphonic acid) (HEPES), 5-hydroxy-indole (5-HI), were from Sigma-Aldrich, Poole, Dorset, UK. Heat-inactivated horse serum (NHS), penicillin and streptomycin were from Gibco BRL, Paisley, UK. Ethanol was from Merck Ltd, Poole, Dorset, UK. Axoclamp 2B was from Axon Instruments, Foster City, CA, USA. The 0.22μM pore filters (Millex-GV) were from Millipore, Bedford, USA. The *Xenopus laevis* toads were from Blades Biological, Edenbridge, Kent, UK. Clark borosilicate glass GC150TF was from Harvard Apparatus Ltd, Kent, UK. The QuikChange^{TM} Site-Directed Mutagenesis Kit was from Stratagene, Amsterdam, NL. The SP6 Mmessage Mmachine kit was from Ambion (Europe) Ltd., Huntingdon, UK.

3.2 Construction of cRNA for oocyte expression

The preparation of the complementary ribonucleic acid (cRNA) was carried out by Uta Schneiders, Jenny Davie, Martina Theuer, Kasia Bera, Skevi Krashia and Dr. Paul Groot-Kormelink and so only a brief description of this protocol will be given here. Complementary deoxyribose nucleic acid (cDNA) for the human $\alpha 2$, $\alpha 3$, $\alpha 4$, $\alpha 6$, $\alpha 7$, $\beta 2$, $\beta 3$ and $\beta 4$ neuronal nicotinic subunits and the $\alpha 1$ glycine subunit (GenBank^{TM} accession numbers Y16281, Y08418, Y08421, Y16281, Y08420, Y08415, Y08417, Y08416 and NM 000171, respectively) containing only coding

sequences and an added Kozak consensus sequence (GCCACC) immediately upstream of the start codon (Groot-Kormelink & Luyten, 1997) were sub-cloned into the pSP64GL vector, which contains 5′- and 3′-untranslated *Xenopus* β-globin regions (Akopian *et al.*, 1996). The mutants in subunits were created using the QuikChange™ Site-Directed Mutagenesis Kit (Stratagene; mutagenesis primer used 5′-GTCGACAGAAAAGACTTCTTCGATAACGGAGAATGG-3′) and the full-length sequence was verified. All cDNA/pSP64GL plasmids were linearised immediately downstream of the 3′ untranslated β-globin sequence and cRNA was transcribed using the SP6 Mmessage Mmachine kit (Ambion (Europe) Ltd., Huntingdon, UK). cRNA quality and quantity were checked by gel-electrophoresis and comparison with RNA concentration and size markers. The cRNA was stored at –80°C and was kept on ice during injection.

Tandem constructs were created by first producing a linker DNA fragment (based on Im *et al.* 1995) by hybridisation of two complimentary olgionucleotides; 5′-GGCCGC**T**CAGCAACAGCAGCAACAGCAGCAAG-3′ and 5′-AATTCTTGCTGCTGTTGCTGCTGTTGCTG**A**GC-3′. The resulting double-stranded DNA linker contains a 5′-end NotI restriction site overhang (underlined) and a 3′-end Eco-RI restriction site overhang (underlined), separated by 25 nucleotides (the first nucleotide [bold] is inserted to bring the NotI site [8-cutter] back into the correct reading frame, whereas the next 24 nucleotides code for the eight glutamine amino acids). The constructs themselves were created by using three unique restriction sites; EcoRI (upstream of the start codon of all subunits and the 3′-end of the linker), NotI (downstream of the coding sequence of all subunits and the 5′-end of the linker), and AgeI (between the Myc and His epitope sequences of the in the pcDNA3.1/Myc-His version C vector). A three way ligation resulted in the following

tandem circular plasmid: * [**AgeI**...His-epitope...stop codon...pcDNA3.1/Myc-His C vector...EcoRI _ *subunit A* _**NotI**] * [**NotI** _ linker _ **EcoRI**] * [**EcoRI** _ *subunit B* _NotI...Myc-epitope...**AgeI**] * (where * represents the ligation sites and [ ] represents purified DNA fragments digested with the restriction sites indicated in bold). To remove the epitope tags (Myc- and His-) all tandems were subcloned in the corresponding pcDNA3.1 vector, using a unique restriction enzyme site in subunit B. For instance, cutting the tandem upstream of the start codon (of subunit A) and somewhere in subunit B and transferring this fragment in the same position of subunit B, previously cloned in the pcDNA3.1 vector. Finally, all the tandem constructs were also subcloned in the pSP64GL vector. The length of the extracellular linkage of the different tandem constructs differs depending on the extracellular region downstream of TM4 of the first subunit and the length of the signal peptide of the second subunit (see Table 7.2). The 9′ mutant tandems were created by swapping the corresponding DNA fragments (using unique enzyme restriction sites upstream and downstream of the L9′T mutation) from $\alpha3^{L279T}$ (for $\beta4\_\alpha3^{L279T}$) and $\beta4^{L272T}$ (for $\beta4^{L272T}\_\alpha3$). The $\alpha3\_\beta4$, $\beta4\_\alpha3$, $\beta4\_\alpha3^{L279T}$, and $\beta4^{L272T}\_\alpha3$ tandem constructs cloned in the pSP64GL vector were sequenced fully to check for PCR and/or cloning artifacts. All other tandem constructs were sequenced only at the outer ends to check for cloning artifacts (Groot-Kormelink *et al.* 2004).

Pentameric constructs were produced from intermediate tandem and trimer constructs. The tandem constructs were created as described above. Trimer constructs were created by cutting and ligating different parts of the tandem and monomeric plasmids described above. The first trimer [β4_β4_α3/ pSP64GL] was created by ligating three DNA-fragments; β4_α3/pSP64GL*EcoRI-XbaI (4583bp), β4/pcDNA3.1/Myc-His*EcoRI-ApaI (1486bp), and β4-α3/pSP64GL*XbaI/ApaI

(1814bp). The mutated [$\beta4^{L272T}$ _β4_α3/pSP64GL] trimer was created as above except for the first DNA-fragment being $\beta4^{L272T}$_α3/pSP64GL*EcoRI-XbaI (4583bp). Pentameric constructs were created by cutting and ligating different parts of the tandem and trimer plasmid constructs described above. The first pentameric construct [β4_β4_α3_β4_α3/pSP64GL] was created by ligating three different DNA-fragments; β4_β4_α3/pSP64GL*KspI-XbaI (6176bp), α3_β4/pcDNA3.1/Myc-His*KspI-ApaI (2986bp), and β4_α3/pSP64GL*ApaI-XbaI (1814bp). Mutant pentameric constructs [β4L272T_β4_α3_β4_α3/pSP64GL, β4_β4_α3_β4_$\alpha3^{L279T}$/pSP64GL, and $\beta4^{L272T}$_β4_α3_β4_$\alpha3^{L279T}$/pSP64GL] were created as above except for using the corresponding mutated β4_$\alpha3^{L279T}$/pSP64GL and/or $\beta4^{L272T}$_β4_α3/pSP64GL DNA-fragments. All trimer and pentameric constructs were checked for cloning artifacts by a minimum of five different restriction enzyme digests.

3.3 cRNA electrophoresis

The RNA electrophoresis was carried out by Dr. Groot-Kormelink. A 1.5% agarose gel was prepared using the 1X gel prep/running buffer (NorthernMax-Gly™ system; Ambion). RNA samples (including the 0.24–9.5 Kb RNA ladder; GIBCO BRL) were diluted 1:1 with Glyoxal sample loading dye (Ambion) and incubated at 50°C for 30 min before loading. Samples were separated at 5 V/cm for 3 h and RNAs were visualized by UV transillumination and a photograph taken (Groot-Kormelink *et al.* 2004).

3.4 Western Blotting

The Western Blotting was carried out by Dr Groot-Kormelink, oocyte protein samples were incubated at 75°C for 8 min just before loading (20 μl each sample) on a 8% Tris-Glycine polyacrylamide gel containing 2% SDS together with the SeeBlue® prestained protein standard (Invitrogen). After PAGE-SDS the proteins were transferred to nitrocellulose membrane (0.2 μm, protran BA83; Schleicher-Schuell). The blots were probed with rabbit antiserum to α3 or β4 (diluted 1:200 from 5-ml stock solution; Research & Diagnostic antibodies, WR-5611 [α3] and WR-5656 [β4]) followed by HRP-labeled goat anti–rabbit IgG (diluted 1:10,000, 10 μg/ml stock solution from supersignal® west femto chemiluminescence substrate kit; Pierce Chemical Co.). After washing, blots were visualized using the supersignal® west femto chemiluminescence substrate kit (Pierce Chemical Co.) and exposure to biomax light films (Kodak) (Groot-Kormelink *et al.* 2004).

3.5 *Xenopus laevis* oocyte preparation

Large, female South African clawed toads (*Xenopus laevis*; *X. laevis*) (Blades Biological) with large ovarian lobes (these are usually noticeable in the intact animal) were selected. The *X. laevis* were anaesthetised by immersion in a 0.4% weight/volume (w/v) solution (pH=5.6) ethyl *m*-aminobenzoate (tricaine, methanesulphonate salt; Sigma) for over 30 minutes. Anaesthesia was confirmed by a lack of reaction to a bone-pinch. Once anaesthesia was confirmed, the *X. laevis* was killed by decapitation and destruction of the brain and spinal cord in accordance with Home Office guidelines. The ovarian lobes were then removed and washed of blood

and other bodily fluids in modified Barth's solution (88mM NaCl, 1mM KCl, 0.82mM $MgCl_2$, 0.77mM $CaCl_2$, 2.4mM $NaHCO_3$, 15mM Tris (Sigma), 50 U/ml penicillin and 50 μg/ml streptomycin (Gibco BRL); made up in HPLC water (Merck); pH adjusted to 7.4 using NaOH and HCl; sterilised by double filtration through a sterile 0.22μM pore Millex-GV filter (Millipore). All work on oocytes was carried out at a room temperature of 18-20°C (controlled by air conditioning).

After washing, smaller, dying and dead cells were removed from the ovarian lobes using forceps, to increase the effectiveness of the enzyme. Clumps of ovarian tissue containing around 60 large, healthy-looking cells each were treated with collagenase (Type 1A, 245 collagen digestion units per ml in Barth's solution) for 65 minutes at 18°C while being shaken at approximately 2Hz. After this treatment the clumps were washed with 60ml Barth's solution and kept at 4°C overnight. The following day, mature (Stage V-VI), healthy oocytes were manually defolliculated using forceps.

3.6 Injection of cRNA

The cytoplasm of the vegetal pole of the defolliculated oocytes were injected with *in vitro* made RNA (46nl/oocyte) with a fire-polished, sharp pipette (12-16 μm tip opening; back filled with mineral oil (M-5904; Sigma) using a Drummond Nanoject injector (Figure 3.1.). A successful injection was confirmed visually by a "plumping up" of the oocyte.

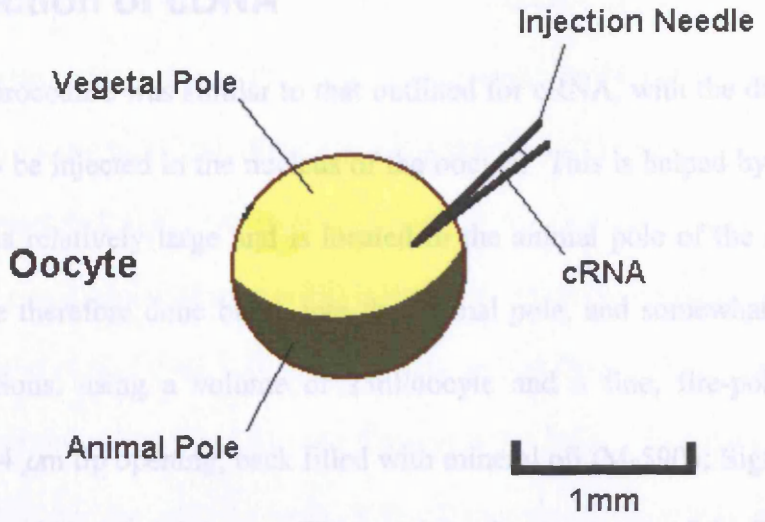

Figure 3.1: Injection of cRNA into the vegetal pole of *X. laevis* oocyte. Adapted from the thesis of James Boorman, 2002.

After injection, the oocytes were placed in individual wells of 24 multiwell plates and incubated at 18°C for approximately 60 hours in modified Barth's solution containing 5% volume/volume (v/v) heat-inactivated horse serum (Gibco BRL) to aid in the healing of the injection wound (Quick *et al.* 1992). The amount of cRNA injected varied between combinations. The aim was to obtain experimental data from oocytes expressing the different nicotinic receptors at levels that would be roughly comparable, sufficiently high to give a good signal to noise ratio, but low enough to avoid excessive series resistance errors (see section 3.6). In order to maintain this level stable from week to week from one batch of oocytes to another, the actual cRNA concentration injected was adjusted appropriately. If required, different cRNA concentrations were injected in order to ensure that at least one batch gave an expression level that satisfied our requirements.

3.7 Injection of cDNA

The procedure was similar to that outlined for cRNA, with the difference that cDNA has to be injected in the nucleus of the oocyte. This is helped by the fact that the nucleus is relatively large and is located in the animal pole of the oocyte. The injections are therefore done blind, into the animal pole, and somewhat deeper than cRNA injections, using a volume of 23nl/oocyte and a fine, fire-polished, sharp pipette (12-14 μm tip opening; back filled with mineral oil (M-5904; Sigma) mounted on a Drummond Nanoject injector. The post-injection treatment of the DNA-injected oocytes was the same as that described above for cRNA-injected oocytes. Of the oocytes injected with $\alpha 3$ + $\beta 4$ cDNA (n=6), all gave robust expression of channels with only one oocyte producing a relatively low current (70nA) the rest being in the range of 4-13 μA, this corresponds well with the circa 98% success rate obtained from cRNA injections and is of a comparable range to the currents seen with high injection concentrations of cRNA.

3.8 Electrophysiological recording

After approximately 60 hours incubation, the cells were stored at 4°C and were used from between three and twelve days after injection. Cell viability and expression levels have been shown to remain adequate for up to two weeks (Groot-Kormelink *et al.* 1998). Due to oocyte-batch variability, the optimal concentration of cRNA injected to record from, was determined on a week-to-week basis, aiming to achieve a maximum ACh-evoked current of 1-1.5 μA. The oocytes were held in a 0.2 ml bath and perfused at 4.5 ml/min with modified Ringer solution (150mM NaCl, 2.8 mM, 2mM $MgCl_2$, 10mM HEPES, pH adjusted to 7.2 with NaOH and HCl) containing

0.5μM atropine solution (to block endogenous muscarinic AChRs) (Davidson *et al.* 1991) and voltage clamped at –70mV, using the two-electrode voltage clamp (TEVC) mode of an Axoclamp-2B amplifier (Axon Instruments). The Ringer was made up in de-ionised water (DI H_2O) which was always stored in glass (rather than plastic) containers to avoid contamination with plasticisers, which have been shown to inhibit nAChRs (Papke *et al.* 1994). Electrodes were pulled from Clark borosilicate glass GC150TF (Harvard Apparatus Ltd.) and filled with 3M KCl. The electrode resistance was 0.5-1.5 MΩ on the current-passing side. Experimental results were included in the analysis of dose response curves only if the total amplitude of the holding current (I_H) together with the agonist evoked current was below 2μA, in order to keep series resistance errors below 2mV (Figure 3.2.). Larger currents (and therefore greater errors) were accepted only if the purpose of the experiment was to establish whether a given combination actually formed a functional receptor. In this case, an approximate measurement of expression level was all that was needed, as the differences between these positive "results" (functional receptors) and the negatives they were compared to, were in the order of 100x.

Additionally, if the I_H of the oocyte exceeded 1μA the cell was judged to be dead or dying and was discarded.

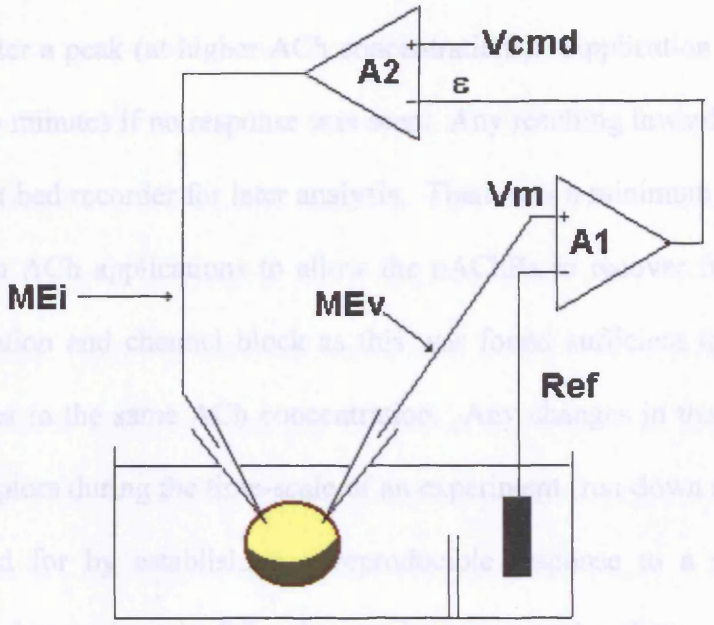

Figure 3.2: A simple representation of the TEVC circuit. Showing the high impedance unity-gain preamplifier (**A1**); the high gain current injecting amplifier of the Axon voltage clamp amplifier (**A2**); ME_v, recording electrode (**ME_v**); current injecting electrode (**MEi**); Ref, bath ground AgCl pellet (**Ref**); measured membrane potential (**Vm**); amplified measured membrane potential (ε); clamp command potential (**V_{cmd}**). (adapted from the thesis of James Boorman, 2002 and Axon Guide)

A nominally Ca^{2+}-free Ringer solution was used in order to minimise possible distortions due to the contribution of the oocyte's endogenous calcium-gated chloride conductance which can be activated by calcium entry through nAChR channels (Sands *et al.* 1993). Mock-injected oocytes (injected with 46ul of MilliQ water, n=19) confirmed that there were no endogenous ACh- or Gly-activated channels in the oocytes. Aliquots of 200mM ACh were made up in plasticiser-free DI H_2O and frozen at -20°C until required. Once defrosted the aliquots were either used or discarded. ACh solutions (prepared daily from the frozen stock aliquots) were applied via the bath perfusion system onto the oocyte for a period of time sufficient to

allow the establishment of a stable plateau (at low ACh concentrations) or the beginning of a sag after a peak (at higher ACh concentrations). Application of ACh was stopped after two minutes if no response was seen. Any resulting inward current was recorded on a flat bed recorder for later analysis. There was a minimum interval of 5 minutes between ACh applications to allow the nAChRs to recover from any short-term desensitisation and channel block as this was found sufficient to ensure reproducible responses to the same ACh concentration. Any changes in the agonist sensitivity of the receptors during the time-scale of an experiment (run-down and run-up) was compensated for by establishing a reproducible response to a standard concentration of ACh (approximately EC_{20}, the agonist concentration that produces a 20% of the maximum response) at the start of the experiment. The standards were judged to be reproducible if three successive applications were within 5% of each other so, for example, the α3β4 dose-response curves were obtained from recordings where the variation in the first and third standard compared to the second were 103.8 ± 1.7% and 96.2 ± 1.4% n=36, respectively. The EC_{20} was used for every third agonist application after that and these responses were compared to the established standard response obtained at the start of in order to calculate the degree of rundown/runup and so compensate for it.

3.9 Negative controls

In some cases, we needed to establish if a combination produced functional receptors. The choice of the amount and ratio of cRNA to be injected into the oocytes for these 'negative controls' was guided by the amount of cRNA expressed to produce responses in all the functional combinations tested. For instance in the tandem experiments, the functional tandem combinations were all found to produce excessive

currents (2μA+) when injected at a ratio of 2ng/μl of tandem to 0.5ng/μl of monomer, therefore this was used as the test concentration for other tandem + monomer combinations (or just 2ng/μl for tandem-only injections) whereas for the β3 experiments an excessive 10ng/μl monomer to 200ng/μl β3 was used to ensure that a "negative" result was due to a non-functional receptor combination rather than too low a level of expression. After the usual incubation time, oocytes were clamped at –70mV and were checked to see if they had any significant response to an application of 1mM ACh; a response was deemed to be significant if it was over 10nA from a low noise base-line. For each combination, at least six oocytes from at least two different batches were tested before concluding that that combination was unable to form a functional receptor. Each batch was from a different frog, processed on different experimental weeks. Every week we made sure that we injected at least one "positive control", namely a subunit combination known to have high functional expression. In all functional combinations tested 1mM was found to be a maximal or supra-maximal concentration of ACh. Higher concentrations began to show significant levels of channel block, so 1mM was chosen as a good compromise of potency, channel block and cost.

3.10 Data analysis

Rundown/runup compensation was calculated using the Excel^{TM} (Microsoft) spreadsheet programme by linear interpolation between EC_{20} standards. Concentration-response curves were fitted separately with the Hill equation with individual response being equally weighted in order to obtain estimates of I_{max}, EC_{50} and n_H (Figure 3.3.) using least squares fitting by the CVFIT programme (courtesy of D. Colquhoun and I. Vais, available from www.ucl.ac.uk/pharmacology/dc.html).

$$I = I_{\max} \frac{[A]^{\eta_H}}{[A]^{\eta_H} + EC_{50}{}^{\eta_H}}$$

Figure 3.3: The Hill equation. **I**, response; $\mathbf{I_{max}}$, maximum response; $\boldsymbol{EC_{50}}$, agonist concentration which produces 50% of the maximum response; ***nH***, Hill coefficient.

Tables and results report the averages and standard errors of the mean for the values obtained from the fit of the individual dose response curves (as these gave a more robust estimate of interoocyte variability). In the figures we show pooled dose-response curves that were obtained by normalising the data as follows. Once the individual concentration-response curves had been separately fitted they were normalised to the fitted I_{max} for that experiment; all the normalised responses for a given combination were then pooled. The pooled normalised datapoints were then fitted again with the Hill equation (with weight given by the reciprocal of their variance) as a free fit to give an average EC_{50} and n_H for each combination. Parameter estimates were similar to those obtained by fitting each curve separately.

When two-components were detected in the concentration-response curve, free fits of the individual dose response curves were attempted. These were usually poorly defined because of the large number of parameters fitted (vs. the number of datapoints). In the of case of $\beta4\_\alpha3 + \beta4^{LT}$, robust fits were usually achieved by fitting all dose-response curves for a combination simultaneously with the constraint that EC_{50} and n_H values for the two components should be the same across oocytes,

while the proportion of the current in the first component was allowed to vary from one oocyte to the other. The multicomponent curves obtained for α3β2 and α4β2 were fitted with individual two-component fits and pooled as this was found to be sufficient to produce reasonable fits.

Analysis of whether EC_{50} or Hill slope values were significantly different between different receptor combinations were carried out using an unpaired two-tailed Student's t-test. Functional expression levels for "knock-out" mutations and β3- and $\beta3^{VS}$-containing receptors were tested for significance using a Kruskal-Wallis one-way non-parametric ANOVA and Dunn's *post-hoc* multiple comparisons test at 5%significance. Significance testing was performed using Graphpad Prism version 4.03 (Trial) for Windows, GraphPad Software Inc. San Diego, California USA (www.graphpad.com), and StatCrunch version 4.0, a free online resource (www.statcrunch.com, West & Ogden, 1997).

CHAPTER 4

Protocol Optimisation

The majority of the experiments to be carried out involved comparing the dose-response curves of different combinations of nAChR subunits in order to detect any changes in the receptors' characteristics caused by, for example, the insertion of a β3 subunit or a subunit carrying a reporter mutation. However, these dose-response curves were not to be interpreted in a mechanistic sense in order to model the channel activation process. Such work is not feasible from macroscopic dose-response curves. This is first of all is because the parameters of the dose-response curves, such as EC_{50} and Hill slope, depend on both the binding and gating constants of the mechanism and these constants therefore cannot be independently determined. Secondly, the experimental dose-response curve depends on the whole mechanism, including desensitisation and agonist channel-block. The extent of the contribution of desensitisation depends greatly on the speed of equilibration of the agonist at the receptor level which is inevitably slow with a cell as large as an oocyte and also varies with the experimental conditions. This slow "on-flow" of agonist compared to the relatively rapid desensitisation and channel block was particularly a problem with α7-containing receptors, although at the highest concentrations of ACh, it was a factor in all the combinations tested. Note that desensitisation does still take place and distorts macroscopic responses even if no sag is detectable in the response to sustained applications (Feltz and Trautmann, 1982). Relatively minor variables such as the volume of the bath, the bore of the agonist tube, the height of the solutions, the positioning of the waste tube and even regularity of maintenance would all affect the speed of solution exchange in the bath and therefore the "on" and "off" rates of agonist application and so affect the responses seen. Add to that differences in the intervals between applications, Ringer recipes, agonist preparation etc.

and the potential for large systematic differences between different research groups exist. This means that the comparison of such things as EC_{50} values between different labs is not particularly informative therefore, all the results produced during my PhD were to be compared to our own internal standards and controls and considerable effort went into maintaining consistent experimental conditions.

The first aim of my project was to establish how to obtain dose-response curves in an efficient, reliable and consistent way. The first thing examined was the different merits of different dosing-order protocols.

4.1 Investigation of the effect of dosing order on the results of experiments.

The examples shown in Figures 4.1 to 4.3 are from experiments which had a protocol requiring the testing of around 12 different concentrations of agonist plus their standards. Instinctively most experimenters use an ascending dose order when carrying out a concentration-effect experiment i.e. they start with the lowest drug concentration and work their way up through higher concentrations until they obtain a plateau for the maximum response. However as will be shown this isn't the most efficient method for a number of reasons. For instance, it is fairly common for a cell to die during an experiment thus ending it, and power cuts and fire alarms halting experiments are certainly not unknown. If this happens during an experiment with an ascending dose order before the responses have reached a maximum (e.g. Figure 4.1A) then the results obtained are of little use, as without a clearly defined maximum response an accurate EC_{50} cannot be obtained and the Hill coefficient is poorly estimated and so this can cause

a lot of wastage. However, if a cell prematurely dies during an experiment with a descending dose order (i.e. starting with the highest concentration and working towards the lowest) as is shown in Figure 4.1B then something of the results can still be salvaged. As can be seen this incomplete concentration-effect curve still gives reasonable estimates for maximum response, EC_{20}, EC_{50} and Hill coefficient and could, at a push, be used in the final fitting. The curve seen in Figure 4.1A on the other hand is of little use whatsoever (other than as a warning) despite representing nine dose "points" and over three-quarters of an experiment compared to the six points, half an experiment, shown in Figure 4.1B.

A

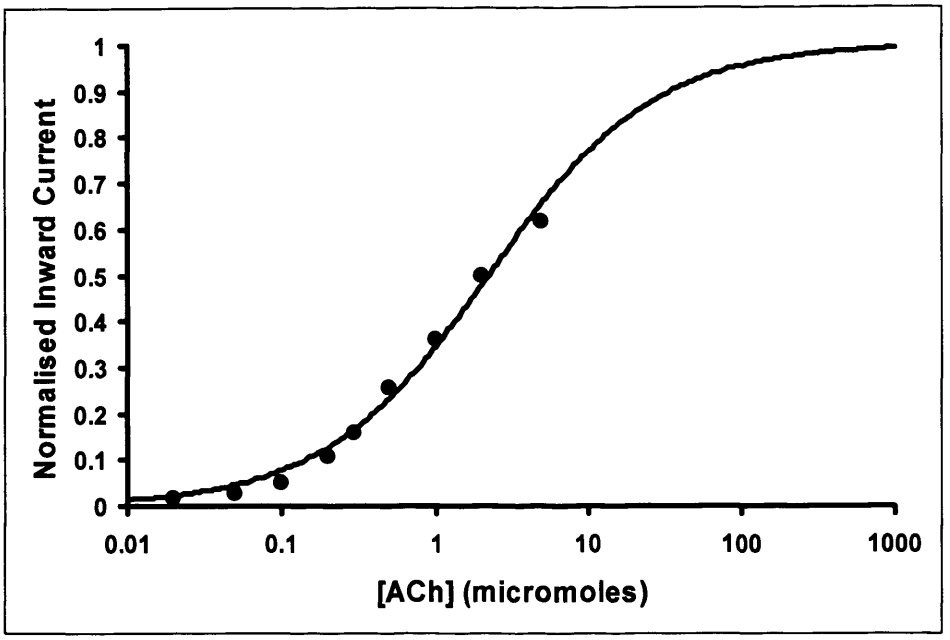

B

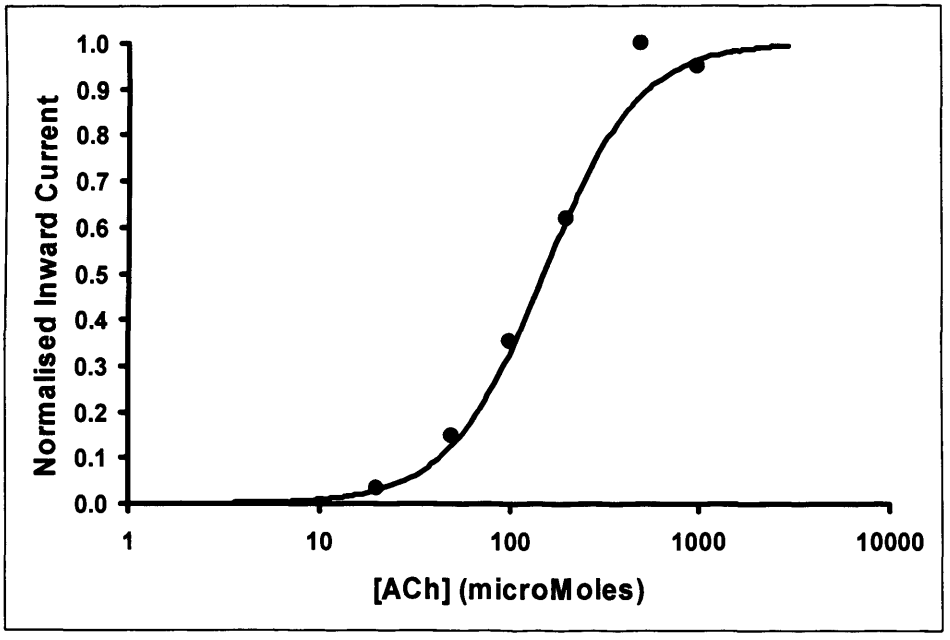

Figure 4.1: Examples of incomplete concentration-effect curves.
A. Three-quarters complete ascending concentration-effect curve for $\beta4^{LT}\alpha3$ + $\beta4^{LT}$ (maximum extrapolated from other $\beta4^{LT}\alpha3$ + $\beta4^{LT}$ curves)
B. Half complete descending concentration-effect curve for $\alpha3$ +$\beta4$.

Even in more extreme examples such as the four-point "curve" in Figure 4.2 the descending protocol allows a reasonable approximation of maximum response, EC_{50} and Hill coefficient, though the curve itself would not be included in the final analysis. A four-point ascending curve wouldn't even be worth plotting. This makes the descending protocol more efficient as it reduces wastage.

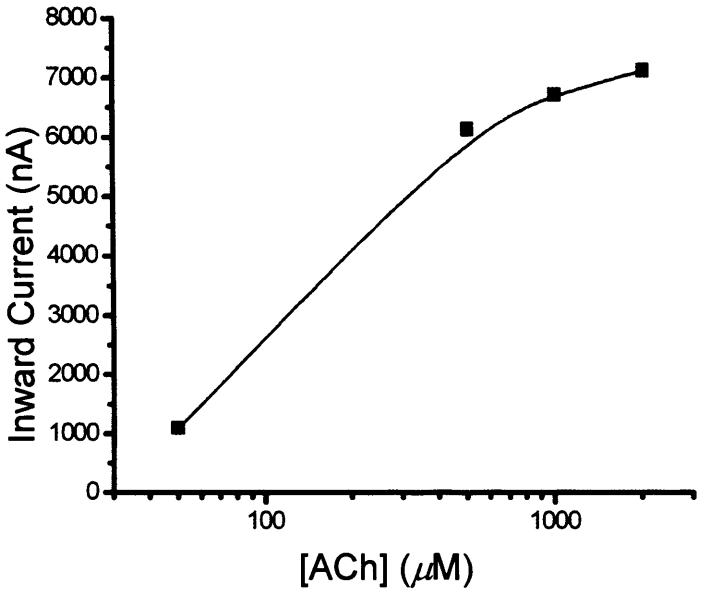

Figure 4.2: Extreme example of an incomplete descending concentration-effect curve. Points fitted with a smoothed line in Excel.

There are also a number of more minor advantages in using a descending over ascending drug application protocol. A quick glance at Figure 4.1A shows that in hindsight the points for 0.2μM and 0.5μM were probably unnecessary, were ultimately a waste of time, Ringer and agonist and had they not been done, in all probability, the experiment may have been completed before it was interrupted. However at the start of

the experiment the experimenter had to guess at where he thought the bottom of the curve would be and in this case he guessed too low. On a descending protocol, however, that problem is avoided as for all combinations I checked where the maximum response was before starting on the dose-response experiments and in the majority of cases 1mM ACh. was found to be near the peak of the dose-response curve of any combination, only when two or more channel mutations are present does the maximum differ significantly therefore as a rule-of-thumb starting the "descent" from 1mM minimises wasted applications. Examination of the curves produced shows that no combination peaks higher than 2mM and most peak within the 50μM-1mM range. Even in the cases where multiple mutations mean a maximum current is evoked at a lower concentration, desensitisation and channel block were not sufficiently large to render a 1mM ACh. application a false negative (see Methods section 3.9).

Another advantage, any errors in the responses obtained are identified by drawing them as a graph during the experiment allowing any unexpected results to be repeated either confirming or correcting them. The graph however can only be drawn in its normalised form once the maximum response has been established. Therefore, for the descending protocol where the maximum is established early on this graph can be drawn during the experiment allowing rapid identification of any outliers whilst for the ascending protocol where the maximum is established last the graph can only be drawn and problems identified after the experiment is finished by which point it may be too late to correct or confirm. It also takes less time to simultaneously draw the graph and do the experiment than to do the experiment and then draw the graph.

A further advantage of the descending protocol is that as the lower concentrations of drug are usually made up from the higher concentrations, therefore for the ascending protocol, before the experiment can be started nearly all the different drug concentrations have to be made up whilst for the descending protocol they can be made up during the experiment thus saving time. All these small advantages not only make the descending protocol more sensitive for identifying problems but also makes it quicker to do; a typical descending protocol takes about 30 minutes less than the equivalent ascending protocol.

Additionally, as stated in the methods, dose-response curves were only accepted for the final fits if their total current i.e. the holding current and the agonist-evoked current did not exceed 2μA for all the application of ACh included in the final curve therefore by testing the highest concentrations first over-expressing oocytes can be identified and the recording halted whereas with the ascending protocol this may not become apparent until near the end of the experiment. This can be compounded by the fact that the holding current of the oocyte tends to increase during the experiment so a 1700nA agonist-evoked response at the start of an experiment may add to a holding current of 100nA to give a total current of 1800nA, well within the maximum-allowed current, whereas near the end of an experiment the holding current may have crept up to 350nA putting the response over the limit and therefore rendering that experiment void. Of course this problem is usually, although not always, cancelled out by the run-down of agonist-evoked responses during the experiment, however it remains an advantage of the descending protocol when the oocytes are in poor health with high holding currents or on the occasions where there is either no run-down or actual run-up.

A potential disadvantage of the "descending" sequence is that applying high concentrations at the beginning of the experiment may produce long-lasting desensitisation that distorts the subsequent data, however as long as all combinations are tested using the same protocol this should be less of an issue, as mentioned earlier we were more interested in comparisons between different combination types rather than the actual "platonic" values of a particular receptor's properties.

The alternative solution for obtaining good estimates of DR curves parameters would be to only get one response and standard from each oocyte (Covernton & Connelly, 2000). This method though is laborious and inefficient and, as stated, we are more interested in getting consistent internal values for these parameters for comparison purposes rather than accurate values for a mechanistic study. Therefore in this case efficiency of data collection is more important than accuracy.

Figure 4.3 shows a typical example of two cells from the same batch of oocytes, from the same week, injected by the same type ($\alpha 3\beta 4$) and concentration of cRNA (0.3:0.3 ng), tested on the same day, by the same experimenter, using the same Ringer, ACh and glass electrodes, at the same temperature. The only difference between the two sets of results is that the top one was carried out using an ascending protocol and the bottom by a descending protocol. As can be seen the ascending protocol has produced a curve without a clear maximum and a shallower slope. Even if the highest concentration of ACh used here (2mM) was producing the maximum response for this curve (of which we cannot be sure) it would produce values for the EC_{50} and nH way off what is expected for $\alpha 3\beta 4$. When analysed by the CVfit programme this experiment gave an EC_{50} of 344μM and a η_H of 1.03 with a warning that this curve was poorly defined. The

descending protocol on the other hand can be seen to give a definite maximum at 500μM and the steep slope expected. Curve fitting gave a well-defined EC_{50} of 106μM and a Hill slope of 1.74, both of these are within the range of our previously determined values for $\alpha 3\beta 4$.

The advantages of a descending protocol (as described above) meant we decided to adopt a descending protocol for future experiments. Although we are more interested in relative differences in values rather than the "true" platonic values we had to see how using a descending protocol affected our values in order to compare them with our own past experiments using ascending protocols. To do this the well-characterised $\alpha 3\beta 4$ nAChRs were examined and compared using ascending and descending protocols. Figure 4.4. show a comparison between the curves produced by ascending and descending protocols and Table 4.1 compares the values obtained with previously published results.

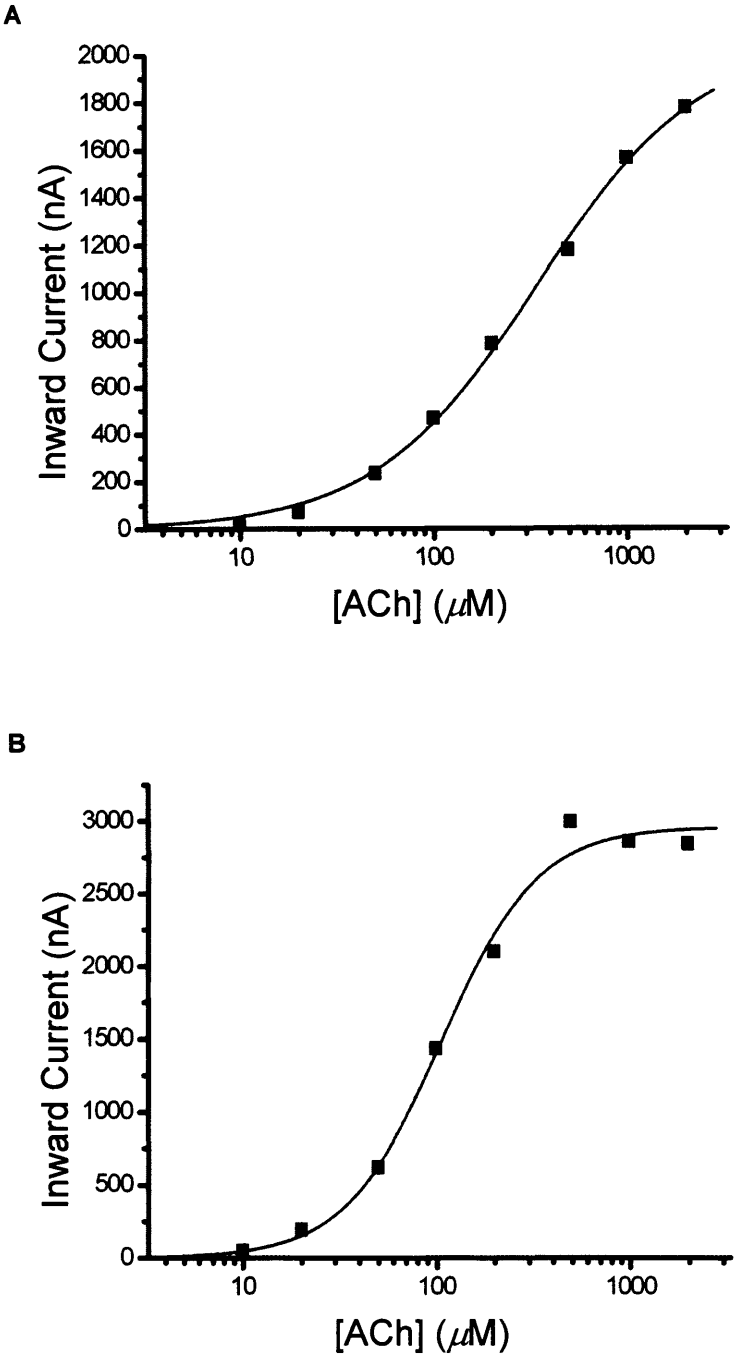

Figure 4.3: Concentration-effect curves for oocytes injected with 0.3ng/μl:0.3ng/μl $\alpha 3$ and $\beta 4$ cRNA to ACh, recorded on 21/05/02.
A. Ascending protocol.
B. Descending protocol.

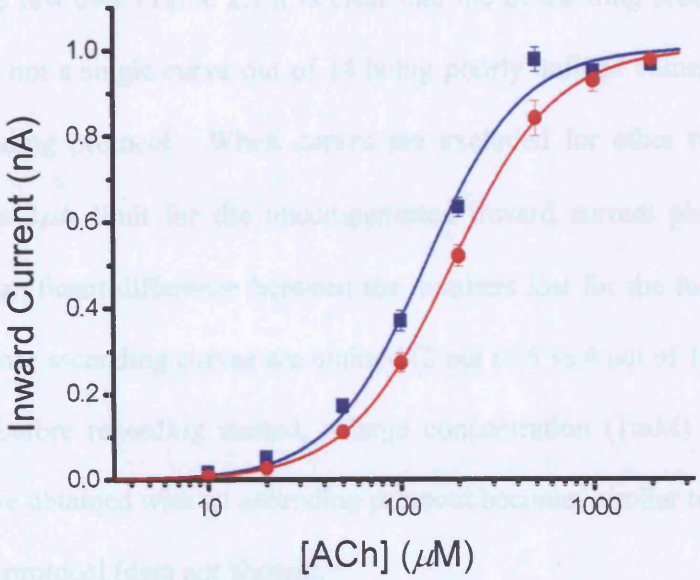

Figure 4.4: Comparison of concentration-effect curves to ACh derived for $\alpha 3\beta 4$ nAChRs using ascending and descending protocols. Max. response (inward current) normalised to 1. The descending protocol (blue squares n=10) produces a curve slightly to the left of the ascending protocol (red circles, n=4).

	No. poorly defined.	n =	ACh EC_{50} (μM)	nH
$\alpha 3\beta 4$ (Up)	6/11	4	185 ± 11	1.61 ± 0.12
$\alpha 3\beta 4$ (Down)	0/14	10	134 ± 6	1.73 ± 0.11
Gerzanich *et al.* (1995)	-	-	160	-
Wang *et al.* (1996)	-	-	163	1.9
Chavez-Noriega *et al.* (1997)	-	-	203	2.2
Groot-Kormelink *et al.* (1998)	-	-	180	1.8

Table 4.1: Comparison of values obtained for ascending and descending protocols and published results for ACh on $\alpha 3\beta 4$ nAChRs.

As can be seen from Table 4.1. although there is a difference between the EC_{50} and *n*H values for the ascending and descending protocols (185 vs 134 μM ; 1.61 vs 1.73) these are quite small with a slight leftward shift and steepening of the curve . When looking at the raw data (Table 2.) it is clear that the descending protocol is much more efficient with not a single curve out of 14 being poorly defined compared to 6 out of 11 for the ascending protocol. When curves are excluded for other reasons (mainly for exceeding the 2μA limit for the uncompensated inward current plus holding current) there is no significant difference between the numbers lost for the two protocols though marginally more ascending curves are omitted (2 out of 6 vs 4 out of 14). Interestingly, if we applied, before recording started, a large concentration (1mM) of ACh, the dose-response curve obtained with an ascending protocol becomes similar to that obtained with a descending protocol (data not shown).

A random protocol would avoid bias introduced by changes in the preparation in time. However, it would be of less use if the responses are not independent and it was decided that it really wasn't feasible because it would be awkward and confusing practically and it would suffer the same problems as the ascending protocol with premature cell death, no monitoring graph and prolonged experiment time. Table 4.2 summarises the pros and cons of the three dosing protocols.

Dosing order	Pros	Cons
Up	Traditional All previous work Less carry-over desensitisation Preferred by supervisor.	Ill-defined maximum. Overestimates maximum. Overestimates EC_{50}. Premature cell death. Longer. Inefficient
Down	Well-defined maximum. More reliable. Shorter. Allows problem monitoring. Efficient.	Underestimates maximum. Underestimates EC_{50}.
Random	Avoids bias	Awkward. Premature cell death. Longer. Long-term desensitisation. Inefficient.

Table 4.2: Summary of pros and cons of the three types of dosing protocol.

4.2 Discussion

In conclusion, these results show that a descending dosing protocol is superior in a number of ways to both random and ascending dosing protocols and produces values comparable to other published results. All the experiments in this thesis use a descending dosing protocol

CHAPTER 5

Development of a Dominant Negative β3 Subunit Mutation

As we have covered in Groot-Kormelink *et al.* 1998, Boorman *et al.* 2000 and Boorman *et al.* 2003, the β3 subunit can co-assemble with α3 and β4 subunits to form a functional receptor with a stoichiometry of 2:2:1 (α3:β4:β3). The insertion of this β3 subunit produced only subtle changes in the receptor compared with the α3β4 pair receptor e.g. decreased potency of lobeline, increased slope conductance and decreased channel mean opening time and left most of the properties of the pair receptor unchanged. In fact the triplet receptor was so similar to the pair receptor that it required the use of a reporter mutation to prove the β3 subunit was actually incorporated into the receptor at all (Groot-Kormelink *et al.* 1998). One of the main thrusts of my PhD research was to check to see if any other β3-containing receptors could be created and if so what effects (if any) did the incorporation of the β3 have.

We were faced with the possibility that any other β3-containing receptors would be as similar to their corresponding pair receptors as the α3β4β3 receptor was to the α3β4. The reporter mutation approach used to show incorporation of β3 into α3β4 receptors requires comparing dose-response curves (e.g. the VT mutation used in Groot-Kormelink *et al.* 1998) so we decided to try to develop a dominant negative β3 subunit mutation ($\beta3^{KO}$) which would allow β3-containing receptors to be quickly flagged up. The simple co-injection of the pair with the $\beta3^{KO}$ would show the β3 subunit was incorporated by knocking out the functional expression of the pair receptor (obviously using multiple batches, expression of functional combinations in the same batch etc. as a control to rule out any injection problems etc.). The development of such a mutation would also give us a potentially useful research tool for the functional knockdown of neuronal nicotinic receptors (say in organotypic preparations).

My colleagues Paul Groot-Kormelink and Jenny Davies produced a range of mutated β3 subunits shown in Table 5.1 which were dubbed the "Delilah" (DEL) mutations and numbered accordingly.

Position	-4'	-3'	-2'	-1'	-1'	0'	1'	2'	3'	4'	5'	6'	7'	8'	9'	10'	11	12	13'	14'	15'	16'	17'	18'	19'	20'	21'
nAChR α7	D	S	G	-	E	K	I	S	L	G	I	T	V	L	L	S	L	T	V	F	M	L	L	V	A	E	I
nAChR β3	D	E	G	-	E	K	L	S	L	S	T	S	V	L	V	S	L	T	V	F	L	L	V	I	E	E	I
Glycine α1	D	A	A	-	E	R	V	G	L	G	I	T	T	V	L	T	M	T	V	Q	S	S	G	S	R	A	S
GABAC ρ1	R	A	V	P	A	R	V	P	L	G	I	T	T	V	L	T	M	S	T	I	I	T	G	V	N	A	S
Delilah mut 1	D	E	G	**P**	E	K	L	S	L	S	T	S	V	L	V	S	L	T	V	F	L	L	V	I	E	E	I
Delilah mut 2	D	E	G	**P**	**A**	K	L	S	L	S	T	S	V	L	V	S	L	T	V	F	L	L	V	I	E	E	I
Delilah mut 3	D	E	G	**P**	**A**	K	L	S	L	S	T	S	V	L	V	S	L	T	**T**	F	L	L	V	I	E	E	I
Delilah mut 4	D	E	G	**P**	**A**	K	L	S	L	S	T	S	V	L	V	S	L	T	V	F	L	L	V	I	E	**N**	I
Delilah mut 5	D	E	G	**P**	**A**	K	L	**G**	L	S	T	S	V	L	V	S	L	T	V	F	L	L	V	I	E	E	I
Delilah mut 6	D	E	G	**P**	**A**	K	L	**G**	L	S	T	S	V	L	V	S	L	T	**T**	F	L	L	V	I	E	E	I
Delilah mut 7	D	E	G	**P**	**A**	K	L	**S**	L	S	T	S	V	L	V	S	L	T	**T**	F	L	L	V	I	E	**N**	I
Delilah mut 8	D	E	G	**P**	**A**	K	L	**G**	L	S	T	S	V	L	V	S	L	T	V	F	L	L	V	I	E	**N**	I
Delilah mut 9	D	E	G	**P**	**A**	K	L	**G**	L	S	T	S	V	L	V	S	L	T	**T**	F	L	L	V	I	E	**N**	I
Delilah mut 10	D	E	G	**P**	**A**	K	L	**G**	L	S	T	S	V	L	V	S	L	T	**T**	F	L	**S**	**G**	I	E	**N**	I
Delilah mut 11	D	E	G	**P**	**A**	K	L	**G**	L	S	T	S	V	L	V	S	L	T	**T**	F	**S**	**S**	**G**	I	**R**	**N**	I
Delilah mut 12	D	**S**	G	**P**	**A**	K	L	**G**	L	S	T	S	V	L	V	S	L	T	**T**	F	**L**	**S**	**G**	I	**E**	**N**	I
Delilah mut 13	D	**S**	G	**P**	**A**	K	L	**G**	L	S	T	S	V	L	V	S	L	T	**T**	F	**S**	**S**	**G**	I	**R**	**N**	I

Table 5.1: The TM2 sequences of the human nAChR α7 and β3 subunits, the rat Glycine α1 and the human GABAC ρ1 subunits compared with the mutations inserted (in bold) to create the Delilah subunits. Residues are numbered according to Miller (1989) where 0′ position is the first residue of M2.

The choice of mutations was based on the work of Galzi *et al.* where the TM2 residues of the cation-selective α7 nAChR were mutated to TM2 residues of anion-selective receptors of the glycine and GABA families ultimately producing an anion-selective α7 receptor (Galzi *et al.* 1992). Their work showed that the minimum set of

mutations required to produce this cation-to-anion switch were a proline insertion at position -1', the charged -1' glutamate mutated to neutral alanine and the substitution of threonine for valine at 13'. This proline insertion is commonly found in anionic but not cationic receptor subunits and has been suggested to cause a major change in the secondary structure of a section of M2 (Galzi *et al.* 1999). The -1' glutamate is part of the intermediate ring of charge thought to control ion permeability in the muscle nicotinic receptor (Imoto *et al.* 1988) and a swap to a neutral alanine in this position may be necessary to allow the passage of anions. Finally, 13' residues are susceptible to sulfhydryl reagent modification both in the absence and in the presence of agonist (Akabas *et al.* 1994) and they are thought to form part of the channel gate (Unwin 2005).

The findings of Galzi and co-workers have since been repeated for the 5-$HT3_A$ receptor (Gunthorpe and Lummis, 2001) and reversed to produce a cation-selective glycine channel (Keramidas *et al.* 2000).

For our work, the first major difference was that here we would be dealing with the mutation of only a single subunit, whereas previously the work has involved homomeric receptors, in which all the subunits in the pentamer would be mutated, therefore we would use the 3 "minimal" mutations identified by Galzi as a starting point and then mutate further residues of the TM2 in case a single copy of the "minimal" mutations weren't enough to produce a complete knock-out of the receptor. The second difference is that we were dealing with the β3 subunit rather than the α7 but as can be seen from Table 5.1 the TM2 sequences are very well conserved between the two subunits and the only differences are relatively minor, certainly less than the differences between cationic and anionic channels, so this didn't pose a problem.

The three "Galzi" mutations were sequentially introduced (DEL1 through to 3) and from these, constructs of subunits with additional mutations (in other positions thought to be of importance in channel conductance) were produced (DEL4 through to 13). No preparation of the DEL8 construct was successful, the sequenced minipreps were found either not to contain the required mutations or to include additional mutations. It was therefore decided not to continue to attempt to produce DEL8 as it was judged that the effects of mutating residues at positions 2', 13' and 20' would be adequately explored by the DEL4, 5, 6, 7 and 9 subunits. Time constraints meant DEL12 was not created initially as it was deemed to be a lesser priority as the effects of its mutations were thought to be covered by the mutation set in DEL13. This left us with 11 usable mutated subunits to test.

As a first step in testing the effectiveness of these mutations, the mutant β3 constructs were expressed in *Xenopus* oocytes (together with wild type α3 and β4 subunit cRNA in a 1:1:20 ratio) and tested by the application of 1mM ACh, a concentration that consistently produces maximum responses in α3β4β3 receptors. Testing several of the mutated subunits within the same batch (i.e. the same frog and experimental week) of injections allowed a more precise direct comparison between the different combinations of mutations to check to see which one was the most powerful. In order to provide a baseline and to allow comparisons between different batches, a number of oocytes from each batch was injected with $\alpha3\beta4\beta3^{WT}$ (in a quantity equal to that of the mutant combinations).

There are a couple of flaws in this approach the main one being the variation in wild-type triplet receptor expression levels between batches, , however by repeating this experiment at least twice and ensuring that each batch was tested on the same days, using the same electrodes, the same Ringer and the same ACh we hoped to

minimise the variation. It must also be remembered that these initial experiments were only intended as a pilot; once the most promising candidates had been identified they could then be re-tested under stricter conditions.

Table 5.2 and Figure 5.1 shows the results obtained from receptors containing Delilah-mutated β3 subunits. Figure 5.2 shows representative traces.

Combination	**Current ± SEM (%)**	***n***	**Batches**	***p* value (vs WT)**
$\alpha3\beta4\beta3^{WT}$	100	35	8	-
DEL1	24.8 ± 10.8	5	2	< 0.05
DEL2	15.3 ± 1.1	5	2	< 0.001
DEL3	21.5 ± 4.2	5	2	< 0.001
DEL4	2.5 ± 0.7	7	2	< 0.001
DEL5	32.7 ± 3.2	7	3	< 0.001
DEL6	11.3 ± 3.7	5	3	< 0.001
DEL7	44.8 ± 10.2	4	3	< 0.05
DEL9	47.1 ± 8.7	5	3	< 0.05
DEL10	17.2 ± 7.8	6	2	< 0.001
DEL11	32.1 ± 12.1	4	3	< 0.01
DEL13	32.3 ± 16.3	5	3	< 0.001

Table 5.2: Currents obtained from receptors containing Delilah-mutated β3 subunits expressed as a percentage of the current obtained from $\alpha3\beta4\beta3^{WT}$ receptors on the same day. Statistical analysis by Kruskal-Wallis one-way nonparametric ANOVA followed by Dunn's *post hoc* multiple comparisons test.

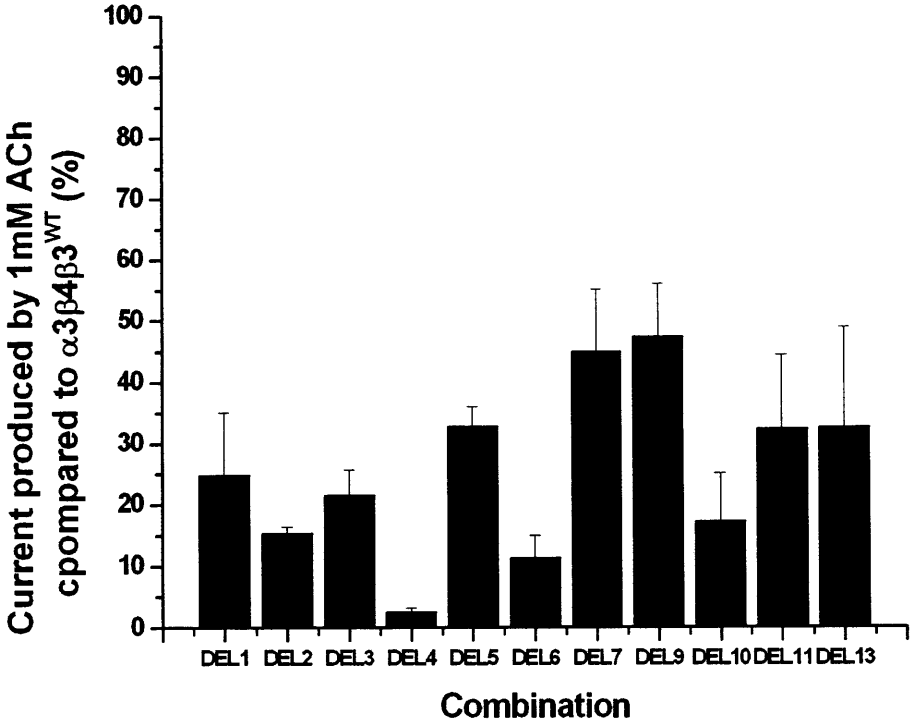

Figure 5.1: Comparison of the relative effectiveness of the Delilah-mutated β3 subunits expressed as a percentage of the current obtained from $\alpha 3\beta 4\beta 3^{WT}$ receptors from1mM ACh on the same day.

As can be seen all the Delilah mutation combinations reduced the current produced by 1mM ACh by at least half, which is very impressive considering there is likely only to be a single mutated subunit in the receptor. DEL4 is consistently the most powerful of the mutation combinations and as such could prove to be a very useful research tool. It isn't clear why this particular combination of mutations should produce the most dramatic fall in whole-cell current particularly when considering most of the other DEL mutations had the same mutations plus a few more and would be expected to be more potent if anything. It is also surprising that Galzi's "minimal" 13' mutation should have less effect than the 20' mutation although this could be due to differences in the channel gate. Another thing we cannot tell from these results is whether the observed "reduction" in ACh-evoked current is genuinely produced by a

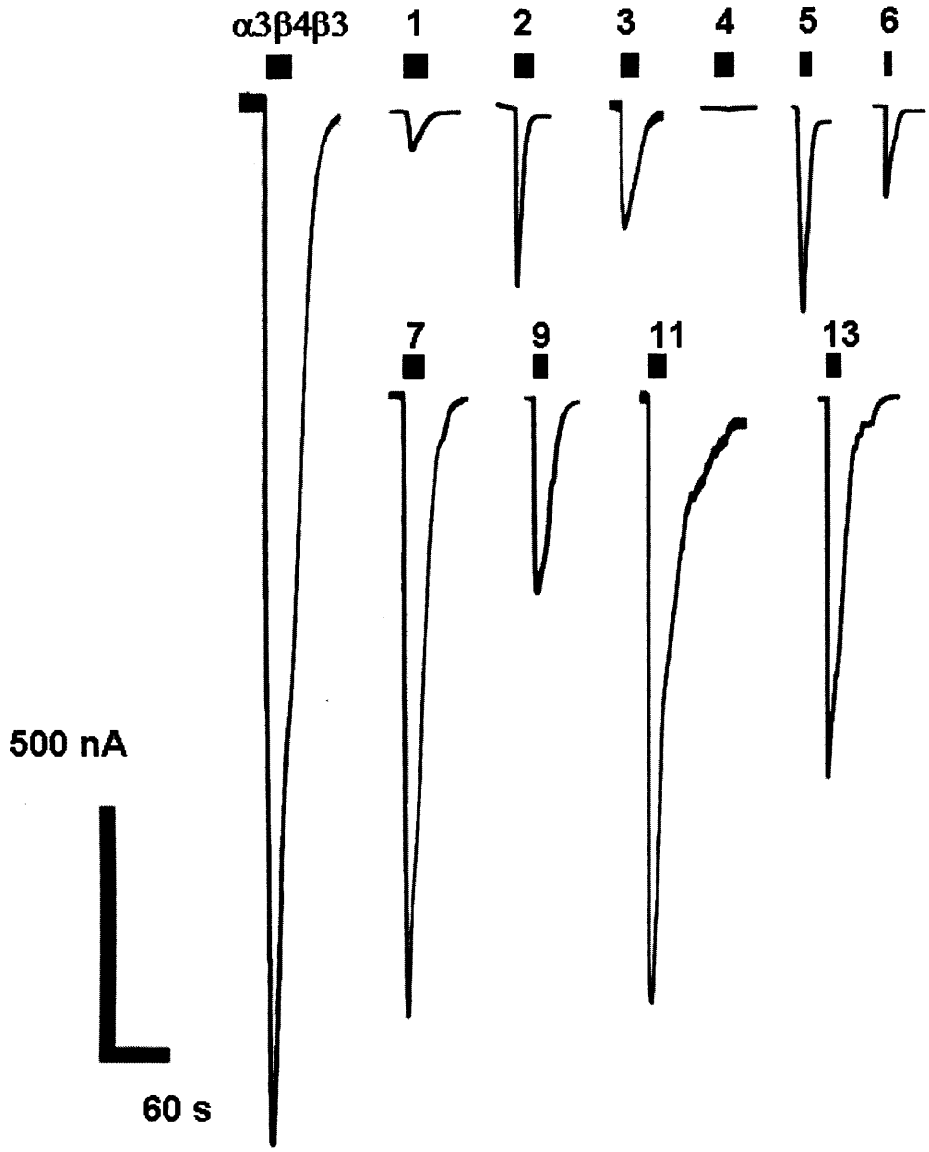

Figure 5.2: Representative traces obtained from $\alpha3\beta4\beta3^{WT}$ and Delilah mutant receptors (numbered) to 1mM ACh at -70mV

reduction in channel conductance or whether the effect is because the mutations have produced an increase in EC_{50} and therefore 1mM ACh is no longer producing a maximal response. It would seem most likely though that the effects are produced by a reduction in channel conductance, given the nature of the mutations. Nevertheless I sought further evidence that a change in ACh sensitivity was not involved in this effect and tested a small range of agonist concentrations.

Figure 5.3 shows the responses (normalised to the response obtained for 1mM ACh in the same oocyte) obtained at ACh concentrations of 200μM, 500μM and 1mM for $\alpha3\beta4\beta3^{WT}$ (n=9) compared to DEL1 (n=3), DEL2 (n=3), DEL3 (n=3), DEL4 (n=1), DEL5 (n=3), DEL9 (n=3), DEL11 (n=1) and DEL13 (n=1). As can be seen all the DEL combinations appear to have reached peak responses by 1mM ACh, if anything the EC_{50} values may have even been decreased compared to the $\alpha3\beta4\beta3^{WT}$ (black squares). It must be borne in mind that these are only partial dose response curves, which have not been compensated for run down and represent only very small n values. It may however be of future interest to see if this reduction in EC_{50} by the DEL mutations is in fact real.

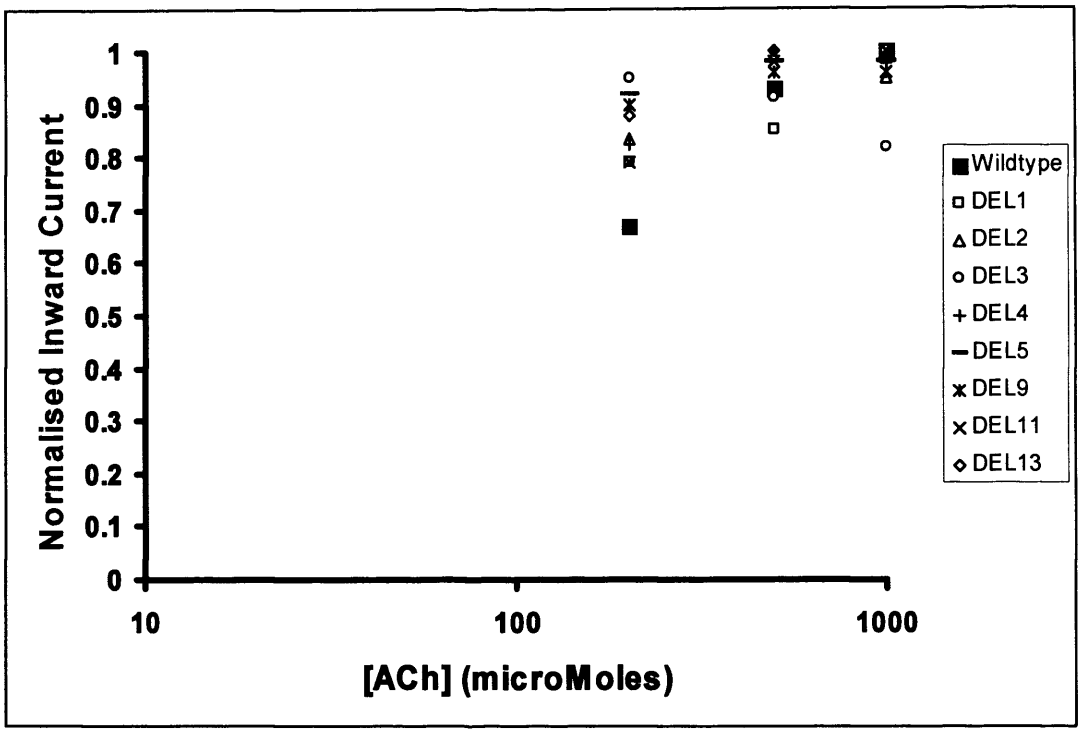

Figure 5.3: Inward currents (±SEM) normalised to the response produced by 1mM ACh to ACh concentrations of 200μM, 500μM and 1mM for $\alpha 3\beta 4\beta 3^{WT}$ (black squares) and various DEL combinations (see box).

For the purposes of our work it doesn't matter whether DEL4 is producing its effect by reducing channel conductance or increasing EC_{50} as the observed effect a massive reduction of response to 1mM ACh is the same and would show the incorporation of the mutated β3 subunit into the receptor tested which was all that we required from the mutant at this point.

All these were questions to be left for some future research project as our primary aim was to develop a dominant negative mutation of the β3 subunit in which we have succeeded. So now armed with the VT and VS "positive" β3 mutations developed for the Groot-Kormelink *et al.* 1998 paper and the negative DEL4 we could now proceed with the testing of other combinations of subunits with the β3 subunit.

CHAPTER 6

The effect of co-expressing the β3 subunit with other nAChRs subunit combinations

A manuscript for this has been submitted for publication.

As described in Chapter 1, the (essentially artificial) criterion for classifying a subunit as a lies in the presence of two adjacent cysteines in the first extracellular domain (Boulter *et al.* 1990; Couturier *et al.* 1990). The successful expression of homomeric and "pair" heteromeric nAChR left two subunits as "orphans", the α5 and the β3. These subunits are quite similar in sequence and have been classed together in tribe III-3 of the nicotinic evolutionary tree (Corringer *et al.* 2000) Both α5 and β3 are expressed in high levels in discrete areas of the brain or autonomic nervous system (Winzer-Serhan & Leslie, 2005; Azam *et al.* 2002). and immunoprecipitation shows that α5 forms one of the main synaptic nAChRs in chick ciliary ganglia (Conroy & Berg, 1995). All of this suggests that, rather than being "evolutionary baggage", both the α5 and β3 subunits must be capable of participating in functional receptors *in vivo* and should have some function.

In 1996, both the groups of Role and Lindstrom showed that α5 could produce functional triplet receptors along with α4β2, α3β2 and α3β4 in heterologous expression systems (Ramirez-Latorre *et al.* 1996; Wang *et al.* 1996). This α5 incorporation was shown to produce a reduction in ACh sensitivity and increase in single channel conductance compared to the "parent" pair receptor (Ramirez-Latorre *et al.* 1996; Sivilotti *et al.* 1997; Nelson & Lindstrom 1999). The effects produced were dependent on the nature of the parent pair so, for instance, α5 incorporation into an α3β4 receptor has less effect on ACh sensitivity but does change the desensitisation and calcium permeability of the receptor (Gerzanich *et al.* 1998). Our group has since shown that the

α3β4α5 receptor contains a single copy of the α5 subunit and it is likely that this 2:2:1 stoichiometry holds for all α5-containing triplet receptors (Groot-Kormelink *et al.* 2001).

With the incorporation and effect of the α5 subunit being shown our group has worked to replicate this work with its sister subunit, the β3. Previously we have proven the incorporation of the β3 subunit into a functional recombinant α3β4β3 receptor (Groot-Kormelink *et a*l. 1998), with a stoichiometry of 2:2:1 (Boorman *et al.* 2000) just as with the α5, but with the difference that the α3β4β3 receptor is very similar to the α3β4 receptor (Boorman *et al.* 2003) in ACh sensitivity, Hill slope, calcium permeability, rank order of potency of agonists and sensitivity to competitive antagonists. The only noticeable difference in the macroscopic properties of the triplet receptor was a three-fold decrease in the potency of lobeline compared to ACh.

Differences were however noticeable at single channel level: β3 incorporation decreased mean opening times and burst length and increased single channel slope conductance. At first sight, this would suggest that any effects of β3 incorporation on α3β4 receptors are fairly minor and it would be hard to justify a significant functional role for the β3 subunit on the α3β4 receptor *in vivo* beyond faster decay kinetics.

This was a little disappointing however, as with the α5 subunit, it was likely that the actual effect of the subunit incorporation would be dependent on the nature of the parent pair and so it was possible more dramatic effects would be seen by β3 co-assembly with other nAChR combinations.

6.1 The $\beta3^{VS}$ reporter mutation

Groot-Kormelink *et al.* 1998 detected the insertion of the β3 into the α3β4β3 receptor through the use of a valine-to-threonine (VT) 9′ mutation in the β3's TM2 domain. However, the literature indicates that a more powerful and therefore noticeable "gain-of-function" mutation would be produced by mutating the 9′ valine to a *serine* (VS) so we set out to see whether this is true for $\beta3^{VS}$.

The $\beta3^{VS}$ mutation was produced and checked by Dr Groot-Kormelink using the method described in Groot-Kormelink *et al.* 1998. This new subunit cRNA was then co-injected with α3 and β4 cRNA with a ratio of 1:1:20 ($\alpha3:\beta4:\beta3^{VS}$) into oocytes in order to produce a pure population of $\alpha3\beta4\beta3^{VS}$ receptors with a stoichiometry of 2:2:1. Dose-response curves were produced for the α3β4 (1:1) and $\alpha3\beta4\beta3^{VS}$ receptors and are shown in Figure 6.1. Ideally the α3β4β3 (1:1:20) receptor should have been used for comparison purposes, however as we had already shown that the α3β4β3 receptor produced dose-response curves indistinguishable from α3β4 (Boorman *et al.* 2003) it seemed an inefficient use of time to duplicate the work done previously and as the α3β4 receptor was being characterised by me anyway for other experiments, it seemed sensible to use that instead. My more recent α3β4 results were used rather than those previously published by our group to compensate for any operator differences and to take into account the different protocol used (detailed in Chapter 4).

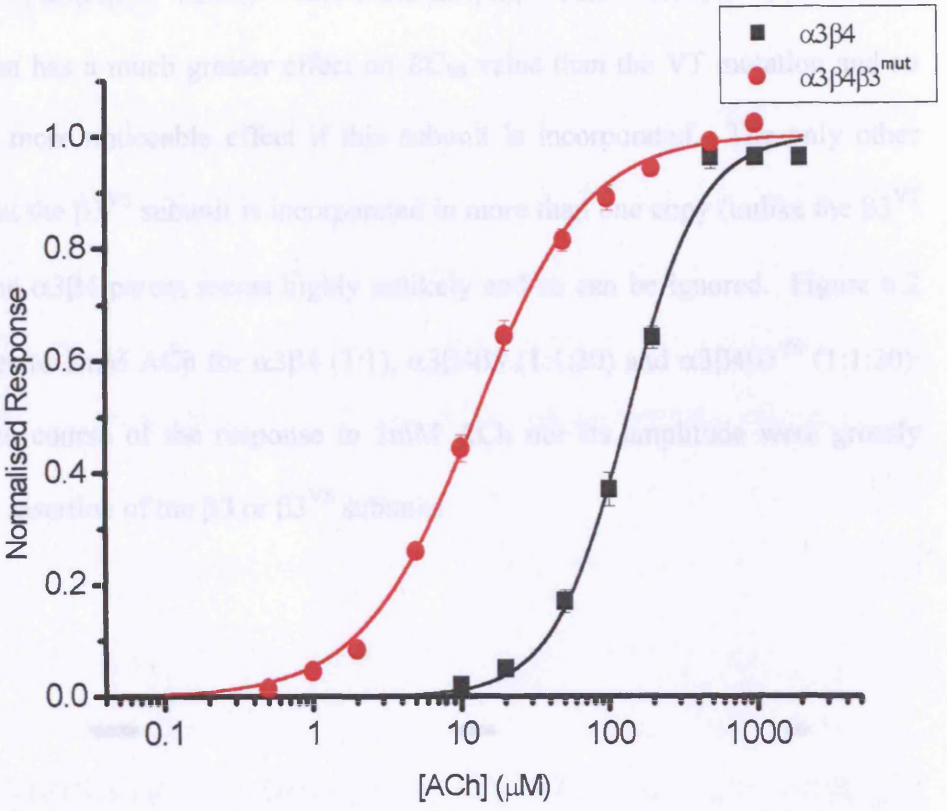

Figure 6.1: The $\beta3^{VS}$ subunit is inserted into the $\alpha3\beta4$ receptor to produce an $\alpha3\beta4\beta3^{VS}$ receptor as shown by the shifted EC_{50} value. Concentration-response curves for $\alpha3\beta4$ receptors (squares) and for the $\alpha3\beta4\beta3^{VS}$ receptors (circles) (n = 15 and 4, respectively). Lines are fits of the data with the Hill equation.
All responses were recorded from *Xenopus* oocytes voltage clamped at -70 mV in nominally calcium-free solution.

Figure 6.1 shows that the $\beta3^{VS}$ subunit has been incorporated into the $\alpha3\beta4$ receptor and so has produced the large shift in EC_{50} value. Comparison of these results ($\alpha3\beta4$ 1:1 : EC_{50} = 149 ± 7 μM, n_H = 1.69 ± 0.05, n=15; $\alpha3\beta4\beta3^{VS}$: EC_{50} = 12.9 ± 1.1 μM, n_H = 1.14 ± 0.05, n=4, EC_{50} and n_H: $p < 0.0001$, two-tailed Student's t-test) with those obtained in Groot-Kormelink *et al.* 1998 ($\alpha3\beta4$ 1:1 : EC_{50} = 180 ± 17 μM, n_H =

1.81 ± 0.09, n=7; α3β4β3^{VT} : EC_{50} = 42.6 ± 2.8 μM, n_H = 1.25 ± 0.04, n=9) shows that the VS mutation has a much greater effect on EC_{50} value than the VT mutation and so will provide a more noticeable effect if this subunit is incorporated. The only other explanation, that the β3^{VS} subunit is incorporated in more than one copy (unlike the β3^{VT} subunit) into the α3β4 parent seems highly unlikely and so can be ignored. Figure 6.2 shows responses to 1mM ACh for α3β4 (1:1), α3β4β3 (1:1:20) and α3β4β3^{VS} (1:1:20): neither the time course of the response to 1mM ACh nor its amplitude were grossly changed by the insertion of the β3 or β3^{VS} subunits.

Figure 6.2: Examples of current responses elicited by 1mM ACh on the three types of α3β4* receptors.

6.2 $\beta3^{VS}$ controls

Before the $\beta3^{VS}$ could be used, some control experiments needed to be carried out. The wild-type β3 subunit doesn't form functional homomeric or pair receptors, and we had to check that was true of the $\beta3^{VS}$ in the highly unlikely event that a TM2 mutation would massively change the properties of the subunit. Thus $\beta3^{VS}$ cRNA was injected at a high concentration either alone (10ng/μl) or together with α2, α3, α4, α6, β2 or β4 cRNA at a ratio of 1:20 (10:200 ng/μl) into oocytes. After incubation, oocytes were tested with 1mM bath-applied ACh. None of these combinations proved functional (all n=10).

6.3 Co-assembly of the β3 subunit with α3 and β2 subunits

Having proved β3 co-assembly with the α3 and β4 subunits, we proceeded to test β3 with other combinations and started with α3β2. Wildtype β3 subunit cRNA was co-injected with α3 and β2 subunit cRNA at the ratio of 1:1:20 into oocytes. For comparison purposes, α3 and β2 cRNA was also injected into oocytes within the same batch to produce α3β2 nAChRs. Whilst we observed robust functional expression in the α3 + β2 injected oocytes (n=13), the α3 + β2 + β3 injected oocytes responded to 1mM ACh with much smaller currents (4.3 ± 1.2 % of those measured in the α3β2 control oocytes, n=9). Even if we injected less β3 construct and used a ratio of 1:1:1 (n=7),

responses to 1mM ACh were effectively halved (55.0 ± 32.8 % of the α3β2 control oocytes).

The fact that increasing the amount of β3 construct expressed decreased the size of the functional response strongly suggests that receptors α3β2-type receptors that incorporate β3 are somehow "less functional" or indeed completely non-functional. The residual response we recorded could be produced by α3β2 receptors *without* β3. These could be expected to be present in larger numbers after the 1:1:1 injections than after 1:1:20 injections.

This dominant negative effect of β3 was totally unexpected, so what could have caused this decrease in current? One possibility that I easily tested and excluded was that the β3 subunit has caused the EC_{50} value to increase massively and that at 1mM ACh I am no longer measuring the maximum receptor response: similar results were obtained with the application of 20mM ACh concentration, the practical maximum ACh concentration possible using my standard stock solutions.

How could the incorporation of the β3 subunit reduce the total maximum current response to ACh of the cell (I_{max})?

I_{max} is dependent on a number of factors summarised in the equation in Figure 6.3.

$$\mathbf{I_{max} = N \bullet P_{open} \bullet \gamma \bullet V}$$

Figure 6.3: Equation for the maximum cell current (I_{max}) through a given receptor channel as a function of the number of receptor channels present (**N**), the maximum Popen value of the receptor (P_{open}), the conductance of the channel (γ) and the driving force (**V**).

The driving force V depends on the holding potential, which is clamped at -70 mV and can be excluded, and on the reversal potential. The latter could change only if the permeability of channels containing β3 is grossly different (unlikely, given that the TM2 sequence of β3 is very similar to that of nicotinic α subunits and that incorporation of β3 does not affect the calcium permeability of α3β4 receptors; Boorman *et al.* 2003) or if the expression of β3 has somehow destroyed the physiological ionic gradients in the oocyte, which is highly unlikely.

This leaves the other three variables to consider. N, the number of the receptors present at the cell surface could have been reduced, if β3 is interfering with receptor assembly or trafficking. Perhaps the maximum Popen of the resulting receptor has been reduced and therefore the receptor is in the membrane in large numbers but just doesn't happen to be particularly functional. Finally it is also possible that γ, the single-channel conductance of the receptor has been reduced. Perhaps it was a combination of all three.

We can test for an effect on the number of receptors (N) in the cell membrane by measuring the total number of specific binding sites through the use of radioliganded binding studies. Dr. Patricia Harkness has carried out this work which will be mentioned later on in this chapter (and excludes major decreases in surface expression).

Has β3 reduced the single-channel conductance (γ) of the receptor? This doesn't seem too likely. If the β3 subunit replaces a "classical" β in the pentamer, β3 should actually increase single channel conductance, because of net -2 change in the charge of the outer ring of charges in TM2. Indeed we found that α3β4β3 has a higher conductance than α3β4 (Boorman *et al.* 2003).

This leaves us with the possibility that it is the Popen of the receptor that is changed by β3 incorporation into α3β2. A way to test that is to express rather than β3, the $\beta3^{VS}$ mutant subunit. This is because it is likely that the main effect of the V to S mutation in the 9' position of TM2 is to destabilize the closed state and favour the opening of the receptor. So by co-injecting α3β2 with $\beta3^{VS}$ at a 1:1:20 ratio this could counteract any Popen lowering effect of the β3 subunit in its wild-type form.

6.4 Rescue of the α3β2β3 receptor by $\beta3^{VS}$

Figure 6.4: Examples of current responses elicited by 1mM ACh on the three types of α3β2* receptors.

Figure 6.4 shows representative traces of the responses to 1mM ACh for α3β2, α3β2β3 and α3β2β3^{VS}. As can be seen the β3^{VS} appears to have reversed the effect caused by β3 on α3β2-containing receptors. The response of α3β2β3^{VS} receptors to 1mM ACh (n=4) averaged 104 ± 25 % of those of α3β2 (n=13) receptors. This strongly suggests that the effect of β3 on I_{max} is due to a reduction in the Popen of the receptor. It is difficult to see how an effect of β3^{WT} on receptor number or on single-channel conductance could be reversed by expressing β3^{VS}.

It is possible (though unlikely) that the rescue we observed is due to the fact that the mutant β3^{VS} subunit (contrary to the WT subunit) is somehow not assembled and therefore what is being recorded is actually the response of pure α3β2 receptors. We can exclude this possibility by examining the concentration-response curves for α3β2 alone and α3β2β3^{VS} in Figure 6.5. It is clear that the β3^{VS} is incorporated along with the α3 and β2 subunits to produce a distinct receptor.

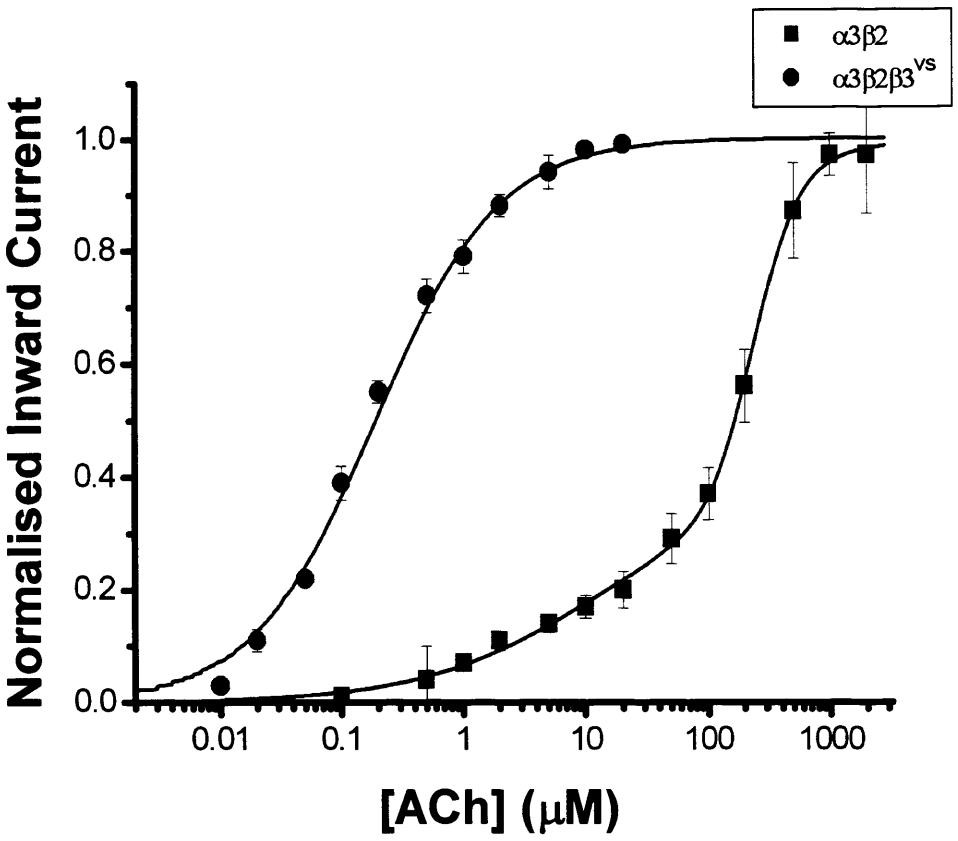

Figure 6.5: The $\beta3^{VS}$ subunit is inserted into the $\alpha3\beta2$ receptor to produce a functional $\alpha3\beta2\beta3^{VS}$ receptor. This insertion is confirmed by the shifted EC_{50} value due to the mutation in the β3 subunit. Concentration-response curves for $\alpha3\beta2$ receptors (squares) and for the $\alpha3\beta2\beta3^{VS}$ receptors (circles) (n = 4, for both). Note the two-component fit of the pair receptor compared to the single-component fit of the triplet receptor. It is possible that this is due to alternate stoichiometries for the pair receptor (see Chapter 9). Lines are fits of the data with the Hill equation.
All responses were recorded from *Xenopus* oocytes voltage clamped at -70 mV in nominally calcium-free solution.

Figure 6.5 shows that $\alpha3\beta2$ produces a biphasic curve with two components having EC_{50} of 11.6 ± 9.4 and 238 ± 11μM (n_H = 0.62 ± 0.1 and 2.34 ± 0.32, respectively, n = 4). A possible explanation of this phenomenon is that $\alpha3\beta2$ may exist in two different stoichiometric forms (probably $2\alpha:3\beta$ and $3\alpha:2\beta$; see Chapter 9 and

Nelson *et al.* 2003 for a similar observation for α4β2 receptors). Both forms are present when a 1:1 cRNA injection ratio is used, but the insertion of the $\beta3^{VS}$ subunit makes the curve monophasic, possibly because most receptors now are $\alpha3\beta2\beta3^{VS}$ in a 2:2:1 ratio ($\alpha3\beta2\beta3^{VS}$: EC_{50} = 0.19 ± 0.02 μM, n_H = 0.86 ± 0.03, n=4, comparison with α3β2 EC_{50}: $p < 0.05$, n_H: $p < 0.005$, two-tailed Student's t-test). This work is covered in more detail in Chapter 9.

These data showed an unexpected effect for the β3 subunit, after leaving the α3β4β3 receptor infuriatingly similar to the α3β4 receptor suddenly the β3 was almost completely knocking out the α3β2 receptor, the question now was did the β3 co-assemble with any of the other nAChR subunit combinations and if so did they produce unchanged α3β4β3-like receptors or knocked-out α3β2β3-like receptors. The next one tested was β3 with α4 and β2.

6.5 Co-assembly of the β3 subunit with α4 and β2 subunits

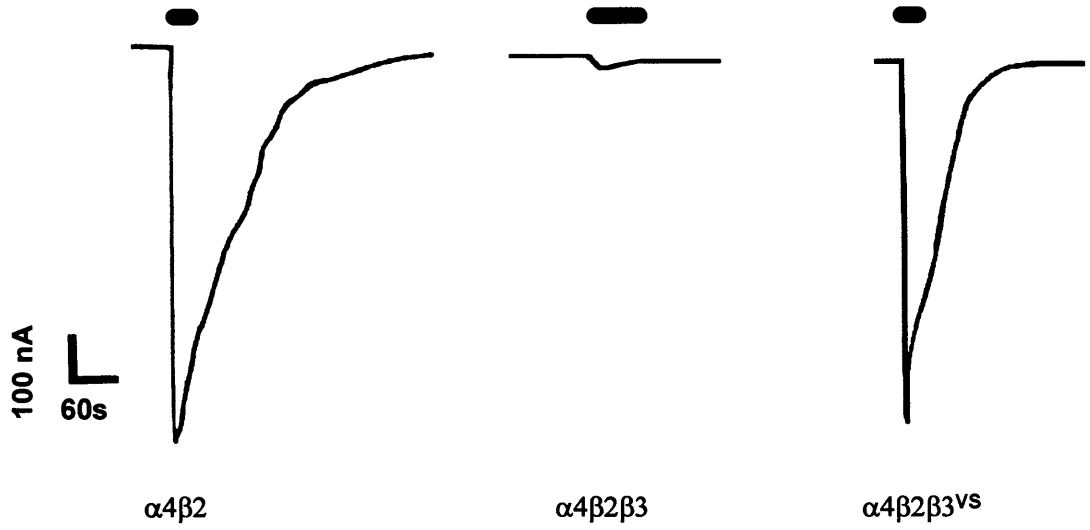

Figure 6.6: Examples of current responses elicited by 1mM ACh on the three types of α4β2* receptors.

Oocytes were injected with α4β2 (1:1), α4β2β3 (1:1:20) and α4β2β3^{VS} (1:1:20) and their responses to 1mM ACh are shown in Figure 6.6. Again the robust expression of the pair α4β2 receptor was knocked out by β3 incorporation but rescued by the co-injection of β3^{VS}. The average current response to 1mM ACh of α4β2β3 (n=17) was 1.7 ± 0.4 % of the response recorded in "control" α4β2 receptors, whereas in α4β2β3^{VS} (n=10) the response was 334 ± 33 % of α4β2 (n=7). Similar results were seen with ratios to 1:1:1 (n = 5; 3.6 ± 0.8 % of control).

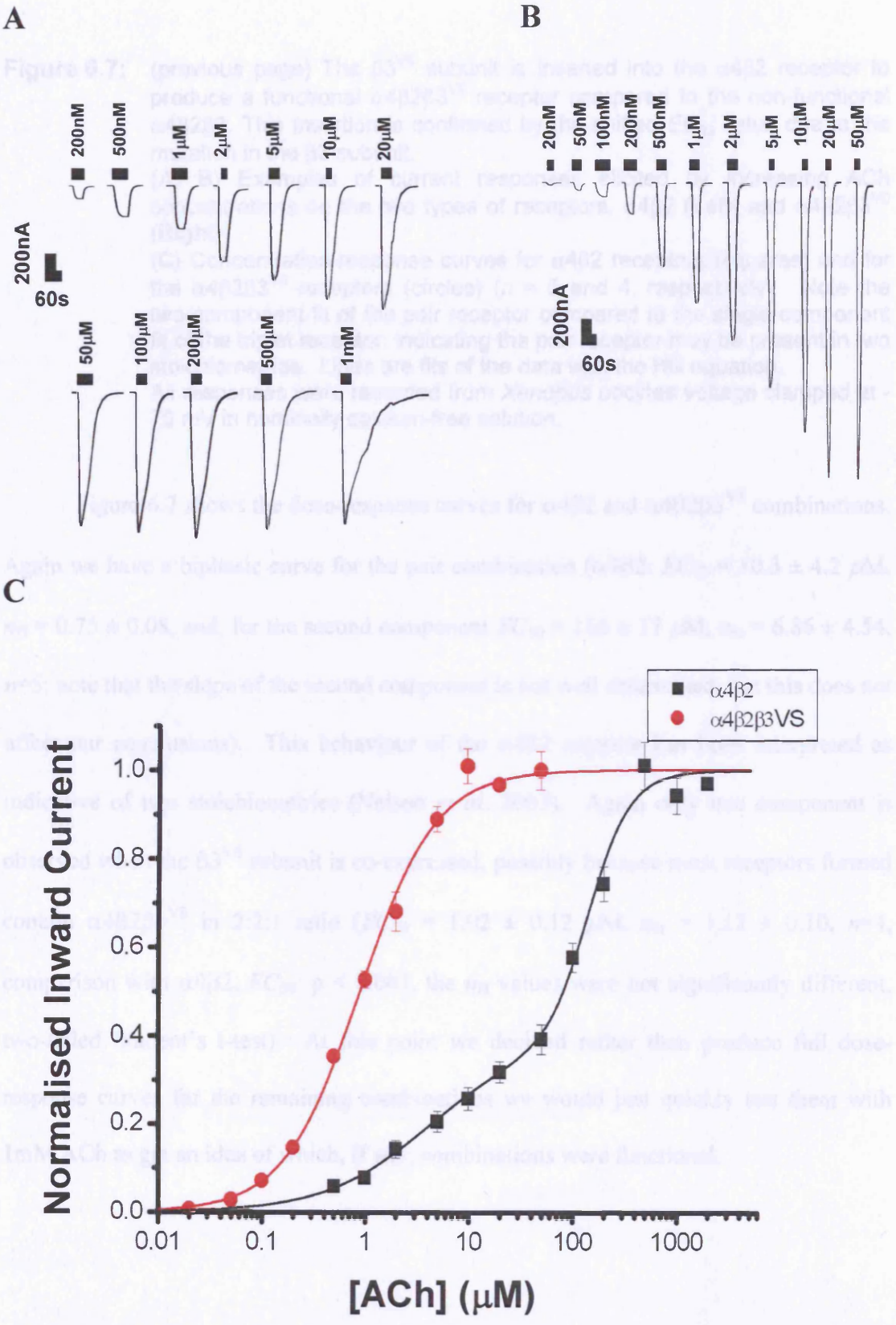
A
200nM
500nM
1μM
2μM
5μM
10μM
20μM
200nA
60s
50μM
100μM
200μM
500μM
1mM
B
20nM
50nM
100nM
200nM
500nM
1μM
2μM
5μM
10μM
20μM
50μM
200nA
60s
C
α4β2
α4β2β3VS
Normalised Inward Current
1.0
0.8
0.6
0.4
0.2
0.0
0.01
0.1
1
10
100
1000
[ACh] (μM)

Figure 6.7: (previous page) The $\beta3^{VS}$ subunit is inserted into the $\alpha4\beta2$ receptor to produce a functional $\alpha4\beta2\beta3^{VS}$ receptor compared to the non-functional $\alpha4\beta2\beta3$. This insertion is confirmed by the shifted EC_{50} value due to the mutation in the $\beta3$ subunit.
(**A, B**) Examples of current responses elicited by increasing ACh concentrations on the two types of receptors, $\alpha4\beta2$ (**Left**) and $\alpha4\beta2\beta3^{VS}$ (**Right**)
(**C**) Concentration-response curves for $\alpha4\beta2$ receptors (squares) and for the $\alpha4\beta2\beta3^{VS}$ receptors (circles) (n = 5 and 4, respectively). Note the two-component fit of the pair receptor compared to the single-component fit of the triplet receptor, indicating the pair receptor may be present in two stoichiometries. Lines are fits of the data with the Hill equation.
All responses were recorded from *Xenopus* oocytes voltage clamped at -70 mV in nominally calcium-free solution.

Figure 6.7 shows the dose-response curves for $\alpha4\beta2$ and $\alpha4\beta2\beta3^{VS}$ combinations. Again we have a biphasic curve for the pair combination ($\alpha4\beta2$: EC_{50} = 10.3 ± 4.2 μM, n_H = 0.75 ± 0.08, and, for the second component EC_{50} = 166 ± 17 μM, n_H = 6.86 ± 4.54, n=5; note that the slope of the second component is not well determined, but this does not affect our conclusions). This behaviour of the $\alpha4\beta2$ receptor has been interpreted as indicative of two stoichiometries (Nelson *et al.* 2003). Again only one component is observed when the $\beta3^{VS}$ subunit is co-expressed, possibly because most receptors formed contain $\alpha4\beta2\beta3^{VS}$ in 2:2:1 ratio (EC_{50} = 1.02 ± 0.12 μM, n_H = 1.12 ± 0.10, n=4, comparison with $\alpha4\beta2$, EC_{50}: $p < 0.001$, the n_H values were not significantly different, two-tailed Student's t-test). At this point we decided rather than produce full dose-response curves for the remaining combinations we would just quickly test them with 1mM ACh to get an idea of which, if any, combinations were functional.

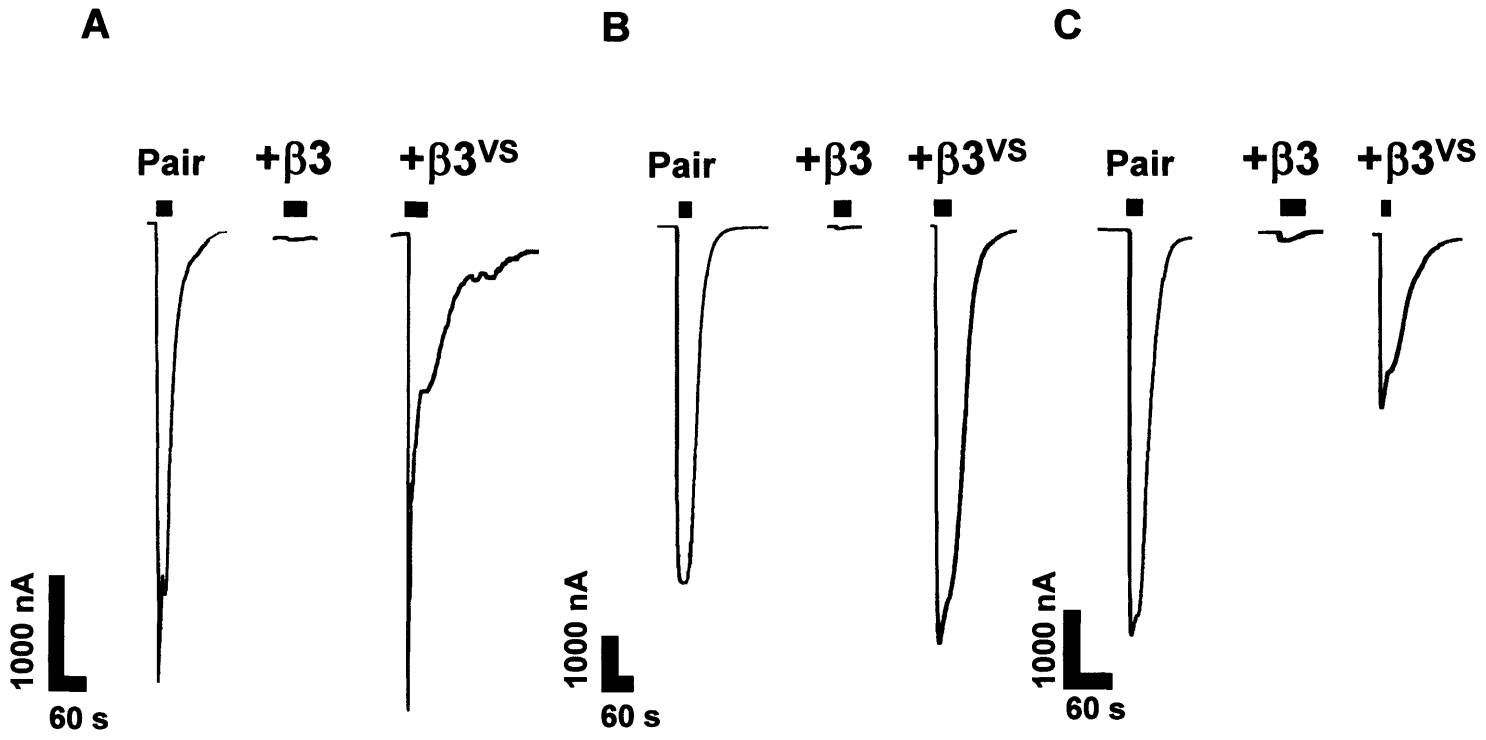

Figure 6.8: Examples of current responses elicited by 1mM ACh on the three types of receptors for α2β2 (**A**), α2β4 (**B**) and α4β4 (**C**) background pair receptors alone (co-expressed with wildtype β3 or with $\beta3^{VS}$. Note the knock-out of the response by the β3 and the rescue by $\beta3^{VS}$.

6.6 Co-assembly of the β3 subunit with α2β2, α2β4 and α4β4

Figure 6.8 shows that the β3 and $\beta3^{VS}$ subunits have the same effect when co-injected with α2β2, α2β4 and α4β4 as they had on α3β2 and α4β2. The average current responses to 1mM expressed as percentage of the response of the "control" pair receptor expressed alone were α2β2β3 (0 ± 0 %, *n*=11), $\alpha2\beta2\beta3^{VS}$ (372 ± 51 %, *n*=10) α2β4β3 (0.9 ± 0.3 %, *n*=5), $\alpha2\beta4\beta3^{VS}$ (22 ± 5 %, *n*=8), α4β4β3 (2.7 ± 0.7 %, *n*=9), $\alpha4\beta4\beta3^{VS}$ (72 ± 21 %, *n*=10) compared to the corresponding pair parent combination (α2β2: *n*=12; α2β4 *n*=5; α4β4: *n*=11, see Table 6.1). The β3 subunit appears to exert a strong dominant negative effect on all the functional pair receptor combinations with the possible exception of the α3β4 combination. We tested again this combination, measuring just responses to 1mM ACh rather than dose-response curves and found that the α3β4β3 receptor produced around 73 ± 12 % the current seen with α3β4. The table below summarises all the results of β3 and $\beta3^{VS}$ coexpression with pair receptors.

Combo Injected (1:1/1:1:20)	Response to 1 mM ACh ± SEM (nA)	Functional Expression as a Percentage ± SEM (parent pair =100)	*n*	*p* value (vs pair receptor)	*p* value (vs pair + β3 receptor)
α2 + β2	216 ± 36	100 ± 17	12	-	-
α2 + β2 + β3	0 ± 0	0 ± 0	11	< 0.01	-
α2 + β2 + $β3^{VS}$	799 ± 110	372 ± 15	10	< 0.05	< 0.001
α2 + β4	13450 ± 1599	100 ± 12	5	-	-
α2 + β4 + β3	124 ± 42	0.9 ± 0.3	5	< 0.01	-
α2 + β4 + $β3^{VS}$	3018 ± 678	22 ± 5	8	NS	< 0.05
α3 + β2	1853 ± 352	100 ± 19	13	-	-
α3 + β2 + β3	79 ± 23	4 ± 1.2	9	< 0.001	-
α3 + β2 + $β3^{VS}$	1929 ± 466	104 ± 25	4	NS	< 0.05
α3 + β4	3583 ± 290	100 ± 23	16	-	-
α3 + β4 + β3	2616 ± 430	73 ± 12	34	< 0.001	-
α3 + β4 + $β3^{VS}$	2629 ± 680	73 ± 19	7	NS	NS
α4 + β2	1083 ± 139	100 ± 13	7	-	-
α4 + β2 + β3	18 ± 4	1.7 ± 0.4	17	< 0.01	-
α4 + β2 + $β3^{VS}$	3621 ± 355	334 ± 33	10	NS	< 0.001
α4 + β4	2556 ± 867	100 ± 34	11	-	-
α4 + β4 + β3	68 ± 17	2.7 ± 0.7	9	< 0.001	-
α4 + β4 + $β3^{VS}$	1970 ± 315	77 ± 12	10	NS	< 0.05

Table 6.1: Summary of the effect of co-injecting β3 and $β3^{VS}$ with various pair combinations at a ratio of 1:1 and 1:1:20. Statistical analysis by Kruskal-Wallis one-way nonparametric ANOVA followed by Dunn's *post hoc* multiple comparisons test. NS = not significant.

Our next question then was does this dominant negative effect of β3 also apply to native neuronal nAChRs?

6.7 Effect of β3 on native nAChRs in primary hippocampal cultures (data courtesy of Dr Marco Beato)

Clearly, if we wish to transfect the β3 subunit into neurones we need either an organotypic slice or a dissociated primary culture. In our Dept. the latter technique is in routine use by Dr Phil Thomas, who kindly provided us with primary cultures of hippocampal neurones obtained from embryonic rats (E17). Untransfected neurones were compared to hippocampal neurones transfected (Effectene©) with either α7, β3 or $\beta3^{VS}$ cDNA. Dr. Marco Beato recorded from these cells using whole-cell patch clamp at -70mV. 3mM ACh was applied using a U-tube to produce a rapid application of agonist. The neurones were co-transfected with green-fluorescent-protein (GFP) and only the cells which glowed green were considered transfected. The near totality (25 out of 27) of the untransfected neurones responded to 3mM ACh with fast inward currents: these are thought to represent responses through α7 receptors (for a review see Albuquerque, 1997). The α7-nature of these responses was confirmed by transfecting with α7 producing increased currents of the same type. These two findings provided us with controls to show the transfection worked and didn't produce unexpected side-effects and an estimation of the proportion of false negatives we were likely to come across. Transfection with β3 had a striking dominant negative effect: 34 out of 38 transfected (i.e. fluorescing) neurones did not respond to 3mM ACh at all. Transfection with $\beta3^{VS}$ did produce a rescue of nicotinic responses and 48 out of 53 $\beta3^{VS}$ transfected neurones produced currents comparable to the α7 untransfected neurones. This is summarised in Figure 6.9.

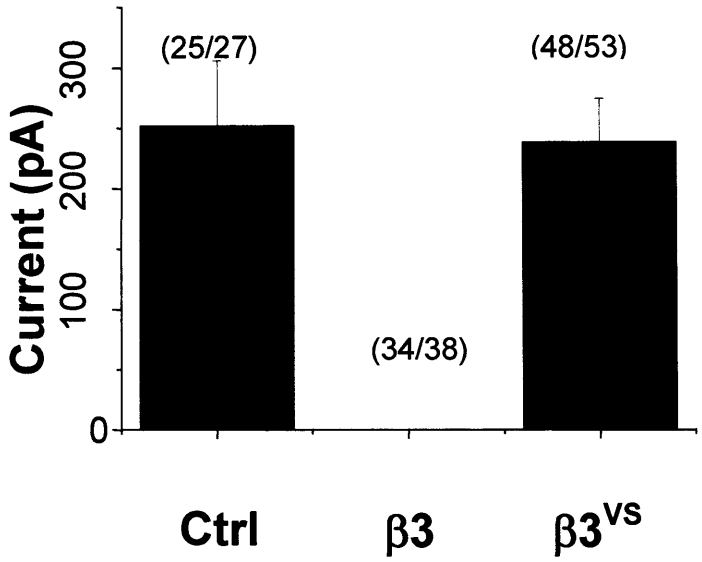

Figure 6.9: Summary of the average maximum currents elicited by 3mM ACh on hippocampal neurones either untransfected (**Ctrl**) or transfected with β3 (**β3**) or $\beta3^{VS}$ (**$\beta3^{VS}$**). Numbers in brackets above show the number of cells corresponding to the types of response shown in Figure 6.11. All responses were recorded from whole-cell patch-clamped neurones at -70 mV in nominally calcium-free solution.

Figure 6.10 shows example responses obtained by Dr. Beato. As can be seen, while the β3 transfected neurones show no response to 3mM ACh, $\beta3^{VS}$ transfected neurones produce relatively large currents which are markedly different in shape from the untransfected, α7-only neurones, proof that the $\beta3^{VS}$ subunit has been incorporated into the α7 receptor.

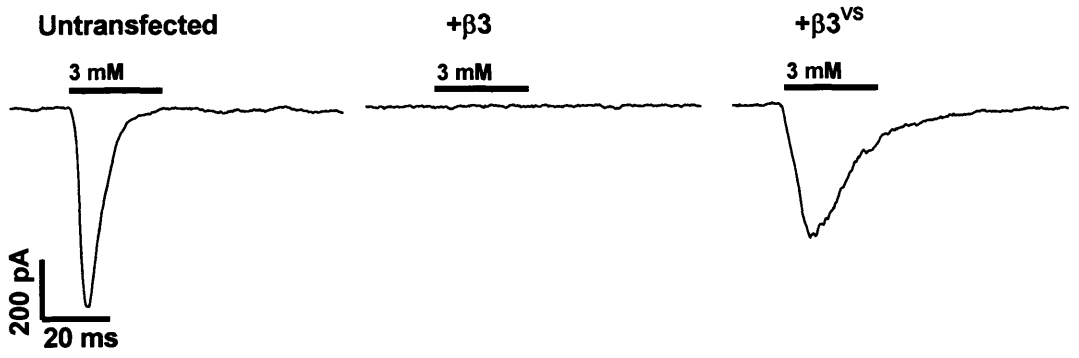

Figure 6.10: Examples of current responses elicited by 3mM ACh concentrations on neurones which were either untransfected or transfected with β3 or $\beta3^{VS}$. All responses were recorded from whole-cell patch-clamped neurones at -70 mV in nominally calcium-free solution. Note the knock-out of the intrinsic receptors by the β3 subunit and their return and change of shape of their responses by the transfection of $\beta3^{VS}$.

We then proceeded to test this effect for oocyte-expressed α7 receptors.

6.8 Co-assembly of the β3 subunit with α7 in oocyte-expressed receptors

Previously the co-injection of β3 subunit has been shown to reduce the ACh-evoked current of α7-injected oocytes without affecting the number of surface receptors measured by α- bungarotoxin binding (Palma *et al.* 1999). Co-injection of the β3 with α7 carrying a leucine-to-threonine mutation at residue 247 ($\alpha7^{L247T}$) produced a functional receptor markedly different with reduced nAChR activity, amplitude of current, transmitter sensitivity and faster rate of desensitisation when compared to the

nAChRs produced by $\alpha7^{L247T}$ alone so it was clear that the β3 was co-assembling with the α7 subunits. The precise stoichiometry of the α7β3 heteromer remains unclear.

To check whether the α7β3 receptor would be "rescued" by our VS mutation in the β3 subunit(s) present, we co-expressed α7 with β3 or $\beta3^{VS}$ at ratios of 1:10 and 1:20 and measured responses to 1mM ACh. As before, co-expression with β3 almost abolished functional expression of the α7-containing receptor to 12.4 ± 3.5 % (1:10, n=14) and 4.3 ± 2.3 % (1:20, n=8) of that of the α7 monomer alone reproducing the findings of Palma *et al.* 1999 and illustrating the relationship between amount of β3 present and the resulting reduction in current (Table 6.2).

However, in this case the $\beta3^{VS}$ mutation failed to produce a significant recovery in the ACh-evoked current with $\alpha7\beta3^{VS}$ having 12 ± 3 % of the functional expression of the α7 receptor compared to 4 ± 2 % of α7β3. This result is in contrast to the "rescue" observed with $\beta3^{VS}$ expression in hippocampal primary cultures by my colleague Dr Marco Beato (see above). An obvious difference in the experimental conditions for the work on oocytes and on neurones lies in the effective agonist application rate for the two systems. This is much slower for the oocyte, because of size of the oocyte, irrespective of the perfusion rate and bath volume. This factor poses an important limitation to the precision with which responses of a fast-desensitising receptor such as α7 can be measured. It is hard to know whether this likely underestimate of the real response could be greater for α7 + $\beta3^{VS}$ and thus introduce a systematic bias in our results. The ideal control would be to express α7 with and without β3 in a mammalian cell line.

Unfortunately, successful expression of α7 in a mammalian cell line requires stable transfection and is far from trivial (Puchacs *et al.* 1994; Zhao *et al.* 2003)

It has recently been reported that 5-hydroxyindole (5-HI) potentiates α7 nAChR mediated currents in oocytes (Gurley *et al.* 2000). It is completely unclear what the mechanism is for this enhancement and whether it can be ascribed to a slowing of α7 desensitisation, but we thought that it was worth testing on an empirical basis.

Table 6.2 summarises the maximum current recorded from 1mM ACh in the presence and absence of 5mM 5-HI for all three receptor combinations. As can be seen, whereas in the absence of 5HI, $\beta3^{VS}$ only produced a marginal increase in the ACh-evoked current (33.6 ± 7.2 nA vs 11.8 ± 6.4 nA, n=8), this recovery was much more substantial in the presence of indole (383 ± 57 nA vs 98.4 ± 28 nA, n=8, $p< 0.05$ Kruskal-Wallis one-way nonparametric ANOVA and Dunn's *post hoc* multiple comparisons test). Figure 6.11 shows some representative traces produced by 1mM ACh co-applied with 5mM 5-HI.

	Average maximum current to 1mM ACh ± SEM (nA)		*n*	*p* value (vs α7)		*p* value (vs α7β3)	
	control	+ 5mM Indole		Ctrl	Indole	Ctrl	Indole
α7	**273 ± 54** (100%)	**968 ± 145** (100%)	**8**	-	-	-	-
α7β3	**11.8 ± 6.4** (4.3 ± 2.3 %)	**98.4 ± 28.0** (10.2 ± 2.9 %)	**8**	**<0.001**	**< 0.01**	-	-
$\alpha7\beta3^{VS}$	**33.6 ± 7.2** (12.3 ± 2.6 %)	**383 ± 57** (39.5 ± 5.9 %)	**8**	**< 0.05**	**NS**	**NS**	**< 0.05**

Table 6.2: Summary of the average maximum currents elicited by 1mM ACh for oocytes injected with different α7 cRNA combinations in the presence and absence of 5mM 5-hydroxy-indole. All responses were recorded from *Xenopus* oocytes voltage clamped at -70 mV in nominally calcium-free solution. Statistical analysis by Kruskal-Wallis one-way nonparametric ANOVA followed by Dunn's *post hoc* multiple comparisons test. NS = not significant.

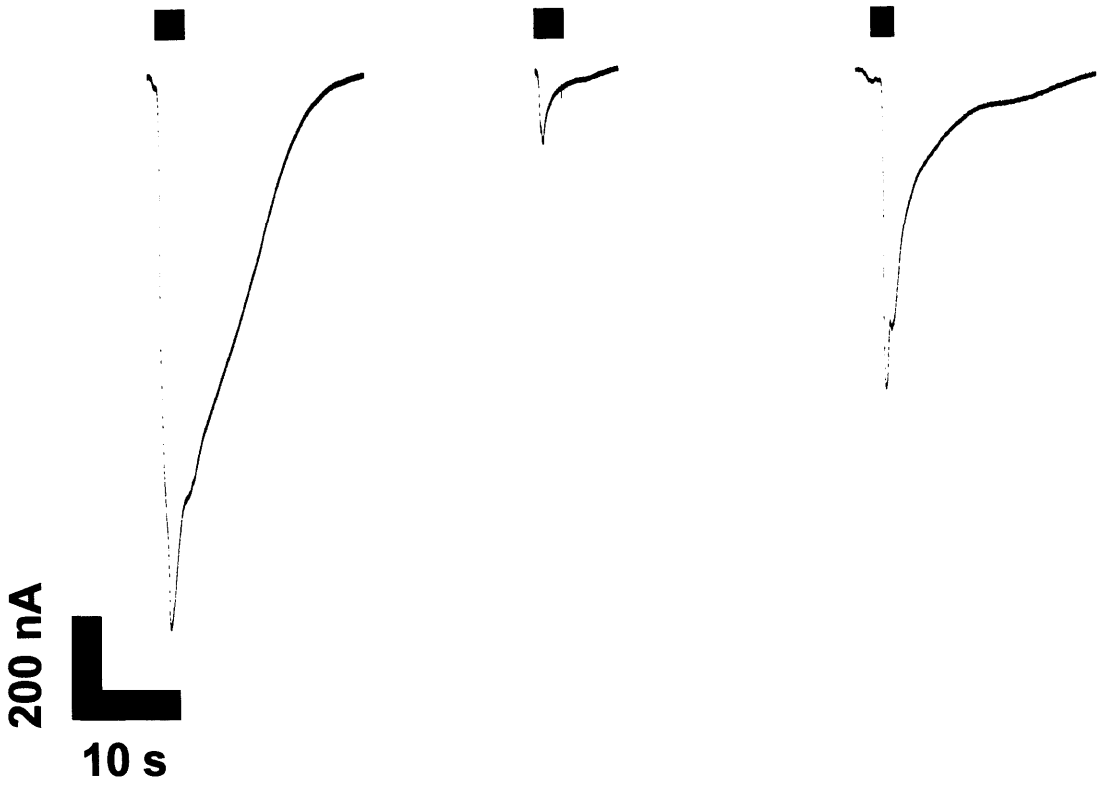

Figure 6.11: Examples of current responses elicited by 1mM ACh on the three types of receptors for α7*. α7 (left), α7β3 (middle) and α7β3^{VS} (right). Note the knock-out of the response by the β3 and the rescue by β3^{VS}. Also note the fast timescale of the responses.

It is hard to explain why the β3^{VS} rescue of α7 responses could be observed only in 5HI and it would be pointless to speculate in the absence of data on the mechanism of action of 5HI. Nevertheless, this uncertainty does not affect our main finding that, for α7 native and recombinant receptors functional expression was knocked out by β3 and resurrected by the β3^{VS} subunit, in a pattern similar to that observed for other neuronal nicotinic combinations.

6.9 β3 co-assembles with α6-containing receptors

It was ironic after spending so long trying to detect any major differences caused by the incorporation of the β3 subunit into α3β4 receptors that we should have had a clean sweep of knock-outs for all the major functional pair receptor combinations and the α7 monomeric receptor. One subunit we hadn't tested was the α6 subunit. Importantly, this subunit appears to co-localise with β3 subunit in native tissues and a selective α6α3β2β3 conotoxin (α-conotoxin PIA) has been identified (Dowell *et al.* 2003). Would α6 receptors also be knocked-out by β3?

Despite there being plenty of evidence of functional α6 receptors in native tissues, functional α6 receptors are notoriously difficult to express in heterologous expression systems such as the oocyte. The α6 (cloned in 1991, Deneris *et al.* 1991) had previously been considered another "orphan" receptor as it doesn't form functional receptors when expressed either alone or with any other single nAChR subunit. In 1997, the co-expression of chicken α6 and human β4 in oocytes was found to produce only barely detectable currents to high concentrations of ACh with an average maximum of <100nA compared to 2-3μA for the equivalent amount of α3β2 and α3β4 RNA (Gerzanich *et al.* 1997). As will be shown in Chapter 7, we ourselves tried to produce β2_α6 and β4_α6 tandem constructs, none of which were functional (Groot-Kormelink *et al.* 2004). We decided to test α6-containing receptors with the β3 and $\beta3^{VS}$. The first test was to co-inject α6 and β3 or $\beta3^{VS}$ subunits (at a ratio of 1:20) to check whether they produced functional pair receptors. Unsurprisingly they failed to produce any response to 1mM ACh (*n*= 19-20) as shown in Figure 6.12.

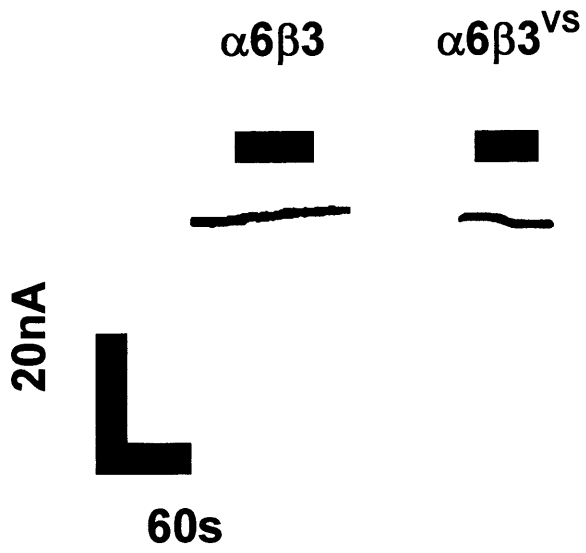

Figure 6.12: Examples of current responses elicited by 1mM ACh on α6 and β3 pair receptors. Note the lack of response even in the presence of $\beta3^{VS}$.

Having confirmed that α6 and β3 didn't form a functional pair receptor we decided to look to see whether they could produce a functional triplet receptor by expressing the β3 with α6 and either β2 or β4 at a ratio of (α6:β2-4:β3) 1:1:20. In parallel we checked to see whether the function of α6β2 and α6β4 was improved by inserting the 9' leucine-to-threonine mutation (LT) into the β subunits we have used previously at a ratio of 1:1 (Boorman *et al.* 2000). Judging by the >75% sequence homology between α6 and α3 (Le Novere *et al*, 1995) the α6 would be expected to form a receptor of a 2:3 stoichiometry with β2 or β4 subunits. It was possible that this receptor does assemble and is present in the membrane and therefore it was possible that the presence of multiple copies of the LT mutation could improve this receptor's function. Using a similar line of reasoning we also checked the effect of inserting the $\beta3^{VS}$ into a

possible α6β2-4β3 receptor (injection ratio 1:1:20). These were all injected into oocytes and tested with 1mM ACh (Figure 6.13).

As can be seen the α6β2* receptors did not produce any significant ACh-evoked currents even with the presence of LT mutations or the β3 subunit. However with the $\beta3^{VS}$ larger responses began to appear (average response to 1mM: 124 ± 27 nA, *n*=8). This pattern was repeated with the α6β4* receptors. All the pair and the wildtype triplet receptors produced small currents to 1mM ACh, currents which were not increased by the presence of multiple LT mutations however the presence of the $\beta3^{VS}$ subunit produced large currents (average response to 1mM: 556 ± 140 nA, *n*=15). These findings are summarised in Table 6.3.

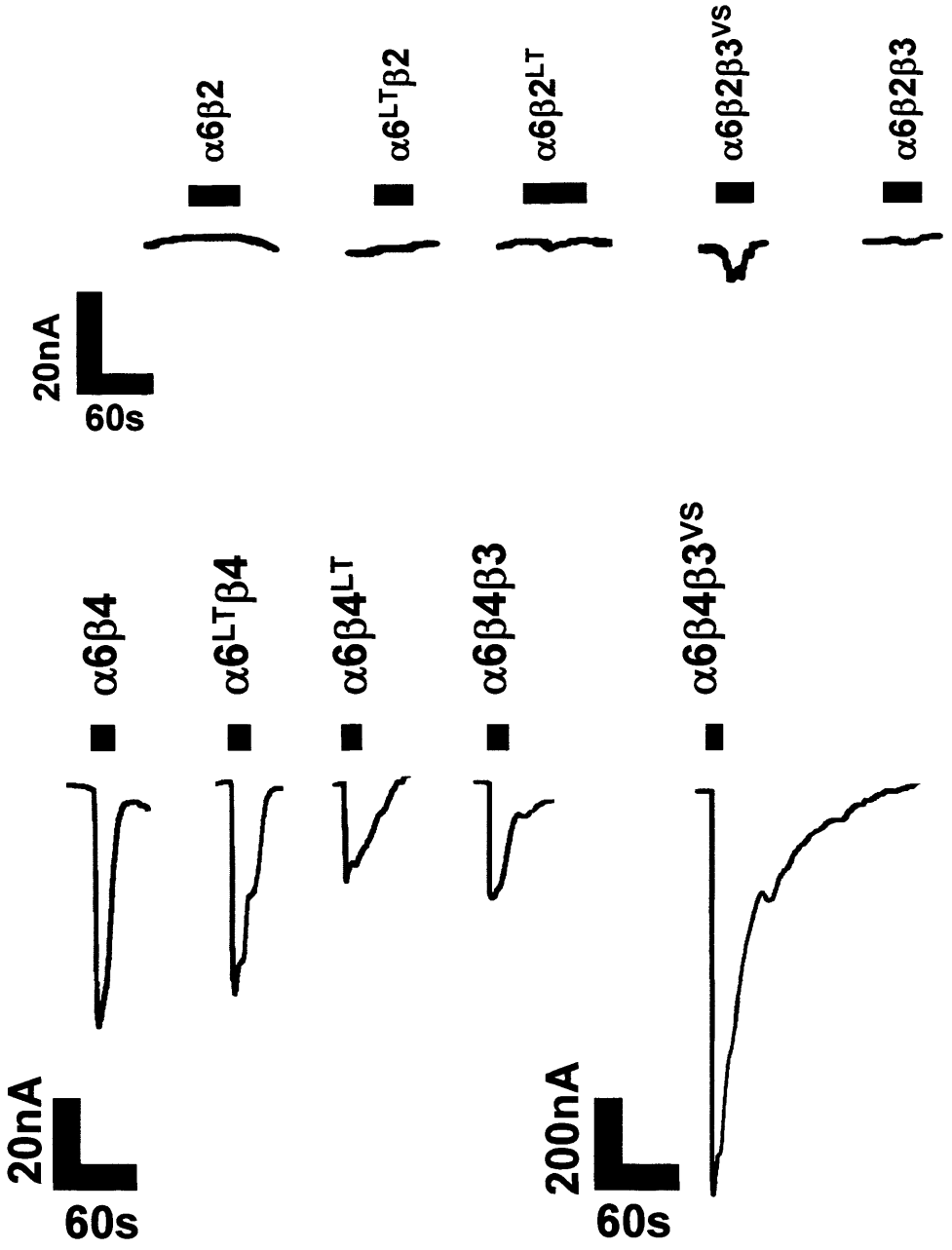

Figure 6.13: Examples of current responses elicited by 1mM ACh on different α6* receptors. Note the lack of response in α6β2* receptors even in the presence of $\alpha6^{LT}$ or $\beta2^{LT}$, with small but noticeable currents apparent only when $\beta3^{VS}$ is added. Also note the size of responses in α6β4* receptors even in the presence of $\alpha6^{LT}$ or $\beta4^{LT}$ compared with the large currents apparent when $\beta3^{VS}$ is introduced shown by the differences in scale used.

	Average maximum current to 1mM ACh ± SEM (nA)	*n* =	*p* value (vs pair)	*p* value (vs β3 receptor)
α6β2	3.0 + 2.5	8	-	-
$\alpha6^{LT}\beta2$	0 ± 0	4	NS	-
$\alpha6\beta2^{LT}$	0.75 ± 0.75	4	NS	-
α6β2β3	1 ± 0.68	8	NS	-
$\alpha6\beta2\beta3^{VS}$	124 ± 27	8	< 0.001	< 0.001
α6β4	49.4 ± 14.9	8	-	-
$\alpha6^{LT}\beta4$	31.8 ± 10.4	4	NS	-
$\alpha6\beta4^{LT}$	14.3 ± 5.7	4	NS	-
α6β4β3	13.7 ± 5.1	8	NS	-
$\alpha6\beta4\beta3^{VS}$	556 ± 141	8	< 0.001	< 0.001

Table 6.3: Summary of the average maximum currents elicited by 1mM ACh for oocytes injected with different cRNA combinations. All responses were recorded from *Xenopus* oocytes voltage clamped at -70 mV in nominally calcium-free solution. Statistical analysis by Kruskal-Wallis one-way nonparametric ANOVA followed by Dunn's *post hoc* multiple comparisons test. NS = not significant.

These results show that there is little or no functional expression following the expression of α6 with β2 or β4 and β3 and obviously beg the question of how receptors containing the α6 subunit can be functional in neurones. While it has been suggested that β3 may be important in the expression of such receptors (Kuryatov 2000), it is clearly not sufficient on its own to produce functional α6-containing receptors. The possibility is

that the α5 subunit is also required, as the surface binding produced by the expression of α6β4β3 is massively increased if α5 is co-expressed (Grinevich *et al.* 2005).

6.10 Conclusion

The progress of this project has following an interesting path and we have had more than our fair share of good fortune in the precise order we carried the experiments out.

β3 co-assembled with α3 and β4 subunits in oocytes but did not substantially change the properties of the resulting triplet receptor compared to the parent pair receptor. Subsequent testing of the β3 subunit with α2β2, α2β4, α3β2, α4β2, α4β4 and α7 receptors has shown that the β3 co-assembles and produces an almost complete knock-out of the functional expression of these receptors (see Figure 6.14 for a summary).

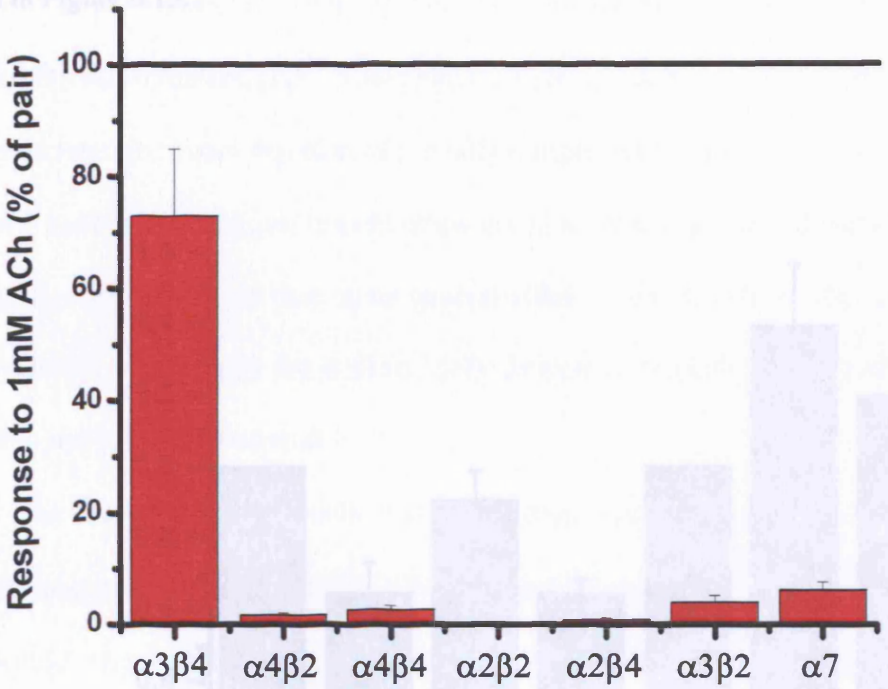

Figure 6.14: Summary of the effect of β3 incorporation on a range of functional nAChR combinations injected into *Xenopus* oocytes. The effect is shown as a percentage of the current evoked by 1mM ACh compared to the equivalent amount of cRNA injected without the β3 (ratios = 1:1:20 or 1:20). All responses were recorded from *Xenopus* oocytes voltage clamped at -70 mV in nominally calcium-free solution.

Our interpretation of these results, namely that β3 reduced the receptor's maximum Popen value rather than the number of receptors on the surface of the cell was confirmed by the work of Dr. Patricia Harkness who carried out binding studies on transiently transfected tsA cells (oocyte work was attempted but the levels of all receptor types were too low to measure). Her findings for ^{3}H-epibatidine on α3β4, α3β4β3,

$\alpha3\beta4\beta3^{VS}$, $\alpha3\beta4\beta3^{KO}$ (Delilah 4, see Chapter 5), $\alpha4\beta2$, $\alpha4\beta2\beta3$ and $\alpha4\beta2\beta3^{VS}$ are shown in Figure 6.15.

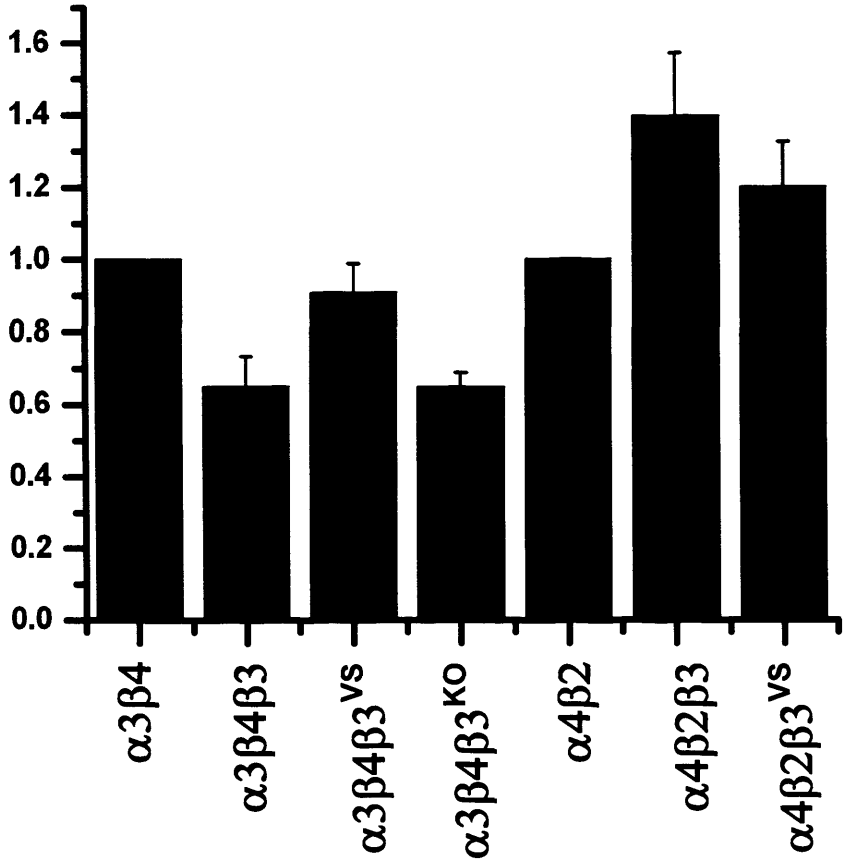

Figure 6.15: Normalised binding of ^{3}H-epibatidine to the surface of transiently transfected tsA cells corrected for protein (mean ± SEM, *n*=7, for all).

The binding studies show that the co-expression of β3 subunits has relatively minor effects on the surface expression of nAChRs. None of these small changes are sufficient to explain the approximately 97% decrease in $\alpha4\beta2$ responses produced by β3

co-expression in oocytes, or their reversal by $\beta3^{VS}$ expression. The same reasoning applies to $\alpha3\beta4$ receptors, where the functional knockout produced by co-transfection with the Delilah 4 mutant, $\beta3^{KO}$ (Chapter 5) is only associated with a small reduction in surface expression. From this data, along with our previous work, it is clear that for both Delilah 4 and the β3 wildtype, the reduction in cell current is due to a direct effect on the receptor's properties rather than some general effect on expression levels. In both case large numbers of receptors are present, fully formed in the cell surface membrane but happen to not be very functional.

The similarity of the results that we obtained with α7 receptors in hippocampal neurones suggests that the effect of β3 may apply to native receptors in native tissues. This would mean β3 could have an important effect on the regulation of nAChR responses and potentially on all the aspects of nervous system transmission downstream regulated by nAChRs in turn.

So why is the $\alpha3\beta4$ receptor "spared" when all the other functional combinations of nAChRs are knocked-out by β3 insertion? The maximum Popen value of a receptor is determined by the following equation, where E is the efficacy:-

$$\textbf{Maximum Popen} = \frac{E}{E+1}$$

The value of E is only known for the muscle-type nAChR as its determination requires single-channel methods, so what follows is essentially plausible speculation. If

the α3β4 had a particularly high E value of say 100, giving a maximum Popen value of 0.99 and the insertion of a β3 subunit reduced the E value by 90% (for arguments' sake) then the α3β4β3 receptor would still have an E of 10 and therefore a maximum Popen value of 0.909 and so the two receptors would be barely distinguishable from each other. However if the other receptors, for example α4β2, have low efficacies, for instance 1, the effect of a 90% reduction in E value would change the maximum Popen from a reasonable 0.5 to a barely detectable 0.091 causing a marked reduction in the Popen values and therefore in the recorded current. With no idea of the E values for neuronal nAChRs, or the amount it is reduced by β3 insertion, this remains purely speculation, although if it is correct you can see how it might explain our findings and the sparing of α3β4. It must be noted that the above maximum Popen equation only really holds for a simple del Castillo-Katz type receptor mechanism (del Castillo & Katz, 1957), as the receptor mechanism for the nAChR receptor is almost certainly more complicated than this a different maximum Popen equation is likely to hold (see Colquhoun, 1998 for some examples). This however doesn't necessarily mean our speculation on an effect on E by β3 insertion is incorrect just that it may be more complicated than illustrated here and as such the above del Castillo-Katz maximum Popen equation is a handy rough first approximation. Further research into the possible effect of β3 on receptor E would require single channel recording and as such is, again, beyond the remit of my PhD.

So what role do these findings suggest for the β3 subunit *in vivo*?

At its most general, if the β3 knock-out effect on the majority of nAChRs combinations occurs *in vivo*, it would give the β3 subunit the capability to act as a global "volume-control" for most neuronal nicotinic receptors. In principle, spatial and temporal changes in β3 expression could, if they occur, control overall nicotinic signals, while mostly sparing α3β4 (and maybe even up-regulating α6* receptors).

What this would mean to the nicotinic network as a whole is unclear at this time along with its significance, if any, to nicotinic pharmacology, pathophysiology, development and in addiction.

The expression of the β3 subunit is very localised in the CNS, where it is expressed mostly in dopaminergic and catecholaminergic areas. In these areas a variety of other subunits are expressed, including α3 and α4: if our results can be extrapolated to neurones, the presence of β3 would basically reduce the effect of receptors formed by α4 and spare those formed by α3. It is hard to deduct what the functional consequences of this switch towards α3β4-type receptors would be, given that it is not clear what the physiological role of such receptors is and most importantly what are the physiologically relevant concentrations of ACh that activate them. The α3β4β3 triplet receptor was found to be almost indistinguishable from the α3β4 receptor with a stoichiometry of 2α:3β, however as will be shown in Chapter 9 the α3β4 can also exist in a stoichiometry of 3α:2β with markedly different properties and pharmacology and we have evidence that this may be the dominant stoichiometry *in vivo*. In that case insertion of the β3 subunit

may be a method of selecting for receptors which are 2α:3β-like, which (as will be discussed) are more sensitive to ACh than receptors with 3 α subunits.

It is possible that in the midbrain dopaminergic neurones, the balance between α4- and α6-type receptors is what is regulated by β3. Populations of α6β2* receptors are know to be co-expressed pre-synaptically in the same neurones as populations of α4β2* receptors. These neurones also have high levels of α5 and β3 expression (Azam *et al.* 2002) so, if α6β2α5β3 receptors are functional, it could be that in these neurones, the levels of β3 would determine the balance between α6β2* and α4β2* mediated ACh current. What the physiological significance of this may be I cannot say, given that the biophysical properties of α6-type receptors have not been characterised.

The phenomenon of cells producing subunits which regulate the function of ion channels is not unknown, voltage-gated potassium channel are known to be differentially regulated by the KCNE proteins, one-transmembrane spanning subunits with intracellular are known to interact with a range of potassium channels producing a number of effects including the inhibition of KCNQ1 channels by the KCNE4 protein (Grunnet *et al.* 2002) and the NR3A subunit (Das *et al.* 1998) and the NR3B subunit (Nishi *et al.* 2001) of the NMDA receptor have been shown to have a similar dominant-negative effect on NMDA heteromeric receptors.

In conclusion, our research has highlighted a possible important effect for the β3 in the regulation of neuronal nicotinic signals (and therefore all the systems downstream regulated by nAChRs).

CHAPTER 7

Development and Evaluation of a Subunit Tandem Approach for nAChRs

This work has been published as:-

"Incomplete Incorporation of Tandem Subunits in Recombinant Neuronal Nicotinic Subunits" (2004) Paul J. Groot-Kormelink, Steven D. Broadbent, James P. Boorman and Lucia G. Sivilotti. *J. Gen Physiol.* 123 697-708

7.1 Background

Previously I have shown data obtained from relatively simple subunit combinations and in the majority of cases the assumption has been that the receptor populations have been "pure" i.e. the currents recorded from a cell have all come from one type of channel with a single make-up and stoichiometry. In heterologous expression systems such as the *Xenopus* oocyte this assumption is fairly robust when recording from receptors made up of a single subunit such as the homomeric α7, α8 and α9 nAChRs or heterologous "pair" receptors, made up from a combination of an α subunit (α2, α3 or α4) and a β subunit (β2 or β4) where neither individual subunit can form a functional receptor on its own. Also, in the case of the two "orphan" subunits, α5 and β3, which form neither homomeric nor "pair" receptors, "triplet" receptors can be created by co-injecting these subunits at high concentrations along with a functional pair combination (Ramirez-Latorre *et al.* 1996; Groot-Kormelink *et al.* 1998). The high concentrations of α5 or β3 (in our case 1:1:20) is used to ensure that as much as possible of the functional receptor population contains all three subunits (Groot-Kormelink *et al.* 1998). However these "simple" subunit combinations probably do not resemble the make-up of native receptors, given that there is strong evidence that native nAChRs can be made up of at least four different subunits (Conroy and Berg, 1995) subpopulations of which could

form functional receptors in their own right. For instance, in the case of the main synaptic nAChR in chick parasympathetic ciliary ganglia, a suspected α3β2β4α5 receptor, the injection of these subunits' cRNA into an oocyte would also result in the formation of sub-populations of at least α3β2 and α3β4 receptors, with possibly α3β2β4, α3β2α5 and α3β4α5 nAChRs as well, not to mention all the possible variations in stoichiometry ratios. Any α3β2β4α5 receptors would likely be a minority population and would almost certainly not be readily distinguishable from the other subpopulations present.

Another situation in which our capability of expressing recombinant receptors is insufficient is when we want to study channelopathy mutations that have autosomal dominant inheritance (such as Autosomal Dominant Nocturnal Frontal Lobe Epilepsy). Affected patients carry both the wild-type and the mutant alleles and their nicotinic receptors in are thought to contain a mixed population of both the mutated subunits (α4 usually) and the corresponding wild-type subunits (see Rozycka *et al.* 2003 for an overview). Such a complicated receptor could not be homogenously expressed in heterologous expression systems using traditional techniques. Further work has shown that even the "simple" combinations mentioned earlier are more complicated than they appeared at first. For instance, α9 can form homomers and also a pair receptor with α10 (Grantham *et al.* 2004) and similarly the α7 is now known to form a non-functional receptor with β3 (Palma *et al.* 1999), work which I have expanded on in Chapter 6. The "pair" α4β2 receptor is now known to exist in two possible forms that differ in their stoichiometry and in their pharmacological properties (Nelson *et al.* 2003). Alternate stoichiometries are likely to be possible for a range of other combinations. See for instance, the biphasic curve for α3β2 shown in Chapter 6, which hints that it too may

have multiple stoichiometries. In addition, Chapter 9 provides evidence that even our old faithful α3β4 receptor is more complicated than it first appeared.

Finally we know that when we express triplet receptors such as α3β4β3, the high concentration of the third subunit ensures that the majority of the receptors are triplet receptors, but does not guarantee that some pair receptors may not also form. Certainly the small currents seen in the "knocked-out" β3 combinations could just as easily be from residual amounts of pair receptors rather than the current from a barely functional triplet receptors or both. In an attempt to restrict the stoichiometry of ligand-gated and other ion channels concatemeric i.e. linked subunits have been examined starting with tandem subunits where two subunits are linked together. Tandem subunits were first used to prove the heteromultimeric nature of *Shaker* K^+ channels (Isacoff *et al.* 1990) and have since been applied to cyclic nucleotide-gated channels (Varnum and Zagotta, 1996), the epithelial Na^+ channel (Firsov *et al.* 1998), the mechanosensitive channel MscL of *Escherichia coli* (Blount *et al.* 1996), the cystic fibrosis transmembrane conductance channel (Zerhusen *et al.* 1999), $P2X_2$ receptors (Newbolt *et al.* 1998) and a range of transport proteins (Emerick and Fambrough, 1993; Sahin-Toth *et al.* 1994; Kohler *et al.* 2000). This eclectic mix of channels and transport proteins all share one common feature; the N- and C-terminals of these proteins are all intracellular allowing their linkage by short amino-acid linkers. It isn't a massive leap to recognise that this technique could be adapted for LGICs whose proteins tend to have extracellular N- and C-terminals. As shown by Schorge and Colquhoun, 2003, this approach can be used even when the terminals are not on the same side of the membrane such as with NMDA receptors through the use of truncated subunits, although this was found to significantly change the

properties of the receptor. The tandem + monomer technique has already been reported being successful for the study of $GABA_A$ receptors (Im *et al.* 1995) and the neuronal nicotinic α4β2 receptors (Zhou *et al.* 2003). So as a first step in restricting the stoichiometry of the other nAChRs, we attempted to create tandems of nAChR subunits.

7.2 Production of a functional nAChR tandem construct

As a starting point we decided to concentrate on the α3β4 receptor, it being the receptor we were most familiar with; under normal circumstances (injection of α3 and β4 constructs in a 1:1 ratio), the α3β4 receptor has a stoichiometry in oocytes of 2α:3β (Boorman *et al.* 2000) with a probable arrangement of αβαββ if analogous to the muscle nicotinic receptor. We were aiming to produce a pure population of receptors from injecting a single tandem construct and a single monomer. Therefore, of the four possible types of α3β4 tandem construct, α3_α3, β4_β4, α3_β4 and β4_α3, only the α3_β4 and β4_α3 had the possibility to form a functional receptor when expressed with a single monomer (i.e. β4). These two tandem constructs were prepared by Dr. Paul Groot-Kormelink, as described in Groot-Kormelink *et al.* 2004. The linker used for the α3_β4 construct was a 45 amino-acid (aa) sequence made up of the signal peptide (21 aa), the C′ domain of the α3 (9 aa) and the linker itself (15 aa) (adapted from Im *et al.* 1995). For the β4_α3 construct a slightly longer 60 aa sequence was used due to the longer C' domain of the β4 (19 aa) and the longer signal peptide (26 aa). The linker sequence was ...AAAQQQQQQQQEFAT.... The inclusion of the signal peptide by Im *et al.* has been recently criticised (Minier and Sigel; 2004) as it may interfere with insertion etc. of the

protein. The possible formation of a secondary structure in the signal peptide may also overly shorten the linker. The net effect of either of these problems would be a non-functional tandem construct (for an example see Baumann *et al.* 2001), and this proved not to be the case for our constructs (see below).

Once the constructs were created, oocytes were injected with linked constructs of either α3_β4 or β4_α3 together with a β4 monomer (in a molar ratio of 2:1 tandem:monomer). This would potentially produce receptors looking like the two cartoons in Figure 7.1.

A

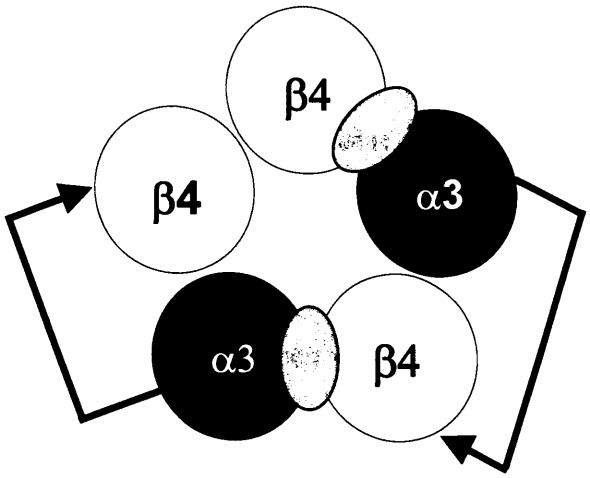

B

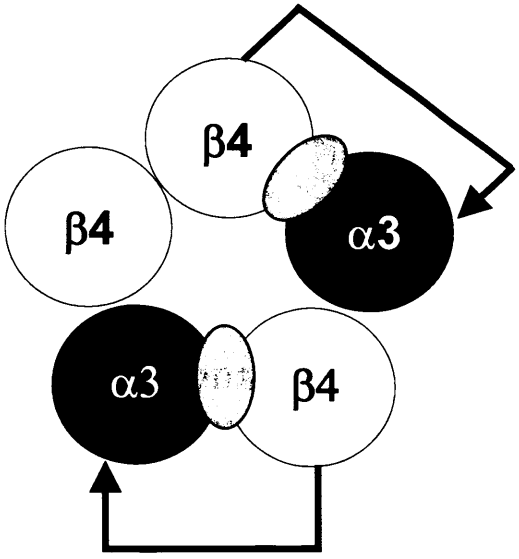

Figure 7.1: Representations of the putative formations of receptors created by (**A**) α3_β4 + β4 and (**B**) β4_α3 + β4. Linkers shown by the black lines, with the presumed direction of linker shown by arrow. Note the differences in position relative to the putative binding sites (grey ovals) of the unlinked β4 monomer in each case.

The α3_β4 construct failed to produce a functional channel i.e. oocytes injected with this combination failed to produce a response to 1mM ACh (n=5). In contrast to that, the β4_α3 construct produced robust expression when expressed with β4 monomer, giving an average maximum inward current of 2.6μA to 1mM ACh. (n=10, cRNA concentration 2ng:0.5ng tandem:monomer, see Table 7.1). The failure of the α3_β4 construct could be due to its slightly shorter linker preventing assembly. This is unlikely as its 45 aa length is well in excess of the linker lengths that work for other LGICs e.g. linkers of lengths as short as 11 aa have been reported to be functional for $GABA_A$ tandems (albeit minus the signal peptide) (Baumann *et al.* 2001).

Another possibility is that α3_β4 does not express functional receptors because the position of the linker with respect to the agonist binding site (which differs between the two orientations, Zhou *et al.* 2003) interferes with the receptor function. A third possibility is that the α_β orientation does not allow the assembly of the receptor subunits in the correct order if neuronal nAChR assembly is analogous to the model postulated for muscle nicotinics (Green, 1999).

7.3 nAChR tandem constructs only produced functional receptors when expressed with β4 monomers

Once we had a functional tandem construct, this allowed us to ask our first question, namely did the tandem strictly require the β4 subunit for function or could other monomers also form functional receptors with it? In order to test this, β4_α3 was

expressed with each of all the other non-homomeric nAChR subunits i.e. α2 to α6, β2 and β3, at the same concentration as before (2ng:0.5ng) and tested with 1mM ACh, the results are shown in Table 7.1. As can be seen, only when the β4_α3 tandem was expressed with the β4 monomer were large currents observed. This was both good news but also a bit perplexing, on the one hand this meant that as the construct formed receptors with significant currents only with β4 we shouldn't have any problems with contaminant and endogenous subunits and could be useful if this technique were ever to be extended to cells with already existing populations of ion channels that did not include β4. On the other hand, when the conventional expression technique is used, it is known that α3, α5 and β3 can form functional receptors together with α3 and β4. Hence we would have expected that α3, α5 and β3 subunits, at least, should also produce a functional receptor with significant currents when expressed with the β4_α3 tandem. In addition the formation of some hybrid of the tandem construct with β2 or one of the other α subunits wouldn't have been too surprising (Boorman *et al.* 2000; Groot-Kormelink *et al.* 2001). This failure to produce functional tandem-containing "triplet" receptors is surprising, although explanations could include the possibility the linker was affecting assembly (although it leaves the question why would that affect β2 insertion but not β4?), as mentioned earlier, or that β4 is the only subunit that can take up the position that is available for the monomer in the tandem expression, whereas the other subunit types need to occupy another position in the pentamer, i.e. one of the positions taken up by a linked subunit. As will be seen, some of the later work may shine a bit of light on this quandary. The α3_β4 construct (i.e. the one with the opposite orientation) was also

tested with all the other non-homomeric nAChR subunits, none of which produced receptors with any significant function.

β4_α3 +	I_{max} (*n*A)	cRNA (*n*g)	*n* = oocyte	*n* = batch
—	0 ± 0	2	6	2
α2	13 ± 7	2:0.5	6	2
α3	0 ± 0	2:0.5	6	2
α4	0 ± 0	2:0.5	6	2
α5	7 ± 4	2:0.5	5	2
α6	0 ± 0	2:0.5	5	2
β2	5 ± 5	2:0.5	6	2
β3	0 ± 0	2:0.5	6	2
β4	2587 ± 702	2:0.5	10	3

Table 7.1: Maximum currents (mean ± SEM) obtained by 1mM ACh application for the β4_α3 tandem constructs expressed alone (—) or with a nicotinic monomer at V_H = -70 mV

7.4 No evidence of proteoysis of the tandem linker into functional monomeric subunits

Other questions for us were whether the tandem construct was being proteolysed at the linker into functional monomeric subunits (a phenomenon seen with $P2X_1$ trimeric receptors at low efficiency, Nicke *et al.* 2003) and whether tandem-only receptors were possible, the so-called dipentamers (as was later reported by Zhou *et al.* 2003). In order to test these possibilities both the tandems alone and the α3_β4 and β4_α3 tandems together were expressed in oocytes (n=6-9) none of which produced functional receptors (data not shown). The failure of the β4_α3 tandem to produce functional receptors with any of the other monomers (Table 7.1) was already evidence that proteolysis was not occurring (or more accurately, if it was occurring, it was not producing functional monomers) and this is supported by the inability of either tandem to produce a functional receptor when expressed on its own.

7.5 No evidence of the formation of dipentamers

This failure, together with the failure of the two tandems to produce a functional receptor when co-injected, also meant it was unlikely that α3*β4 tandem (where * means constructs of either orientation) constructs were able to form the dipentamers seen with α4*β2 tandem constructs by Lindstrom and his colleagues.

Production of monomer subunits from tandem constructs could only be by breakdown at the level of either cRNA or protein. Further evidence for lack of breakdown into functional monomers was provided by cRNA gel-electrophoresis results

confirming the absence of any monomer cRNA from β4_α3 preparations (Figure 7.2A, courtesy of Dr Paul Groot-Kormelink) and by Western blots from both oocytes and HEK cells, as these failed to show any evidence of monomer protein in cells expressing only β4_α3 (Figure 7.2B, courtesy of Dr Paul Groot-Kormelink). However, it must be noted that, while β4 monomer protein was detected by this technique in the control cells (lane β4), the antibodies used failed to produce a signal from tandem proteins (lane T). This has been reported before for $GABA_A$ tandems (Baumann *et al.* 2001) and could be due to insufficient amounts of antigen being formed to be detected above background by the antibodies used or by deformation of the epitope region by the presence of the linker.

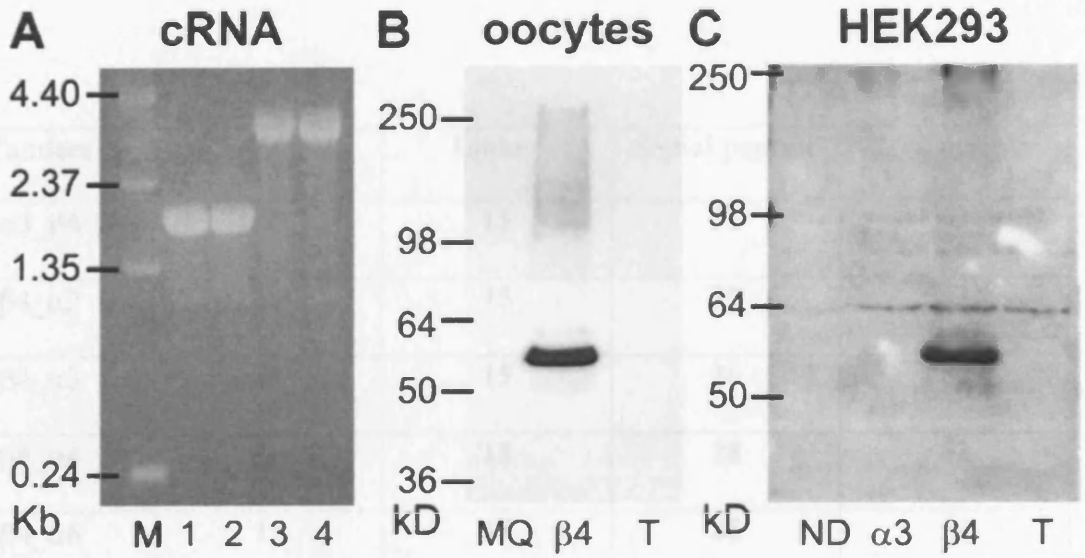

Figure 7.2: cRNA gel-electrophoresis (**A**) and Western Blots of expressed proteins in oocytes (**B**) and HEK293 cells (**C**). Approximately 1μg of α3 (**1**), β4 (**2**), α3_β4 tandem (**3**) and β4_α3 tandem (**4**). Beside the RNA ladder (**M**) were separated on a 1.5% agarose-gel (**A**). The Western Blot in B was obtained from oocytes injected with MilliQ water only (**MQ**), β4 only or β4_α3 tandem (**T**) and the Western in C is from HEK293 cells transfected with no DNA (**ND**), α3 only, β4 only or β4_α3 tandem (**T**). Detection by β4 antibody and visualisation by chemoluminesence. Bands for the β4 subunit were detected at the expected size of 56kD for both blots after 30s exposure. No breakdown products were observed for the tandem subunit in either blots, even for longer exposure times up to 1 h. Note that the tandem fusion protein (predicted size of 115 kD) was not detected by the β4 antibody used.

7.6 Production of other functional nAChR tandem constructs

The same techniques were used to create and test other nAChR tandems, of a β_α + β template. The linker regions are summarised in Table 7.2, all contain the same 15 aa linker section as the α3*β4 constructs.

Tandem	C' domain	Linker	Signal peptide	Total
α3_β4	9	15	21	45
β4_α2	19	15	29	63
β4_α3	19	15	26	60
β4_α4	19	15	28	62
β4_α6	19	15	25	59
β2_α2	23	15	25	63
β2_α3	23	15	29	67
β2_α4	23	15	28	66
β2–α6	23	15	25	63

Table 7.2: Linker regions of tandems from presumed $-NH_2$ end of TM4 region (extracellular region) of the first subunit up to start of the mature second subunit.

The response to 1mM ACh of these tandem constructs with and without the appropriate monomer is shown in Table 7.3 and Figure 7.3. As can be seen, while none of the α6-containing constructs produced functional receptors, all the other constructs of the form β4_α + β4 produced large inward currents, whereas the β2-containing constructs were less successful with only the β2_α4 producing significant amounts of current (even that was far less than what was seen for the β4 constructs). Several of the

constructs also generated significant amounts of current when injected alone, particularly the β2_α4, so there is a strong possibility of either proteolysis or, as reported by Zhou *et al.* 2003, the formation of dipentamers by these constructs.

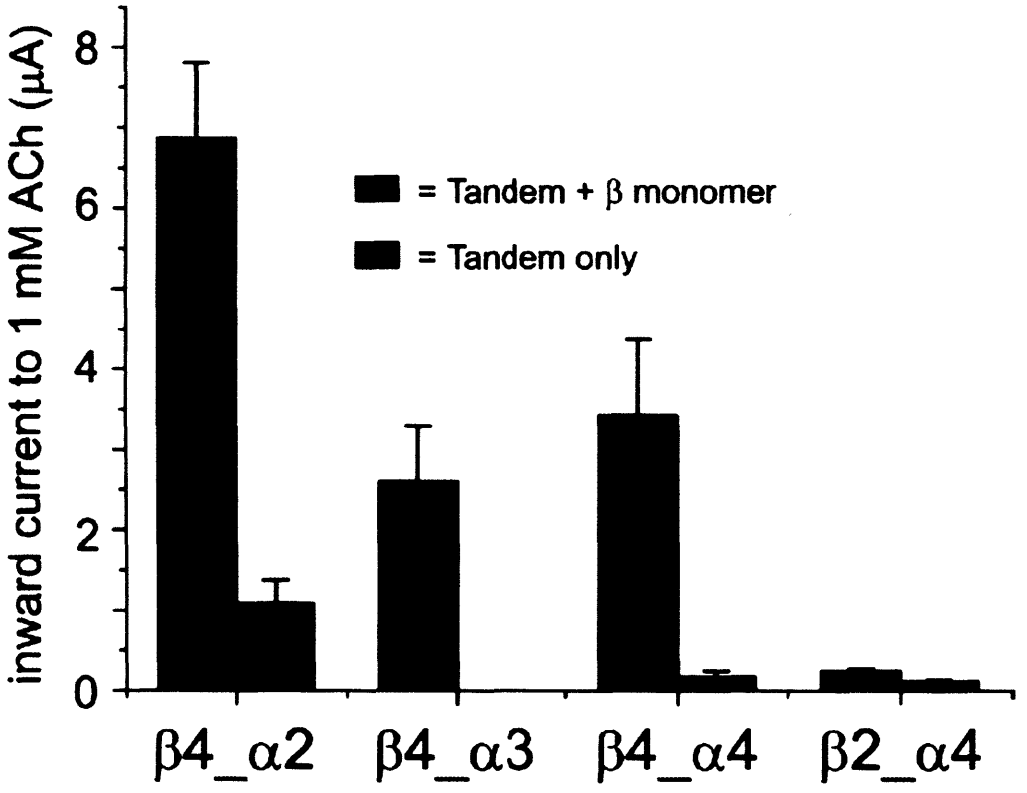

Figure 7.3: Maximum currents obtained from application of 1mM ACh on tandem constructs expressed in oocytes with and without the appropriate β2 or β4 monomer (2ng/μl:0.5ng/μl).

Combo	Imax (nA) to 1 mM ACh	cRNA injected	n (oocytes)	n (batches)
β2_α2	0 ± 0	0.5 ng	6	2
β2_α2 + β2	0 ± 0	2 ng : 0.5 ng	5	2
β2_α3	0 ± 0	0.5 ng	5	2
β2_α3 + β2	6 ± 4	2 ng : 0.5 ng	5	2
β2_α4	99 ± 35	0.5 ng	6	2
β2_α4 + β2	216 ± 46	2 ng : 0.5 ng	6	2
β2_α6	0 ± 0	0.5 ng	6	2
β2_α6 + β2	0 ± 0	2 ng : 0.5 ng	6	2
β4_α2	1077 ± 287	0.5 ng	5	2
β4_α2 + β4	7044 ± 912	2 ng : 0.5 ng	5	2
β4_α3	1.7 ± 5	0.5 ng	9	3
β4_α3 + β4	882 ± 195	2 ng : 0.5 ng	5	2
β4_α4	678 ± 496	0.5 ng	5	2
β4_α4 + β4	3079 ± 693	2 ng : 0.5 ng	7	2
β4_α6	0 ± 0	0.5 ng	6	2
β4_α6 + β4	0 ± 0	2 ng : 0.5 ng	5	2

Table 7.3: Maximum inward current (mean ± SEM) produced by bath-applied 1mM ACh on a series of tandem constructs expressed, with and without the appropriate monomer, in oocytes held at V_H = -70mV. Note the failure of some constructs to produce current and the relatively large currents seen with some tandem-only injections.

The possibility that for some tandem constructs, we may encounter the formation of tandem-only receptors and/or proteolysis re-affirmed our decision to concentrate on the β4_α3 construct.

7.7 Receptors formed by β4_α3 tandem constructs have similar macroscopic pharmarmacological properties to receptors formed by α3 and β4 monomers

Having shown that β4_α3 tandems produced functional receptors that were faithful to β4 monomers, unable to form dipentamers and didn't appear to proteolyse, the most important question then was, do these receptors have the same properties as the analogous α3β4 monomeric receptor? Dose-response curves were obtained for both types of receptors and as can be seen by Figure 7.4 both the shape of the responses and the pooled and fitted dose-response curves are indistinguishable, (α3β4: EC_{50} = 134 ± 5 μM, nH = 1.70 ± 0.10, n=9; β4_α3 + β4: EC_{50} = 122 ± 8 μM, nH = 1.98 ± 0.21, n=4).

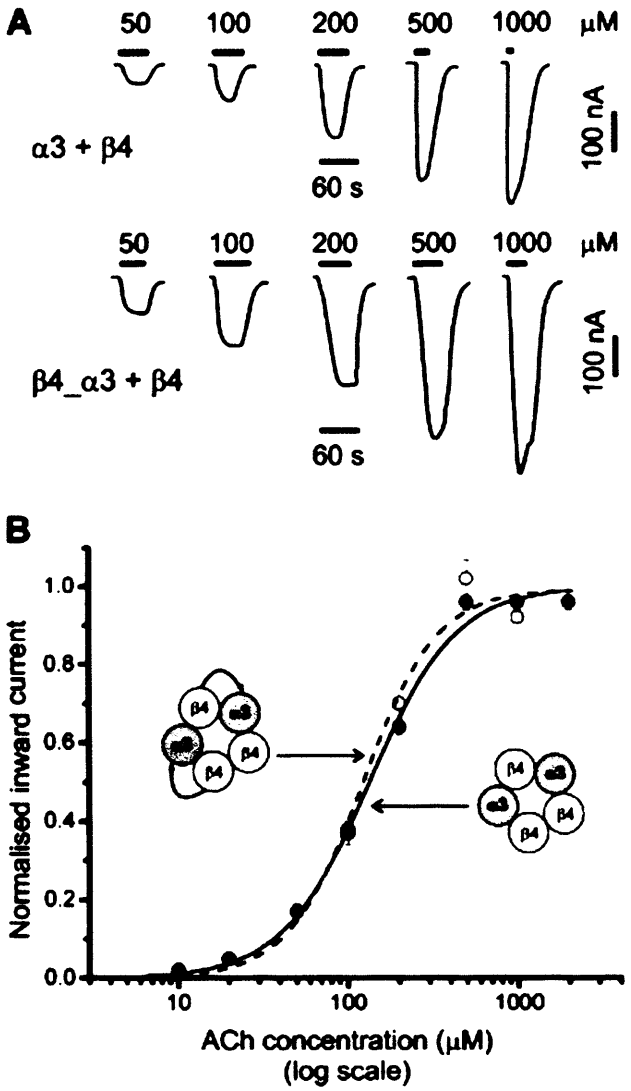

Figure 7.4: ACh concentration-response curves of α3β4 nAChR expressed in oocytes from monomer or tandem constructs are indistinguishable. (**A**) Traces are inward current recorded at a holding potential of -70mV in response to bath-applied ACh. (**B**) ACh concentration-response curves from experiments such as the ones shown in A, performed in oocytes injected with either α3 or β4 monomer cRNAs (filled circles, *n*=9) or β4_α3 tandem together with β4 monomer cRNAs (open circles, *n*=4). Full sets of peak responses to ACh from each oocyte were fitted with the Hill equation and normalised to the fitted maximum response before pooling. The curves shown are the results of the fitted data.

7.8 Tandem-containing receptors have the same number and ratio of α3 and β4 subunits forming the channel pore as receptors produced by monomers

Everything appeared to be going to plan and this was as much validation of tandem-containing LGICs as any group had ever done. Nevertheless, we decided to check that the stoichiometry of the receptors formed was the 2α:3β seen with α3β4 monomeric-construct receptors through the use of our 9′ LT mutation (Boorman *et al.* 2000). Figure 7.5 is taken from Boorman *et al.* 2000 and shows the effect of mutating either all the α or all the β subunits with a 9′ LT TM2 mutation. This mutation is thought to disrupt the closed state of the receptor resulting in a reduction in the EC_{50} value of the receptor (Revah *et al.* 1991). The degree of reduction is thought to be proportional to the number of copies of the mutation present in the channel pore. Using this mutation for the study of stoichiometry also relies on the assumption that the different possible positions of the mutation are equivalent. As can be seen in Figure 7.5 a larger shift was produced by the mutation being present in the β4 subunit than the α3 and the degree of shift corresponded well with a stoichiometry of 2α:3β.

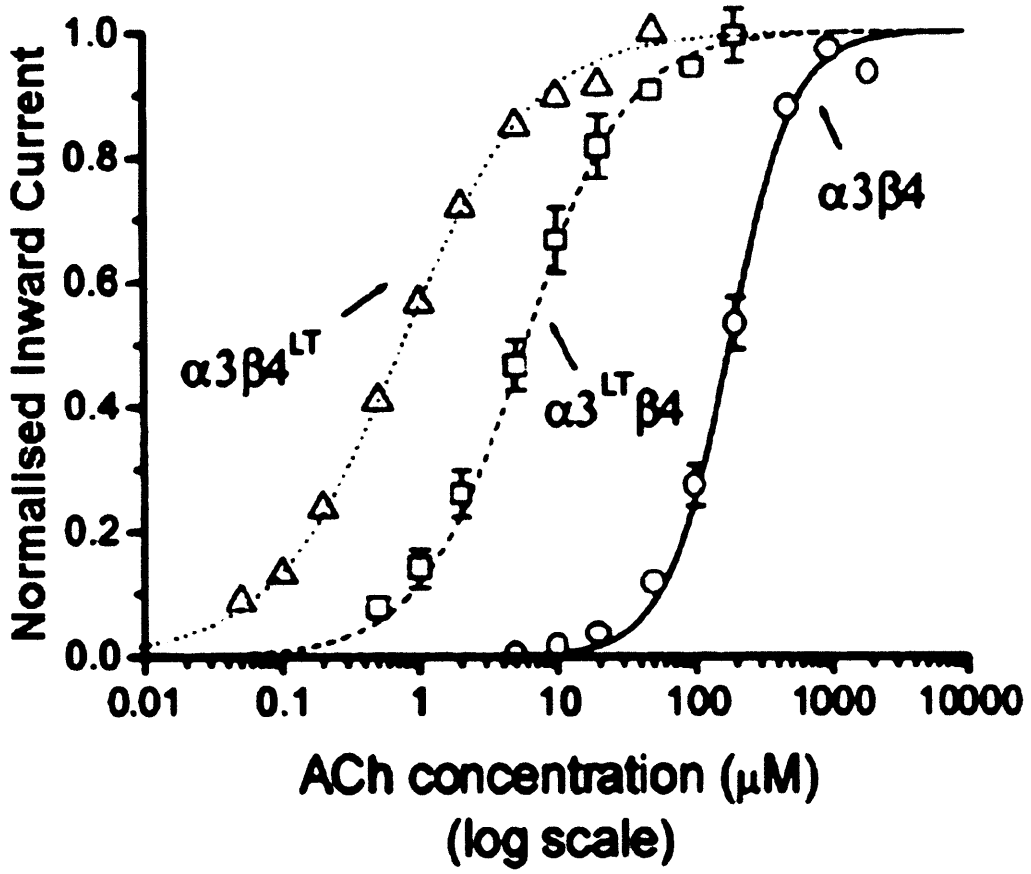

Figure 7.5: Stoichiometry of α3β4 nAChR expressed in oocytes from monomers cRNA is 2α:3β. Curves show normalised inward current recorded at a holding potential of -70mV in response to bath-applied ACh for α3 + β4 wildtype (circles,), $\alpha3^{LT}$ + β4 (squares) and α3 + $\beta4^{LT}$ (triangles). Full sets of peak responses to ACh from each oocyte were fitted with the Hill equation as a free fit and normalised to the fitted maximum response before pooling. The curves shown are the results of the fitted data. Note the greater increase in ACh sensitivity when β4 was mutated. (from Boorman *et al.* 2000)

Therefore we created a β4_$\alpha3^{LT}$ mutant construct and expressed it at the usual 2:1 molar ratio with β4 monomer. If the resulting receptor has the same stoichiometry as the monomeric receptors, this should produce a channel containing two copies of the $\alpha3^{LT}$ subunit. Similarly the $\beta4^{LT}$_α3 was also created and expressed with $\beta4^{LT}$ monomer to hopefully produce a receptor containing 3 $\beta4^{LT}$ subunits. Figure 7.6 shows the traces and

dose-response curves obtained from these two receptor combinations. When Fig. 7.6 is compared to Fig. 7.5 it can be seen the two graphs appear very similar, even the "discrepancy" of the decrease in Hill slope seen for three copies of the mutation in Figure 7.5 is reproduced by the all-$\beta4^{LT}$ mutations curve in Figure 7.6 (this decrease might be due to the impact of mono-liganded, or even spontaneous, openings of receptors containing three or more mutations). The numbers are summarised in Table 7.4 and as can be seen neither the EC_{50} nor Hill slope values differ significantly between the monomeric receptors and the corresponding tandem-construct receptor (unpaired two-tailed Student's t-test). The difference in the actual EC_{50} values between the Boorman results and the tandem were probably due to the differences in protocol covered in Chapter 4, but the relative changes in values caused by the mutations are remarkably consistent.

At this stage it certainly seemed that the β4_α3 tandem receptor had the same stoichiometry of the α3β4 receptor, or more precisely, that it incorporated two α and three β subunits in the channel-gating domain. Furthermore, it appeared that the use of concatenated subunits didn't interfere with the effect of the 9′ TM2 LT mutations, suggesting that the presence of the linker hadn't greatly disrupted the either the binding or gating function of the receptor.

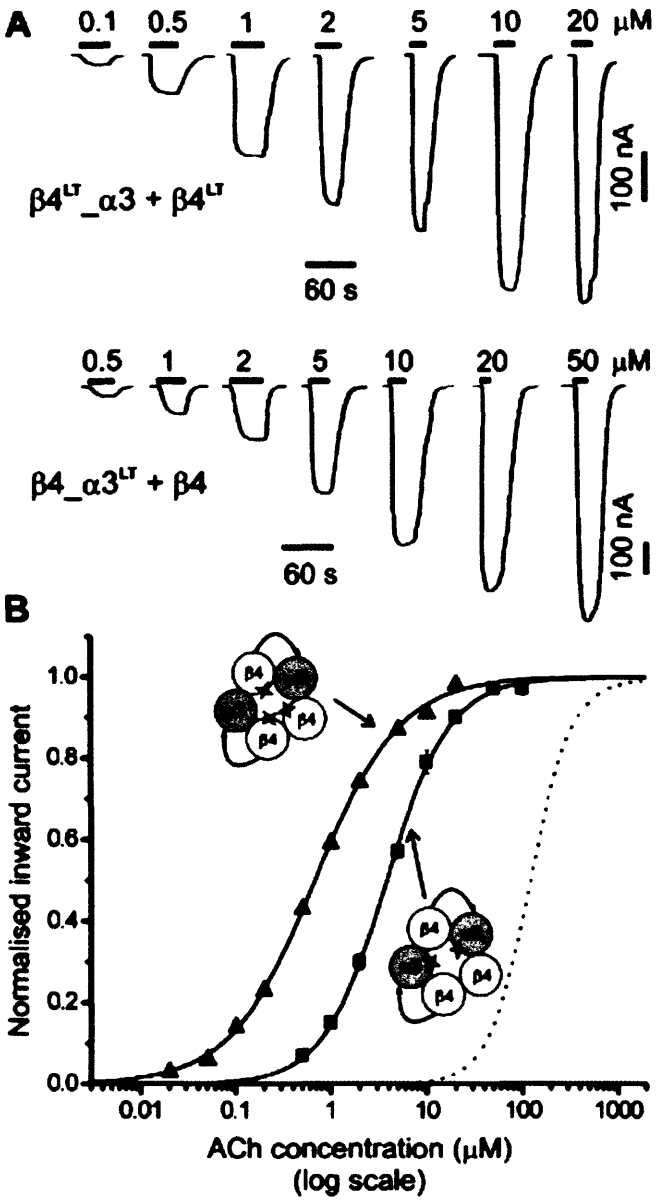

Figure 7.6: The effects of inserting a L9′T reporter mutation into all the α or all the β subunits in tandem construct receptors. (**A**) Examples of inward currents elicited by bath-applied ACh in oocytes expressing $\beta4^{LT}$_α3 + $\beta4^{LT}$ (top) or β4_$\alpha3^{LT}$ + β4 (bottom). (B) Concentration-response curves from oocytes injected with $\beta4^{LT}$_α3 + $\beta4^{LT}$ cRNAs (filled triangles, *n* = 7) or β4_$\alpha3^{LT}$ + β4 cRNAs (filled squares, *n* = 8). The concentration-response curve for the β4_α3 + β4 wildtype nAChR is shown for reference (dotted line). The EC_{50} shifts produced by the mutations are similar to those observed in α3 + β4 receptors (see Figure 7.5) and suggest that the channel gate is made up of two α and three β subunits both in linked-subunit and monomer construct receptors.

	EC_{50} (μM)	nH	n	Probable no. of mutations	p value (monomer vs tandem)	
					EC_{50}	n_H
$\alpha3\beta4$	180 ± 17	1.81 ± 0.09	7	0	-	-
$\alpha3^{LT}\beta4$	5.8 ± 1	1.15 ± 0.08	6	2	-	-
$\alpha3\beta4^{LT}$	0.75 ± 0.05	0.92 ± 0.08	4	3	-	-
$\beta4\_\alpha3 + \beta4$	122 ± 8	1.98 ± 0.21	4	0	NS	NS
$\beta4\_\alpha3^{LT} + \beta4$	3.81 ± 0.18	1.34 ± 0.06	8	2	NS	NS
$\beta4^{LT}\_\alpha3 + \beta4^{LT}$	0.68 ± 0.02	0.98 ± 0.03	7	3	NS	NS

Table 7.4: Comparison of the EC_{50} values and Hill slopes of the wildtype, all α and all β mutant receptors for both monomer and tandem construct receptors. Note the comparable amounts of shift for the all α and all β mutations between both types of receptor construct. Statistical analysis by unpaired two-tailed Student's t-test. NS = not significant.

7.9 Reporter mutations revels that tandem-containing receptors are misassembled

The final and most vital test to check that the use of concatenated subunits had effectively restricted stoichiometry was to ensure that each concatenated receptor contained only one monomer and two tandem constructs. A moment's thought should allow the realisation that although mutating all the α subunits proves the, at least partial, incorporation of the tandem construct, the mutation of all the β subunits cannot identify where the individual $\beta4$ subunits come from, either from the monomer or from the tandem. To check this it is necessary to mutate either just the monomer or just the tandem's $\beta4$ subunits. If the receptor is forming correctly, the $\beta4^{LT}\_\alpha3 + \beta4$ should produce a leftward shift comparable to that obtained for the $\beta4\_\alpha3^{LT} + \beta4$ and if our

findings are transferable from Boorman *et al.* 2000 then the β4_α3 + $\beta4^{LT}$ should be similar to the $\alpha3\beta4\beta3^{VT}$ receptor in producing a leftward parallel shift intermediate between the wildtype and "two-mutations" curves. Figure 7.7 shows the traces and curves obtained for $\beta4^{LT}$_α3 + β4, as can be seen the curve (solid line) bears no resemblance to the expected two-mutation curve (dash and dot) and instead is virtually indistinguishable from the wild type line (dotted line) (β4_α3 + β4: EC_{50} = 122 ± 8 μM, n_H = 1.98 ± 0.21, n=4; $\beta4^{LT}$_α3 + β4: EC_{50} = 100 ± 4 μM, n_H = 1.55 ± 0.10, n=11). There is possibly a small shift but it is barely significant and certainly nowhere near the ~30-fold shift we were expecting. From this data it would appear that the β4 subunits of the tandem construct are not in the channel in the majority of receptors formed and that the bulk of the β4 subunits in the receptors must be non-mutated monomers.

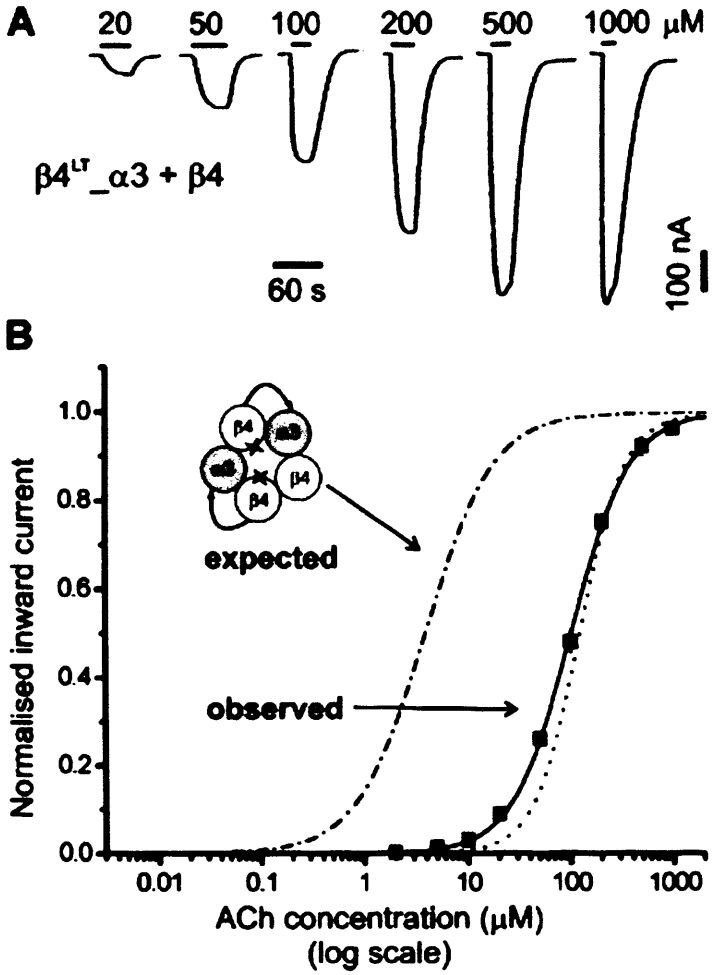

Figure 7.7: Low ACh sensitivity of linked subunit receptors carrying the L9′T mutation in the tandem β4 only. (**A**) Examples of inward currents elicited by bath-applied ACh in oocytes expressing $\beta4^{LT}$_α3 + β4. (**B**) Data from oocytes injected with $\beta4^{LT}$_α3 + β4 cRNAs (filled squares, *n* = 7). The concentration-response curve for β4_α3 + β4 (dotted line) and β4_$\alpha3^{LT}$ + β4 (dashed line) are shown for comparison purposes: the later showing the EC_{50} shift expected from two L9′T mutations.

This problem was confirmed when just the monomer was mutated. As mentioned above, had the receptor been forming properly, we would expect β4_α3 + $\beta4^{LT}$ to produce a curve intermediate between the wild-type and two-mutation curves, the dashed line in Figure 7.8 shows their geometric mean (22 μM) as a guideline of where a one-

mutation copy curve ought to be. However, the actual data from β4_α3 + $β4^{LT}$ shows a biphasic curve. The top part of the curve is near where the one-mutation guideline but the larger part of the curve (average = 58.6 ± 7.3 %, n=13) was closer to the expected curve for three mutations. This is agrees with our interpretation of the results of mutating only the tandem β4 subunits, and confirms that the majority of the β4 subunits in the channel derived from the monomer construct i.e. mutated rather than from the tandem i.e. non-mutated. Fitting the curve with a two-component Hill equation gave EC_{50} values of 0.67 ± 0.1 and 31.7 ± 1.9 μM (n=8). As can be seen the values of the two components are close to the values obtained for three mutations ($β4^{LT}$_α3 + $β4^{LT}$; EC50 = 0.68 ± 0.02 μM, n_H = 0.98 ± 0.03, n=7) and to that expected and calculated for a one mutation curve (22 μM) by taking the geometric mean between no-mutation and two-mutation curves. However there was a large amount of variability from one oocyte to the next in the proportion of the two components. Thus the higher ACh sensitivity accounted for 21 to 100 % of the total current (n =13; cfr. 59% average). For display purposes, a subset of four oocytes with roughly comparable high- and low-sensitivity components was used to illustrate the biphasic nature of β4_α3 + $β4^{LT}$ in Figure 7.8.

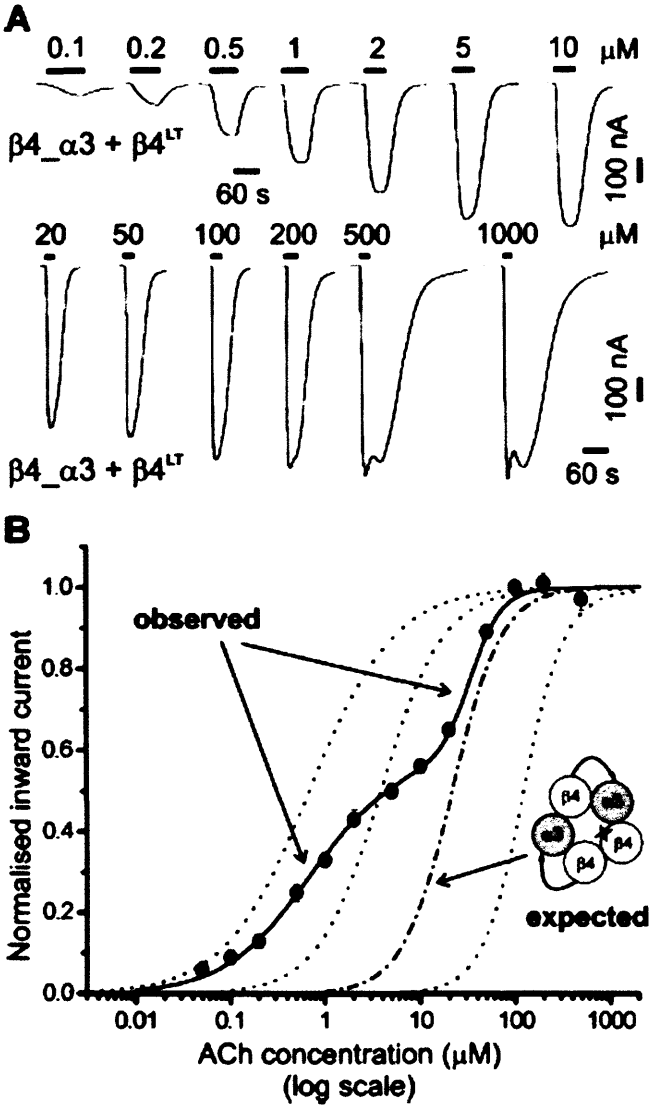

Figure 7.8: Inserting the L9′T reporter mutation in the β4 monomer subunit of linked subunit in nAChRs reveals multiple receptor population. (**A**) Examples of inward current elicited by bath-applied ACh in oocytes expressing β4_α3 + $β4^{LT}$. (B) Concentration-response curves for oocytes injected with β4_α3 + $β4^{LT}$ cRNAs (filled circles, *n*=4). The initial fit was a simultaneous fit of a two component Hill equation to each dose-response curve, with the constraint of equal EC_{50} and Hill slope across oocytes (the proportion of the first component was allowed to vary). The three dotted curves shown for reference are, respectively, (right to left), the concentrations-response curves for no mutations (β4_α3 + β4), two mutation copies (β4_$α3^{LT}$ + β4) or three mutation copies ($β4^{LT}$_ α3 + $β4^{LT}$). The dashed curve shows the concentration-response curve expected for complete tandem incorporation as depicted in the cartoon (i.e. one mutation copy) calculated from the geometric mean of the none and two mutation curves.

This hypothesis was confirmed with experiments carried out on oocytes injected with $\beta4\_\alpha3^{LT}$ + $\beta4^{LT}$ at a molar ratio of 2:1. If everything was working correctly you would expect this to form a receptor containing three mutations which should be comparable to the $\beta4^{LT}\_\alpha3$ + $\beta4^{LT}$ or the $\alpha3\beta4^{LT}$ receptors.

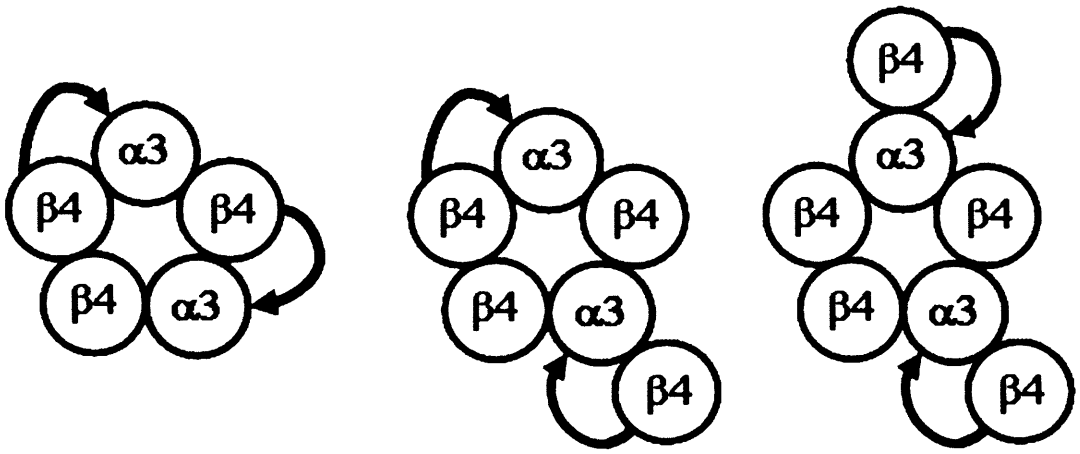

Figure 7.9: Diagrammatic representation of how the misassembly of a tandem-containing receptor results in the tandems β4 subunits "hanging-out". Note that there are two possible forms of misassembly, the partial misassembly (centre) with one tandem hanging out and the full misassembly (right) with both tandems hanging out. This would result in the incorrect no. of mutation being incorporated into the receptor if just the monomer or tandem β4 subunits are mutated (see Figure 7.11D, E & F).

However, if our interpretation of the data from the experiments with the tandem- and monomer-only mutations is correct, it implies that of the tandem construct "hanging out" this would produce a mixed population of receptors with the majority of $\beta4\_\alpha3^{LT}$ + $\beta4^{LT}$ receptors would contain four or five copies of the mutation (Figure 7.11). Receptors with more than three mutations are likely to give rise to a significant amount of

spontaneous activity, which would manifest itself as high cell mortality and a high holding current which should be sensitive to a nicotinic channel blocker such as trimetaphan. Certainly our previous attempts to record from oocytes injected with $\alpha3^{LT}$ + $\beta4^{LT}$ (expected to contain 5 mutations) resulted in a mortality rate of 16 out of 17 oocytes, over multiple injection batches. Even incubation with 10μM trimetaphan starting immediately after injection could not totally abolish mortality. With trimetaphan incubation, we still observed a 20% mortality with an average holding current of -2663 ± 339 nA for the survivors (n=5) rendering them unusable. These data can be compared with the 100% survival rate, and low holding current (-90 ± 24 nA; n=5) seen for wild-type $\alpha3\beta4$ receptors in trimetaphan. Sure enough, $\beta4\_\alpha3^{LT}$ + $\beta4^{LT}$ injected oocytes had a survival rate of 43% (n=14) and an average holding current of -550 ± 75 nA (n=6) in the survivors. If injected cRNA levels were doubled to 8ng:2ng (tandem:monomer) this mortality rate reached 100% (n=10) good evidence that this mortality was due to spontaneously opening channels. This holding current was decreased 46 ± 6 % (n=3) by application of 10 μM trimetaphan (Figure 7.10), a phenomenon not seen with receptors (both monomeric and concatemeric) with three or less mutations. Average mortality rates and holding currents for a range of injected oocytes are summarised in Table 7.5. Out of the $\beta4\_\alpha3^{LT}$ + $\beta4^{LT}$ oocytes which survived, some were healthy enough for us to obtain dose-response curves even if the holding currents were too high to allow enough confidence that the oocytes' were clamped at precisely the correct voltage to allow them to be "officially" accepted. The properties of these dose-response curves tallied reasonably well with a receptor containing three copies of the mutation (EC_{50} = 1.35, nH = 0.8, n=6). It appears, for whatever reason, these cells survived because they produced a

greater proportion of correctly assembled receptors which were less prone to spontaneous opening and so produced curves closer to what was expected. In fact, if anything, these receptors had EC_{50} values higher than what was expected for three mutations, an observation we now believe we can explain and will below.

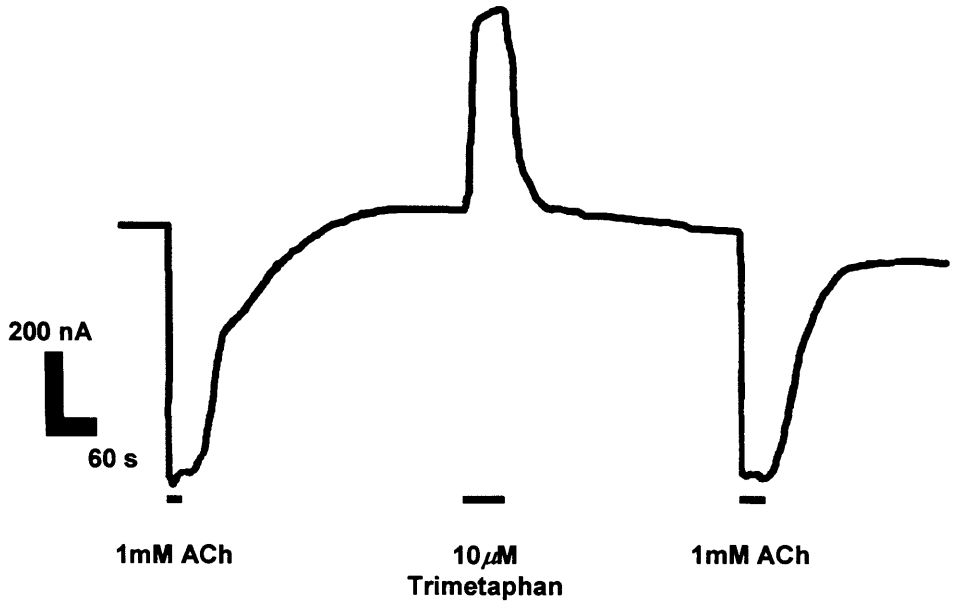

Figure 7.10: Representative trace obtained from an oocyte injected with $\beta4\_\alpha3^{LT}$ + $\beta4^{LT}$ to bath applications of 1mM ACh and 10μM Trimetaphan. Note the agonist-like response to Trimetaphan and the full reversibility of its action. 10μM Trimetaphan didn't produce any response in any receptor complex known to have three or less mutations.

	Mean I_H (nA)	Mortality (%)	*n*=
MQ	-92 ± 13	0	11
α3 + β4	-122 ± 26	10	20
$\alpha3^{LT}$ + β4**LT**	-	94	17
α3 + β4 **(in Tri)**	-90 ± 24	0	5
$\alpha3^{LT}$ + $\beta4^{LT}$ **(in Tri)**	-2663 ± 339	100	5
β4α3 + β4	-130 ± 33	-	4
$\beta4^{LT}$α3 + $\beta4^{LT}$	-549 ± 102	-	7
β4$\alpha3^{LT}$ + $\beta4^{LT}$	-550 ± 75	75	24
(Low concentration)	-550 ± 75	57	14
(High concentration)	-	100	10

Table 7.5: Summary of the mean holding current, I_H (± SEM) and mortality rates of a oocytes for a range of injected combinations. A cell was classed as "dead" if it had lysed or had a holding current in excess of 1μA. Also given are the values for cells incubated in 10μM trimetaphan after injection "(in Tri)". The results for β4_$\alpha3^{LT}$ + $\beta4^{LT}$ are also separated into "low concentration" (4ng:1ng) and "high concentration" (8ng:2ng) injections.

Constructs for the remaining combination $\beta4^{LT}$_$\alpha3^{LT}$ + $\beta4^{LT}$ was not even prepared as we decided early on that it would shed no light on the receptor's stoichiometry or this problem with mis-assembly and in all likelihood would experience all the problems with high mortality rates and holding currents seen with $\alpha3^{LT}$ + $\beta4^{LT}$ and β4_$\alpha3^{LT}$ + $\beta4^{LT}$.

Figure 7.11: (following page) Diagrammatic representations of different nAChR assemblies which may be formed by complete (left) or partial (centre and right) incorporation of linked constructs into the receptor. **B-F** show the effects of introducing a reporter mutation (a Thr in the 9′ position of the second transmembrane domain) in different subunits. The number under each cartoon shows the number of mutation copies expected to be in the channel gate for each receptor assembly. Note that no heterogeneity in the number of mutation copies is predicted if all α, all β or no subunits are mutated (**A-C**) in accord with the experiments shown in Figures 7.4 and 7.6. Mutating β only in the monomer construct or only in the tandem construct (**D** and **E**) can detect the different receptor forms (Figures 7.7 and 7.8). If receptors are expressed in which both the tandem α and β monomer bear the mutation, some receptors will bear five copies of the mutation (**F**).

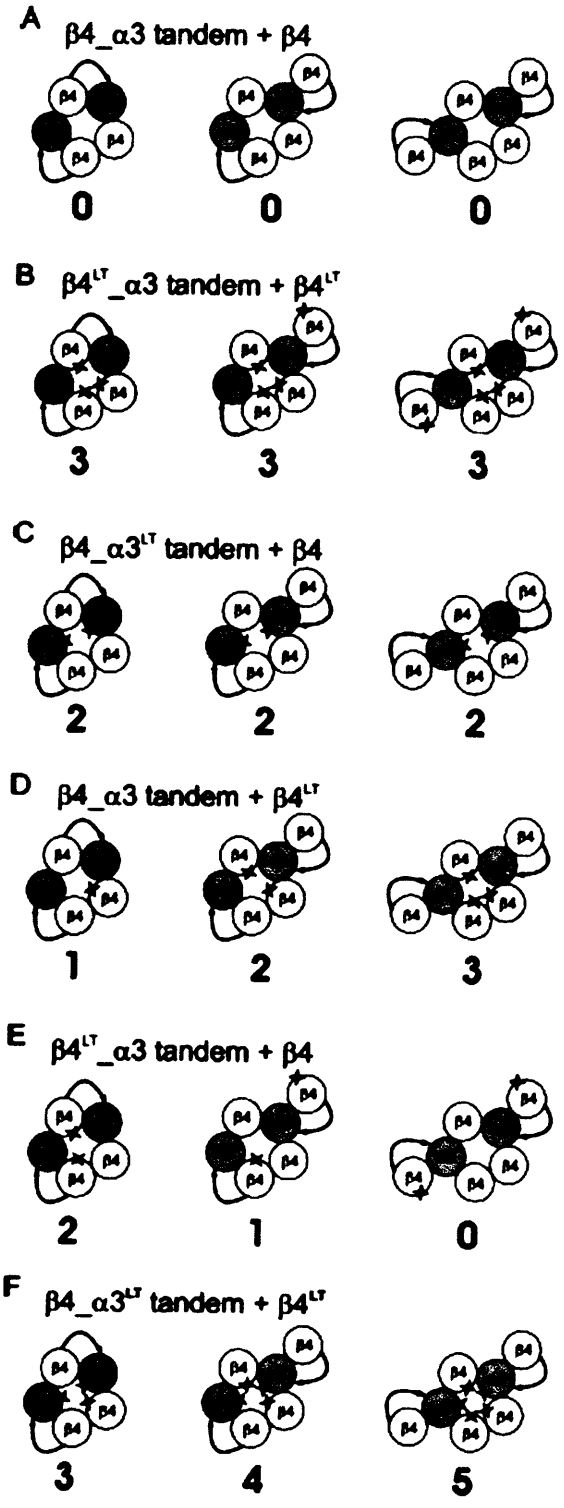
A
β4_α3 tandem + β4
0
0
0
B
β4LT_α3 tandem + β4LT
3
3
3
C
β4_α3LT tandem + β4
2
2
2
D
β4_α3 tandem + β4LT
1
2
3
E
β4LT_α3 tandem + β4
2
1
0
F
β4_α3LT tandem + β4LT
3
4
5

7.10 Discussion

The cartoon in Figure 7.11 summarises our interpretation for our observations when mutations were inserted in the different subunits with β4_α3 tandem receptors. As can be seen the problem of incomplete incorporation would not be apparent when the subunits expressed were either all wildtype, or when all α or all β were mutated (7.11A, B & C), This is because, whatever the exact formation of the receptors, the same number of mutations would be present in the gate of each receptor assembly. Mutation of just the monomer (7.11D) or just tandem (7.11E) β4 subunits would produce the unexpected shifts we saw in Figures 7.7 and 7.8 whilst 7.11F shows how receptors with more than 3 mutations would be produced.

At the time of publication there was one inconsistency in our data we had difficulty explaining. The $\beta4^{LT}$_α3 + β4 data suggest that in the majority of receptors all the β4 subunits came from the monomer. If that has been the case for β4_α3 + $\beta4^{LT}$, we should have seen a single component curve representing receptors with three mutant subunits. The biphasic curves obtained suggested at least two stoichiometries were present and it was assumed this was due to the presence of both the correctly assembled (one mutation) and completely incorrectly (three mutations) receptors. The intermediate stoichiometry (two copies of the mutation, with one β4 subunit coming from a tandem and the other two coming from the monomer), couldn't be ruled out because of the limited sensitivity of fitting multiple components to a dose-response curve. There was great variability in the proportion of the two main components present, with three of the

13 oocytes tested having just the high sensitivity component i.e. the majority of receptors being totally mis-assembled, just like $\beta4^{LT}\_\alpha3 + \beta4$, in those that did display two-components the high sensitivity component still made up the majority of the receptors (~60%). This inconsistency was only a minor irritant and didn't detract from our main conclusion that tandem constructs can mis-incorporate and therefore can not be trusted to restrict stoichiometry. Later work, covered in the next chapter, may go some way into resolving this apparent inconsistency.

The assumption in the interpretation is that the same mutation has the same effect regardless of which subunit carries it and where the subunit is within the receptor. This assumption could not be tested until the use of concatenated subunits, and there was evidence for and against it. On the one hand, in Boorman *et al.* 2000 for instance, the effect of mutating an individual α3 subunit (dose ratio = 6.11) was comparable to mutating an individual β4 subunit (dose ratio = 6.63) although it must be borne in mind that these finding were the averages of two or three mutations and as such may obscure individual variations due to exact subunit position not to mention the possibility and effect of multiple α3β4 stoichiometries. However, in the muscle nicotinic receptor mutations of the 12′ residue in TM2 has a greater effect for the δ than for the α subunit (Grosman and Auerbach, 2000). Of course the problem with the evidence that the effect of the mutations were not equivalent in muscle receptors subunit is that the actual subunit with the mutations differs from position to position. One of the whole points of using concatenated subunits was to answer this equivalent/non-equivalent dilemma. As will be shown in the next chapter, we have since discovered that a TM2 9′ leucine to threonine mutation of β4 is less effective if the β4 is the non-binding site β4 subunit, with a dose-

ratio of around 3.2 rather than the ~6.6 expected. This position corresponds to that taken by β3 and is the subunit provided by the monomer in a correctly assembled tandem receptor.

In that case a reappraisal of Figure 7.8 shows that the component that was originally suspected of being the correctly-formed, one-mutation, receptor is more likely to be the partially mis-assembled, two mutation receptor meaning the correctly formed receptor must only constitute a very small sub-population of the receptors formed and whose component is probably "smeared" into the two-component curve thus making its EC_{50} slightly higher that that predicted for two mutations.

This reappraisal helps to resolve better the apparent discrepancy between Figures 7.7 and 7.8 as both now represent receptor populations where the large majority of receptors are mis-assembled. This realisation that the mutated monomer β4 subunit in a correctly assembled receptor has only a limited effect on the receptors EC_{50} also explains the observation with $\beta4\_\alpha3^{LT}$ + $\beta4^{LT}$ receptors, that whilst the majority of oocytes expressed mostly mis-assembled receptors resulting in spontaneous openings and high cell mortality those few cells which, for what ever reason, produced correctly assembled receptors and survived to be recorded from, produced curves with a higher EC_{50} than would be expected from three mutations. What in fact we were seeing was the addition of the less effective non-binding site β4 mutations with the two α3 subunit mutations to produce a curve only slightly to the left of that obtained from the two α3 subunits mutated alone. If what we suspect is correct about the non-equivalence of mutations in concatenated subunits applies to monomeric subunits this would explain why the all α- and all β- mutant curves for both tandem- and monomer-containing receptors match so

well as the net effect of this non-equivalence would apply to both sets of receptors and would average out.

An argument could be made that, like the α4β2 receptor (Nelson *et al.* 2003), α3β4 receptors may not be all of a 2α:3β stoichiometry but instead might display alternate stoichiometries, the most likely one being a 3α:2β one and this might be a contributory factor to the problems seen with our research on tandem constructs of the α3β4 receptor. This possibility was examined in detail (see Chapter 9): although our data show that α3β4 can produce receptors of a 3α:2β stoichiometry, this only occurs in oocytes when the conditions are changed to force it, with extreme expression ratios. Under normal conditions the vast majority of α3β4 receptors produced by oocytes have a stoichiometry of 2α:3β. This was confirmed in our paper, Boorman *et al.* 2000. Examination of our data also helps to rule out alternate stoichiometries in the tandem experiments as a significant factor. Firstly, for α3β4 tandem-constructs to produce a functional receptor with 3α, the third α would have to be provided by the tandem either through proteolysis or through the creation of a dipentamer, neither of which we could detect. Secondly, β4_α3 + α3 does not produce significant amounts of functional receptors. Finally, it is hard to see how the clear cut differences witnessed in Figure 7.6 between all-α and all-β mutated receptors could occur if the two different ratio stoichiometries were both present in significant amounts even with the complicating factor of non-equivalence. If both stoichiometry ratios were present you'd expect both the all-α and all-β mutants to average out at two and a half mutations each, with the non-equivalence factors probably cancelling out, causing the two dose-response curves for these receptors to be identical. There was no evidence of this and therefore we can

conclude that, irrespective of the problems in interpreting the data, alternate stoichiometries are not a significant factor in these β4_α3 tandem-construct receptors.

Although the mis-assembly of tandem constructs is the simplest explanation of the problems with our data, a more convoluted hypothesis is that the receptors are forming correctly but that the linker has changed the properties of the receptor so as to produce the odd results we see in Figures 7.7, 7.8 and Table 7.5. Although we have no direct evidence against this, it is hard to see how such an effect could explain why the receptors appear to be assembling correctly when all the α or all the β subunits were mutated in Figures 7.4 and 7.6 yet misbehave when it came to mutating the monomer or tandem alone. Even if this more unlikely hypothesis was correct, it would imply that tandem-containing receptors were acting differently from monomeric. In itself this would mean the tandem technique had failed to reproduce a monomeric-like channel.

These findings on their own are disappointing for our hopes of using concatamers as a tool for restricting the stoichiometry of α3β4* receptors, but they may have a wider importance namely is this problem unique to β4_α3 constructs or is it common to all tandem constructs? Problems had already been noted with proteolysis ($P2X_1$ receptors, Stoop *et al.* 1999; Nicke *et al.* 2003), dipentamers (α4*β2, Zhou *et al.* 2003) and mis-assembly (K^+ channels, Liman *et al.* 1992). Furthermore the initial work on cyclic nucleotide-gated channels using concatenated subunits has since been contradicted by more recent findings (Zimmerman, 2002) and rearrangement of the tandem dimer has been reported in $GABA_A$ constructs (Baumann *et al.* 2001). So can we conclude that these problems are endemic to the use of all tandem concatemers? Well at the moment we can't say for sure: however, the fact that these errors have emerged every time these

problems have been checked for is worrying. What adds to this worry is the fact the receptors superficially appeared to be working perfectly and the problem with mis-assembly only became apparent after an extensive amount of work. It was dangerously tempting to have just carried out the basic tests on the tandem constructs i.e. check there was no proteolysis and that the tandem receptor was similar to the monomeric receptor and then assumed everything else was fine, publish and carry on our research with our work based on flawed assumptions. The majority of concatemer construct research has just carried out these basic tests and then leap-frogged onto doing more "interesting" work with the assumption that everything is OK. For absolute peace of mind, however, these other groups should return to their basic work on concatemers and ensure that their stoichiometries are correct. This however is unlikely to happen and this means a large body of research from the last decade may be fatally flawed.

I shall use a more recent paper as an example of this. It has been suggested that the rearrangement of tandem dimers and dipentamers only occurs if monomer subunits are also expressed and as such only dimer/triplet combinations i.e. a dual and triple subunit constructs should be used (Minier and Sigel, 2004). It could be argued that the problems we see were only due to the presence of monomers and may have been avoided had we used a dual and triplet construct combination. The Berezhnoy *et al.* paper of 2005 is a study of the benzodiazepine action on $GABA_A$ channels and uses a $\gamma2\_\beta2\_\alpha1$ and $\beta2\_\alpha1$ combination of concatenated constructs to restrict stoichiometry and allow the mutation of a single α subunit at a time, therefore only affecting one binding site. Amongst the findings of this paper was one glaring inconsistency, which the Authors could not explain but however was perfectly understandable if their constructs were not

assembling correctly and as such might render their entire findings null and void. They used tandems and trimers to restrict the stoichiometry of the $GABA_A$ receptor so that an inserted mutation would only be present in just the benzodiazepine-binding site and so the covalent modification of the receptor by the NCS-compound should be prevented by the presence of the benzodiazepine, Ro-15-1788. In fact the NCS-compound caused covalent modification even in the presence of Ro-15-1788 and was only blocked when GABA was present as well. This indicates that the mutation wasn't restricted to just the BZD site and was present in the GABA-binding site and therefore the receptor was misassembled, probably with hanging subunits. They tried to explain away their problem citing thermal mobility of the receptor. This demonstrates that the problem with mis-assembly is wider spread than just the β4_α3 constructs, is affecting the interpretation of data and can also affect the dimer/triplet combinations suggested as a solution to some of the tandem approach's problems.

So can the use of tandem (and triplet) constructs be saved?

One possible remedy would be to change the linker. Lengthening the linker is more likely to increase mis-assembly, but it is possible that shortening the linker may restrict the assembly better so the β4 subunit of the tandem is preferentially inserted ahead of rogue β4 monomers. However against this possibility we must count the fact that maybe the α3_β4 construct did not work because the α3_β4 linker (45 residues) was too short (cfr. the 60 residue in the β4_α3 linker). Also there is the possibility that shorter linkers may encourage the formation of dipentamers and tandem-only receptors. The

inclusion of the signal peptide could also be reconsidered, although it is hard to predict what its effects are removing it may cause proteolysis or affect membrane insertion, subunit assembly etc. Paradoxically though, via the creation of secondary structures, the signal peptide may actually shorten the linker, which in this context can only be beneficial and problems with proteolysis, subunit assembly etc. are not what we are faced with. The main practical problem is that the amount of work needed to create the new constructs, test them for function and then check their stoichiometry in assembling is prohibitive: the amount of work covered in this chapter took over two years, on and off, and as such would be unlikely to be worth it even if it succeeded.

Another possibility would be to change the tandem:monomer ratio injected. The choice of a molar 2:1 ratio for the injection was based on the assumption that tandem fusion proteins were translated with the same efficiency as the equivalent weight of monomer cRNA would produce. If this was the case exactly twice as many tandem constructs would be created as monomers avoiding any excess or rogue subunits to be left without a receptor. This assumption appears flawed in hindsight, the tandem + monomer combinations injected produced substantially lower currents than the equivalent amount of monomer cRNA did. The less efficient translation efficiency of concatenated constructs has also been reported elsewhere (e.g. 5:1 ratio needed for triplet:tandem receptors Baumann *et al.* 2001). Also, as will be seen in the next Chapter the efficiency of expression of the more complicated constructs is massively lower than that of monomers. The net result of this is that maybe our 2:1 ratio resulted in an effective excess of β4 monomers, which might explain why the mis-assembled stoichiometries appear to the preferred formation of receptor. Therefore, a possible way forward may lie

in increasing the relative amount of tandem injected (or decreasing the amount of monomer). The problems with this would be, first, the prohibitive amount of work required to optimise the correct ratios and secondly the possibility of going too far the other way and producing an excess of tandems which could result in the formation of dipentamers.

Even if either of these modifications solved the problem of mis-incorporation of β4_α3 tandem constructs, it wouldn't change the wider point that the rest of the "tandem" field have, for the most part, not optimised their linkers or injection ratios and as such may still have drawn erroneous conclusions from their data. To go back and check all these different constructs and modify their parameters would be a Herculean task. Instead we decided to take the approach covered in the next Chapter, the creation of a pentameric construct.

CHAPTER 8

The Creation and Evaluation of Pentameric Constructs of a LGIC

This work has been published as:-

Groot-Kormelink P.J, Broadbent S.D., Beato M, and Sivilotti L.G.
Constraining the expression of nicotinic acetylcholine receptors using pentameric constructs. *Mol Pharm.* (2006) **69**(2): 558-63. (see White, 2006 for a review).

As discussed in the last chapter, an important aim of heterologous expression is the production of receptors with the complex stoichiometries of native receptors and the patterns of mutations seen in channelopathies. This problem was thought to have been solved by the development of concatenated subunit techniques. As detailed in the previous chapter, problems have now become apparent which may throw the whole concatenated approach and the findings obtained from them into doubt. Possible solutions to these problems were covered at the end of Chapter 7. With a tremendous amount of work, extreme vigilance and exhaustive controls, it could be possible to use tandem and triplet constructs and be sure that the receptors produced do have the stoichiometry and make-up wanted. Alternatively, the problems uncovered could be circumvented by producing a pentameric construct. In this chapter I shall record our attempts to produce a functional pentameric concatemer of a nAChR free of the problems associated with the tandem and triplet concatemers.

It had always been a long-term goal to use the tandem and triplet concatemers as stepping-stones for the production of a pentameric concatemer i.e. a functional channel made up of five linked subunits. Such molecules are not totally unknown in nature; the voltage-gated sodium channel is comprised of a large 260kDa channel-forming α subunit in association with one or more auxiliary β subunits. This α subunit is made up of four

linked domains (I-IV) each made up of six transmembrane segments (S1-S6) (see Figure 8.1) and as such is analogous to other receptor channels made up of concatenated monomers (compare with the cartoon in Figure 8.2) .

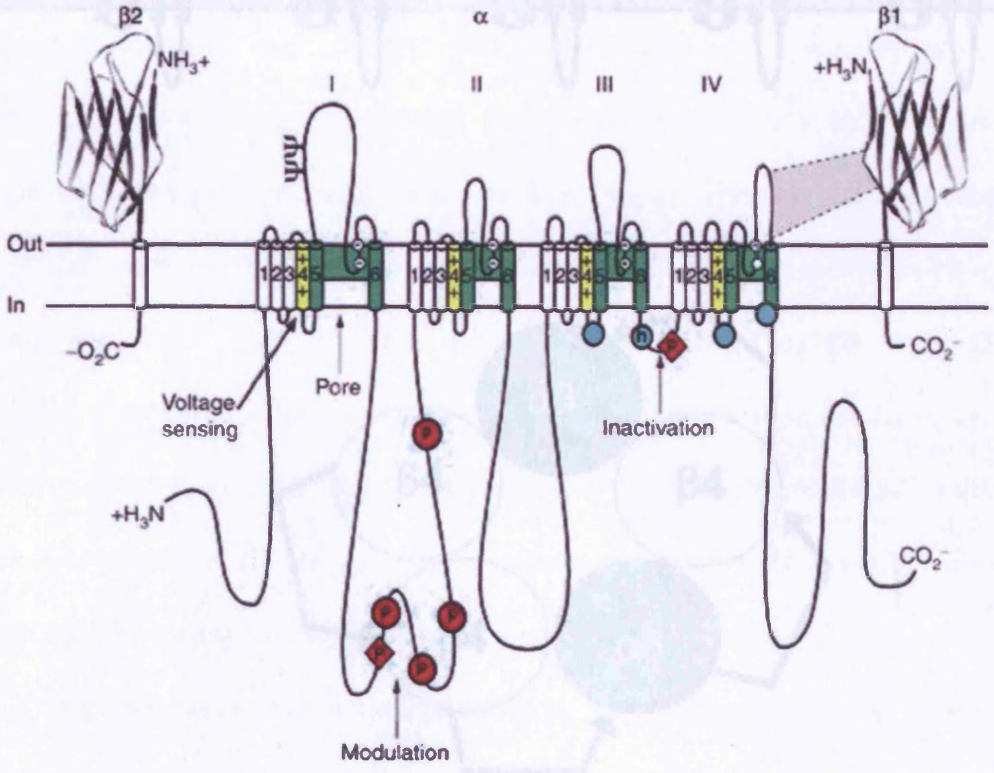

Figure 8.1: Schematic representation of the sodium-channel subunits The α subunit of the $Na_v1.2$ channel is illustrated together with the β1 and β2 subunits. (from Yu and Catterall 2003)

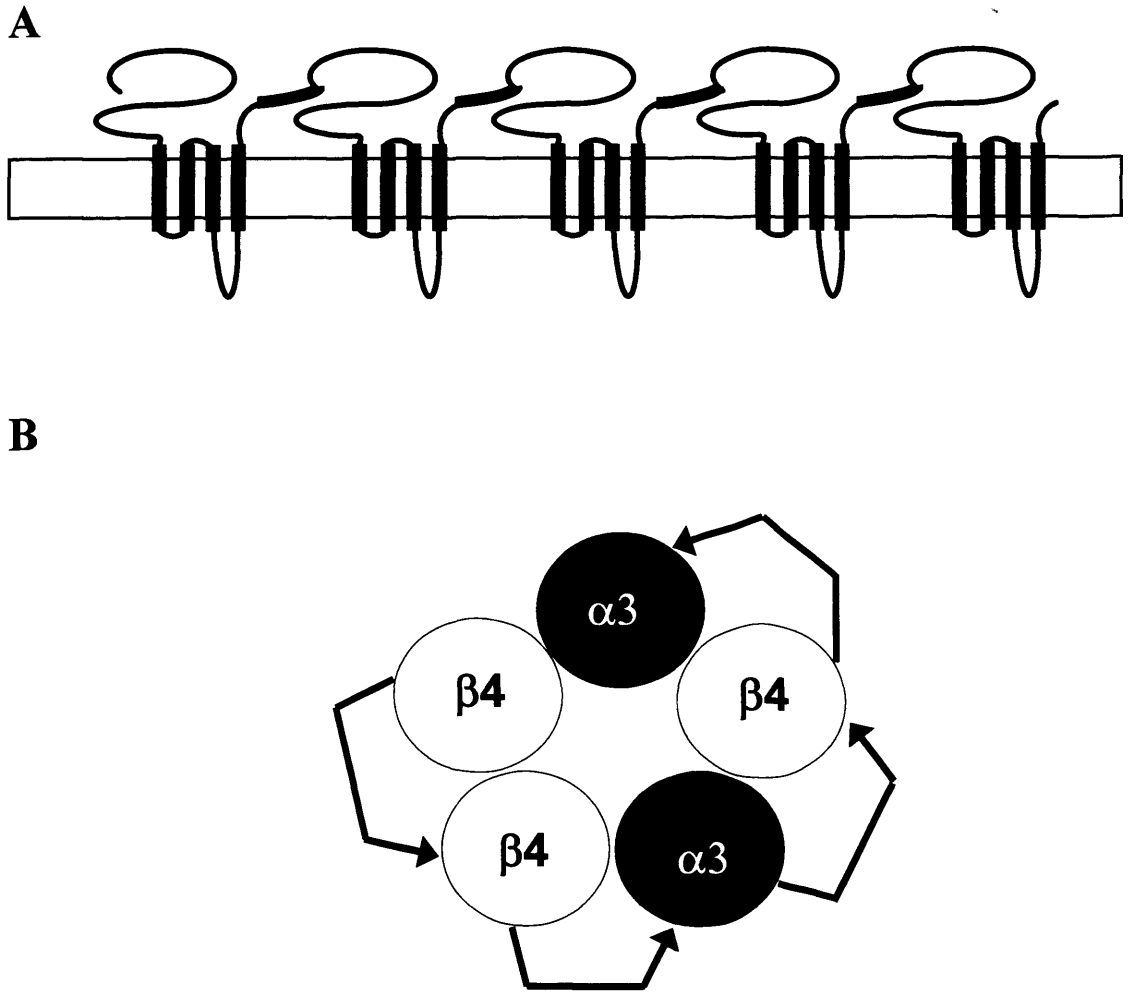

Figure 8.2: **A)** Linear representation of the pentamer construct in the cell membrane. Inserted linkers indicated by black rectangles.
B) Expected orientation of the β4β4α3β4α3 construct. Linkers shown by arrows.

Even without the tandem/triplet problems of dipentamers, proteolysis and mis-assembly reported by Zhou *et al.* 2003, Nicke *et al.* 2003 and Groot-Kormelink *et al.* 2004, functional pentamers may well be preferable as they may in principle offer a far greater control of stoichiometry and allow the precise insertion of one or more mutations anywhere within the receptor complex.

8.1 Creation of a pentameric channel

As in previous work, we focussed on the α3β4 receptor, as this was the combination we were most familiar with, was thought at the time to have a set stoichiometry, had produced functional β4_α3 tandem-containing receptors and we already had existing α3*β4 trimer constructs. These trimer constructs had been produced and partially tested before the project was abandoned due to the mis-assembly of the tandem constructs. Some trimer + dimer combinations (β4_α3_β4 + β4_α3 and β4_β4_α3 + β4_α3) had been found to express functional receptors, producing currents in the tens-of-nA range for a 10ng:2ng injection (n = 2). Due to the "success" of tandems of the β_α orientation and the initial findings from the trimer + dimer work, a pentamer construct of the stoichiometry β4_β4_α3_β4_α3 (ββαβα) was created.

The pentamer constructs were produced by Dr Paul Groot-Kormelink as described previously: the existing dimer and trimer cDNAs were linked into a pentameric construct which was then used to prepare the cRNA.

8.2 Comparison of the pentameric vs the monomeric receptor

These constructs were injected into oocytes, which were then tested for ACh sensitivity. The ββαβα construct was found to produce sizeable inward currents of a similar shape to those seen for α3 + β4 and β4_α3 + β4 receptors.

The first question is whether it does resemble the monomeric receptor. Figure 8.3 shows the traces and concentration-response curves obtained for the monomeric α3β4 (1:9 ratio) receptor and the ββαβα receptor. The 1:9 α3β4 ratio is used in the comparison, in order to ensure the majority of the monomeric construct receptors were of the same 2α:3β stoichiometry as the ββαβα receptor (it will be shown in Chapter 9 that α3β4 can also form receptors of a 3α:2β stoichiometry and that at 1:1 ratio a small proportion of these may be present). As can be seen, the responses are very similar both in time course and ACh sensitivity. Analysis of the concentration-response curves revealed small differences in the EC_{50} values (137.8 ± 13.7 μM vs. 95.0 ± 10.7 μM, n=6 and 4, for the monomer and pentamer constructs, respectively; p<0.05, two-tailed Student t-test), but not in the Hill slopes of the two receptors (1.79 ± 0.14 and 1.71 ± 0.13, difference not significant, unpaired two-tailed Student's t-test). The pentamer values do not compare too badly with the wildtype β4_α3 + β4 receptor either (EC_{50} = 122 ± 8 μM, nH = 1.98 ± 0.21, n=4, differences not significant, unpaired two-tailed Student's t-test). This is not a perfect match but it is reasonable for a linked receptor.

It would not be too surprising if it turned out the pentamer linkers have affected the properties of the channel. Other possible explanations include the presence of small residual populations of the 3α:2β receptor, which would be expected to increase the EC_{50}

value in the monomer-injected oocytes. This is pretty unlikely as receptor heterogeneity should also decrease the Hill slope.

Another possibility is that that the monomeric 2α:3β receptor (but not the pentamer-expressed receptor) might exist in different topologies, with slightly different properties. Different formations of the 2α:3β receptor sound unlikely but can not be ruled out at this stage; a monomeric receptor of a βββαα formation seems unlikely but must be borne in mind.

The responses produced by the ββαβα injection were large enough to allow us to obtain concentration-response curves (mean I_{max} = 222 ± 49, n=13) with individual I_{max} values reaching up to a respectable 610nA. These results were however achieved by injecting high cRNA concentrations (100 ng/μl) and we found that further increasing the cRNA concentration up to 2 and 3 μg/μl (the realistic upper limit of cRNA concentration), failed to increase the size of current produced (if anything it declined).

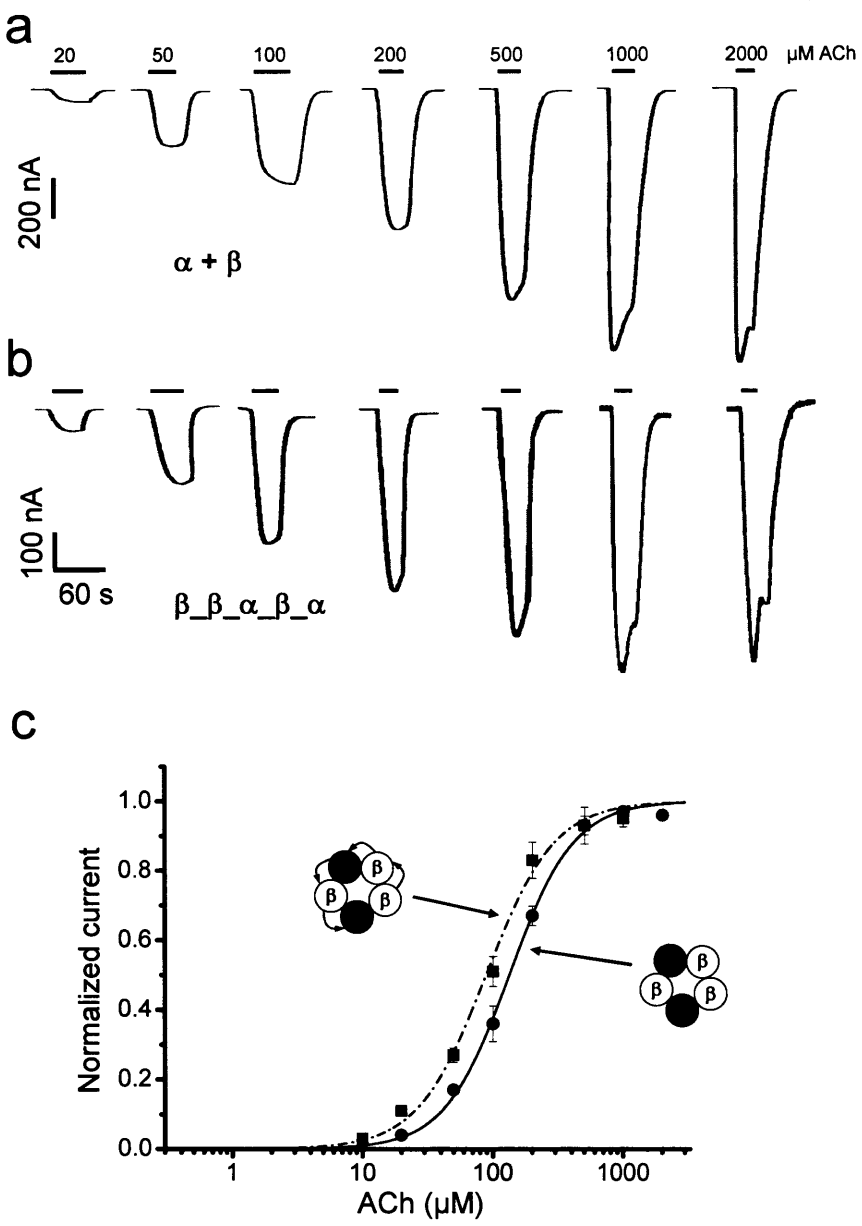

Figure 8.3: α3β4 neuronal nicotinic receptors expressed from the pentameric cRNA construct have ACh sensitivity similar to that of receptors expressed from monomeric cRNA constructs

(**a, b**) examples of current responses elicited by increasing ACh concentrations on the two types of receptors

(**c**) concentration-response curves for α3 + β4 (monomeric) receptors and for the α3 + β4 (pentameric) receptors (*n* = 4 and 6, respectively). Lines are fits of the data with the Hill equation.

All responses were recorded from *Xenopus* oocytes voltage clamped at -70 mV in nominally calcium-free solution.

8.3 Action of a competitive antagonist on the pentameric receptor

The EC_{50} and Hill slope of a receptor are fairly unsatisfactory ways of comparing receptors. A much more robust comparison can be obtained by measuring the shift produced by a competitive antagonist in the concentration dependence of agonist responses (i.e. dose-ratios). We have in the past done this for the competitive antagonist trimetaphan and α3β4 receptors expressed from unlinked constructs (Boorman *et al.* 2003). We now found that dose-ratios to 0.2 μM trimetaphan are very similar in pentamer-expressed receptors, with values of 4.35 ± 0.38 (n = 10) and 5.01 ± 0.37 (n = 4) for unlinked and linked constructs, respectively. Because the magnitude of this shift is a direct expression of antagonist affinity, this indicates that the (overlapping) agonist/antagonist binding site is very similar in the two types of recombinant receptors.

8.4 Does the pentamer assemble correctly?

Thus, we have shown that the pentamer constructs form receptors similar to monomeric receptors in its ACh and trimetaphan sensitivity. However, having detected mis-assembly of tandem-containing receptors, we now have to make sure that the same does not apply to pentameric construct receptors and that these receptors contain the correct complement of subunits as dictated by the construct design. This also entails checking that there is no significant proteolysis (at least into functional fragments) and no formation of dipentamer receptors etc.

First we checked if the *in vitro* synthesised cRNA was of the correct length and that no RNA breakdown had happened. Conceivably, if there is sufficient contamination

by breakdown products, the functional receptors we observed may not be produced by the linked, five-subunit construct as we wish, but by the contaminant. The cRNA gel electrophoresis experiment shown in Figure 8.4 allowed us to discount this possibility: all the constructs used showed one clean band of the appropriate molecular weight on the gel, indicating that construct impurity or breakdown was not a problem at RNA level.

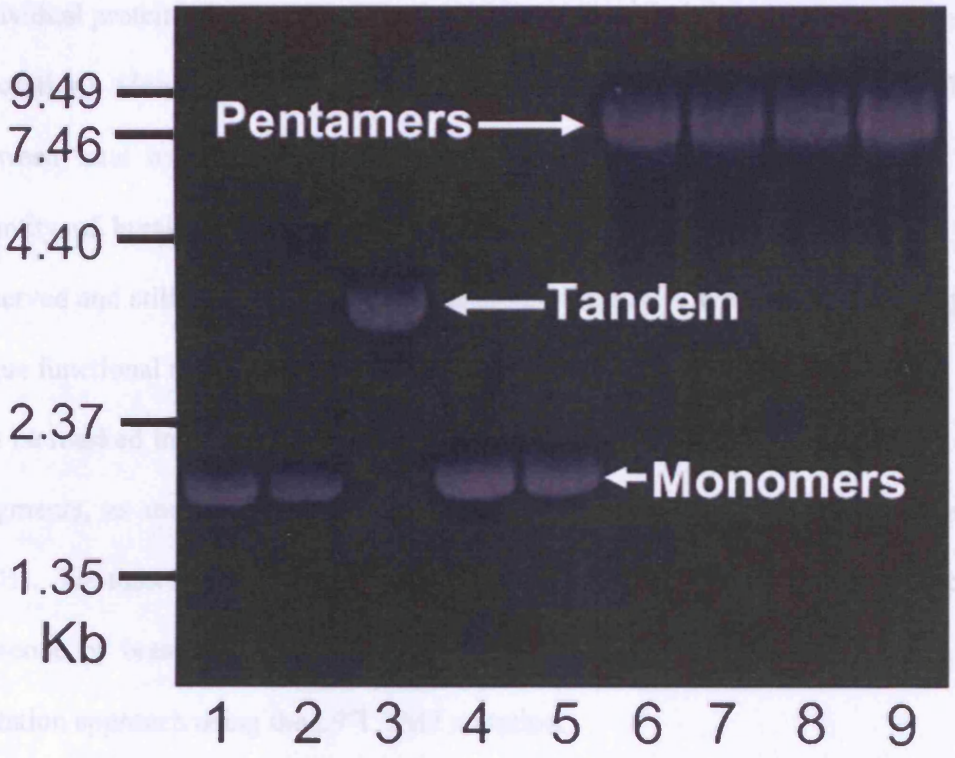

Figure 8.4: RNA gel-electrophoresis of capped cRNA constructs used for *Xenopus laevis* oocyte injections. Approximately 1 μg of α3 (**1**), β4 (**2**), β4_α3^{LT} tandem (**3**), α3^{LT} (**4**), β4^{LT} (**5**), β4_β4_α3_β4_α3 penta (**6**), β4^{LT}_β4_α3_β4_α3 mutant penta (**7**), β4_β4_α3_β4_α3^{LT} mutant penta (**8**), and β4^{LT}_β4_α3_β4_α3^{LT} mutant penta (**9**) were separated on a 1.5% agarose-gel. The 0.24-9.5 Kb RNA ladder is indicated on the left. The predicted cRNA sizes are; 1.8 kb for α3 and β4 monomers, 3.4 kb for β4_α3 tandem, and 8 kb for the pentameric constructs.

It is of course possible that problems may arise *after* the cRNA is injected into the oocyte: our pentameric fusion protein may not really assemble as a pentamer because either the cRNA is broken down in the oocyte or because degradation occurs at protein level. It is important to assess whether this happens, because such a process could in principle render pointless our effort in constraining the topology and composition of the receptor. A straightforward way of testing this would be to check the size of either the individual proteins (by Western Blotting) or the assembled complex (by sucrose-gradient separation). However, these methods are not very sensitive and cannot differentiate between total receptor protein and surface-expressed functional receptors. A small quantity of breakdown products could be enough to produce the functional channels observed and still escape biochemical detection. Similarly, Western Blotting may pick up rogue functional monomer subunits but, given that the epitope recognised by the antibody can be masked in linked subunits, wouldn't necessarily detect functional dimer or trimer fragments, as mentioned in the last chapter and reported elsewhere (Baumann *et al.* 2001). We therefore decided to perform a more sensitive functional test to check for the presence of breakdown products and incomplete incorporation, and chose a reporter mutation approach using the L9′T TM2 mutation.

Co-injecting the pentameric construct with excessive levels of mutated monomer or tandem construct would "kill two birds with one stone".

One possibility was that the channels we are detecting are the result of the pentamer being proteolysed into functional monomeric, dimeric, trimeric and even tetrameric fragments which then reassemble into a receptor (obviously with unconstrained stoichiometry). By co-injecting with an excess amount of mutated

subunits (note that the mutated subunit alone is incapable of forming a receptor homomerically) these proteolytic fragments would preferentially form receptors with the mutated subunits resulting in receptors incorporating one or more of the L9'T mutations. Therefore the concentration-response curves of these mis-assembled receptors would display a shift in their EC_{50} values. Even if our assumption that the mutated subunits were not in excess we would still expect a sizeable subpopulation of the formed receptors to contain the mutations and therefore the concentration-response curves would at least become multi-phasic. Injection with a high concentration of $\alpha3^{LT}$ should detect any rogue β4 monomers, β4_β4 dimers or β4_β4_α3_β4 tetramers and it would also show if any 3α:2β receptors were forming, possibly by co-assembling with β4_α3 and α3_β4 dimers or β4_α3_β4_α3 tetramers. Injection with a high concentration of $\beta4^{LT}$ should detect any rogue α4 monomers, β4_α3 dimers, α3_β4 dimers, α3_β4_α3 trimers or β4_α3_β4_α3 tetramers. Even unexpected formations of, say, a trimer-only receptor formed by partial incorporation of constructs leaving hanging subunits should be detected. Of the different possible functional fragments there was one which wouldn't be detected by co-injection with a single $\alpha3^{LT}$ or $\beta4^{LT}$ subunit, the β4_β4_α3 fragment. Such a fragment could however assemble into a receptor with its cleaved end β4_α3 dimer or form a receptor with another trimer, leaving a hanging subunit. Obviously we couldn't co-inject the pentamer with *both* $\alpha3^{LT}$ and $\beta4^{LT}$ monomers as these could form receptors in their own right. Therefore, in order to check for this fragment we also co-injected the pentamer with excess $\beta4\_\alpha3^{LT}$ tandem. This could assemble with the β4_β4_α3 fragment, to form a receptor containing a single $\alpha3^{LT}$ mutation.

The other possibility was that unconstrained receptors could form because of multiple pentameric fusion proteins participating to the same receptor assembly. At one end of the spectrum, it may be only two pentamers and a single hanging subunit, at the other it could five individual pentamers coming together and contributing one subunit each. These in turn could in principle produce higher order structures with "rafts" of pentamers forming multiple channels. It is hard to know whether these channels would be functional or indeed if their low level of function is the cause of the low functional "expression" of pentamers discussed at the end of this chapter. The real nightmare scenario would be a combination of both functional proteolytic fragments and pentamer rafts producing a complete mess which somehow still seemed to resemble the monomeric receptor in pharmacological properties. Such scenarios do not sound likely, but our experience with mis-assembled tandem receptors taught us to take nothing for granted. For example, who would have believed that not only was the completely mis-assembled tandem receptor possible but was actually the preferred stoichiometry! Either way all our hopes of constraining stoichiometry would go out of the window.

These possibilities ought also to be detected by the co-injection of mutated subunits in excess, as these should be the preferential candidates for mis-incorporation and should produce mutation-containing receptors causing changes in the concentration-response curves of the resulting receptors.

As previously noted, the efficiency of expression appears to be impaired for concatenated subunits. An alternative explanation could be that expression has not been affected greatly by linking, but that receptors made up by concatenated subunits are less functional than monomeric receptors, with a lower *P*open, for instance. This appears

unlikely: concatenated subunit receptors have EC_{50} that is very similar to monomeric construct receptors and this could not be if their maximum *P*open were grossly reduced. Also when Dr. Marco Beato attempted to perform single-channel studies on pentamer-injected oocytes he found that the large majority of the patches pulled were "blank" rather than that they were expressing "low *P*open" functional receptors, further anecdotal evidence that the low currents seen are a problem with expression rather than function (see discussion at the end of this chapter).

An important decision in the experimental design is how much mutant monomer should be injected in these tests vs. the pentamer. Because efficiency of expression and incorporation are much greater for monomer construct, deciding simply considering the ratio between the quantity of cRNA injected for monomer and pentamer grossly underestimates the size of the excess in monomer. A better quantification of that is given by the level of functional expression achieved by the different constructs. The top traces of Figure 8.5 show that functional expression of monomers (estimated by measuring maximum ACh responses to 1mM) is approximately an order of magnitude larger than that of monomer plus pentamer, even though the actual ratio of cRNA concentration was actually 0.25ng:100ng (mutated subunit:pentamer). Thus, 0.25 ng of $\alpha3^{LT}$, $\beta4^{LT}$ or $\beta4\_\alpha3^{LT}$ cRNA produced several μA of current if injected together with the appropriate wild type monomer at the correct concentration (5570 ± 890 nA, n = 10, 2342 ± 393 nA, n=6 and 1790 ± 500 nA, n=8 respectively) but only half a μA if injected with pentamer cRNA (570 ± 151, 621 ± 97 and 119 ± 38 nA, respectively).

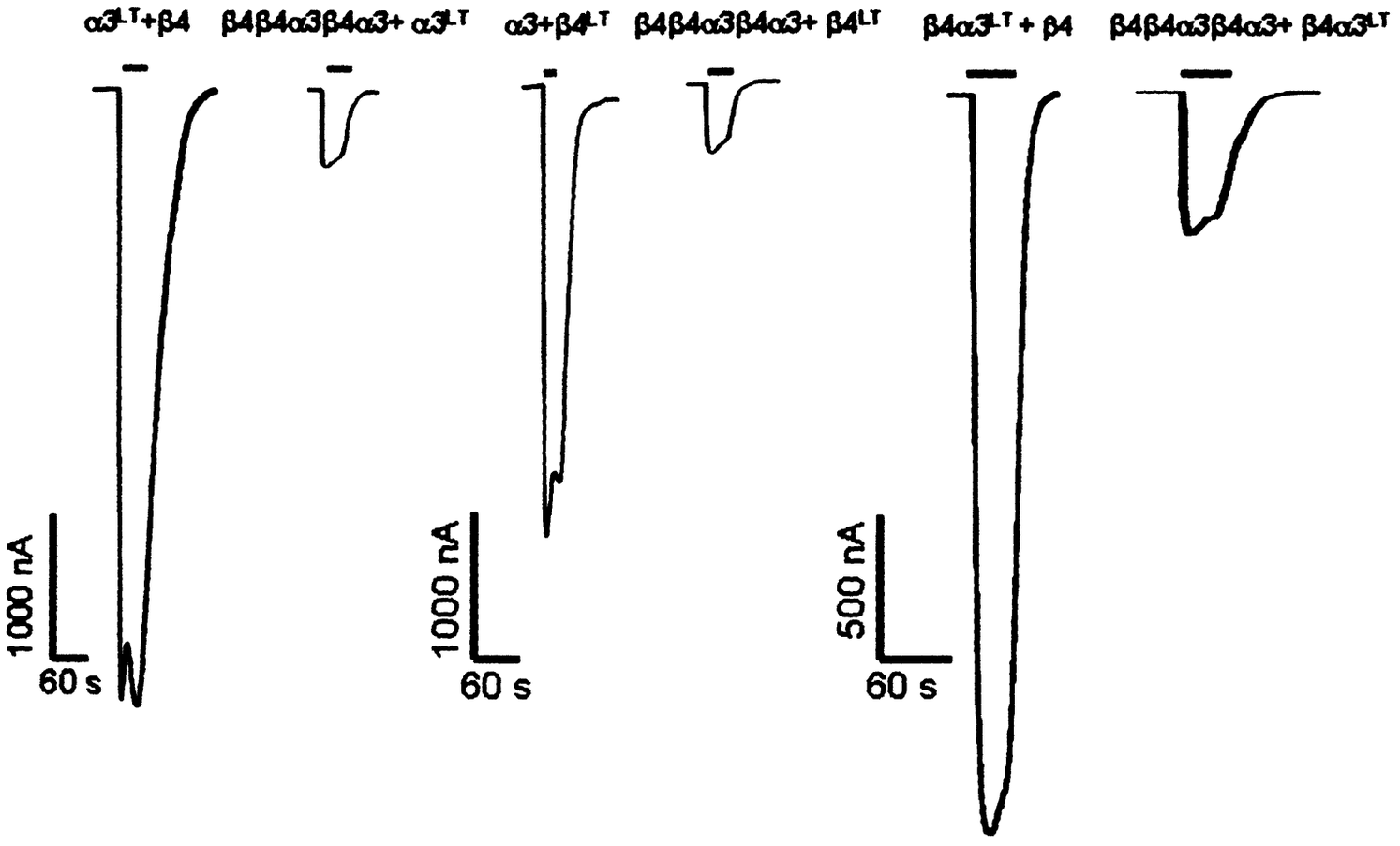

Figure 8.5: Example traces give an estimate of the extent of the functional excess of $\alpha3^{LT}$, $\beta4^{LT}$ and $\beta4\_\alpha3^{LT}$ subunit cRNA injected, compared to the pentamer, by showing that the same quantity of monomer or tandem cRNA produced very large functional responses if co-expressed with the appropriate monomer.

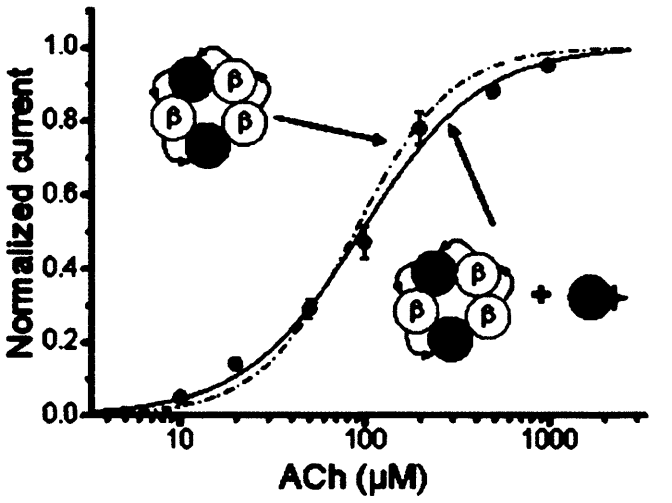
Normalized current
1.0
0.8
0.6
0.4
0.2
0.0
10
100
1000
ACh (μM)

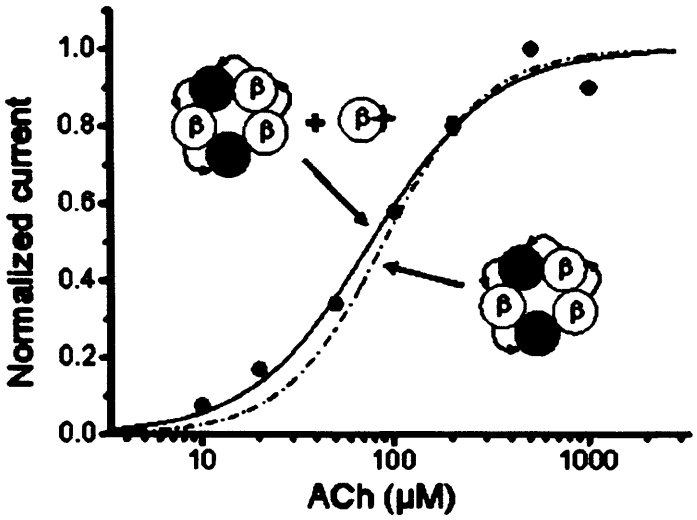
Normalized current
1.0
0.8
0.6
0.4
0.2
0.0
10
100
1000
ACh (μM)

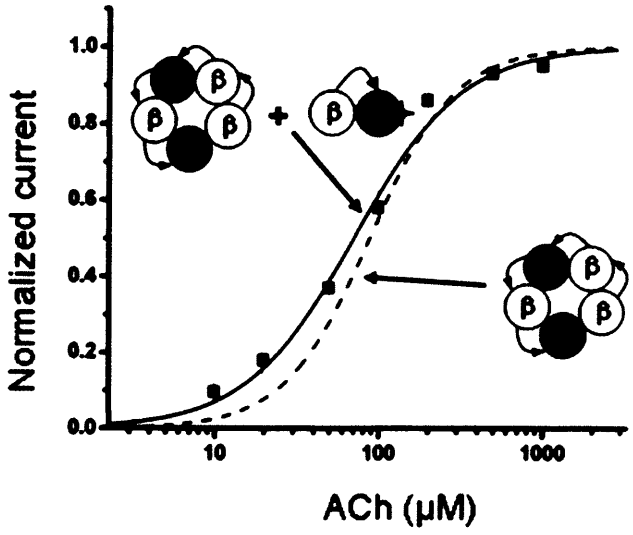
Normalized current
1.0
0.8
0.6
0.4
0.2
0.0
10
100
1000
ACh (μM)

Figure 8.6: (previous page) Expression of an excess of $\alpha3^{LT}$ (**Top**), $\beta4^{LT}$ (**Middle**) or $\beta4\_\alpha3^{LT}$ (**Bottom**) together with the pentamer construct does not result in incorporation of the mutant monomers into functional receptors. The concentration response curves obtained from receptors expressed after co-injection of mutant monomer with wild-type pentamer constructs (full circles and continuous lines, n=4 for all) were not significantly different from those obtained after expression of wild-type pentamer alone (dashed curves) (unpaired two-tailed Student's t-test).

Figure 8.6 shows the concentration-response curves obtained when the pentamer was injected with high concentrations of mutated monomer or tandem. As can be seen there is very little difference between the dose-response curves obtained from the pentamer in the absence or presence of high concentrations of "loose" mutated subunits (wild-type pentamer alone, i.e. $\beta4\_\beta4\_\alpha3\_\beta4\_\alpha3$: EC_{50} = 95.0 ± 10.7 μM n_H = 1.71 ± 0.13, n=4; wild-type pentamer + $\alpha3^{LT}$: EC_{50} = 95.0 ± 10.7 μM n_H = 1.35 ± 0.13, n = 4; wild-type pentamer + $\beta4^{LT}$: EC_{50} = 75.8 ± 5.1 μM n_H = 1.39 ± 0.11, n=4; wild-type pentamer + $\beta4\alpha3^{LT}$: EC_{50} = 71.0 ± 6.7 μM n_H = 1.32 ± 0.14, n=4, differences not significant, unpaired two-tailed Student's t-test). If there were any breakdown or mis-assembly, these curves would be expected to be closer to those obtained from receptors containing one, two or even three copies of the mutation.

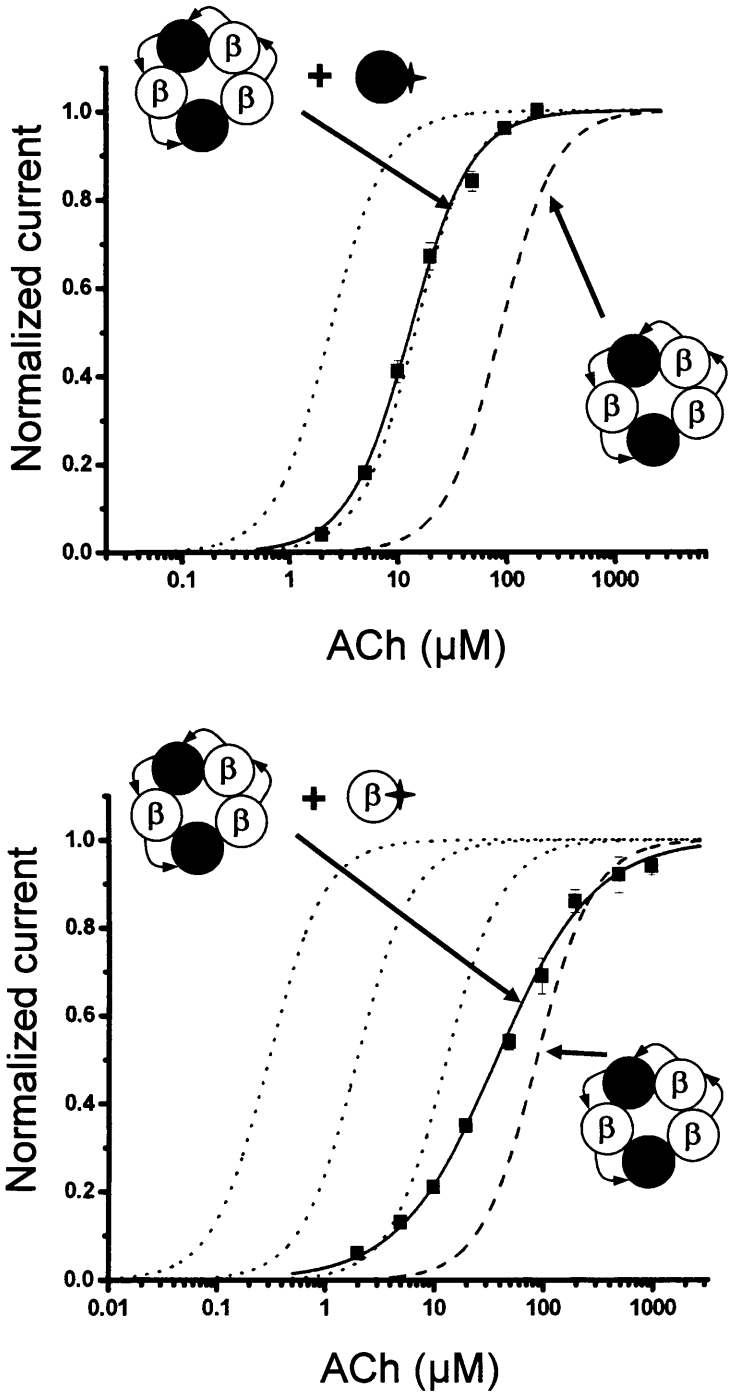

Figure 8.7: Expression of a vast excess of $\alpha 3^{LT}$ (**Top**) or $\beta 4^{LT}$ (**Bottom**) together with the pentamer construct results in partial incorporation of the mutant monomers into functional receptors. The concentration response curves obtained from receptors expressed after co-injection of mutant monomer with wild-type pentamer constructs (full circles and continuous lines, n=4 for all) differ from those those obtained after expression of wild-type pentamer alone (dashed curves).

If the injected concentration of rogue monomer ($\alpha3^{LT}$ or $\beta4^{LT}$) was further increased to the equivalent of that needed to produce over twenty-five-fold the current of that produced by the injected pentamer RNA concentration (wild-type pentamer $\beta4\beta4\alpha3\beta4\alpha3$ + $\alpha3^{LT}$: I_{max} = 326 ± 147 nA; $\alpha3^{LT}$ + $\beta4$: I_{max} = 7235 ± 1187 nA; wild-type pentamer + $\beta4^{LT}$: I_{max} = 525 ± 196; $\alpha3$ + $\beta4^{LT}$: 50 μM produced a current in excess of 13 μA, amplifier saturated) some mis-assembly could be produced (Figure 8.7). As can be seen, the pentamer plus $\alpha3^{LT}$ curve was significantly different from the wild-type pentamer (EC_{50}: $p < 0.001$, n_H: not significant, unpaired two-tailed Student's t-test) shifted to where we would predict an $\alpha3\beta4$ monomeric receptor containing a single $\alpha3^{LT}$ mutation would be. This suggests that a single rogue mutant monomer subunit was incorporated into most or all of pentameric construct receptors. The pentamer plus $\beta4^{LT}$ curve was intermediate between the wild-type pentamer and the predicted single $\beta4^{LT}$ mutation curve indicating partial mis-assembly although neither EC_{50} nor Hill slope values were significantly different from the wild-type pentamer (unpaired two-tailed Student's t-test). These results are not really worrying as they conclusively prove there is no complete breakdown and they show that, if mis-assembly was occurring when we injected less monomer in the experiments shown in Figure 8.6, it would have been detected.

These results are very reassuring and suggest that gross misassembly of the pentamer constructs is unlikely to occur in normal circumstances.

These experiments may also provide some insight into the post-translational assembly of receptor complexes. The most likely explanation of the $\alpha3^{LT}$ subunit

induced mis-assembly was that it replaced the "trailing" α3 subunit as replacement of the "central" α3 would necessitate the disruption of the receptor complex and the replacement of the missing subunits with either a triplet fragment or another pentamer, an overly complicated hypothesis none of which we have any evidence for. A similar line of reasoning would conclude that the most likely β4 subunit to be displaced by a single $\beta4^{LT}$ monomer would be the "leading" β4 subunit. The shallow slope of the pentamer plus $\beta4^{LT}$ curve of Fig. 8.7 would indicate a mixed population of receptors, most probably a roughly equal split between correctly assembled pentamers and receptors with a single incorporated $\beta4^{LT}$ monomer, rather than a single population of pentamers all incorporating one $\beta4^{LT}$ monomer but with a lesser effect on the EC_{50} value due to mutation non-equivalence. It is tempting to conclude from this that the "trailing" subunits may be more "floppy" i.e. more easily displaced than the "leading" subunits.

These experiments not only suggest that there is no breakdown, but also confirm that the receptor expressed from pentamer constructs contains the pentameric fusion protein in its entirety, as intended, in all but the most extreme circumstances. If this was not the case and more than one pentamer participated to the formation of a single receptor, for instance contributing one or two subunits, we would expect to see preferential incorporation of monomer or tandem constructs into such receptors and therefore shifts in the dose-response curves. Having developed a functional pentamer, shown it resembles monomeric receptors and, after exhaustive testing, found no significant evidence of breakdown or mis-assembly can we use pentamers to help study LGICs.

8.5 Testing a pentamer mutant construct

As mentioned earlier one of the big unknowns about LGICs is whether the effect of mutations in specified subunits is equivalent, and independent of subunit type and position. This was one of the questions we hoped would be answered by the development of functional pentamers. Therefore we decided to apply the pentamer technique first to producing functional pentamers with mutations in specified positions.

Incidentally, these experiments could act as a further control to ensure that there was no significant pentamer breakdown or mis-assembly, because if these phenomena were occurring it would be likely that mutated pentamers would produce multi-phasic or surprisingly shifted concentration-response curves.

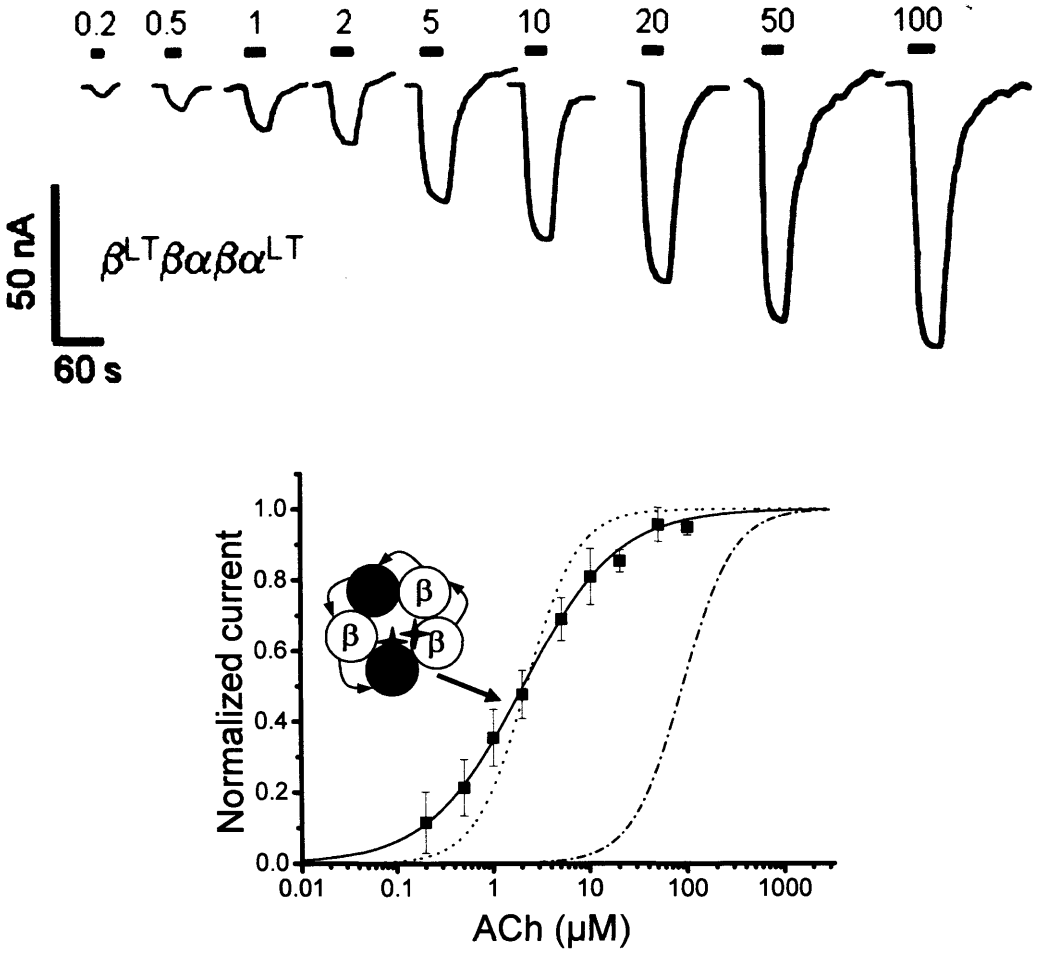

Figure 8.8: Example traces and concentration-response curves showing the effect of inserting two TM2 leucine-to-threonine 9' mutations into the pentamer construct, (filled squares, continuous line, *n* = 4), where the dotted line is the 36-fold shift, expected on the basis of the previous data (Boorman *et al.* 2000), from the wildtype pentamer (dashed line).

The first mutated construct to be tested was the β4β4α3β4α3 pentamer with its first β4 and last α3 subunit mutated at 9′ from leucine to threonine ($\beta4^{LT}\beta4\alpha3\beta4\alpha3^{LT}$). This was chosen because it was the easiest construct to produce. Future work will deal with other two-mutant pentamers such as $\beta4\beta4\alpha3^{LT}\beta4\alpha3^{LT}$, $\beta4^{LT}\beta4^{LT}\alpha3\beta4\alpha3$ or $\beta4^{LT}\beta4\alpha3\beta4^{LT}\alpha3$. The obvious term of comparison are two-mutant $\alpha3^{LT}\beta4$, $\alpha3^{LT}\beta4\beta3$ and $\alpha3\beta4^{LT}\beta3$ monomeric receptors. Figure 8.8 shows the traces and concentration-

response curve obtained for $\beta4^{LT}\beta4\alpha3\beta4\alpha3^{LT}$. As can be seen from the graph the degree of shift produced by the two mutations in the pentamer was almost identical to that calculated (from Boorman *et al.* 2000) for the combined effect of a single α3 and β4 mutant subunit (EC_{50} = 2.03 ± 0.46 μM, n = 4 vs 2.19 μM calculated). The Hill slope is a little bit reduced when compared to the calculated two mutation curve but the calculated curve was generated on the assumption that the two-mutation curve would be parallel to the wildtype pentamer curve (n_H = 1.67), of course as has been discussed earlier receptors with mutations tend to have reduced Hill slope possibly due to monoliganded and spontaneous openings. Hence the Hill slope of $\beta4^{LT}\beta4\alpha3\beta4\alpha3^{LT}$ (0.9 ± 0.16, n = 4) compares reasonably well to the Hill slopes values we have recorded for other two-mutation α3β4 monomeric receptors ($\alpha3^{LT}\beta4$ 1:1, 1.15 ± 0.08, n = 6, $\alpha3^{LT}\beta4$ 1:9, 1.32 ± 0.07, n = 5). It must be borne in mind that these two-mutant monomeric receptors, although providing better expected Hill slope guidelines than the calculated curve, aren't perfect comparisons as they are taking from receptors with two α3 mutations rather than the single α3 and β4 of the pentamer.

Overall, these findings suggests that the presence of the linkers has not significantly altered the properties of the receptor and as such mutated pentamer constructs provide a good model for nAChR LGICs with complicated patterns of mutations.

8.6 Checking the equivalence of individual subunit mutations

A

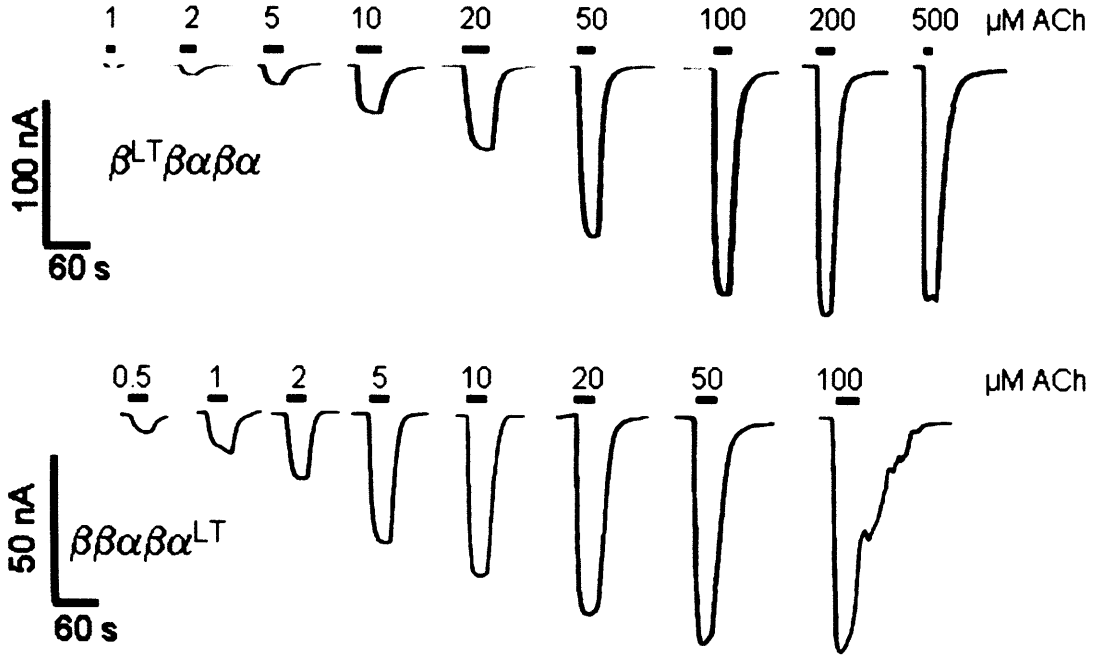

B

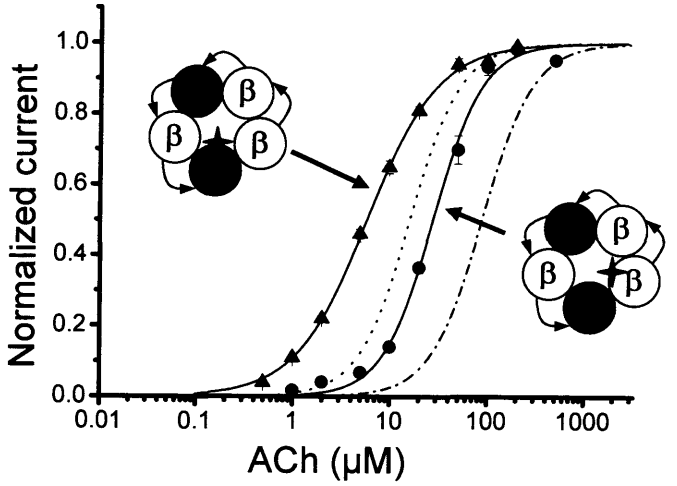

Figure 8.9: (previous page) Non-equivalent effects of TM2 L9'T mutations inserted into a single α or a single β subunit.
(**A**) Example current responses elicited by increasing concentrations of ACh.
(**B**) Comparison of the concentration-response relation for pentamer-expressed receptors bearing an L9'T mutation on a single α subunit (β4_β4_α3_β4_$\alpha3^{LT}$) or a single β subunit ($\beta4^{LT}$_β4_α3_β4_α3). Note that the increase in agonist sensitivity produced by a single mutation copy is greater if the mutation is in α. (filled triangles, *n*=4). This single-mutation shift is greater than the approximately 6-fold shift expected from previous experiments in which all α or all β were mutated (shown for reference by the dotted line, (Boorman *et al.* 2000). Conversely, the increase in ACh sensitivity is less than expected when the mutation is inserted in β (filled circles, *n*=5).

Having shown that the pentamer produced a reasonable model of a two-mutant LGIC, we then produced pentameric constructs with either the first β4 subunit or the last α3 subunit mutated to test, for the first time, the assumption on equivalence of effect of 9′ mutations. The traces and curves obtained are shown in Figure 8.9. The graph shows, the actual effects of mutating a single subunit in a specified position and as can be seen while the β4β4α3β4$\alpha3^{LT}$ (EC_{50}: 5.9 ± 0.2 μM, n = 4) produced a greater than expected shift (around 16-fold compared to the 6-fold expected from the Boorman interpolation), the $\beta4^{LT}$β4α3β4α3 (EC_{50}: 28.5 ± 1.8 μM, n = 5) produced a smaller shift of around 3-fold (EC_{50}: $p < 0.005$, n_H; not significant, unpaired two-tailed Student's t-test). The net effect of combining these two mutations would be to produce an intermediate shift close to that seen for the two mutations together as seen for $\beta4^{LT}$β4α3β4$\alpha3^{LT}$ in Figure 8.8.

It is not clear yet why a mutation in that particular α3 should be more potent than a mutation in the neighbouring β4: clearly considerable further work is needed, and each subunit will have to be mutated in turn alone and in combination with other mutations. The differences could be due to differences in their proximity to the binding sites or some

other important region of the receptor or it could reflect some difference in the exact positioning of the 9′ residues of each subunit in the channel. It can not be ruled out at this point that this difference is not due to some artefact caused by the linkers in the pentamer and their effects on the insertion or activity of the receptor.

All the curves produced by mutated pentamers were well fitted by one-component fits which further indicates there was no significant breakdown or misassembly of the pentamers.

8.7 Discussion

The low currents obtained from pentamer constructs are a serious limitation of the technique. As discussed above, it is likely to be due to low surface expression, maybe because of poor translation of such large constructs. This is a serious limitation, given that one of our aim was to use linked-subunit receptors for single-channel work. This phenomenon of low currents was a common feature and was to dog the whole project; it may be related to the decrease in expression levels noted for tandems and triplets and commented on in Chapter 7. The cause of this low current is unclear, it maybe due to proteolysis (although, as shown, there is no evidence of functional proteolysed fragments), a "maxing-out" of protein production or the resulting pentameric receptor may just have a low *P*open or channel conductance. For the sake of brevity I shall refer to the level of currents seen as "expression" levels although they may not actually be due to low expression levels but may be due to low *P*open, conductance etc. Attempts at single-channel recordings from pentamer-injected oocytes provides some evidence that this problem is due to expression level, given that as many as 95% of the patches pulled

were "blank" whilst the "non-blank" patches contained receptor channels with normal *P*open and channel conductance values.

How to increase expression? We haven't explored the relation between quantity of cRNA injected and expression enough to be sure, but given we found that increasing cRNA concentration slightly decreased current levels, it is possible that there is a "bell curve" relationship between concentration of cRNA injected and receptor expression levels. It could well be that the quantity we injected was not optimal and expression levels may be increased, counter-intuitively, by injecting *less* cRNA. Another possible avenue to explore would be molecular biological techniques, for instance we saw a trend towards a small increase in I_{max} (from 293 ± 71 to 351 ± 52, n = 5-6) when cRNA created with an extra 1μl GTP as suggested in the mMESSAGE mMACHINE Kit instruction manual for optimising the yield of long transcripts. While the aim of the work covered in this chapter was proof of concept, optimising expression will be important as the low "expression" levels witnessed were about 10-fold too low to allow single-channel work.

In summary, we have shown that the concatemer approach can be extended to produce constructs of up to five subunits which produce functional receptors. While expression of such a complete-receptor concatemer has been obtained for other types of channel, notably potassium channels see for instance (Liman *et al.*, 1992) and TRP channels (Hoenderop *et al.*, 2003), to our knowledge this is the first time that this approach has been used in the nicotinic superfamily of ligand-gated channels. These receptors appear to be similar to those obtained with monomeric constructs, and do not appear to suffer from the problems noted for other, smaller constructs. Though there is a small difference in the EC_{50} of the pentameric and monomeric construct receptors these

results compare well with those obtained by Sigel and co-workers in their expression of $GABA_A$ receptors from trimer + dimer constructs (Baumann *et al.*, 2002). Use of these constructs can be exploited for a huge variety of experiments that were simply not possible until now. As such this technique could provide a powerful tool for electrophysiological studies of recombinant receptors in heterologous expression systems. With the recent development of higher throughput, automated recording systems for *Xenopus* oocytes such as the Roboject, the ability to produce native-like, complicated receptors containing multiple subunits with specified mutations in heterologous systems should also be of great use to the pharmaceutical industry.

CHAPTER 9

Alternate Stoichiometries of the α3β4 nAChR

A manuscript on the findings in this chapter is in preparation.

A substantial body of biochemical and electron microscopy work has shown the muscle nicotinic receptor to be a heteropentamer with a stoichiometry of $\alpha 1\beta 1\gamma(\delta/\varepsilon)$ at a ratio of 2:1:1:1 (for a review see Karlin, 1991) and this has been accepted for over two decades (Lindstrom *et al.* 1979). In comparison the stoichiometry of the neuronal nAChRs is still the subject of much research and debate. Early work showed that the $\alpha 2$, $\alpha 3$ and $\alpha 4$ subunits when co-expressed in oocytes individually with $\beta 2$ produced receptors with two conductances. Varying the injection ratios of $\alpha 2\beta 2$ changed the proportion of each conductance present indicative of two different stoichiometries (Papke *et al.* 1989). Estimating the proportion of different channel types by counting single channels is difficult and prone to errors. Furthermore these experiments had low *n* and showed poor quality of the recordings. It is not therefore surprising that these data had little impact on the general opinion that all types of nicotinic receptors, including the neuronal receptors, have only a single stoichiometry. Further work on oocyte-expressed chick $\alpha 4\beta 2$ receptors using site-directed mutagenesis suggested a stoichiometry ratio of 2:3 (Cooper *et al.* 1991; see also Anand *et al*, 1991) and this was thought to hold for all the neuronal nicotinics, especially since the two alpha, three non-alpha subunit stoichiometry tallies well with the muscle nAChR stoichiometry. In addition to that, two α subunits would form two ligand binding sites in agreement with Hill slope values, which also suggested that neuronal nAChRs required the binding of two ACh molecules. Nevertheless, the expression of rat $\alpha 4\beta 2$ subunits has since been shown to produce receptors with two apparent stoichiometries with distinct pharmacologies, most likely

2α:3β and 3α:2β (Zwart & Vijverberg, 1998). Reporter mutation work, however, confirmed that in oocytes at equimolar injection ratios, the stoichiometry of the α3β4 receptor is 2α:3β (Boorman *et al.* 2000). Most recently, extensive work has shown that human α4β2 does exist in two stoichiometries when expressed in HEK cells and the relative proportions of each stoichiometry could be forced and changed, not only by changing injection ratios but also by changing temperature and through exposure to nicotine (Nelson *et al.* 2003).

Following on from our work in 2000 (Boorman *et al.* 2000), the use of first tandem then pentameric constructs had confirmed that an α3β4 nAChR with two α subunits is functional and resembles the receptor expressed by oocytes injected at an α:β 1:1 ratio. However, as shown earlier, α3β2 and α4β2 dose-response curves are biphasic (and become monophasic when $\beta3^{VS}$ is co-expressed) suggesting that at a 1:1 ratio these two combinations were likely to exist in two stoichiometries. The questions I address in this chapter are:-

1) What is the α3β4 primary stoichiometry?
2) Can that stoichiometry be changed?
3) If so, what effect does changing the stoichiometry have on that receptor?

9.1 Primary Stoichiometry of the α3β4 nAChR: expression of wild-type subunits at 1:1 ratio

In Boorman *et al.* 2000, reporter mutations showed that the injection of α3 and β4 subunits at equimolar ratios produced a receptor which displayed a greater shift when the mutation was present in the β4 subunit then the α3 subunit (Figure 9.1). Comparison of the dose-ratio values gave the likeliest stoichiometry to be the 2α:3β as seen with oocyte-expressed chick α4β2 by Cooper *et al.*

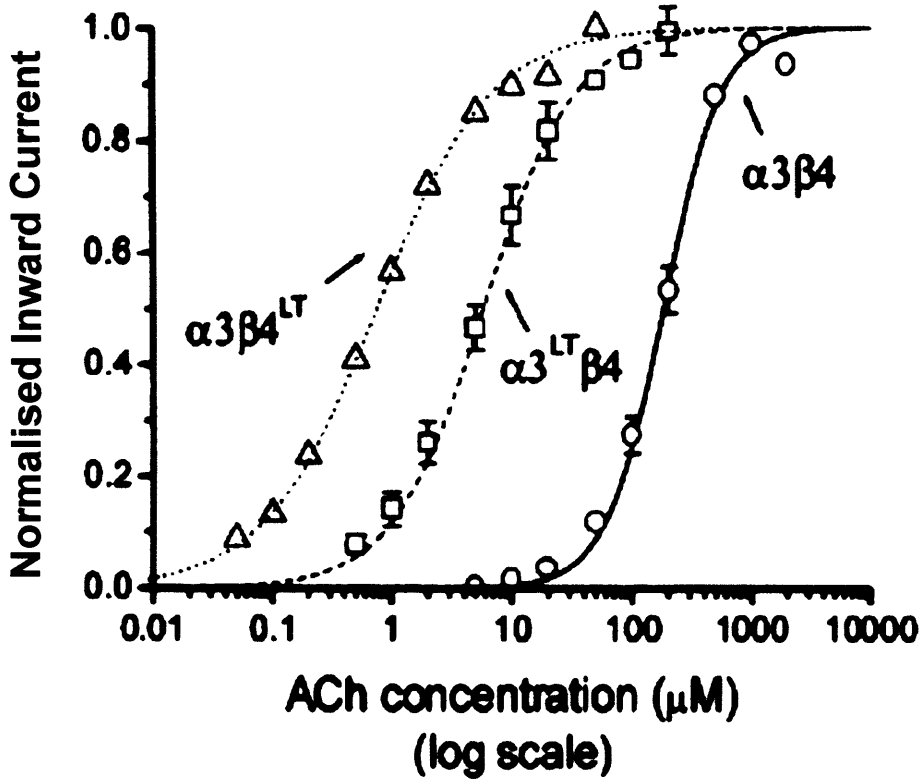

Figure 9.1: ACh-concentration-response curves showing the effect of incorporation of the 9′ LT mutation into the α3 (open squares) and β4 (open triangles) subunits compared with the wildtype (open circles). Pooled normalised curves were fitted with a Hill equation as a free fit (n=4-7). Note the greater effect of the mutation in β4 than α3, consistent with there being more β than α subunits present in the receptor. (from Boorman *et al.* 2000)

Our first set of experiments was to characterise the receptors produced by injecting the wild-type subunits at ratios of 1:9 and 9:1. If the α3β4 can only adopt one stoichiometry we would expect to see the same dose-response curves irrespective of subunit ratio.

This was not what we observed. Figure 9.2 shows the curves obtained for the 1:1 injection ratio of α3β4 compared to those produced by 1:9 and 9:1.

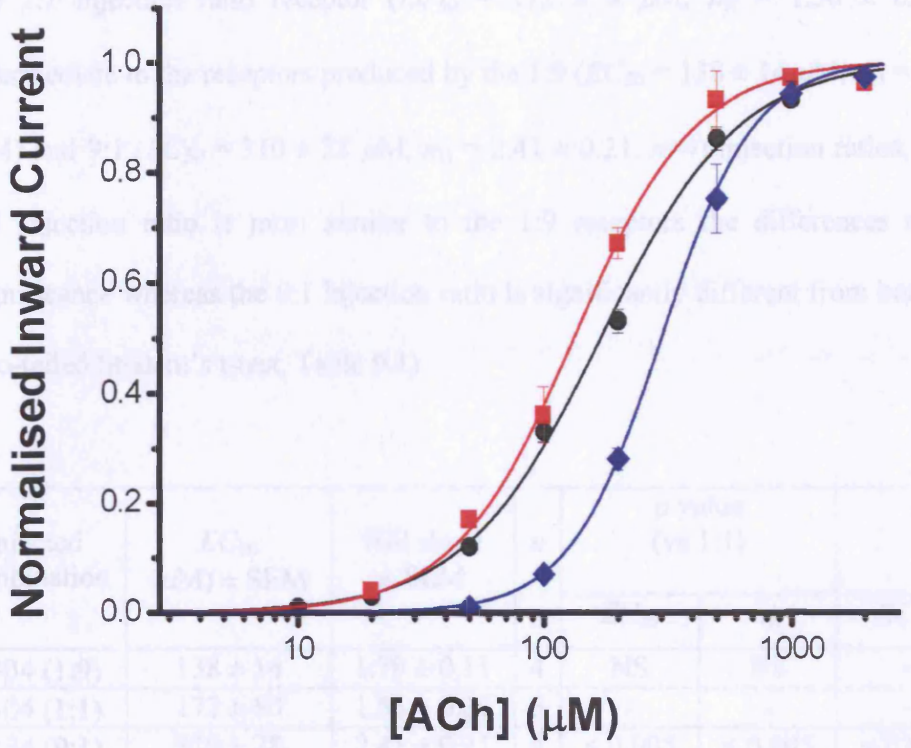

Figure 9.2: Comparison of ACh-concentration-response curves obtained from oocytes injected with α3β4 cRNA at either an equimolar (1:1 black line, circles) or extreme ratio (1:9, red line squares; 9:1, blue line, diamonds). Pooled normalised curves were fitted with a Hill equation as a free fit (n=4-5). There is a clear difference between the curves. Note that the equimolar curve, although intermediate between the two extreme ratio curves, is most similar to the 1:9 wildtype curve.

As can be seen there are marked differences between some of the curves. Receptors expressed from a 9:1 ratio are much less sensitive to ACh than the 1:9 receptors and their dose-response curve has a steeper Hill slope (p<0.01 and p<0.05, two-tailed Student's t-test). While the dose-response curve for 1:9 receptors looks somewhat to the left of the 1:1 curve and appears steeper, the two curves are close to each other, and neither of these differences is significant.

Comparison of the parameters fitted to the different curves show that the curve for the 1:1 injection ratio receptor (EC_{50} = 172 ± 8 μM, n_H = 1.56 ± 0.07, n=5) is intermediate to the receptors produced by the 1:9 (EC_{50} = 138 ± 14 μM, n_H = 1.79 ± 0.11, n=4) and 9:1 (EC_{50} = 310 ± 28 μM, n_H = 2.41 ± 0.21, n=4) injection ratios, and that the 1:1 injection ratio is most similar to the 1:9 receptors the differences not reaching significance whereas the 9:1 injection ratio is significantly different from both (unpaired, two-tailed Student's t-test, Table 9.1).

Injected combination	EC_{50} (μM) ± SEM	Hill slope ± SEM	n	p value (vs 1:1)		p value (vs 1:9)	
				EC_{50}	n_H	EC_{50}	n_H
α3β4 (1:9)	138 ± 14	1.79 ± 0.11	4	NS	NS	-	-
α3β4 (1:1)	172 ± 80	1.56 ± 0.07	5	-	-	-	-
α3β4 (9:1)	310 ± 28	2.41 ± 0.21	4	< 0.005	< 0.005	< 0.005	< 0.05

Table 9.1: Comparison of the EC50 and Hill slopes for α3 + β4 receptors produced by cRNA injected into oocytes at different ratios. Note the significant differences between the 9:1 injection ratio and the 1:1 and 1:9 injection ratios. Statistical analysis by unpaired two-tailed Student's t-.test. NS = not significant.

We already know that at 1:1 injection ratio most of the receptors are 2α:3β; if we want to interpret the trend towards a lower EC_{50} in the 1:9 receptors, it is possible that these receptors contain a small but sizeable proportion of 3α:2β receptors and that this decreases or disappears when we inject 1:9 ratios. The 9:1 receptors are likely to represent a majority of 3α:2β receptors (this will be proven in the next section). The lower Hill slope of the 1:1 injection ratio could be the product of a two-component curve where the two components, representing the two stoichiometries, are too close to be

separated. Our data resemble the findings of Nelson *et al.* 2003 who found that the 2α:3β form of α4β2 had higher ACh sensitivity. Thus, α3β4 receptor stoichiometry in oocytes can be changed and forced by varying the injection ratios.

All this worked on the assumption that the only possible stoichiometries were 2:3 or 3:2 (i.e. that 4:1 and 1:4 stoichiometries are not possible) and that the extreme ratios used would produce pure populations of a certain stoichiometry. To confirm that the two stoichiometries were 2:3 and 3:2 and to check that the two extreme ratios were producing fairly pure populations we then decided to repeat the reporter mutation experiments carried out on α3β4 (1:1 ratio) as reported in Boorman *et al.* 2000 on the 1:9 and 9:1 receptors.

9.2 Investigating the Stoichiometry of the α3β4 Receptor (Injection Ratio 1:9) by the LT Reporter Mutation

$\alpha3^{LT}\beta4$ and $\alpha3\beta4^{LT}$ subunit combinations were injected into oocytes at a ratio of 1:9, the curves obtained are shown in Figure 9.3.

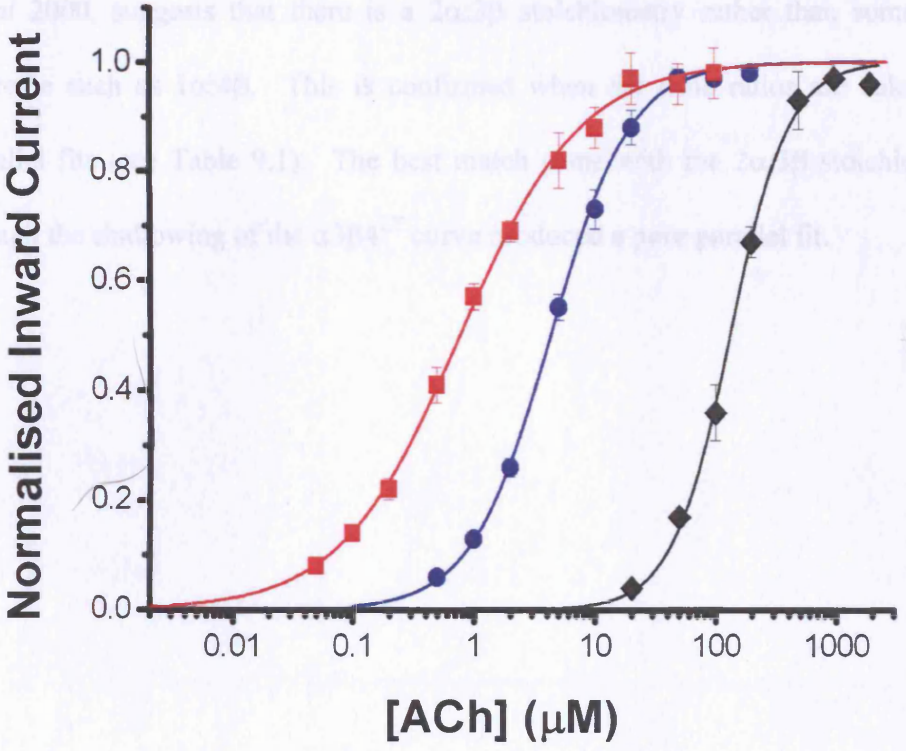

Figure 9.3: ACh-concentration-response curves showing the effect of incorporation of the 9′ LT mutation into the α3 (blue line, circles) and β4 (red line, squares) subunits compared with the wildtype (black line, rhombuses) for α3β4 receptors injected at a ratio of 1:9. Pooled normalised curves were fitted with a Hill equation as a free fit (*n*=4-5). Note the greater effect of the mutation in β4 than α3, consistent with there being more β than α subunits present in the receptor with the same pattern as seen in Figure 9.1.

As shown by the figures, the curves produced by the $\alpha 3^{LT}\beta 4$ and $\alpha 3\beta 4^{LT}$ at a 1:9 injection ratio reproduced the same pattern seen in Boorman *et al.* 2000 with the 1:1 ratio (even down to the shallowing of the Hill slope for the $\beta 4^{LT}$ mutation), with the largest shifts produced by the insertion of the mutation into the β4 subunit (EC_{50} = 0.92 ± 0.13 μM, n_H = 0.90 ± 0.12, n=4) rather than the α3 (EC_{50} = 4.48 ± 0.38 μM, n_H = 1.33 ± 0.09, n=5). By eye, the similarity in the magnitude of the shifts to those observed by Boorman *et al* 2000, suggests that there is a 2α:3β stoichiometry rather than something more extreme such as 1α:4β. This is confirmed when the dose ratios are calculated from parallel fits (see Table 9.1). The best match came with the 2α:3β stoichiometry even though the shallowing of the $\alpha 3\beta 4^{LT}$ curve produced a poor parallel fit.

9.3 Investigating the Stoichiometry of the α3β4 Receptor (Injection Ratio 9:1) by the LT Reporter Mutation

The injection ratios were then reversed to 9:1 for $\alpha3^{LT}\beta4$ and $\alpha3\beta4^{LT}$ combinations. The resulting curves are shown in Figure 9.4.

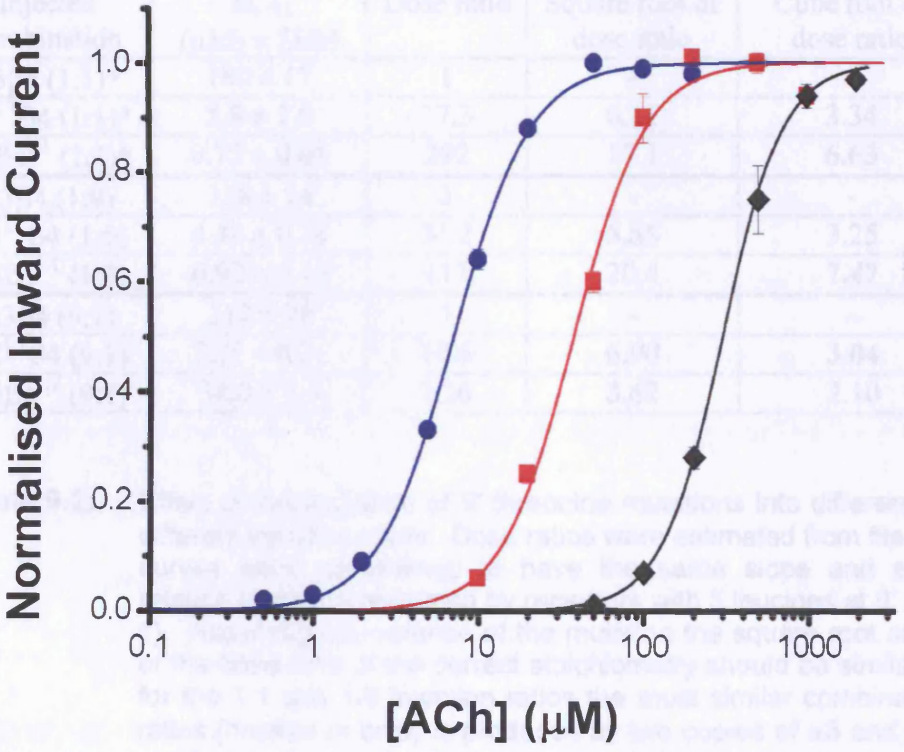

Figure 9.4: ACh-concentration-response curves showing the effect of incorporation of the 9′ LT mutation into the α3 (blue line, circles) and β4 (red line, squares) subunits compared with the wildtype (black line, rhombuses) for α3β4 receptors injected at a ratio of 9:1. Pooled normalised curves were fitted with a Hill equation as a free fit (*n*=4-5). Note the greater effect of the mutation in α3 than β4 the exact opposite of what is seen with the 1:1 and 1:9 ratios, this is consistent with there being more copies of α3 in the receptor than β4.

Comparing Figure 9.4 with Figures 9.1 and 9.3 shows the pattern of shifts of the mutations has entirely changed and the largest effect is now seen with the insertion of the $\alpha3^{LT}$ mutation (EC_{50} = 7.2 ± 0.2 μM, n_H = 1.91 ± 0.05, n=5) rather than the $\beta4^{LT}$ (EC_{50} = 38.8 ± 1.4 μM, n_H = 2.05 ± 0.15, n=4). Once more the stoichiometry which gives the best dose-ratios calculated from parallel fits was the 2:3 stoichiometry but this time with 3α to 2β (Table 9.2).

Injected combination	EC_{50} (μM) ± SEM	Dose ratio	Square root of dose ratio	Cube root of dose ratio	n
α3β4 (1:1)*	180 ± 17	1	-	-	7
$\alpha3^{LT}\beta4$ (1:1)*	5.8 ± 1.0	37.3	**6.11**	3.34	6
$\alpha3\beta4^{LT}$ (1:1)*	0.75 ± 0.05	292	17.1	**6.63**	4
α3β4 (1:9)	138 ± 14	1	-	-	4
$\alpha3^{LT}\beta4$ (1:9)	4.48 ± 0.38	34.2	**5.85**	3.25	5
$\alpha3\beta4^{LT}$ (1:9)	0.92 ± 0.13	417	20.4	**7.47**	4
α3β4 (9:1)	310 ± 28	1	-	-	4
$\alpha3^{LT}\beta4$ (9:1)	7.21 ± 0.21	47.6	6.90	**3.04**	5
$\alpha3\beta4^{LT}$ (9:1)	38.8 ± 1.4	9.26	**3.62**	2.10	4

Table 9.2: Effect of incorporation of 9′ threonine mutations into different subunits at different injection ratios. Dose ratios were estimated from fits in which the curves were constrained to have the same slope and expressed in relation to curves produced by receptors with 5 leucines at 9′ (dose ratio = 1). Assuming equivalence of the mutation the square root and cube root of the dose ratio of the correct stoichiometry should be similar. Note that for the 1:1 and 1:9 injection ratios the most similar combination of dose ratios (marked in bold) is produced by two copies of α3 and three copies of β4 while for the 9:1 ratio the most similar combination is produced by three copies of α3 and two copies of β4. The EC_{50} and the Hill slopes for the two extreme ratios are significantly different for both $\alpha3^{LT}\beta4$ ($p < 0.001$ and $p < 0.05$, respectively, two-tailed Student's t-test) and $\alpha3\beta4^{LT}$ ($p < 0.005$ and $p < 0.05$, respectively, two-tailed Student's t-test). Data marked with * reproduced from Boorman *et al* 2000.

One of the noticeable features of the 3α:2β stoichiometry was the steepness of the Hill slopes, which lead us to wonder whether the 3 alpha form of the α3β4 nAChR had three binding sites? This is a line of speculation we have not yet had an opportunity to follow further.

9.4 Expression of a Pentameric 3-alpha α3β4 Receptor

Given our success with our work on pentameric constructs for α3β4 receptors in their 2α:3β form, we wondered whether it would be possible to produce a pentameric receptor made up by three α3 subunits and two β4 subunits. If such a functional receptor could be produced would it resemble the 3α:2β monomeric receptors we had produced with the 9:1 injection ratio? There are two ways 3α and 2β subunits could be arranged around the pore, namely either with all three α subunits together e.g. α_α_α_β_β or with two together and one separated by β subunits (a sort of "negative" of the putative 2α:3β formation) e.g. α_α_β_α_β.

We thought the likeliest arrangement would be the α_α_β_α_β template. Given that we found that of the two tandem constructs α3_β4 and β4_α3 only the latter produced functional receptors, we would expect to see a similar picture for pentameric constructs and that only some of the possible pentameric constructs (α_α_β_α_β, α_β_α_β_α, β_α_β_α_α and β_α_α_β_α) that follow this chosen pattern would express. With our experience with functional constructs of the β_α template and the functional β_β_α_β_α pentamer we decided to test the nearest variation, β4_α3_α3_β4_α3. High concentrations of this pentamer construct were injected into

oocytes (i.e. 10ng-1000ng, n=6-24) and were tested for function. As with the 2α pentamer constructs, low expression levels were a problem (average I_{max}= 97 ± 14 nA n=12), but the receptor was found to be functional and full dose response curves were obtained (Figure 9.5.). The variation α_β_α_β_α did not express functional receptors

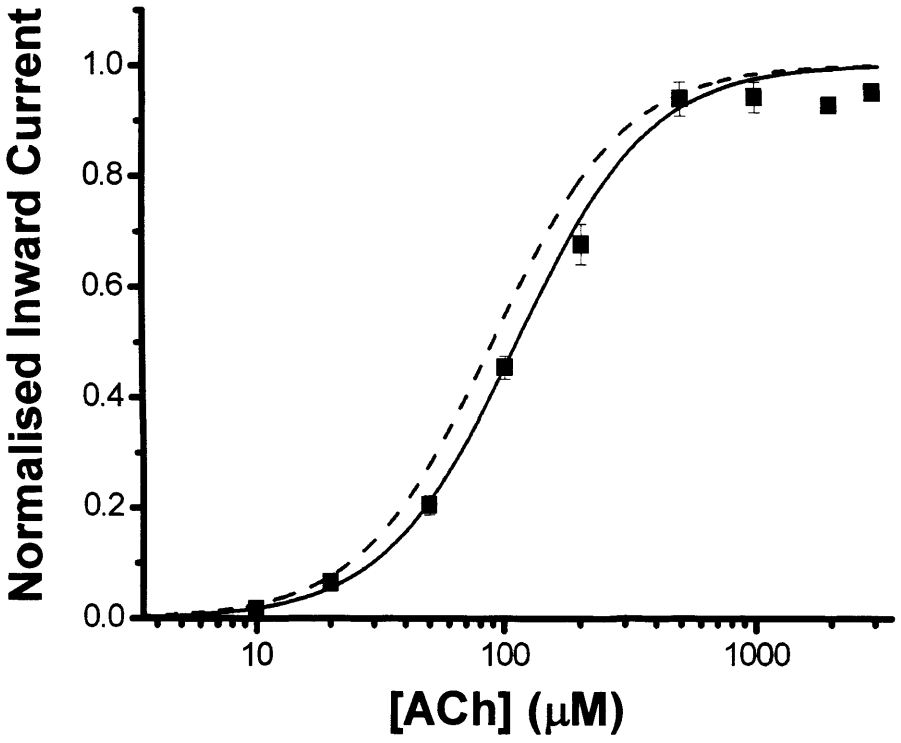

Figure 9.5: ACh-concentration-response curves comparing the β4_β4_α3_β4_α3 pentamer construct (dashed line) with the wildtype β4_α3_α3_β4_α3 (black line, squares). Pooled normalised curves were fitted with a Hill equation as a free fit (n=6-12). Note the only minor differences between the two constructs.

Figure 9.5, shows there was a small shift in the EC_{50} of the 3α pentamer (EC_{50} = 124 ± 11 μM, n_H = 1.74 ± 0.19, n=12) compared to that of the 2α pentamer (EC_{50} = 95 ±

11 μM, n_H = 1.71 ± 0.13, n=6). Not only was this shift too small and variable to reach significance (two-tailed Student's t-test), but also this was nowhere near as large as the shift observed in receptors expressed from monomer construct. In addition to that, the Hill slope was nowhere as steep as in the monomer-expressed 9:1 receptor.

Possibly another variation on the α_α_β_α_β or even the α_α_α_β_β template would produce results more similar to that obtained from the monomeric receptors but without further work, it is hard to give a convincing explanation of these differences, other than just say that this may be a flaw in the use of pentameric constructs, in that they don't always reproduce the properties of monomeric receptors. However, one thing this work does show is that it is possible to produce other functional pentameric constructs other than β4_β4_α3_β4_α3.

My initial work on the two stoichiometries of α3β4 has been expanded on by other members of my group, I will briefly summarise their findings below to help put my work into context; even though I have had only been marginally involved in this work.

9.5 Differences in Pharmacology Between the Two Stoichiometries

My colleague Skevi Krashia checked the potency ratios of a variety of nAChR agonists on the two different stoichiometries in oocytes to produce the following rank orders of potency (n = 6-19).

For the 1:9 injection ratio:-

epibatidine >> lobeline > nicotine ≈ cytisine > DMPP ≈ ACh >> carbachol

For the 9:1 injection ratio:-

epibatidine >> lobeline > DMPP > nicotine > cytisine > ACh >> carbachol

The most obvious changes being the increases in relative potencies of DMPP and cytisine as well as large changes in the absolute values for each agonist (data not shown), From this it was clear that the two different stoichiometries have distinctly different pharmacologies.

9.6 The Stoichiometry of the α3β4 Receptor when Expressed in HEK Cells

My colleagues Seb Kracun and Giovanna Hofmann attempted to repeat this experiment in HEK cells and although experimental problems meant they were unable to fully characterise all the combination ratios, examining the HEK cells transfected at 1:1 shows the primary α3β4 stoichiometry to be the 3α:2β form, the opposite of the findings in oocytes (Figure 9.6 & Table 9.3) and that if forced the other stoichiometry can be formed.

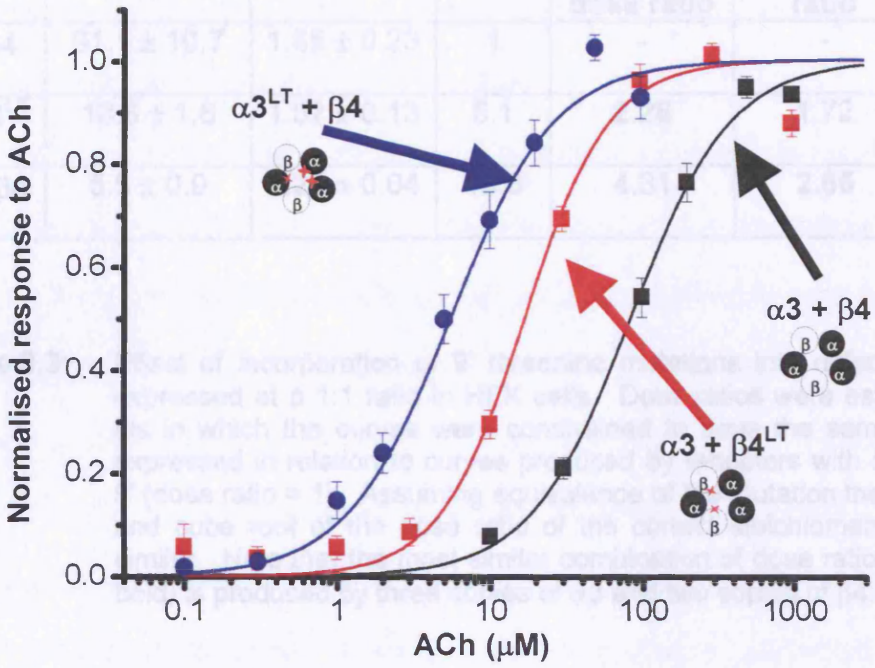

Figure 9.6: ACh-concentration-response curves showing the effect of incorporation of the 9′ LT mutation into the α3 (blue circles) and β4 (red squares) subunits compared with the wildtype (black squares) when expressed in HEK cells at a ratio of 1:1. Pooled normalised curves were fitted with a Hill equation as a free fit (*n*=7-8). Note the greater effect of the mutation in α3 than β4, consistent with there being more α than β subunits present in the receptor, the opposite to what is seen in oocytes. Data courtesy of Seb Kracun and Giovanna Hofmann.

	EC_{50} (μM) ± SEM	n_H ± SEM	Dose ratio	Square root of dose ratio	Cube root of dose ratio	*n*
α3β4	91.1 ± 10.7	1.65 ± 0.23	1	-	-	8
$\alpha3\beta4^{LT}$	18.6 ± 1.6	1.52 ± 0.13	5.1	**2.26**	1.72	7
$\alpha3^{LT}\beta4$	5.5 ± 0.9	1.27 ± 0.04	18.6	4.31	**2.65**	7

Table 9.3: Effect of incorporation of 9′ threonine mutations into different subunits expressed at a 1:1 ratio in HEK cells. Dose ratios were estimated from fits in which the curves were constrained to have the same slope and expressed in relation to curves produced by receptors with 5 leucines at 9′ (dose ratio = 1). Assuming equivalence of the mutation the square root and cube root of the dose ratio of the correct stoichiometry should be similar. Note that the most similar combination of dose ratios (marked in bold) is produced by three copies of α3 and two copies of β4.

Our group have attempted to examine single channel recordings from both stoichiometries, with and without mutations, in order to see if there is any marked difference. However as of writing, this has yet to be analysed and so I will go no further into it.

9.7 Discussion

The results of expressing extreme injection ratios in oocytes confirm that α3β4 is capable of adopting two stoichiometries with distinct properties and that the relative proportions of each receptor population can be changed by changing the transfection ratios. The follow up work has shown the two receptors have distinct pharmacologies, that the predominant stoichiometry in mammalian cell lines is 3α:2β.

The reporting of the presence of two stoichiometries for α4β2, also thought to be 2α:3β and 3α:2β, and the ability for them to be changed led Nelson *et al.* to indulge in some interesting speculation (Nelson *et al.* 2003).

It is known that during development the majority of muscle nicotinic receptor change their formation by one subunit, a γ subunit is replaced by an ε subunit (Naranjo & Brehm, 1993). This confers a number of changes in the resulting receptor properties, the adult receptor has a reduced sensitivity to ACh with shorter mean opening time and increased desensitisation. This change is thought to mark the change in the receptor from embryonic volume transmission to adult synaptic transmission (Sanes & Lichtman, 2001). In volume transmission in embryonic muscle the distances between site of ACh release can be large therefore it is beneficial for the receptor to be activated by relatively low concentrations of ACh. In comparison, in synaptic receptors as the concentration of ACh in the cleft is high and the distance low there is less need for such a sensitive receptor and were a highly ACh-sensitive receptor present there would be the risk of inappropriate activation caused by the firing of neighbouring neurones. The nature of the signal is different as well, synaptic transmission should be faithful, produce large currents in the target muscle fibre but only for a short period before shutting off, whereas in volume transmission longer, more sustained signalling is required. These requirements nicely dove-tail with the properties of embryonic vs. adult muscle nicotinic receptors.

When compared with the different properties of the two stoichiometries of α4β2 neuronal nicotinics it was clear that the 2α:3β stoichiometry with its higher ACh-sensitivity and lower conductance resembles the embryonic muscle nicotinics while the 3α:2β (low ACh-sensitivity, high conductance) resembles the adult. Nelson *et al.*

speculated that the 2α:3β stoichiometry might represent the pre-terminal form of nAChRs where transmitter diffuses from adjacent synapses whereas the 3α:2β is optimal where α4β2 serves a traditional postsynaptic role. However without knowing the physiological concentrations of ACh present in the synaptic cleft and extrasynaptically we cannot say whether this is correct. Similarly we can only speculate whether the developmental change postulated by Sanes and Lichtman (2001) in ganglionic nicotinics has a parallel in the CNS receptors.

As well as being of interest in the stoichiometry and developmental studies of nAChRs the presence of two changeable stoichiometries for α4β2 may be of great importance in the action of nicotine in smoking and particularly the effect of nicotine exposure on the unborn. To these findings we now add proof of there being two stoichiometries for α3β4.

In Boorman *et al.* 2000, it was found that a 1:1 injection ratio of α3 and β4 produced a receptor with a 2α:3β stoichiometry. The new work broadly confirms this, in that it is clear from Figure 9.2 that the 1:1 injection ratio produces a dose-response curve that is very close to the curve produced by the 1:9 injection ratio, which corresponds to the 2α:3β stoichiometry. A question that arises is whether the 1:1 receptors are a mixed population of the two α3β4 stoichiometries, with the majority of the 2α:3β form. If that is the case, can we estimate how many receptors are of the other, 3α:2β form, or at least how much of the current is carried by them? If we can assume that the extreme injection ratios produce pure stoichiometries, the greatest difference between the EC_{50} of the 2α vs the 3α form is seen when we express $\alpha3\beta4^{LT}$ and it is approximately 8-fold (i.e. 0.92 vs 7.21 μM, respectively). Nevertheless, it is hard to see how we could reliably fit the $\beta4^{LT}$

curve resulting from 1:1 injections with two components (Fig. 9.1) and this indicates that the proportion of 3α receptors is too small to be detected, with this mutation and this technique.

It is apparent that in oocytes injected with equimolar concentrations of cRNA produce mixed populations of different stoichiometries for the α4β2 nAChRs and possibly the α2β2 and α3β2 as well, whereas the α3β4 appears to form a fairly pure population of the 2α:3β stoichiometry. We do not know the reason for the difference between the different subunit combinations. In contrast HEK cells predominantly express the 3α:2β form of α3β4. This difference in stoichiometry depending on the expression system used may be due to differences in the respective cell-types membrane insertion, protein assembly etc. machinery or could just reflect differences in expression efficiency between, for instance, α3 and β4 DNA vs. RNA constructs.

An alternative explanation is that the difference is due to the difference in incubation temperature for mammalian cell lines and oocytes, in a manner similar to that reported by Nelson *et al* (2003)

One observation that can be made about α3β4 having two distinctly different stoichiometries is that this may provide the β3 subunit with an additional unexpected role. As noted earlier the α3β4β3 triplet receptor is infuriatingly similar to the α3β4 receptor injected into oocytes at a 1:1 ratio i.e. mostly the 2α:3β form. We have also shown that there is a considerable difference in the properties between the 2α:3β and the 3α:2β forms of the α3β4 receptor. This all suggests a possible role for the β3 subunit in native nAChRs. A neuron expressing α3β4 without the presence of β3 would produce a receptor population mostly made up from the 3α:2β form of the receptor with the

resulting lower sensitivity to ACh, different pharmacology etc. typical of this stoichiometry. Conversely, a neuron expressing α3β4 with β3 would mostly express a population of receptors of the α3β4β4 (2:2:1) form which has similar characteristics to the 2α:3β form of the α3β4 receptor when it comes to ACh sensitivity and pharmacology. Therefore it is possible, if not yet proven, that β3 expression may be a mechanism by which the relative proportions of 3α:2β and 2α:3β-like α3β4 nAChRs are controlled. What the physiological significance of such a control mechanism would be is currently not clear. Even without a clear physiological role if the effect of nicotine on α4β2 is replicated in α3β4 this could be a source of pharmacologically induced plasticity and so may be important in nicotine addiction.

The most pessimistic conclusion would be that in recombinant receptors we see different stoichiometries simply because we are expressing the minimally functional subunit combination, which may never be found in neurones, in which only one of the stoichiometries may be produced.

CHAPTER 10

Summary

Chapter 2 outlined the main aims of my project, so to what extent have these aims been met?

The primary aim of my PhD was to examine which combinations of nAChR subunits could form receptor complexes with the β3 subunit and what effect did the β3's insertion have on the properties of these receptors. We believe the evidence presented here, through both the knock-out of receptors when co-injected with β3 and their recovery by the $\beta3^{VS}$ mutation, shows that, in the oocyte at least, β3 can form receptor complexes with α2β2, α2β4, α3β2, α4β2, α4β4 and α7 subunits. These receptors are present in the membrane of the cell but are virtually non-functional, probably because of a β3-induced decrease in the P_{open} values of these receptors. This effect can also be observed in native α7-type receptors from primary hippocampal cultures. We have also begun to show the possibility that the β3 subunit is a vital requirement in producing functional receptors containing the α6 subunit. All this along with our previous findings on the effect of β3 on the α3β4 receptor suggests an intriguing and significant role of the β3 subunit. Whereas the α3β4 nAChR, the main peripheral nervous system nicotinic receptor, is unaffected by the insertion of a β3 subunit to an almost infuriating degree, all the other nAChRs combinations (which are likely to represent the central nervous system receptor types) are almost totally "knocked-out" by the β3 subunit. The only exception is α6 receptors whose function appears to be dependent on β3's presence. What makes this α6 finding to be of particular interest is the high degree of overlap between α6 and β3 expression (Le Novere *et al.* 1996). It is still unclear what the exact role of the β3 subunit is, particularly the relevance of α6 versus the other CNS nAChRs findings. Nevertheless

it is plausible that control of β3 expression could give neurones a tremendous amount of control over nicotinic transmission both in a general sense (of increasing and decreasing total-cell nicotinic current) and in a more selective way, namely to control which nAChR subtypes are functional in a given cell at a given time. This selection between PNS and CNS nicotinic transmission might be an important factor in the control of nicotinic activity in development and β3 could provide both general and highly specific temporal and spatial control over nAChR-mediated current.

nAChRs are thought to have a general modulatory role over the actions of a wide range of neurones which release a host of different neurotransmitters. Thus, β3 levels may provide a means of controlling a large number of neuronal systems and as such may have a pivotal role in neuronal development, neuronal activity, neuropathology and neuropharmacology.

Of the other secondary aims of the project, the development of the TM2 9′ β3 mutations have proven their worth in researching the action of β3 on nAChRs and while, as events transpired, the Delilah mutants where found to be unnecessary for the research of the majority of the nAChR combos we examined they may still prove to be a useful research tool in the examination of the α6/β3 story. Our work on tandem constructs has highlighted a possible major flaw in the interpretation of the results obtained using these, a finding which could undermine the validity of a large amount of work carried out, not only on nAChRs, but also other LGICs, VGICs and transport proteins which have utilised this approach. Having uncovered this problem with tandems we have then developed a possible solution in the form of pentameric constructs which, even if tandems were flawless, provided a superior amount of control over receptor stoichiometry and despite exhaustive testing have not been shown to suffer the problems associated with tandem constructs. This pentamer

approach has the potential to revolutionise the use of heterologous expression systems to model native type receptors and other proteins far beyond just the nicotinics or even the LGICs as a whole.

Our other work has also produced interesting findings. The discovery of multiple α3β4 subunit stoichiometries and the evidence of this also being present in α3β2 receptors, and perhaps others, supports the findings of Nelson *et al.* 2003 with α4β2. These authors have hypothesised that these two stoichiometries are important for the role of nAChRs in embryonic vs mature CNS and in volume vs synaptic transmission and that they can be affected by nicotine exposure. If this hypothesis is correct, then this may underlie an important effect in nicotine addiction and may be of great importance in the development of the nicotinic system, even for peripheral receptors

I hope you will agree this all adds up to a fairly constructive PhD research project.

CHAPTER 11

Future Work

Below follow a list of potential avenues of future research:-

Beta3

Is the stoichiometry of all the β3-containing triplet receptors 2:2:1?

What is the stoichiometry of α7β3 receptors? Is this changeable?

Is the β3 KO effect seen in other native type tissues?

What regulates β3 levels and do they change in disease states, development, pharmaceutical treatment or smoking?

Are our initial findings on the role of β3 with α6 correct?

Will Delilah-mutated β3 subunits knock out functional α6β3* receptors?

Can the Delilah mutations be used to produce functional knock-down in organotypic preparations?

Pentamers

Can we increase pentamer expression level enough to facilitate more efficient single channel recording and other research?

Can we create pentamers with more complicated stoichiometries?

Can we use pentamers to further explore the non-equivalence of mutations story?

Can we use pentamers to examine the difference between the nAChRs binding sites?

Can we express pentameric constructs in other cell lines?

Can we create pentamers of other types of LGIC?

Can we adapt pentamers to help us with our research on β3, stoichiometries and our other lines of work?

Stoichiometry

Do the other nAChRs have variable stoichiometries?

What governs the control of stoichiometry? What role does nicotine, temperature etc. play?

Do other heteromeric LGICs display this variability?

CHAPTER 12

References

Akabas, M. H., Kaupmann, C., Archdeacon, P. & Kablin, A. (1994). Identification of acetylcholine receptor channel-lining residues in the entire M2 segment of the α subunit. *Neuron.* **13.** 919-927.

Akk, G., Sine, S. & Auerbach, A. (1996). Binding sites contribute unequally to the gating of mouse nicotinic αD200N acetylcholine receptors. *J. Physiol. (Lond.).* **496**:185-196

Akk, G., Zhou, M., & Auerbach A. (1999). A mutational analysis of the acetylcholine receptor channel transmitter binding site. *Biophys J.* **76**(1 Pt 1):207-18.

Akopian, A. H., Sivilotti, L. and Wood, J. N. (1996). A tetrodotoxin-resistant voltage-gated sodium channel expressed by sensory neurones. *Nature* **379** (6562):257-262.

Almeida, O.P., Hulse' G.K., Lawrence' D. & Flicker, L. (2002). Smoking as a risk factor for Alzheimer's disease: contrasting evidence from a systematic review of case–control and cohort studies *Addiction* **97**(1) 15.

Anand, R., Conroy, W. G., Schoepfer, R., Whiting, P., & Lindstrom, J. (1991). Neuronal nicotinic acetylcholine receptors expressed in Xenopus oocytes have a pentameric quaternary structure. *J.Biol.Chem.* **266**, 11192-11198.

Anderson, A. D., Troyanovskaya, M., & Wackym, P. A. (1997). Differential expression of α2-7, α 9 and β2-4 nicotinic acetylcholine receptor subunit mRNA in the vestibular end-organs and Scarpa's ganglia of the rat. *Brain Research* **778**, 409-413.

Ascher, P., Large, W. A., & Rang, H. P. (1979). Studies on the mechanism of action of acetylcholine antagonists on rat parasympathetic ganglion cells. *J.Physiol* **295**, 139-170.

The Axon Guide For Electrophysiology & Biophysics: Laboratory Techniques (1993). Axon Instruments, Inc.

Azam, L., Winzer-Sehan, U.H., Chen, Y. & Leslie, F.M. (2002). Expression of neuronal nicotinic acetylcholine receptor subunit mRNAs within midbrain dopamine neurons. *J Comp Neurol.* **444**(3):260-74.

Baumann, S.W., Baur, R. & Sigel E. (2001). Subunit arrangement of γ-aminobutyric acid type A receptors. *J. Biol. Chem.* **276**:36275–36280.

Baumann, S.W., Baur, R. & Sigel E. (2002). Forced subunit assembly in α1ß2γ2 $GABA_A$ receptors: insight into the absolute arrangement. *J. Biol. Chem.* **277**:46020–46025.

Beckstein, O. & Sansom, M.S. (2004). The influence of geometry, surface character, and flexibility on the permeation of ions and water through biological pores. *Phys Biol.* **1**(1-2):42-52.

Berezhnoy, D., Baur, R., Gonthier, A., Foucaud, B., Goeldner, M. & Sigel, E. (2005). Conformational changes at benzodiazepine binding sites of GABA(A) receptors detected with a novel technique. *J Neurochem.* **92**(4):859-66.

Bertrand, D., Bertrand, S., & Ballivet, M. (1992). Pharmacological properties of the homomeric α7 receptor. *Neurosci.Lett.* **146**, 87-90.

Blount, P., Sukharev, S.I, Moe, P.C., Schroeder, M.J., Guy, H.J. & Kung, C. (1996). Membrane topology and multimeric structure of a mechanosensitive channel protein of Escherichia coli. *EMBO J.* **15**(18): 4798–4805.

Booker T.K., Tritto T., Colman J., Cui C., Collins A.C. & Heinemann S.F. (2000) β3 subunits in regulation of anxiety: analysis of β3-null mutant mice. In: *The 20th Neuropharmacology Conference*, p 65. New Orleans: Elsevier Science.

Boorman, J.P. (2002). The molecular composition of neuronal nicotinic acetylcholine receptors: The role of β3.

Boorman J. P., Beato M., Groot-Kormelink P. J., Broadbent S. D. & Sivilotti L. G. (2003). The effects of β3 subunit incorporation on the pharmacology and single channel properties of oocyte-expressed human α3β4 neuronal nicotinic receptors. *J Biol Chem* **278**:44033-44040.

Boorman, J.P, Groot-Kormelink, P.J. & Sivilotti, L.G. (2000). Stoichiometry of human recombinant neuronal nicotinic receptors containing the β3 subunit expressed in Xenopus oocytes. *J.Physiol* 529 Pt 3:565-577.

Boulter, J., O'Shea-Greenfield, A., Duvoisin, R.M., Connolly, J.G., Wada, E., Jensen, A.,Gardner, P.D., Ballivet, M., Deneris, E.S., McKinnon, D., Heinemann, S. & Patrick, J. (1990). Alpha 3, alpha 5, and beta 4: three members of the rat neuronal nicotinic acetylcholine receptor-related gene family form a gene cluster. *J Biol Chem.* **265**(8):4472-82.

Bouzat, C., Gumilar, F., Spitzmaul, G., Wang, H., Rayes, D., Hansen, S., Taylor, P., & Sine, S.M. (2004). Coupling of agonist binding to channel gating in an ACh-binding protein linked to an ion channel *Nature* **430**, 896-900.

Brejc K, van Dijk WJ, Klaassen RV, Schuurmans M, van Der Oost J, Smit AB, & Sixma TK (2001) Crystal structure of an ACh-binding protein reveals the ligand-binding domain of nicotinic receptors. Nature **411**: 269–276.

Butt, C.M., King, N.M., Sterling, C.R., Tank, A.W., Collins, A.C. & Wehner, J.M. (2004). Tyrosine hydroxylase activity and genetic background effects on phenotypes observed in mice lacking the β3 nicotinic subunit. Program No. 48.20. *2004 Abstract Viewer/Itinerary Planner.* Washington, DC: Society for Neuroscience

Cachelin, A. B. & Rust, G. (1995). β-subunits co-determine the sensitivity of rat neuronal nicotinic receptors to antagonists. *Pflügers Archiv-European Journal of Physiology* **429**, 449-451.

Caulfield, M. P. (1993). Muscarinic receptors-characterization, coupling and function. *Pharmacology and Therapeutics* **58**, 319-379.

Celie, P.H.N., Klaassen, R.V., van Rossum-Fikkert, S.E., van Elk, R., van Nierop, P., Smit, A.B. & Sixma, T.K. (2005). Crystal Structure of Acetylcholine-binding Protein from Bulinus truncatus Reveals the Conserved Structural Scaffold and Sites of Variation in Nicotinic Acetylcholine Receptors *J. Biol. Chem.*, **280**(28): 26457 – 26466.

Chang, Y. & Weiss, D.S. (1999). Allosteric activation mechanism of the alpha1beta2gamma2 gamma- aminobutyric acid type A receptor revealed by mutation of the conserved M2 leucine. *Biophys.J.* **77** (5):2542-2551.

Changeux, J.P. (1990). Fidia Research Foundation Neuroscience Award lectures, Vol. 4. 21-168. Raven Press, New York.

Chavez-Noriega, L.E., Crona, J.H., Washburn, M.S., Urrutia, A., Elliott, K.J. & Johnson, E.C. (1997). Pharmacological characterization of recombinant human neuronal nicotinic acetylcholine receptors h alpha 2 beta 2, h alpha 2 beta 4, h alpha 3 beta 2, h alpha 3 beta 4, h alpha 4 beta 2, h alpha 4 beta 4 and h alpha 7 expressed in Xenopus oocytes. *J.Pharmacol.Exp.Ther.* **280** (1):346-356.

Charpantier, E., Barneoud, P., Moser, P., Besnard, F., & Sgard, F. (1998). Nicotinic acetylcholine subunit mRNA expression in dopaminergic neurons of the rat substantia nigra and ventral tegmental area. *Neuroreport.* **9**, 3097-3101.

Chen, G.Q., Lin, B., Dawson, M.I. & Zhang, X.K. (2002). Nicotine modulates the effects of retinoids on growth inhibition and RAR beta expression in lung cancer cells. *Int J Cancer.* **99**(2):171-8.

Coggan, J. S., Paysan, J., Conroy, W. G., & Berg, D. K. (1997). Direct recording of nicotinic responses in presynaptic nerve terminals. *Journal of Neuroscience* **17**, 5798-5806.

Colquhoun, D (1998) Binding, gating, affinity and efficacy: the interpretation of structure-activity relationships for agonists and of the effects of mutating receptors. *Br J Pharmacol.* **125**(5):924-47.

Colquhoun, D. and Sakmann, B. (1985). Fast events in single-channel currents activated by acetylcholine and its analogues at the frog muscle end-plate. *J.Physiol* **369**:501-557.

Combi, R., Dalprà, L., Tenchini, M.L. & Ferini-Strambi, L. (2004) Autosomal dominant nocturnal frontal lobe epilepsy--a critical overview. *J Neurol.* **251**(8):923-34

Conroy, W. G. & Berg, D. K. (1995). Neurons can maintain multiple classes of nicotinic acetylcholine receptors distinguished by different subunit compositions. *J.Biol.Chem.* **270**, 4424-4431.

Cooper, E., Couturier, S., & Ballivet, M. (1991). Pentameric structure and subunit stoichiometry of a neuronal nicotinic acetylcholine receptor. *Nature* **350**, 235-238.

Cordero-Erausquin, M., Marubio, L. M., Klink, R., & Changeux, J.-P. (2000). Nicotinic receptor function: new perspectives from knockout mice. *Trends in Pharmacological Sciences* **21**, 211-217.

Corringer, P-J., Le Novère, N. and Changeux, J-P. (2000). Nicotinic receptors at the amino acid level. *Annu Rev Pharmacol Toxicol.* **40**:431-58.

Couturier, S., Erkman, L., Valera, S., Rungger, D., Bertrand, S., Boulter, J., Ballivet, M. & Bertrand, D. (1990). Alpha 5, alpha 3, and non-alpha 3. Three clustered avian genes encoding neuronal nicotinic acetylcholine receptor-related subunits. *J Biol Chem.* **265**(29):17560-7.

Covernton PJ & Connolly JG. (2000). Multiple components in the agonist concentration-response relationships of neuronal nicotinic acetylcholine receptors. *J Neurosci Methods* **96(1),** 63-70.

Cui, C., Booker, T.K., Allen, R.S. Grady, S.R., Whiteaker, P., Marks, M.J., Salminen, O., Tritto, T., Butt, C.M., Allen, W.R., Stitzel, J.A., McIntosh, J.M., Boulter, J., Collins, A.C. & Heinemann, S.F. (2003).The beta3 nicotinic receptor subunit: a component of alpha-conotoxin MII-binding nicotinic acetylcholine receptors that modulate dopamine release and related behaviors. *J Neurosci.* **23**(35):11045-53.

Dale, H. H. (1914). *J. Pharmacol. Exp. Ther.* **6**:147-190.

Dale, H.H, Feldberg, W. and Vogt, M. (1936). Release of acetylcholine at voluntary motor nerve endings. *J. Physiol.* **86**:353-380.

Das S, Sasaki Y.F., Rothe T., Premkumar L.S., Takasu M., Crandall J.E., Dikkes P., Connor D.A., Rayudu P., Cheung W., Chen H-S.V., Lipton S.A. & Nakanishi N. (1998). Increased NMDA current and spine density in mice lacking the NMDAR subunit, NR3A. *Nature* **393**: 377-381.

Davidson, A., Mengod, G., Matus-Leibovitch, N. & Oron, Y. (1991). Native Xenopus oocytes express two types of muscarinic receptors. *FEBS Lett.* **284** (2):252-256.

De Haan, L., Booij, J., Lavalaye, J., van Amelsvoort T. & Linszen, D. (2005). Occupancy of dopamine D_2 receptors by antipsychotic drugs is related to nicotine addiction in young patients with schizophrenia. *Psychopharmacology (Berl).* **183**(4):500-5. Epub 2005 Nov 15

De Luca, V., Wang, H., Squassina, A., Wong, G.W.H., John Yeomans, J. & Kennedy, J.L (2004). Linkage of M5 muscarinic and alpha7-nicotinic receptor genes on 15q13 to schizophrenia. *Neuropsychobiology.* **50**(2):124-7.

Del Castillo, J. and Katz, B. (1957). Interaction at end-plate receptors between different choline derivatives. *Proc R Soc Lond B Biol Sci* **146**:369 –381.

Deneris, E. S., Boulter, J., Swanson, L. W., Patrick, J., & Heinemann, S. (1989). β3: a new member of nicotinic acetylcholine receptor gene family is expressed in brain. *Journal of Biological Chemistry* **264**, 6268-6272.

Deneris ES, Connolly J, Rogers SW, Duvoisin R (1991) Pharmacological and functional diversity of neuronal nicotinic acetylcholine receptors. *Trends Pharmacol Sci.* **12**(1):34-40.

Dowell, C., Olivera, B.M., Garrett, J.E., Staheli, S.T., Watkins, M., Kuryatov, A., Yoshikami, D., Lindstrom, J.M. & J. McIntosh, M. (2003). Alpha-conotoxin PIA is selective for alpha6 subunit-containing nicotinic acetylcholine receptors. *J Neurosci.* **23**(24):8445-52.

Drescher, D. G., Khan, K. M., Green, G. E., Morley, B. J., Beisel, K. W., Kaul, H., Gordon, D., Gupta, A. K., Drescher, M. J., & Barretto, R. L. (1995). Analysis of nicotinic acetylcholine receptor subunits in the cochlea of the mouse. *Comp.Biochem.Physiol.* **112C**, 267-273.

Durner, M., Zhou, G., Fu, D., Abreu, P., Shinnar, S., Resor, S. R., Moshe, S. L., Rosenbaum, D., Cohen, J., Harden, C., Kang, H., Wallace, S., Luciano, D., Ballaban-Gil, K., Klotz, I., Dicker, E., & Greenberg, D. A. (1999). Evidence for linkage of adolescent-onset idiopathic generalized epilepsies to chromosome 8-and genetic heterogeneity. *American Journal of Human Genetics* **64**, 1411-1419.

Eccles, J. C., Fatt, P., & Koketsu, K. (1954). Cholinergic and inhibitory synapses in a pathway from motor-axon collaterals to motoneurones. *Journal of Physiology* **126**, 524-562.

Ehrlich, P., (1897). Uber die Constitution des Diphtheriegiftes. In: Himmelweit, F., Editor. *The Collected Papers of Paul Ehrlich* **vol. 2 (1957)**, Pergamon Press, London, pp. 126–133 (4 vols).

Elgoyhen, A.B., Johnson, D.S., Boulter, J., Vetter, D.E., & Heinemann, S. (1994). Alpha 9: an acetylcholine receptor with novel pharmacological properties expressed in rat cochlear hair cells. *Cell* **79**, 705-715.

Elgoyhen A.B., Vetter D.E., Katz E., Rothlin C.V., Heinemann S.F., Boulter J. (2001). alpha 10: A determinant of nicotinic cholinergic receptor function in mammalian vestibular and cochlear mechanosensory hair cells. *Proc Natl Acad Sci USA* **98**: 3501-3506.

Emerick, M.C. & Fambrough, D.M. (1993). Intramolecular fusion of Na pump subunits assures exclusive assembly of the fused alpha and beta subunit domains into a functional enzyme in cells also expressing endogenous Na pump subunits. *J Biol Chem.* **268**(31):23455-9.

Engel, A.G., Lambert, E.H., Mulder, D.M., Torres, C.F., Sahashi, K, Bertorini, T.E & Whitaker, J.N. (1982). A newly recognized congenital myasthenic syndrome

attributed to a prolonged open time of the acetylcholine-induced ion channel. *Ann Neurol.* 11(6):553-69.

Feller, M. B., Wellis, D. P., Stellwagen, D., Werblin, F. S., & Shatz, C. J. (1996). Requirement for cholinergic synaptic transmission in the propagation of spontaneous retinal waves. *Science* **272**, 1182-1187.

Feltz, A & Trautmann, A. (1982). Desensitization at the frog neuromuscular junction: a biphasic process. *J. Physiol.* **322**:257-72.

Fenster, C.P., Beckman, M.L., Parker, J.C., Sheffield, E.B., Whitworth, T.L., Quick, M.W. & Lester, R.A.J. (1999). Regulation of α4β2 Nicotinic Receptor Desensitization by Calcium and Protein Kinase C. *Mol Pharmacol.* **55**(3):432-43.

Filatov G.N., & White M.M. (1995) The role of conserved leucines in the M2 domain of the acetylcholine receptor in channel gating. *Mol Pharmacol* **48**:379-384.

Firsov, D., Gautschi, I., Merillat, A.M, Rossier, B.C. & Schild, L. (1998). The heterotetrameric architecture of the epithelial sodium channel (ENaC*). EMBO J.* **17**(2): 344–352.

Forsayeth, J. R. & Kobrin, E. (1997). Formation of oligomers containing the β3 and β4 subunits of the rat nicotinic receptor. *Journal of Neuroscience* **17**, 1531-1538.

Fruton, J. S. (1979). Claude Bernard the scientist. In E. D. Robin (Ed.) *Claude Bernard and the internal environment. A memorial symposium.* Marcel Dekker, New York.

Fucile, S., Matter, J. M., Erkman, L., Ragozzino, D., Barabino, B., Grassi, F., Alema, S., Ballivet, M., & Eusebi, F. (1998). The neuronal alpha6 subunit forms functional heteromeric acetylcholine receptors in human transfected cells. *Eur.J.Neurosci.* **10**, 172-178.

Galzi, J-L., Devillers-Thiery, A., Hussy, N., Bertrand, S., Changeux' J-P. & Bertrand, D. (1992). Mutations in the channel domain of a neuronal nicotinic receptor convert ion selectivity from cationic to anionic. *Nature.* **359**(6395):500-5.

Galzi, J-L., Edelstein, S.J & Changeux J. (1996). The multiple phenotypes of allosteric receptor mutants. *Proc Natl Acad Sci USA.* **93**(5):1853-8.

Gao, F., Bren, N., Burghardt, T.P. Hansen, S., Henchman, R.H, Taylor, P., McCammon, J.A & Sine, S.M. (2005) Agonist-mediated Conformational Changes in Acetylcholine-binding Protein Revealed by Simulation and Intrinsic Tryptophan Fluorescence *J. Biol. Chem.* **280**, (9,) 8443-8451.

Gerzanich, V., Kuryatov, A., Anand, R. & Lindstrom, J. (1997). "Orphan" alpha6 nicotinic AChR subunit can form a functional heteromeric acetylcholine receptor. *Mol Pharmacol.* **51**(2):320-7.

Gerzanich, V., Peng, X., Wang, F., Wells, G., Anand, R., Fletcher, S. & Lindstrom, J.. (1995). Comparative pharmacology of epibatidine: a potent agonist for neuronal nicotinic acetylcholine receptors. *Mol.Pharmacol.* **48** (4):774-782.

Gerzanich, V., Wang, F., Kuryatov, A., & Lindstrom, J. (1998). α5 subunit alters desensitization, pharmacology, Ca^{++} permeability and Ca^{++} modulation of human neuronal α3 nicotinic receptors. *Journal of Pharmacology and Experimental Therapeutics* **286**, 311-320.

Gotti, C., Fornasari, D., & Clementi, F. (1997). Human neuronal nicotinic receptors. *Progress in Neurobiology* **53**, 199-237.

Gotti, C., Moretti, M., Clementi, F., Riganti, L., McIntosh, J.M., Collins, A.C., Marks, M.J. & Whiteaker, P. (2005). Expression of nigrostriatal alpha 6-containing nicotinic acetylcholine receptors is selectively reduced, but not eliminated, by beta 3 subunit gene deletion. *Mol Pharmacol.* **67**(6):2007-15.

Green, W.N. (1999). Ion channel assembly: creating structures that function. *J. Gen. Physiol.* **113**:163–169.

Grinevich, V.P., Letchworth, S.R., Lindenberger, K.A., Menager, J., Mary, V., Sadieva, K.A., Buhlman, L.M., Bohme, G.A., Pradier, L, Benavides, J., Lukas, R.J & Bencherif, M. (2005). Heterologous expression of human alpha6beta4beta3alpha5 nicotinic acetylcholine receptors: binding properties consistent with their natural expression require quaternary subunit assembly including the alpha5 subunit. *J Pharmacol Exp Ther.* **312**(2):619-26.

Groot-Kormelink, P.J., Broadbent, S., Beato, M. & Lucia Sivilotti (2006) Constraining the expression of nicotinic acetylcholine receptors using pentameric constructs. *Mol Pharmacol.* **69**(2); 558-63.

Groot-Kormelink PJ, Broadbent S D, Boorman J P & Sivilotti L G (2004). Incomplete incorporation of tandem subunits in recombinant neuronal nicotinic receptors. *J Gen Physiol* **123**:697-708.

Groot Kormelink, P.J. & Luyten, W.H. (1997). Cloning and sequence of full-length cDNAs encoding the human neuronal nicotinic acetylcholine receptor (nAChR) subunits beta3 and beta4 and expression of seven nAChR subunits in the human neuroblastoma cell line SH-SY5Y and/or IMR-32. *FEBS Lett.* **400** (3):309-314.

Groot-Kormelink, P.J., Luyten, W.H., Colquhoun, D. & Sivilotti, L.G. (1998). A reporter mutation approach shows incorporation of the "orphan" subunit beta3 into a functional nicotinic receptor. *J.Biol.Chem.* **273** (25):15317-15320.

Grosman C & Auerbach A (2000) Asymmetric and independent contribution of the second transmembrane segment 12' residues to diliganded gating of acetylcholine receptor channels: a single-channel study with choline as the agonist. *J Gen Physiol* **115**:637-651.

Grunnet, M., Jespersen, T.,Rasmussen, H.B., Ljungstrøm, T., Jorgensen, N.K., Olesen, S-P. & Klaerke, D.A. (2002). KCNE4 is an inhibitory subunit to the KCNQ1 channel. *J Physiol.* **542**(Pt 1):119-30.

Gunthorpe, M.J. & Lummis, S.C.R. (2001). Conversion of the ion selectivity of the 5-HT(3A) receptor from cationic to anionic reveals a conserved feature of the ligand-gated ion channel superfamily. *J Biol Chem.* **276**(24):10977-83.

Gurley D, Harris E.W., Li C,. Johnson E.C. & Lanthorn T. (2000) 5-Hydroxyindole potentiates the nicotinic acetylcholine receptor alpha7 subtype. *Soc Neurosci Abstr* **26:** 827

Harvey, S. C. & Luetje, C. W. (1996). Determinants of competitive antagonist sensitivity of neuronal nicotinic receptor α subunits. *Journal of Neuroscience* **16**, 3798-3806.

Hefft, S., Hulo, S., Bertrand, D., & Muller, D. (1999). Synaptic transmission at nicotinic acetylcholine receptors in rat hippocampal organotypic cultures and slices. *Journal of Physiology* **515**, 769-776.

Hernandez, M.-C., Erkman, L., Matter-Sadzinski, L., Roztocil, T., Ballivet, M., & Matter, J.-M. (1995). Characterization of the nicotinic acetylcholine receptor β3 gene. Its regulation within the avian nervous system is effected by a promoter 143 base pairs in length. *Journal of Biological Chemistry* **270**, 3224-3233.

Hoenderop JG, Voets T, Hoefs S, Weidema F, Prenen J, Nilius B & Bindels R J (2003) Homo- and heterotetrameric architecture of the epithelial Ca2+ channels TRPV5 and TRPV6. *EMBO J* **22**:776-785.

Hunt, R. (1901). Further observations of the blood-pressure-lowering bodies in extracts of the supradrenal gland. *Amer. J. Physiol.* **5**.

Im, W.B., Pregenzer, J.F., Binder, J.A., Dillon, G.H. & Alberts, G.L. (1995). Chloride channel expression with the tandem construct of α6-ß2 $GABA_A$ receptor subunit requires a monomeric subunit of α6 or γ2. *J. Biol. Chem.* **270**:26063–26066.

Imoto, K., Busch, C., Sakmann, B., Mishina, M., Konno, T., Nakai, J., Bujo, H., Mori, Y., Fukuda, K., & Numa, S. (1988). Rings of negatively charged amino acids determine the acetylcholine receptor channel conductance. *Nature* **335**, 645-648.

Imoto, K., Konno, T., Nakai, J., Wang, F., Mishina, M., & Numa, S. (1991). A ring of uncharged polar amino acids as a component of channel constriction in the nicotinic acetylcholine receptor. *FEBS Lett.* **289**, 193-200.

Isacoff, E.Y, Jan, Y.N. & Lily Yeh Jan (1990). Evidence for the formation of heteromultimeric potassium channels in Xenopus oocytes. *Nature*. **345**(6275):530-4.

James I of England (1604). "A Counterblaste to Tobacco".

Johnson, D. S., Martinez, J., Elgoyhen, A. B., Heinemann, S. F., & McIntosh, J. M. (1995). α-conotoxin Iml exhibits subtype-specific nicotinic acetylcholine receptor blockade: Preferential inhibition of homomeric α7 and α9 receptors. *Molecular Pharmacology* **48**, 194-199.

Karlin, A. (1993). Structure of nicotinic acetylcholine receptors. *Curr.Opin.Neurobiol.* **3**, 299-309.

Karlin, A. & Akabas, M. H. (1995). Toward a structural basis for the function of nicotinic acetylcholine receptors and their cousins. *Neuron* **15**, 1231-1244.

Katz, B. & Thesleff, S. (1957). A study of "desensitisation" produced by acetylcholine at the motor end plate. *J. Physiol (Lond).* **138**:63-80.

Keramidas, A., Moorhouse, A.J., French, C.R, Schofield, P.R. & Barry, P.H (2000). M2 pore mutations convert the glycine receptor channel from being anion- to cation-selective. *Biophys J.* **79**(1):247-59.

Köhler, K., Forster, I.C., Lambert, G., Biber, J. & Murer, H. (2000). The functional unit of the renal type IIa Na+/Pi cotransporter is a monomer. *J Biol Chem.* **275**(34):26113-20.

Kuryatov, A., Olale, F., Cooper, J., Choi, C. & Lindstrom, J. (2000). Human alpha6 AChR subtypes: subunit composition, assembly, and pharmacological responses. *Neuropharmacology.* **39**(13):2570-90.

Labarca, C., Nowak, M. W., Zhang, H., Tang, L., Deshpande, P., & Lester, H. A. (1995). Channel gating governed symmetrically by conserved leucine residues in the M2 domain of nicotinic receptors. *Nature* **376**, 514-516.

Langley, J.N. and Anderson H.K. (1892). The actions of nicotine on the cillary ganglion on endings of the third cranial nerve. *J. Physiol (Lond).* **13**:460-468.

Langley, J.N. (1905). On the reaction of cells and of nerve-endings to certain poisons chiefly as regards the reaction of striated muscle to nicotine and curare. *J. Physiol (Lond).* **33**:374-413.

Langley, J.N. (1907). On the contraction of muscle chiefly in relation to the presence of receptive substances. Part 1. *J. Physiol (Lond).* **36**:347-384.

Le Novere, N. & Changeux, J. P. (1995). Molecular evolution of the nicotinic acetylcholine receptor: an example of multigene family in excitable cells. *J.Mol.Evol.* **40**, 155-172.

Le Novere, N., Zoli, M., & Changeux, J. P. (1996). Neuronal nicotinic receptor alpha 6 subunit mRNA is selectively concentrated in catecholaminergic nuclei of the rat brain. *Eur.J.Neurosci.* **8**, 2428-2439.

Liman, E.R., Tytgat, J. & Hess, P. (1992). Subunit stoichiometry of a mammalian K^+ channel determined by construction of multimeric cDNAs. *Neuron.* **9**:861–871.

Lindstrom, J. (1997). Nicotinic acetylcholine receptors in health and disease. *Molecular Neurobiology* **15**, 193-222.

Lindstrom, J. M (2000). Acetylcholine receptors and myasthenia. *Muscle Nerve.* 23(4):453-77.

Listerud, M., Brussaard, A. B., Devay, P., Colman, D. R., & Role, L. W. (1991). Functional contribution of neuronal AChR subunits revealed by antisense oligonucleotides [published erratum appears in Science 1992 Jan 3;255(5040): 12]. *Science* **254**, 1518-1521.

Liu, L., Chang, C. Q., Jiao, Y. Q., & Simon, S. A. (1998). Neuronal nicotinic acetylcholine receptors in rat trigeminal ganglia. *Brain Research* **809**, 238-245.

Loewi, O. (1921). Uber humorale ubertragbartkeit der herzenervenwirkung. *Pflugers Arch.* **189**:239-242.

Luetje, C.W. & Patrick, J. (1991). Both alpha- and beta-subunits contribute to the agonist sensitivity of neuronal nicotinic acetylcholine receptors. *J Neurosci.* **11**(3):837-45.

Luetje, C. W., Piattoni, M., & Patrick, J. (1993). Mapping of ligand-binding sites of neuronal nicotinic acetylcholine receptors using chimeric α subunits. *Molecular Pharmacology* **44**, 657-666.

Lukas, R.J. (1991) Effects of chronic nicotinic ligand exposure on functional activity of nicotinic acetylcholine receptors expressed by cells of the PC12 rat pheochromocytoma or the TE671/RD human clonal line. *J Neurochem* **56:** 1134-1145.

Luo, S., Kulak, J. M., Cartier, G. E., Jacobsen, R. B., Yoshikami, D., Olivera, B. M., & McIntosh, J. M. (1998). α-Conotoxin AuIB selectively blocks α3β4 nicotinic acetylcholine receptors and nicotine-evoked norepinephrine release. *J.Neurosci.* **18**, 8571-8579.

Marubio, L. M., Arroyo-Jiménez, M. d. M., Cordero-Erausquin, M., Léna, C., Le Novère, N., de Kerchove d'Exaerde, A., Huchet, M., Damaj, M. I., & Changeux, J.-P. (1999). Reduced antinociception in mice lacking neuronal nicotinic receptor subunits. *Nature* **398**, 805-810.

Matsubayashi, H., Alkondon, M., Pereira, E. F., Swanson, K. L., & Albuquerque, E. X. (1998). Strychnine: a potent competitive antagonist of α-bungarotoxin-sensitive nicotinic acetylcholine receptors in rat hippocampal neurons. *Journal of Pharmacology and Experimental Therapeutics* **284**, 904-913.

McCreadie, R.G. (2003). Diet, smoking and cardiovascular risk in people with schizophrenia: descriptive study. *Br J Psychiatry.* **183**:534-9.

McGehee, D. S., Heath, M. J. S., Gelber, S., Devay, P., & Role, L. W. (1995). Nicotine enhancement of fast excitatory synaptic transmission in CNS by presynaptic receptors. *Science* **269**, 1692-1696.

McIntosh, J.M., Gardner, S., Luo, S., Garrett J.E. & Yoshikami, D. (2000). Conus peptides: novel probes for nicotinic acetylcholine receptor structure and function. *Eur J Pharmacol.* **393**(1-3):205-8.

Miller, C (1989). Genetic manipulation of ion channels: a new approach to sructure and mechanism. *Neuron.* **2.** 1195-1205.

Minier F & Sigel E (2004) Techniques: Use of concatenated subunits for the study of ligand-gated ion channels. *Trends Pharmacol Sci* **25**:499-503.

Miyazawa, A., Fujiyoshi, Y., Stowell, M. & Unwin, N. (1999). Nicotinic acetylcholine receptor at 4.6 A resolution: transverse tunnels in the channel wall. *J Mol Biol.* **288**(4):765-86.

Miyazawa, A., Fujiyoshi, Y. & Unwin, N. (2003). Structure and gating mechanism of the acetylcholine receptor pore. *Nature.* **423**(6943):949-55.

Morley, B.J., Li, H-S., Hiel, H., Drescher, D.G., & Elgoyhen, A.B. (1998). Identification of the subunits of the nicotinic cholinergic receptors in the rat cochlea using RT-PCR and in situ hybridization. *Molecular Brain Research* **53**, 78-87.

Moss, S. J., McDonald, B. J., Rudhard, Y., & Schoepfer, R. (1996). Phosphorylation of the predicted major intracellular domains of the rat and chick neuronal nicotinic acetylcholine receptor α7 subunit by cAMP-dependent. *Neuropharmacology* **35**(8):1023-8.

Nelson, M.E., Kuryatov, A., Choi, C.H., Zhou, Y. & Lindstrom, J. (2003). Alternate stoichiometries of α4ß2 nicotinic acetylcholine receptors. *Mol. Pharmacol.* **63**:332–341.

Nelson, M. E. & Lindstrom, J. (1999). Single channel properties of human alpha3 AChRs: impact of beta2, beta4 and alpha5 subunits. *J.Physiol* **516 (Pt 3)**, 657-678.

Nicke, A., Rettinger, J. & Schmalzing, G. (2003). Monomeric and dimeric byproducts are the principal functional elements of higher order $P2X_1$ concatamers. *Mol. Pharmacol.* **63**:243–252

Nishi, M., Hinds, H., Lu, H-P., Kawata, M. & Hayashi, Y. (2001). Motoneuron-Specific Expression of NR3B, a Novel NMDA-Type Glutamate Receptor Subunit That Works in a Dominant-Negative Manner. *J. Neurosci.* **21**(23):RC185.
O'Leary, M.E., Filatov, G.N. & White, M.M. (1994). Characterization of d-tubocurarine binding site of Torpedo acetylcholine receptor. *Am J Physiol.* **266**(3 Pt 1):C648-53.

Orr-Urtreger, A., Broide, R. S., Kasten, M. R., Dang, H., Dani, J. A., Beaudet, A. L., & Patrick, J. W. (2000). Mice homozygous for the L250T mutation in the α7 nicotinic

acetylcholine receptor show increased neuronal apoptosis and die within 1 day of birth. *Journal of Neurochemistry* **74**, 2154-2166.

Orr-Urtreger, A., Goldner, F. M., Saeki, M., Lorenzo, I., Goldberg, L., De Biasi, M., Dani, J. A., Patrick, J. W., & Beaudet, A. L. (1997). Mice deficient in the α7 neuronal nicotinic acetylcholine receptor lack α-bungarotoxin binding sites and hippocampal fast nicotinic currents. *Journal of Neuroscience* **17**, 9165-9171.

Palma, E., Bertrand, S., Binzoni, T., & Bertrand, D. (1996). Neuronal nicotinic α7 receptor expressed in *Xenopus* oocytes presents five putative binding sites for methyllycaconitine. *Journal of Physiology* **491**, 151-161.

Palma, E., Maggi, L., Barabino, B., Eusebi, F., & Ballivet, M. (1999). Nicotinic acetylcholine receptors assembled from the alpha7 and beta3 subunits. *Journal of Biological Chemistry* **274**, 18335-18340.

Papke, R.L., Boulter, J., Patrick, J. & Heinemann, S.F. (1989). Single-channel currents of rat neuronal nicotinic acetylcholine receptors expressed in Xenopus oocytes. *Neuron.* **3**(5):589-96.

Papke, R.L., Duvoisin, R.M., & Heinemann, S.F. (1993). The amino terminal half of the nicotinic β–subunit extracellular domain regulates the kinetics of inhibition by neuronal bungarotoxin. *Proceedings of the Royal Society of London Series B-Biological Sciences* **252**, 141-148.

Papke, R.L., Craig, A.G. & Heinemann, S.F. (1994). Inhibition of nicotinic acetylcholine receptors by bis (2,2,6,6- tetramethyl- 4-piperidinyl) sebacate (Tinuvin 770), an additive to medical plastics. *J.Pharmacol.Exp.Ther.* **268** (2):718-726.

Paton, W. D. M. & Zaimis, E. J. (1949). The pharmacological actions of polymethylene bistrimethylammonium salts (Reprinted from Brit J Pharmacol, vol 4, pg 381, 1949). *British Journal of Pharmacology* **120**, 60-79.

Paton, W. D. M. & Zaimis, E. J. (1951). Paralysis of autonomic ganglia by methonium salts. *British Journal of Pharmacology* **6**, 155-168.

Pereira, E. F. R., Alkondon, M., McIntosh, J. M., & Albuquerque, E. X. (1996). α-conotoxin-ImI: A competitive antagonist at α-bungarotoxin-sensitive neuronal nicotinic receptors in hippocampal neurons. *Journal of Pharmacology and Experimental Therapeutics* **278**, 1472-1483.

Picciotto, M. R., Zoli, M., Rimondini, R., Léna, C., Marubio, L. M., Merlo Pich, E., Fuxe, K., & Changeux, J.-P. (1998). Acetylcholine receptors containing the β2 subunit are involved in the reinforcing properties of nicotine. *Nature* **391**, 173-177.

Puchacz, E., Buisson, B., Bertrand, D. & Lukas, R.J. (1994). Functional expression of nicotinic acetylcholine receptors containing rat alpha 7 subunits in human SH-SY5Y neuroblastoma cells. *FEBS Lett.* **354**(2):155-9.

Quick MW, Naeve J, Davidson N, & Lester HA. (1992) Incubation with horse serum increases viability and decreases background neurotransmitter uptake in Xenopus oocytes. *Biotechniques.* **13**(3):357-61.

Quik, M., Polonskaya, Y., Gillespie, A., Jakowec, M., Lloyd, G.K. & Langston, J.W. (2000). Localization of nicotinic receptor subunit mRNAs in monkey brain by in situ hybridization. *J Comp Neurol.* **425**(1):58-69.

Ramirez-Latorre, J., Yu, C. R., Qu, X., Perin, F., Karlin, A., & Role, L. (1996). Functional contributions of α5 subunit to neuronal acetylcholine receptor channels. *Nature* **380**, 347-351.

Revah, F., Bertrand, D., Galzi, J.-L., Devillers-Thiéry, A., Mulle, C., Hussy, N., Bertrand, S., Ballivet, M., & Changeux, J-P. (1991). Mutations in the channel domain alter desensitization of a neuronal nicotinic receptor. *Nature* **353**, 846-849.

Roerig, B., Nelson, D. A., & Katz, L. C. (1997). Fast synaptic signaling by nicotinic acetylcholine and serotonin 5-HT_3 receptors in developing visual cortex. *Journal of Neuroscience* **17**, 8353-8362.

Role, L.W. & Berg, D.K. (1996). Nicotinic receptors in the development and modulation of CNS synapses. *Neuron* **16**, 1077-1085.

Rozycka, A. & Trzeciak, W.H. (2003). Genetic basis of autosomal dominant nocturnal frontal lobe epilepsy. *J Appl Genet.* **44**(2):197-207.

Sahin-Tóth, M., Lawrence, M.C. & Kaback, H.R. (1994). Properties of permease dimer, a fusion protein containing two lactose permease molecules from Escherichia coli. *Proc Natl Acad Sci USA.* **91**(12):5421-5.

Sands, S.B., Costa, A.C.S. & Patrick, J.W. (1993). Barium permeability of neuronal nicotinic receptor $\alpha 7$ expressed in *Xenopus* oocytes. *Biophys. J.* **65**:2614–2621.

Schorge, S. & Colquhoun, D. (2003). Studies of NMDA receptor function and stoichiometry with truncated and tandem subunits. *J. Neurosci.* **23**:1151–1158.

Schuller, H.M., Jull, B.A, Sheppard B.J. & Plummer, H.K. (2000). Interaction of tobacco-specific toxicants with the neuronal alpha(7) nicotinic acetylcholine receptor and its associated mitogenic signal transduction pathway: potential role in lung carcinogenesis and pediatric lung disorders. *Eur J Pharmacol.* **393**(1-3):265-77.

Sgard, F., Charpantier, E. Bertrand, S., Walker, N., Caput, D., Graham, D., Bertrand, D. & Besnard, F. (2002). A novel human nicotinic receptor subunit, alpha10, that confers functionality to the alpha9-subunit. *Mol Pharmacol.* **61**(1):150-9.

Shelley, C. & Colquhoun, D. (2005). A human congenital myasthenia-causing mutation ({varepsilon}L78P) of the muscle nicotinic acetylcholine receptor with unusual single channel properties. *J. Physiol.* **564**(2): 377 - 396.

Sivilotti, L. G., Colquhoun, D., & Millar, N. (2000). Comparison of native and recombinant neuronal nicotinic receptors: problems of measurement and expression. In *Neuronal Nicotinic Receptors*, eds. Clementi, F., Fornasari, D., & Gotti, C., pp. 379-416. Springer Verlag, Berlin Heidelberg.

Sivilotti, L. G., McNeil, D. K., Lewis, T. M., Nassar, M. A., Schoepfer, R., & Colquhoun, D. (1997). Recombinant nicotinic receptors, expressed in *Xenopus* oocytes, do not resemble native rat sympathetic ganglion receptors in single-channel behaviour. *Journal of Physiology* **500**, 123-138.

Smit, A.B., Syed, N.I., Schaap, D., van Minnen, J., Klumperman, J., Kits, K.S., Lodder, H., van der Schors, R.C., van Elk, R., Sorgedrager, B., Brejc, K., Sixma, T.K. & Geraerts, W.P.M (2001) A glia-derived acetylcholine-binding protein that modulates synaptic transmission. *Nature* **411**, 261-268.

Steinlein, O. K., Magnusson, A., Stoodt, J., Bertrand, S., Weiland, S., Berkovic, S. F., Nakken, K. O., Propping, P., & Bertrand, D. (1997). An insertion mutation of the CHRNA4 gene in a family with autosomal dominant nocturnal frontal lobe epilepsy. *Human and Molecular Genetics* **6**, 943-947.

Steinlein, O. K., Mulley, J. C., Propping, P., Wallace, R. H., Phillips, H. A., Sutherland, G. R., Scheffer, I. E., & Berkovic, S. F. (1995). A missense mutation in the neuronal nicotinic acetylcholine receptor alpha 4 subunit is associated with autosomal dominant nocturnal frontal lobe epilepsy. *Nat.Genet.* **11**, 201-203.

Stoop, R., S. Rassendren, T.F. Kawashima, E., Buell, G., Surprenant, A. & North, R.A. (1999). Contribution of individual subunits to the multimeric $P2X_2$ receptor: estimates based on methanethiosulfonate block at T336C. *Mol. Pharmacol.* **56**:973–981.

Tapper, A.R., McKinney, S.L., Nashmi, R., Schwarz, J., Deshpande, P., Labarca, C., Whiteaker, P., Marks, M.J., Collins, A.C. & Lester, H.A. (2004). Nicotine activation of alpha4* receptors: sufficient for reward, tolerance, and sensitization. *Science.* **306**(5698):1029-32

Tsunoyama, K. & Gojobori, T. (1998). Evolution of nicotinic acetylcholine receptor subunits. *Mol.Biol.Evol.* **15**, 518-527.

Unwin, N. (1993). Nicotinic acetylcholine receptor at 9 A resolution. *J.Mol.Biol.* **229**, 1101-1124.

Unwin, N. (1995) Acetylcholine receptor channel imaged in the open state. *Nature.* **373**(6509):37-43

Unwin, N. (1998). The nicotinic acetylcholine receptor of the Torpedo electric ray. *J.Struct.Biol.* **121**, 181-190.

Unwin, N. (2000). The Croonian Lecture 2000. Nicotinic acetylcholine receptor and the structural basis of fast synaptic transmission. *Philos.Trans.R.Soc.Lond B Biol.Sci.* **355**, 1813-1829.

Unwin N (2005) Refined structure of the nicotinic acetylcholine receptor at 4Å resolution. *J Mol Biol* 346: 967–989

Unwin, N., Miyazawa, A., Li, J. & Fujiyoshi, Y. (2002). Activation of the nicotinic acetylcholine receptor involves a switch in conformation of the alpha subunits. *J Mol Biol.* **319**(5):1165-76.

Van Duijn, C.M., Clayton, D.G., Chandra, V., Fratiglioni, L., Graves, A.B., Heyman, A., Jorm, A.F., Kokmen, E., Kondo, K. & Mortimer, J.A. (1994). Interaction between genetic and environmental risk factors for Alzheimer's disease: a reanalysis of case-control studies. EURODEM Risk Factors Research Group. *Genet Epidemiol.* **11**(6):539-51.

Varnum, M.D. & Zagotta, W.N. (1996) Subunit interactions in the activation of cyclic nucleotide-gated ion channels. *Biophys J.* **70**(6):2667-79.

Vernallis, A.B., Conroy, W.G., & Berg, D.K. (1993). Neurons assemble acetylcholine receptors with as many as three kinds of subunits while maintaining subunit segregation among receptor subtypes. *Neuron* **10**, 451-464.

Vetter, D. E., Liberman, M. C., Mann, J., Barhanin, J., Boulter, J., Brown, M. C., Saffiote-Kolman, J., Heinemann, S. F., & Elgoyhen, A. B. (1999). Role of α9 nicotinic ACh receptor subunits in the development and function of cochlear efferent innervation. *Neuron* **23**, 93-103.

Wang, F., Gerzanich, V., Wells, G.B., Anand, R., Peng, X., Keyser, K. & Lindstrom, J. (1996). Assembly of human neuronal nicotinic receptor alpha5 subunits with alpha3, beta2, and beta4 subunits. *J.Biol.Chem.* **271** (30):17656-17665.

West, R.W. & Ogden, R.T. (1997) Statistical Analysis with Webstat, a Java applet for the World Wide Web. *J.Stat.Soft* **2**(3). Epub www.jstatsoft.org.

Wheeler, S. V., Chad, J. E., & Foreman, R. (1993). Residues 1 to 80 of the N-terminal domain of the β subunit confer neuronal bungarotoxin sensitivity and agonist selectivity on neuronal nicotinic receptors. *FEBS Letters* **332**, 139-142.

White, M.M. (2006). Pretty subunits all in a row: using concatenated subunit constructs to force the expression of receptors with defined subunit stoichiometry and spatial arrangement. *Mol. Pharmacol..***69**(2): 407-10.

Williams, B. W., Temburni, M. K., Schwartz Levey, M., Bertrand, S., Bertrand, D., & Jacob, M. H. (1998). The long internal loop of the α3 subunit targets nAChRs to subdomains within individual synapses on neurons *in vivo*. *Nature Neuroscience* **1**, 557-562.

Winzer-Serhan, U.H. & Leslie, F.M, (2005). Expression of alpha5 nicotinic acetylcholine receptor subunit mRNA during hippocampal and cortical development. *J Comp Neurol.* **481**(1):19-30.

Wonnacott, S. (1997). Presynaptic nicotinic ACh receptors. *Trends in Neurosciences* **20**, 92-98.

Xu, W., Gelber, S., Orr-Urtreger, A., Armstrong, D., Lewis, R. A., Ou, C. N., Patrick, J., Role, L., De Biasi, M., & Beaudet, A. L. (1999a). Megacystis, mydriasis, and ion channel defect in mice lacking the alpha3 neuronal nicotinic acetylcholine receptor. *Proceedings of the National Academy of Sciences U.S.A.* **96**, 5746-5751.

Xu, W., Orr-Urtreger, A., Nigro, F., Gelber, S., Ballard Sutcliffe, C., Armstrong, D., Patrick, J. W., Role, L. W., Beaudet, A. L., & De Biasi, M. (1999b). Multiorgan autonomic dysfunction in mice lacking the β2 and the β4 subunits of neuronal nicotinic acetylcholine receptors. *Journal of Neuroscience* **19**, 9298-9305.

Yu' F.H & Catterall, W.A. (2003). Overview of the voltage-gated sodium channel family. *Genome Biol.* **4**(3):207

Yu, C. R. & Role, L. W. (1998a). Functional contribution of the α5 subunit to neuronal nicotinic channels expressed by chick sympathetic ganglion neurones. *Journal of Physiology* **509**, 667-681.

Yu, C. R. & Role, L. W. (1998b). Functional contribution of the α7 subunit to multiple subtypes of nicotinic receptors in embryonic chick sympathetic neurones. *Journal of Physiology* **509**, 651-665.

Zerhusen, B., Zhao, J., Xie, J., Davis, P.B. & Ma, J. (1999). A Single Conductance Pore for Chloride Ions Formed by Two Cystic Fibrosis Transmembrane Conductance Regulator Molecules. *J Biol Chem*, Vol. **274**, Issue 12, 7627-7630.

Zhang, Y., Chen, J., & Auerbach, A. (1995). Activation of recombinant mouse acetylcholine receptors by acetylcholine, carbamylcholine and tetramethylammonium. *J.Physiol (Lond)* **486 (Pt 1)**, 189-206.

Zhao, L., Kuo, Y-P., George,A.A., Peng, J-H., Purandare, M-S., Schroeder, K.M., Lukas, R.J. & Jie Wu (2003). Functional Properties of Homomeric, Human α7-Nicotinic Acetylcholine Receptors Heterologously Expressed in the SH-EP1 Human Epithelial Cell Line *J Pharmacol Exp Ther.* **305**(3):1132-41

Zhou, F-M., Liang Y. & Dani, J.A. (2001). Endogenous nicotinic cholinergic activity regulates dopamine release in the striatum. *Nat Neurosci.* **4**(12):1224-9.

Zhou, Y., Nelson, M.E., Kuryatov, A., Choi, C., Cooper, J. & Lindstrom, J. (2003). Human α4ß2 acetylcholine receptors formed from linked subunits. *J. Neurosci.* **23**:9004–9015.

Zimmerman, A.L. (2002). Two B or not two B? Questioning the rotational symmetry of tetrameric ion channels. *Neuron.* **36**:997–999.

Zwart R & Vijverberg H P (1998) Four pharmacologically distinct subtypes of α4β2 nicotinic acetylcholine receptor expressed in *Xenopus laevis* oocytes. *Mol Pharmacol* **54**:1124-1131.